Decoding the content of cross-modal influences in the brain

Kerri Marie Bailey

100012558

A thesis submitted in partial fulfilment of the requirements of the University of East Anglia for the degree of Doctor of Philosophy

Research undertaken in the School of Psychology, University of East Anglia

January 2020

Decoding the content of cross-modal influences in the brain

Abstract

This thesis examined how context and prior experience can shape the neural computations occurring in the human brain, specifically by using pattern classification analysis to decode the content of cross-modal influences in and around the primary somatosensory cortex (S1). In Chapter 2, fMRI was used to investigate whether simply hearing familiar sounds depicting different hand-object interactions could be discriminated in S1, even though stimulus presentation occurred in the auditory domain and no external tactile stimulation occurred. Results found discriminable patterns of activity about the sound of different hand-object interactions in hand-sensitive areas of S1, and not our two control categories of familiar animal vocalizations and unfamiliar pure tones. Chapter 3 aimed to corroborate the cross-modal effects found in the previous fMRI literature using a high temporal resolution neuroimaging technique: EEG. Specifically, EEG was used to examine whether simply viewing images of different familiar visual object categories which imply rich haptic information could be identified in sensorimotor-related oscillatory responses, even though input was from a visual source and no tactile stimulation occurred. Results found the content of different familiar, but not unfamiliar, visual object categories could be discriminated in the mu rhythm oscillatory response, thus establishing a potential oscillatory marker for the cross-modal effects previously observed. Chapter 4 involved an interactive fMRI paradigm using real 3D objects to test whether the primary function of the cross-modal influences previously detected is a likely result of predictive coding mechanisms. Whilst no reliable evidence for an account of predictive coding was found in this experiment, this study provided critical insight into the development of experiments which can directly test the assumptions of predictive coding with real action. The research conducted in this thesis has, therefore, provided significant contributions to the literature regarding our understanding of cross-modal influences and cortical feedback in the human brain.

***Keywords**:* cross-modal, cortical feedback, multi-voxel pattern analysis, mu rhythm, predictive coding, primary somatosensory cortex. (6)

Contents

List of Figures

Acknowledgements

First and foremost, I thank Dr. Fraser Smith. You have been a fantastic supervisor who I could always depend on to guide me through any problem I was facing. Your exceptional level of knowledge and supervision has shaped me into a person who can achieve things I never realised I was capable of. Not once throughout the time we have worked together have you doubted my potential to excel, and your endless encouragement to aim high has enabled me countless opportunities to present this research at prestigious conferences and attend once in a lifetime courses all around the world to stand me in good stead for my career. For that, I will be eternally grateful. It was a privilege to have taken on a research project that I am truly invested in, and I hope we can continue further collaborations in the future. My deepest and sincerest gratitude goes to you Fraser. It was an honour to have completed my doctorate with you.

Second, I would like to thank all the people who made significant contributions to the three experimental chapters in this thesis. Dr. Bruno Giordano, Dr. Amanda Kaas, the staff at the Scannexus imaging centre in Maastricht, Dr. Saber Sami, Dr. Ethan Knights, Dr. Janak Saada, Dr. Stephanie Rossit, and all the welcoming radiographers during the long scanning days at the Norfolk and Norwich University Hospital. In addition, thank you to all the participants who volunteered their time to make these research projects possible, and to anyone who listened to my presentations at various conferences around the world, offering valuable advice which I could implement into my work. I also thank my second supervisor Prof. John Spencer for your insightful comments on the projects at my annual reviews. Thank you to Dr. Vicky Adams for all your help and advice when I was starting out fresh in my academic path. I could not have hoped for a better lab partner who transitioned into a friend. I also thank Dr. Damian Cruse and Prof. Will Penny for taking the time to read my thesis, in addition to Dr. Natalie Wyer for agreeing to act as independent chair, for my viva examination.

I wish to express a general thank you to all the past and present staff and PhD students in the School of Psychology at UEA who I have got to know over the past seven and a half years. I'll treasure all the fond memories I have shared with so many of you. I would particularly like to voice a special thank you to Jackie Orford for all the hard work she has put in to making the School of Psychology what it is

today, and to Scott Steward-Smith for always resolving any queries I had, in addition to putting up with me at every psychology ball!

Thank you to all my friends and family. You all mean so much to me and I feel very fortunate to have you in my life as a constant source of support. My entire academic experience would have been very different if I did not have you there every step of the way to celebrate the successes but also build me back up at my lowest points. In particular, I thank Megan Rudrum, my work wife, for your eternal words of encouragement and advice given during the many lake walks spent talking through any dilemmas we were facing. I am going to miss our synchronised tea and coffee breaks! Rachel Lambert, thank you for always being there to listen to any problems I had, even though you were probably going through the same thing because that always happened with us! I am also very grateful that you always offered me a place to stay when needed. Dr. Ian Norman, thank you for the numerous conversations when we needed a break from writing. I am very thankful to have had your support and advice right toward the end of the PhD, even when we went into lockdown! I thank all three of you for helping me to keep routine to my days with the scheduled Skype calls during that difficult time. Dr. Ethan Knights, thank you for making each trip to various conferences around the world turn in to a memory I will cherish forever (five stars, would recommend!). I miss the days we spent after work laughing until my face hurt and I want you to know how much I truly value the friendship we developed throughout the PhD.

Last and most definitely not least, I thank my mum, Sandra Bailey, my dad, Kevin Bailey, and my sister, Laura Bailey. I am so proud to be part of such a close-knit, caring, and supportive family who always look out for each other. Mum, I especially want to thank you for everything you have done for me. I am incredibly grateful for the fact I always came home to a cooked meal after a long day, and for your continuous offerings of coffee or wine when I was stressed (depending on the time of day!). Most importantly, I thank all of you for giving me a distinctive work-life boundary. It is never a dull moment in the Bailey household, and I am forever thankful for all the fun “NFB” memories we have shared. I cannot thank you enough for your patience and unwavering support since I decided to go to university, and I love you all unconditionally.

Author's Declaration

I declare that the work contained in this thesis has not been submitted for any other award and that it is all my own work. I also confirm that this work fully acknowledges opinions, ideas and contributions from the work of others.

The research presented in Chapter 2 has been submitted as a preprint:

Bailey, K. M., Giordano, B. L., Kaas, A., & Smith, F. W. (2019). Decoding the sound of hand-object interactions in primary somatosensory cortex. *BioRxiv*, 732669. https://doi.org/10.1101/732669

The research produced in Chapters 2, 3, and 4 has previously been presented, and will be presented, at conferences in oral and poster formats:

Oral Presentations

Bailey, K. M., Giordano, B. L., Kaas, A., & Smith, F. W. (2018, May). *Decoding the sound of hand-object interactions in early somatosensory cortex*. Oral presentation at the meeting of the Concepts, Actions, and Objects Workshop, Rovereto, IT.

Smith, F. W., Giordano, B. L., Kaas, A., & **Bailey, K. M.** (2018, September). Decoding the sound of hand-object interactions in early somatosensory cortex. In S. Rossit (Chair), *Human neuroimaging of predictive processing*. Symposium conducted at the meeting of the British Association for Cognitive Neuroscience, Glasgow, UK.

Poster Presentations

Bailey, K. M., Giordano, B. L., Kaas, A., & Smith, F. W. (2018, May). *Decoding the sound of hand-object interactions in early somatosensory cortex*. Poster session presented at the meeting of the Concepts, Actions, and Objects Workshop, Rovereto, IT.

Bailey, K. M., Giordano, B. L., Kaas, A., & Smith, F. W. (2018, September). *Decoding the sound of hand-object interactions in primary somatosensory cortex*. Poster session presented at the meeting of the British Psychological Society East of England, Norwich, UK.

Bailey, K. M., Giordano, B. L., Kaas, A., & Smith, F. W. (2018, November). *Decoding the sound of hand-object interactions in primary somatosensory cortex*. Poster session presented at the meeting of the Society for Neuroscience, San Diego, CA.

Bailey, K. M., Giordano, B. L., Kaas, A., & Smith, F. W. (2019, January). *Decoding the sound of hand-object interactions in primary somatosensory cortex*. Poster session presented at the meeting of the Experimental Psychological Society, London, UK.

Bailey, K. M., Sami, S., & Smith, F. W. (2019, June). *Is there alpha and beta attenuation in sensorimotor cortex during perception of graspable objects?* Poster session presented at the meeting of the Organisation for Human Brain Mapping, Rome, IT.

Bailey, K. M., Sami, S., & Smith, F. W. (2019, June). *Is there alpha and beta attenuation in sensorimotor cortex during perception of graspable objects?* Poster session presented at the Cognitive and Bodily selves workshop, Norwich, UK.

Smith, F. W., Knights, E., Saada, J., Rossit, S., & **Bailey, K. M.** (2020, May). *Testing predictive processing as an account of visually driven responses to real-*

world objects in primary somatosensory cortex. Poster presentation at the Vision Sciences Society, St. Pete Beach, FL.

Any ethical clearance for the research presented in this thesis has been approved. Approval has been sought and granted by the School of Psychology Ethics Committee at the University of East Anglia.

Name: Kerri Marie Bailey

Signature: 

Date: 30/01/2020

Word Count: 66,089

CHAPTER 1

–

General Introduction

1.1. Prelude

How the human brain processes sensory information is much more complex than a typical textbook definition of cortex function. A standard explanation will likely state that the primary sensory cortical areas in the brain are specialised in passively registering specific types of sensory input (e.g. the primary visual cortex registers incoming visual information). Whilst this is strictly true, in reality it is unlikely that any one sense ever operates independently at any given time in such a simplistic manner. For example, I am currently typing on my keyboard. The feel of the keys on my fingertips is a tactile sensation, yet I am also receiving simultaneous auditory and visual input whenever I press down on the keys and see the letters that appear in front of me on the screen. I am also using my previous experience of typing on keyboards to accurately predict where the next key I plan to use will be. I am using the current context of the particular size of this keyboard to adapt my hand and finger movements accordingly. All this information comprises a simultaneous combination of visual, auditory, and tactile input, adapted to my previous experiences with the world and continuously being updated based on the current context that I am in. As such, moving away from standard textbook definitions of primary sensory cortex function, and instead focusing on how these areas integrate different sensory information and adapt with experience, is an important question and increasingly popular area of investigation in cognitive neuroscience today.

The primary aim of this thesis is to examine how our prior experience with the world, together with the current context, can shape the neural computations that are occurring in the primary sensory cortical regions of the human brain. Specifically, this thesis focuses on how information is processed in and around the primary somatosensory cortex - the first known cortical area to process tactile input. This chapter will provide a detailed review about how we currently understand human cortex function. First, traditional views of cortex function will be reviewed, indicating how these views have changed over the past few decades. Then, research investigating multisensory processes across the primary sensory cortical areas will be introduced. Next, theories to explain how the brain may combine sensory input will be detailed. Following a comprehensive review of the literature, this chapter will subsequently introduce the important unanswered questions around sensory information processing which have been addressed in the present thesis.

1.2. The primary sensory cortical areas

The first known cortical areas in the human brain which process sensory information from the outside world are known as the primary sensory cortices. There are three dominant primary sensory cortices. The primary visual cortex (V1) is centred around the calcarine sulcus of the occipital lobe, the primary auditory cortex (A1) is located in the mid superior temporal lobe, and the primary somatosensory cortex (S1) is located in the most anterior portion of the parietal lobe; these cortical areas are known to process visual, auditory, and tactile information respectively (Crossman & Neary, 2015). Figure 1.1 displays the anatomical location of the primary sensory cortices in the left cerebral hemisphere. This section of the introduction will provide a detailed overview of research which has studied how sensory information is processed in the primary sensory cortices in the human brain.

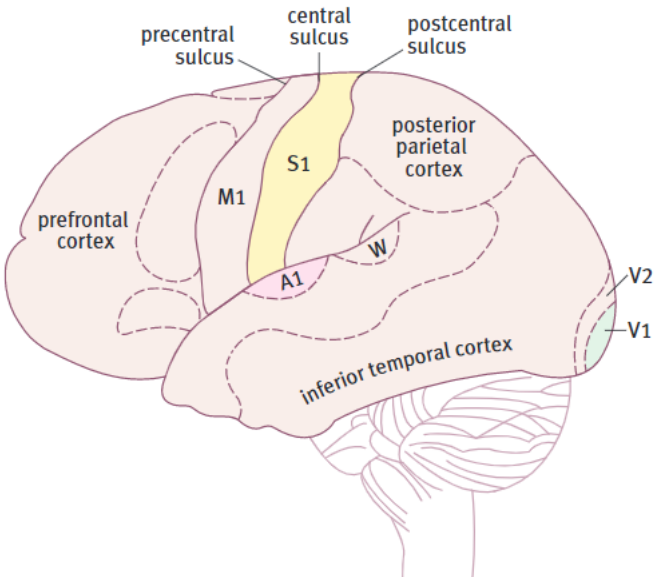

Figure 1.1: The three primary sensory cortices belonging to the senses of vision (V1), audition (A1), and tactile (S1) information, demonstrated in the left cerebral hemisphere. Taken from Watson, Paxinos, and Kirkcaldie (2010).

1.2.1. Traditional models of cortex function in the primary sensory cortices.

The primary sensory cortices are located within the cerebral cortex; a highly convoluted thin sheet of neural tissue approximately 2-3mm thick, enveloping the surface of the human brain. Due to the nature of the many complex folds in this

cortical sheet, the cortex actually accounts for approximately 40-50 per cent of the entire mass of the human brain (Ramachandran, 2002). The cortex is divided in to many different functional areas, each specialised for specific tasks (see Brodmann, 1994; Brodmann & Garey, 2006). These areas can be further organised in to a functional hierarchy of high- and low-level cortical brain regions (Felleman & Van Essen, 1991; C. Koch, 2004; Maunsell & Van Essen, 1983; Mumford, 1991, 1992; Rockland & Pandya, 1979). As explained simply by Hawkins and Blakeslee (2004), these areas are not physically arranged 'above' or 'below' other areas, rather, the level in which a functional area sits in the cortical hierarchy depends on how the areas are connected to one another. Whilst low-level areas send information up to high-level areas via a feedforward pathway, high-level areas can send information back down to low-level areas via a separate feedback pathway (Hawkins & Blakeslee, 2004; Maunsell & Van Essen, 1983; Mumford, 1992). There are also lateral connections which can send information within the same level of a given functional area, such as within V1. Figure 1.2 depicts an example of the feedforward, feedback and lateral connections in the visual system.

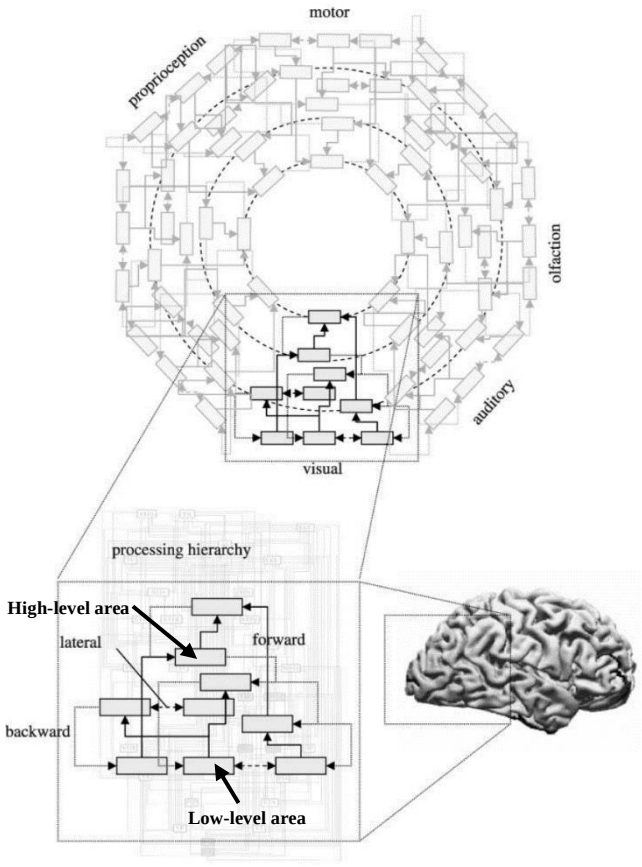

Figure 1.2: An example of the feedforward, feedback, and lateral pathways in the visual processing hierarchy. Taken and slightly adapted from Friston (2005).

Traditional models of sensory information processing indicated all sensory input (e.g. vision, audition, and tactile information) travelled through the cortex from low- to high-level cortical regions along a feedforward pathway (e.g. Lamme, Super, & Spekreijse, 1998). This pathway suggests sensory information enters the brain via the retina of the eye, the cochlea of the ear, or the somatosensory receptors on the skin, and is first transformed to a specific region in the thalamus dedicated to each type of sensory input. For example, visual input enters the lateral geniculate nucleus (LGN), auditory input enters the medial geniculate nucleus (MGN), and tactile input enters the ventral posterior nucleus (VPN); all located within the thalamus (Crossman & Neary, 2015). Sensory information is then relayed from the nuclei in the thalamus to the corresponding primary sensory cortex for each sense (e.g. V1, A1, or S1 respectively). These areas are at the lowest level in the cortical hierarchy and process sensory input at its raw most basic level (S. M. Sherman & Guillery, 2002). The connections between the thalamus and primary cortices are topographic, meaning information projects to a given primary sensory cortex in an ordered fashion. For example, primary visual and somatosensory cortices are spatially organised in such a way that a specific cortical region is representative of the exact location of the sensory surface of the retina or skin (Udin & Fawcett, 1988). In auditory cortex, specific sound frequencies sent from the cochlea are represented in a tonotopically organised map of low to high frequencies from central to outer regions of A1 (Elia Formisano et al., 2003; Talavage, Ledden, Benson, Rosen, & Melcher, 2000). Finally, feedforward models suggest sensory information is then passed from the primary cortical area up the cortical hierarchy to high-level association areas which carry out a more complex analysis of the information. For example, areas such as the superior temporal sulcus (STS) or inferotemporal cortex (IT) can assign meaning to the raw sensory input, and contain rich, abstract information about the world (Felleman & Van Essen, 1991; Maunsell & Van Essen, 1983; Tanaka, 1996).

The feedforward pathway has been extensively studied within the visual system. For example, Serre, Oliva and Poggio (2007) demonstrate a feedforward architecture of visual processing from V1 through to IT during a rapid categorization task (see also Chapman, Zahs, & Stryker, 1991; Reid & Alonso, 1995). The feedforward flow of visual processing has been largely characterised by models which have studied the neuronal response when stimulating a specific region of sensory space, identifying what is known as the receptive field of the neuron (Alonso

& Chen, 2009). For example, a visual receptive field model is concerned with determining exactly what properties of a visual stimulus elicit the maximum response of the receptive field in a given neuron in V1 (Carandini et al., 2005). The classic studies by Hubel and Wiesel (1968; 1959; 1962) described the powerful method of studying the receptive fields of single neurons in V1 in the cat and monkey brain, identifying two main cell types depending on their receptive field structures; simple and complex cells. They found that simple cells in V1 are preferentially activated by specific patterns of light or orientation (Figure 1.3A), whereas complex cells have larger receptive fields and are more responsive to the boundaries and changes between light and dark (Figure 1.3B). Therefore, each neuron in V1 has a specific receptive field which signifies a particular region of visual space it is selective for, with a maximum size of around 1° (Alonso & Chen, 2009). From this research, area V1 was taken to be a stimulus driven feature detector which simply responds to the visual information that is present in the real world, such as changes in light or contrast.

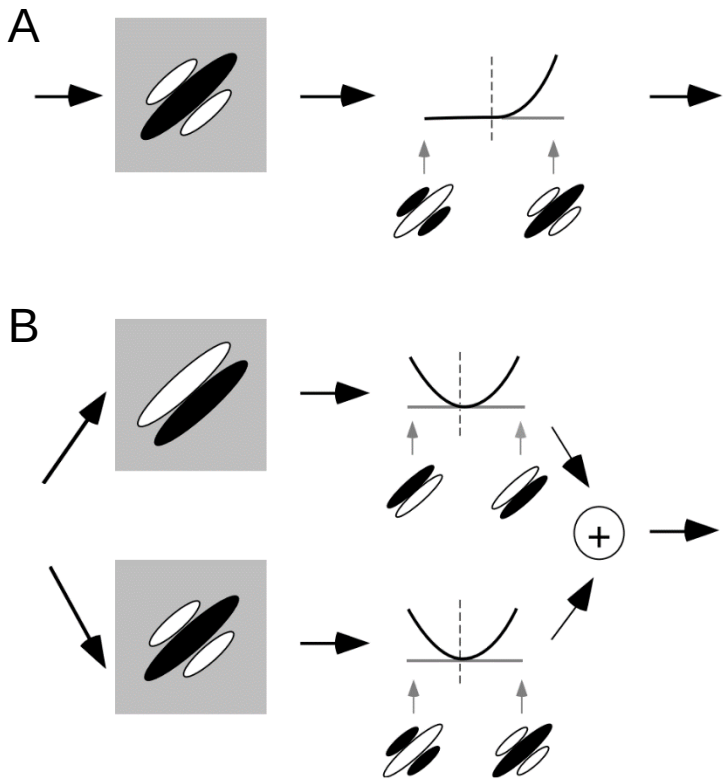

Figure 1.3: A visual example of the receptive field of (A) a simple cell, and (B) a complex cell, in a V1 neuron. (A) Here, cells in V1 are preferentially activated by specific patterns of light or orientation. (B) Here, cells are more responsive to the boundaries and changes between light and dark. Taken from Carandini et al. (2005).

Moving beyond the feature detector in V1, traditional models of visual cortex function suggest this information is subsequently sent up the cortical hierarchy to higher level visual areas, which have broader receptive fields and construct a higher order representation of the visual stimulus (Zeki, 1969). For example, neurons in IT show selectivity to complex objects (Rolls, 1991; Tanaka, 1996), and other areas along the ventral visual stream, such as the inferior occipital and fusiform gyri, are selective to the recognition of objects even when partially occluded (Tang et al., 2014). Whilst receptive field models have been predominantly studied in V1, the same principles have been applied to other primary sensory cortical areas. For example, somatosensory receptive fields comprise a region of space on the surface of the skin which, when stimulated, can subsequently evoke a response in a specific neuron in S1 (Alonso & Chen, 2009). In S1, the accuracy of sensing tactile stimulation varies across the body. For example, receptive fields on the fingertips have a discrimination threshold diameter of around 1-2mm, whereas the diameter on the palms is around 5-10mm (Breedlove, Watson, & Rosenzweig, 2010). Moreover, recent work has found receptive field sizes differ among individual fingers, indicating the index finger contains smaller receptive fields compared to the little finger (Puckett, Bollmann, Junday, Barth, & Cunnington, 2020). As such, discrimination of two spatially separate stimuli is more accurate the smaller the diameter of a receptive field. Once again, traditional research on somatosensory receptive fields would suggest S1 is a simple detector which merely responds to tactile information from specific areas on the sensory surface of the skin, feeding this information up to higher-level brain areas, such as secondary somatosensory cortex (S2), which is involved in tactile object recognition (Gardner & Johnson, 2012).

1.2.2. The missing content of traditional models of cortex function.

A problematic aspect of the conventional feedforward model of cortex function is the fact that this model provides no explanation as to how context and prior experience can influence processing in the primary sensory cortical areas. For example, whilst receptive field models aim to provide all information needed to explain neuronal responses in the primary cortical areas (such as V1; Rust, Schwartz, Movshon, & Simoncelli, 2005), these models do not account for the role of the feedback and lateral pathways in the cortex. It is important to consider feedback and

lateral connections in any model of cortical processing, especially since feedforward models (e.g. Chapman et al., 1991; Reid & Alonso, 1995; Serre et al., 2007) based on Hubel and Wiesel's (1968; 1959; 1962) original studies in V1 have been found to only account for around 40 per cent of the total explainable variance of responses in V1 neurons during natural vision (David & Gallant, 2005). This 40 per cent, as explained by Carandini et al. (2005), is the best estimate of how well the conventional feedforward models account for natural visual responses in V1. Although this is a sizeable amount of explained variance, previous work has estimated around 60-80 per cent of the total response variance of a given V1 neuron remains unexplained from these models, and is likely to be a function of cortical inputs arising from areas other than the LGN (Olshausen & Field, 2005). Further work has also found traditional auditory and somatosensory receptive field models to account for approximately 55 and 40 per cent of the total explainable response variance in A1 and S1 respectively (see Blake & Merzenich, 2002, and DiCarlo & Johnson, 2002; DiCarlo, Johnson, & Hsiao, 1998 respectively).

Furthermore, since most receptive field models are based on data gathered from simple stimuli such as viewing gratings or bars, hearing random tone pips, or feeling random dot patterns, it is important to consider how contextual priors from more complex stimuli may shape processing in the primary sensory cortical areas. A classic illustration of how prior experience can shape processing in the primary cortical areas can be demonstrated with illusions. To give visual illusions as one example, in the famous Kanizsa (1976, 1979) illusion (see Figure 1.4), a non-existent white triangle or square can be clearly perceived, even though in reality the figures simply depict a series of Pac-Man shaped stimuli arranged in a certain position. The illusory contours of the shapes have no physical basis, however, the fact that these contours are so clearly perceived challenges the idea that the visual system merely processes raw sensory input at its most basic level, in turn demonstrating how prior knowledge can influence visual perception. As a result, other theories of cortical processing have suggested phenomena such as the Kanizsa illusion may be the result of a separate neural pathway in the brain. Indeed, we know high-level areas can send information back down to low-level areas via feedback cortico-cortical pathways (Hawkins & Blakeslee, 2004; Maunsell & Van Essen, 1983; Mumford, 1992). This means the primary cortical areas such as V1 must not only receive information entering the brain from the external environment, such as

via the retina, but also from other cortical areas which send information back to V1 via a separate neural path. As a result, other theories, such as Gregory's (1970) visual assumption theory, argues top-down processing via such feedback cortico-cortical pathways must be important to facilitate perception.

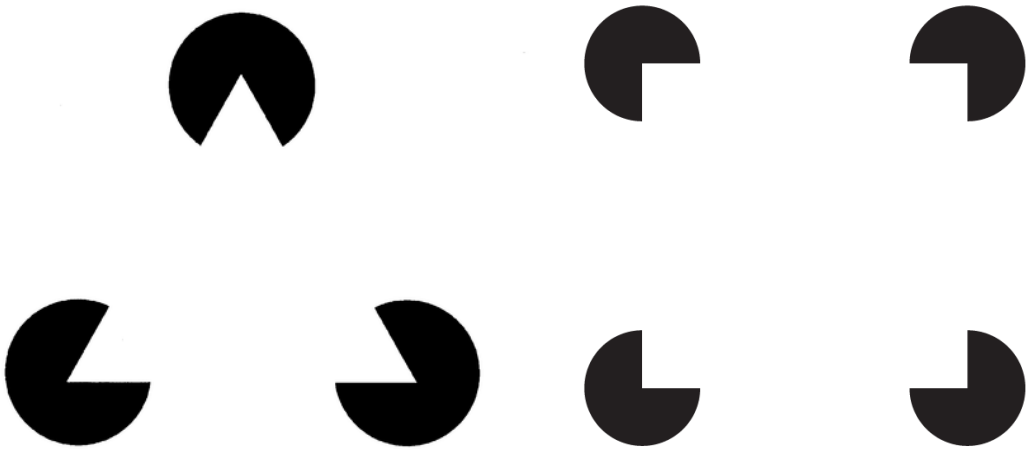

Figure 1.4: The Kanizsa (1976, 1979) illusion. The left image appears to contain a solid white triangle, and the right image appears to include a solid white square, both with well-defined contours. However, these shapes are both subjective, and actually have no physical basis.

Neural evidence to support the idea that a primary sensory region can be influenced from contextual information sent via feedback pathways in the brain has been established using functional magnetic resonance imaging (fMRI) in the visual system. For example, Murray, Boyaci, and Kersten (2006) showed participants visual illusions of two balls which projected the same visual angle yet were perceived to be at different distances. As briefly mentioned in Section 1.2.1., each primary cortical area is spatially organised into a topographic map. For vision, retinotopy can be used to map visual input to the specific location of neurons in V1. Therefore, Murray et al (2006) used retinotopy to find that the region of V1 which retinotopically represented the two balls was larger for the ball that was *perceived* as being larger, despite the fact they were exactly the same size. Furthermore, Muckli, Kohler, Kriegeskorte, and Singer (2005) presented participants with two blinking squares to display an illusion of apparent motion, and found the region of V1 that retinotopically represented the illusory path of the apparent motion showed a significant response, despite the fact there was no physical stimulus on this path.

Additionally, Lee and Nguyen (2001) displayed Kanizsa illusion figures (see Figure 1.4 above) to monkeys whilst monitoring cell responses in V1 and secondary visual area V2. Remarkably, they found neural responses to the illusory contours of the edges of the Kanizsa illusion in both V1 and V2. Other research has also found neuronal responses to the illusory contours of the Kanizsa illusion in visual cortex (Von Der Heydt, Peterhans, & Baumgartner, 1984). Taken together, this research strongly indicates V1 does not merely process the raw visual information present in the outside world. This research therefore challenges the conventional feedforward models of information processing.

Whilst contextual influences on perception have been well documented within the field of vision, we can assume that similar mechanisms can be applied to the other primary sensory cortices. This is due to the uniformity of feedforward, feedback, and lateral pathways across all areas of cortex (Edelman & Mountcastle, 1978). Indeed, despite receiving less attention in the literature, research has found neural evidence for contextual influences in A1. For example, researchers have used fMRI to find activity in A1 reflects a perceived continuity of illusory tones in noise, meaning even if the stimuli were acoustically identical yet were perceived differently, activity in A1 reflected the *perceived* difference (Riecke, Van Opstal, Goebel, & Formisano, 2007). Neural evidence for such contextual effects has also been found in S1. For example, in the cutaneous rabbit illusion (Geldard & Sherrick, 1972), repetitive presentations of brief stimulation at two or more points on the skin can lead to the illusion that areas on the skin situated between the physical stimulation points have been stimulated. Using this illusion in an fMRI study, researchers found activation in S1 at the somatotopic location corresponding to the illusory perception of stimulation on the skin (Blankenburg, Ruff, Deichmann, Rees, & Driver, 2006). Similar effects have also been found in S1 using optical imaging (L. M. Chen, Friedman, & Roe, 2003). Once again, this research demonstrates how the primary sensory cortices must process more than the raw sensory input entering the brain from the external environment.

As such, updated models which account for the role of feedforward, feedback, and lateral pathways in shaping the neural processes even in primary sensory cortices provide a more accurate representation of cortex function. They offer a convincing argument for how context and prior experience can shape information processing in the brain (see Heeger, 2017). Specifically, these models

recognise the importance of the different neuron populations in the layered structure of the cortex, which group together based on similarities in connections and functions to form six basic layers (Ramachandran, 2002); layer I being the most superficial layer (see Figure 1.5). Layer IV is known to be the main receiving layer of cortex, which receives the most input from both thalamic afferents and other cortical structures, mainly consisting of neurons known as stellate cells. On the other hand, layer V provides the main output of the cortex, consisting of large pyramidal neurons which project information to other areas of the brain via long, thick axons (Mumford, 1992; Ramachandran, 2002).

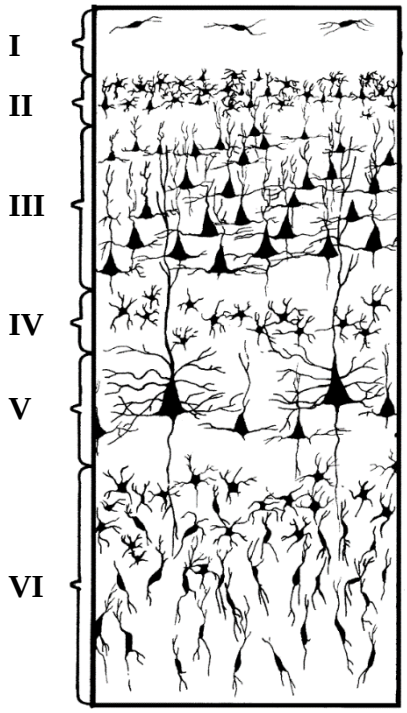

Figure 1.5: Neural populations in the six layers of the cerebral cortex. Layer I is the most superficial layer. Note the stellate cells in layer IV and the pyramidal cells in layer V, the main neurons which receive and project information from and to other areas of cortex respectively. Taken from Ramachandran (2002).

The functional relevance of the laminar organisation of the six layers of cortex was notably studied in the visual system by Rockland and Pandya (1979), who found that visual input travelling through the cortex along the renowned feedforward pathway from the thalamus terminated in layer IV of the corresponding primary cortical area (V1). Since they found layer IV is where the bulk of thalamic afferents terminate, they proposed a highly developed layer IV is a sure indication of

a primary sensory cortical area. This has since been further confirmed in subsequent research (Felleman & Van Essen, 1991), with further work recognizing any given primary cortical area (e.g. V1, A1, and S1) can typically be identified by a mass of densely packed cells in layer IV of cortex (Mesulam, 1998). Rockland and Pandya (1979) also discovered information passing up the cortical hierarchy originated from neurons in layers III and V from a low-level cortical area, terminating in layer IV of the next higher-level cortical region. Finally, they discovered reciprocal connections sent information from high-level visual areas back down the cortical hierarchy towards primary visual area V1. This information flow tended to originate from neurons in the deeper layers such as V and VI of the high-level cortical areas, terminating in layer I of the next area going back down the cortical hierarchy toward primary visual area V1, avoiding layer IV altogether (see also Felleman & Van Essen, 1991). As such, it is clear that the different layers of cortex have a functional purpose in transmitting information up and down the cortical hierarchy. Specifically, this research provides direct neural evidence for exactly how both feedforward and feedback neural pathways in the brain play different fundamental functional roles in shaping the responses of the primary cortical areas, such as V1.

Drawing back upon the empirical research which has investigated the influence of contextual information in the primary cortical areas, Lee and Nguyen (2001) not only found neural responses to the illusory contours of the edges of the Kanizsa illusion in both V1 and V2 (see above), but specifically they found such responses in the *superficial* layers of such regions, thus suggesting high-level areas sent this contextual information back down the cortical hierarchy to V1 via a feedback pathway. Furthermore, subsequent research has found merely 10 per cent of the input to layer IV neurons of primary visual area V1 arise from thalamic afferents (Masland & Martin, 2007), which therefore suggests the remaining input to a given V1 neuron derives from intracortical neurons, or neurons located in distal areas of cortex, via feedback and lateral connections. Since this research suggests feedback and lateral connections to V1 outweigh feedforward connections by over half, this lead researchers to later believe feedforward stimulus driven information is actually a minor task of the cortex (Muckli, 2010), with most activity, even in the primary sensory cortices, being controlled for by contextual influences via feedback or lateral neural pathways in the brain.

Further empirical research has investigated the role of feedback pathways in shaping neural responses in primary cortical regions, such as that of Smith and Muckli (2010), who were particularly interested in the role of feedback pathways when presented with visual stimuli under more natural viewing conditions. In an fMRI experiment, participants were presented with different images of natural visual scenes, in which the lower right quadrant of each scene was occluded from view. Smith and Muckli found that discriminable patterns of information relating to the different scenes could be read out from the region of early visual cortex which retinotopically represented the occluded quadrant of each scene. As this discriminable information was based on activity patterns alone in regions with missing feedforward input, this indicates early visual cortex must have received content-specific information inferred from the context of each scene, supposedly through cortical feedback from high-level areas. This was further supported with a control condition whereby no occlusion was present when viewing the natural scenes. The researchers used cross-classification methods to find that the region of early visual cortex representing the occluded quadrant contained similar patterns of brain activity when stimulated either through feedforward or feedback conditions (see also Muckli & Petro, 2013). Furthermore, this experiment was replicated using 7-Tesla fMRI to enable layer-specific analysis, to find that whilst the control condition of the entire scene produced discriminable patterns of information about each scene in all layers of V1, representations for the partial occlusion conditions were only discriminable in the outer superficial layers (e.g. layers I and II; Muckli et al., 2015). These are the cortical layers that are expected to receive information through cortical feedback (Lee & Mumford, 2003). Overall, the findings thus suggest that non-stimulated regions of V1 contain information about the surrounding visual context, which is also related to the information projected from stimulus driven vision along the renowned feedforward pathway. Other research has also found such context effects in V1 (see Muckli, Kohler, Kriegeskorte, & Singer, 2005; Murray, Boyaci, & Kersten, 2006), further supporting the idea that feedback connections play a critical role in information processing in the primary sensory cortices.

As introduced above, high spatial resolution neuroimaging at 7-Tesla enables segregation of the different layers of cortex, which is becoming an increasingly popular technique for investigating the laminar architecture of feedforward and feedback connections in the cortex. Whilst the studies described to this point have

focused mainly on the visual system (due to vision being the most studied sense), research has also used 7-Tesla fMRI to investigate the laminar architecture of primary cortical areas A1 and S1. For example, 7-Tesla fMRI has been used to examine the columnar organisation of the processing of sound frequency in A1 (De Martino et al., 2015). Furthermore, tactile thalamic input has also been found to terminate in layer IV of S1 (Thomson, 2003), with recent research also demonstrating how the different layers of S1 contain different neuron types with distinct feedforward inputs and feedback projections (Palomero-Gallagher & Zilles, 2019). Whilst the laminar architecture of specific feedforward and feedback processes in S1 has been less studied, recent research has begun to investigate this further. For example, feedforward tactile input has recently been found to preferentially activate the middle layers of S1, whilst expectation of a tactile sensation has been found to evoke activity in superficial and deep layers of S1 (Yu et al., 2019). Taken together, this research further validates the different roles of the six cortical layers for processing sensory feedforward and feedback signals in the primary sensory cortices, thus emphasizing the functional importance of the laminar architecture of the human cerebral cortex and how context can influence processing in the primary cortical areas.

1.3. Multisensory processing across the primary sensory modalities

The multitude of research discussed on cortex function to this point has focused on how sensory input belonging to one independent sensory modality, such as vision, is processed in the human brain. However, when experiencing an event in the real world, it is rare that any one sense would ever operate independently at any given time. For example, typing on a keyboard constitutes an integration of visual, tactile and auditory sensory components. As such, it is important to understand how the brain processes and integrates information from multiple sensory sources at the same time. Furthermore, whilst the sensory representations of an event such as typing on a keyboard would typically be thought to be constructed in multiple individual primary cortical regions (e.g. V1, S1, and A1), it is likely that the brain could form associative links between these senses through experience. Therefore, one could expect that context and prior experience can not only shape processing *within* a sensory modality (see for example Smith & Muckli, 2010; discussed in

detail above), but also *across* modality connections. In this section, classic multisensory studies investigating how the brain integrates multisensory information, along with research that has revealed the influence of one sense on another, will be introduced. This section will proceed to discuss how the wiring between the senses can exhibit neuroplastic changes based on experience and reform following sensory deprivation. Finally, more recent ground-breaking research will be reviewed which has revealed even the primary sensory cortices of the human brain are not only influenced by context within a sensory modality, but can receive contextual influences cross-modally from other independent sensory sources.

1.3.1. Classic studies investigating multisensory processing in the cortex.

Investigating exactly how and where the human brain converges information from independent sensory inputs is essential for understanding cortex function. A celebrated review by Ghazanfar and Schroeder (2006) suggested certain high-level association brain areas, such as the superior temporal sulcus (STS) region, the posterior parietal cortex (PPC), pre-motor cortex (PMC), and areas located within frontal and prefrontal cortices, may receive input from several senses, in turn forming multisensory 'hubs' in the brain. For example, Jones and Powell (1970) discovered each primary sensory cortical area in the brain of the Rhesus monkey contained neural connections to STS and orbito-frontal cortex, classifying such areas as multisensory convergence zones. Furthermore, the superior temporal polysensory (STP) area of the Macaque brain has been found to respond to somatosensory, auditory, and visual stimulation (Bruce, Desimone, & Gross, 1981; Falchier, Clavagnier, Barone, & Kennedy, 2002; Hikosaka, Iwai, Saito, & Tanaka, 1988). As a compliment to the animal studies, Beauchamp (2005) conducted a review of neuroimaging studies which demonstrate multisensory convergence in the lateral occipito-temporal cortex in humans, suggesting this area may be functionally equivalent to the STP areas observed in animal studies. For example, the lateral occipital complex in humans is preferentially activated in response to visual and tactile stimuli (Beauchamp, 2005). Furthermore, an area in human posterior STS has been found to respond to visual, auditory, and somatosensory stimulation (Beauchamp, Yasar, Frye, & Ro, 2008). These areas have all hence been suggested to be cortical regions that converge sensory information from multiple modalities.

Since the multisensory convergence zones identified above are high-level regions, it was generally assumed that convergence of multisensory information occurred only after the primary cortical areas had processed the individual types of sensory input in the corresponding unisensory modality (see for example Massaro, 1999). However, research using electroencephalography (EEG) to investigate the timing of the neural responses to both uni- and multi-sensory stimuli can provide further insight as to at what stage each type of information is likely to be processed in the brain. For example, a study by Giard and Peronnet (1999) found neural responses to a combination of multisensory audio-visual stimuli as early as when either the audio, or the visual, unisensory stimuli were presented alone (all around 40ms post-stimulus), suggesting multimodal information interacts very early in the sensory processing chain. This was further corroborated at a later date, whereby Molholm et al. (2002) found neural responses to audio-visual stimuli were virtually simultaneous to the first neural responses from independent sensory information.

Therefore, another argument outlined in a review by Driver and Noesselt (2008) is that multisensory convergence may occur earlier in the cortical hierarchy than previously thought. For example, Wallace, Ramachandran, and Stein (2004) studied the anatomy of the rat brain to find overlapping cortical areas at the borders between the sensory-specific domains that contained a mixture of neurons representing each individual bordering region, in addition to multisensory neurons that represented the convergence of the overlapping modalities. They suggested such regions not only represent both independent sensory modalities, but may also play important roles in the brains ability to integrate multisensory information. Wallace et al. (2004) mention the pathway of information processing to these transitional areas is yet to be determined, however they suggest the zones may be formed by the convergence of sensory-specific nuclei sent from the thalamus. Therefore, it is possible that multisensory information enters these areas earlier in the cortical hierarchy than the high-level multisensory convergence zones mentioned previously, with such zones existing adjacent to each low-level sensory-specific area.

In fact, research has remarkably found multisensory convergence can occur even in the early sensory areas of the brain; regions which are traditionally considered to be unisensory (for extensive reviews see Driver & Noesselt, 2008; Ghazanfar & Schroeder, 2006; Kayser & Logothetis, 2007; Macaluso & Driver, 2005). For example, Calvert (1997) found linguistic visual cues and silent speech-

like movements activated auditory cortical areas in an fMRI experiment. This was found in the absence of actual auditory input, thus showing that traditional 'unisensory' cortical areas can be influenced from other sensory modalities based on information presented via an entirely independent sensory source. Further work has also used fMRI on the Macaque monkey to find responses to visual (Kayser & Logothetis, 2007) or tactile (Fu et al., 2003; Kayser, Petkov, Augath, & Logothetis, 2005) stimuli in and around A1. Similar effects have also been observed in visual cortices, whereby McIntosh, Cabeza, and Lobaugh (1998) found learned associations between an auditory and visual stimulus resulted in occipital activity when the auditory stimulus was subsequently presented in isolation. In somatosensory cortex, neurons have been found to activate in response to visual (Zhou & Fuster, 1997, 2000) and auditory (Zhou & Fuster, 2004) cues if they are associated with tactile information. Finally, Liang, Mouraux, Hu, and Iannetti (2013) presented participants with visual, auditory, and tactile stimuli in an fMRI study and found the pattern elicited in response to each type of sensory stimulus was discriminable in any primary cortical area. For example, S1 could discriminate between the unique signatures of a visual or an auditory stimulus, in addition to a tactile stimulus. Taken together, this research shows how multisensory integration can occur even in the primary sensory regions of cortex.

The fact research has found multisensory information is present even in the primary sensory cortices of the brain may be a result of information being sent from high-level multisensory convergence zones back down to the primary cortical areas via feedback pathways (see for example Stein, Meredith, & Wallace, 1993). However, another alternative to how this occurs was discussed in a review by Driver and Noesselt (2008), whereby research has suggested direct neural connections may exist between the unisensory modalities. For example, animal studies have found direct cortico-cortical connections from primary auditory to primary visual cortex (Falchier et al., 2002), between primary auditory and primary somatosensory cortex (Budinger, Laszcz, Lison, Scheich, & Ohl, 2008; Henschke, Noesselt, Scheich, & Budinger, 2015), and from visual areas towards areas of primary somatosensory cortex (Cappe & Barone, 2005). In studies such as that by Cappe and Barone, they found information processing along these direct connections can follow either a feedforward or feedback profile, thus arguing against a cortical hierarchy of information processing in the brain in this case. However, Driver and Noesselt note

that such direct neural connections are relatively sparse in comparison to the feedback connections that send information from multisensory convergence zones such as STS to primary sensory cortices. As such, it is unlikely that direct cortico-cortical pathways are a dominant pathway of multisensory convergence in the brain.

1.3.2. Neural plasticity of multisensory processing, and the neuroplastic effects of sensory deprivation.

Understanding the neural pathways for multisensory processing in the brain leads to an interest in how specific experiences may cause neuroplastic changes in and between such underlying cortical brain structures; also known as neural plasticity. Neural plasticity is the ability for the brain to reorganise itself in terms of its functional or structural properties in response to a given event, or a set of events (Huttenlocher, 2002). This can be a learned change, for example, animal studies have revealed multisensory integration improves with maturation, whereby multisensory neurons are unable to synthesize cross-modal information received in early life, with all sensory-responsive neurons being unimodal during early postnatal stages (Stein, Perrault Jr, Stanford, & Rowland, 2009; Wallace, Carriere, Perrault, Vaughan, & Stein, 2006; Wallace & Stein, 1997). Furthermore, Xu, Yu, Rowland, Stanford, and Stein (2014) found neurons in the superior colliculus of cats that were deprived from co-activated visual and auditory experiences could not engage in typical multisensory integration. More recently, research has found a sensory cortex can even rewire specific aspects of the corresponding sense. Studying S1 activity in foot artists who were born without arms, Dempsey-Jones, Wesselink, Friedman, and Makin (2019) found an organised topographic map of the toes in S1 in the specific area which would be typical of a map of the fingers in a control population. Overall, this suggests sensory processing is not hardwired, but rather cross-modal connections are continuously being generated and updated through experience with the world (see also Hebb, 1949; Paraskevopoulos & Herholz, 2013; Paraskevopoulos, Kuchenbuch, Herholz, & Pantev, 2012).

Furthermore, neural plasticity can also occur when a person has undergone sensory deprivation. Unlike traditionally thought, research has found deprivation of a sensory modality (such as deafness and/or blindness) can result in reorganisation of the neural circuitry in the brain (for reviews, see Collignon, Champoux, Voss, &

Lepore, 2011; Collignon, Voss, Lassonde, & Lepore, 2009; Frasnelli, Collignon, Voss, & Lepore, 2011). This can result in a strengthening of nerve impulses in a non-deprived modality, such as an enhanced tonotopic map found in auditory cortex in blind individuals (Elbert et al., 2002). Interestingly, research has also found *cross*-modal changes in areas of cortex which are sensory-deprived. Cross-modal plasticity occurs when neurons or brain regions that would have typically processed a certain type of sensory information (e.g. visual regions process visual information) can adapt to process a completely different kind of sensory information when the person has undergone sensory deprivation to that modality. For example, Sadato et al. (1996) used positron emission tomography (PET) to find activation in V1 during tactile discrimination tasks for blind braille readers when compared to sighted controls. Other research has found activation in V1 in response to auditory change detections in blind individuals (Kujala et al., 2005). Furthermore, when investigating participants who were deaf, Finney, Fine, and Dobkins (2001) found visually evoked activity in auditory brain regions when compared to hearing controls. Together this research suggests neuronal wiring between the sensory areas in the brain is experience-dependent and not hard-wired.

In terms of the neural mechanisms underlying how sensory information can be sent cross-modally after sensory deprivation, it is generally thought to be due to how the synapses are wired in the brain from birth. As explained in a review by Collignon et al. (2009), initial synaptic connections in early life are primarily arbitrary and can consist of connections between multiple senses. For example, from audition to visual cortex in the cat brain (Innocenti & Clarke, 1984). However, following Hebb's (1949) law of plasticity, it is thought the subsequent synaptic pruning phase eliminates any unused connections and causes certain areas to be specialised for different functions, thus eradicating connections such as those between vision and audition (Changeux, Courrpge, & Danchin, 1973). Interestingly, however, such connections between audition and vision in the cat cortex have been found to remain intact if they are visually deprived from birth (Berman, 1991). This is thought to be because auditory input is no longer in competition with visual inputs during the synaptic stabilisation phase, thus the connections do not undergo synaptic pruning. However, this theory posits that redundant connections do not escape the critical period of synaptic pruning, therefore, it does not account for why cross-modal connections still exist in people who have experienced sensory deprivation

after the synaptic pruning phase, nor does this account for why we can find sensory information can be sent cross-modally in healthy participants. Furthermore, the research discussed in Section 1.3.1. above which found direct neural connections between primary sensory cortices (see e.g. Budinger et al., 2008; Cappe & Barone, 2005; Falchier et al., 2002; Henschke et al., 2015) further suggests not all connections are pruned early in life despite the supposed lack of functional significance behind it.

Other theories therefore suggest that cross-modal connections are rather silenced yet remain intact, and the cross-modal plasticity observed in late blindness may be a result of these redundant connections increasing in strength and essentially becoming reactivated upon sensory deprivation (Collignon et al., 2009). For example, a study by Klinge, Eippert, Röder, and Büchel (2010) found stronger cortico-cortical connections between A1 and V1 in blind participants compared to those who were sighted. However, crucially, this research revealed such connections do exist, yet are weakened, in the typically functioning human brain relative to blind individuals. This may explain why we can see cross-modal effects even in the typically functioning brain in people who have not undergone any type of sensory loss. The idea here is that the connections are not pruned entirely, but rather weakened and then brought back to strength following sensory deprivation (Collignon et al., 2009). Furthermore, a review by Bavelier and Neville (2002) also suggests polymodal association areas, such as the superior colliculus, become reorganised following sensory deprivation, whereby there is an increase in the number of neurons that respond to the sensory areas that remain intact. As such, Karlen, Kahn, and Krubitzer (2006) suggest it may be a combination of cortico-cortical connections and connections to polysensory subcortical areas which are modified following sensory deprivation.

1.3.3. Unisensory areas contain content-specific information from other sensory modalities.

Whilst it has been known for some time that the primary sensory cortices can receive sensory information traditionally belonging to other primary sensory modalities (see Section 1.3.1. above for a review), especially when a person has undergone sensory deprivation (see Section 1.3.2. above), it is only within the last

decade that research has examined the specific content of the information which can be sent cross-modally (for a review, see Meyer & Damasio, 2009). This is an interesting avenue of research for the reason that if two sensory modalities are often stimulated simultaneously, experience-based neural plasticity should mean a stimulus presented in one modality could evoke *specific* traces of activity in the primary sensory cortex of an entirely independent sensory region, providing the stimulus implies features representative of that sensory modality (see Figure 1.6 for a visual diagram of this theory). This has already been found in terms of the neural response - for example, as discussed in Section 1.3.1., Zhou and Fuster found neurons in somatosensory cortex activate in response to visual (Zhou & Fuster, 1997, 2000) and auditory (Zhou & Fuster, 2004) cues if they are associated with tactile information. However, what has not been shown from this previous research is whether the specific content of this information can be discriminated within the primary cortical area which is independent to that of stimulus presentation. A popular method for investigating the content of cross-modal information is to use multi-voxel pattern analysis (MVPA); an analysis technique used mainly in fMRI to examine whether distributed patterns of activity across multiple voxels are statistically discriminable across different stimulus conditions (Davis et al., 2014; Norman, Polyn, Detre, & Haxby, 2006).

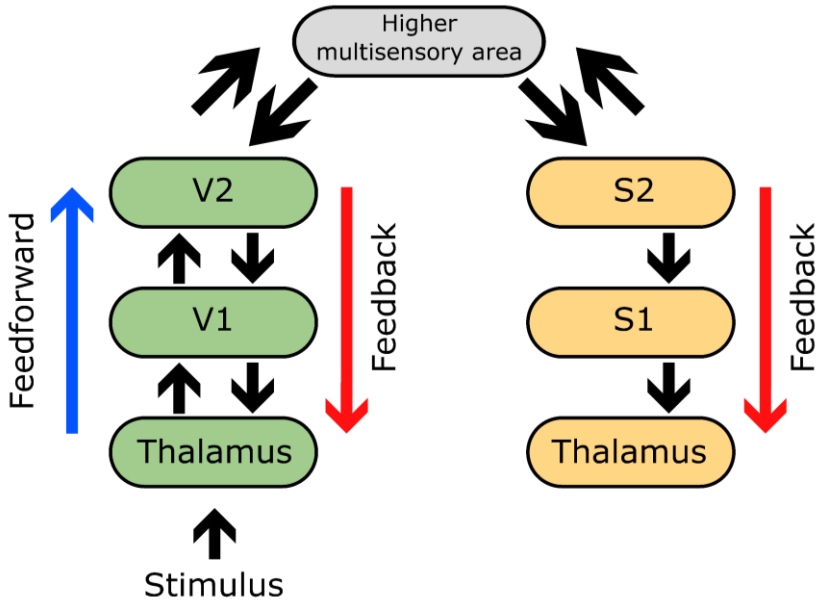

Figure 1.6: A diagram to visually represent how sensory input belonging to one sensory modality (e.g. a visual stimulus) could send information back to the primary cortical area of an entirely independent sensory modality (e.g. S1), providing the visual input implies features representative of the independent modality.

Research over the past decade has indeed found information in a primary sensory cortical area that is independent to the source of stimulus presentation can be reliably discriminated. For example, in an fMRI experiment by Meyer et al. (2010), participants simply viewed different silent yet sound implying video clips (e.g. silent animal calls or musical instruments), and MVPA was used to find each video clip could be significantly discriminated based on the patterns of activity elicited in A1 alone. This suggests content-specific activity was transmitted to A1 even in the absence of external auditory stimulation, supposedly through experience-based plasticity wiring the two modalities together in the brain. In a later study, Meyer, Kaplan, Essex, Damasio, and Damasio (2011) also showed participants different video clips conveying object interactions with the hands (e.g. hands exploring a tennis ball or a light bulb), and found MVPA could significantly discriminate between the different videos by looking at patterns of activity in S1. This suggests information regarding the tactile properties of the objects was sent to S1 in the absence of any external tactile stimulation, again supposedly through associative links between the two areas formed from prior experience of interacting with the objects.

Furthermore, Vetter, Smith, and Muckli (2014) investigated whether content-specific activity could be discriminated in V1 in the absence of external visual stimulation when presenting participants with only the sounds of different rich visual scenes (e.g. the sound of traffic noise, or a rainforest). An interesting aspect of this study was that the researchers also tested whether content-specific activity could be decoded in such areas when the information originated from imagery rather than a stimulus entering the brain from the external environment. They showed that the content of both the sound and imagery of rich visual scenes could be decoded in early visual cortex. This finding is noteworthy, since this provides converging evidence that abstract information implying visual features can be fed back from high-level areas to early visual cortex, which is comparable across auditory or imagery exemplars, thus providing evidence that such information may be category specific rather than stimulus specific. Specifically, Vetter et al. found such discriminable information within the regions which retinotopically represented the *periphery* of visual space, particularly in the far periphery for the auditory stimuli. This is important since previous research has found evidence for direct connections between auditory and visual cortex in the peripheral regions of primary sensory

cortices (e.g. Cate et al., 2009). This may mean peripheral areas of early sensory regions receive the information as a prime for soon-to-appear objects in the visual field, and suggests different areas of V1, specifically peripheral areas, are specialised in receiving feedback information from auditory cortex. A final noteworthy finding from this study is the fact that whole brain searchlight analysis revealed high-level multisensory areas such as posterior STS may be multisensory relay stations in the brain which feedback information to early visual cortex, thus supporting the research mentioned in Section 1.3.1. above which suggests such areas are multisensory convergence zones.

The research discussed in this section until now suggests content-specific information presented via one sense can be sent across to non-stimulated primary sensory modalities, however it does not prove whether prior experience with the stimuli is necessary for successful discrimination. Therefore, the first known study to address the question of whether familiarity is necessary for cross-modal context effects was conducted by Smith and Goodale (2015). In their study, they showed participants still images of three different familiar object categories (wine glasses, mobile phones, or apples), in addition to three unfamiliar object categories (cubies, smoothies, and spikies; Op de Beeck, Torfs, & Wagemans, 2008). Using pattern classification techniques, they found discriminable patterns of information in S1 *only* for the familiar visual object categories, which strongly suggests such cross-modal connections require a high degree of experience with the object, since the artificial objects did not produce comparable effects. Additionally, they were able to find similar patterns of activation across multiple exemplars of the same stimulus. For example, three exemplars of a wine glass all produced statistically similar patterns of activation. This finding is important, since it strongly supports the idea that high-level cortical areas transmit content-specific information about stimulus categories as a whole to other primary sensory cortices, as opposed to simply transmitting fine-grained sensory properties about any familiar stimulus without discriminating the unique tactile properties associated with each individual stimulus. Additionally, whole brain searchlight analysis revealed decoding in high-level areas within the parietal lobe, such as the superior parietal lobule, which have previously been suggested to be involved in multimodal integration (Hsiao, 2008), thus further supporting the idea of such high-level areas being multisensory relay stations for transmitting sensory information cross-modally.

Whilst this research has found discriminable patterns of activity in a primary sensory cortex independent to that of stimulus presentation, the underlying theory as to why such cross-modal effects exist remains unclear. Furthermore, this research has not examined cross-modal effects between all pairs of sensory modalities, such as the potential cross-modal links between audition and touch. Therefore, it would be interesting to investigate whether the dominant sense of vision (Colavita, 1974; Mumford, 1991) is needed in order to observe these cross-modal effects. Additionally, given this is a relatively novel area of study, this research has only examined such effects using 3-Tesla fMRI. Therefore, interesting avenues for future research to pursue could use 7-Tesla fMRI to examine the underlying laminar architecture of these cross-modal effects to further understand the role of different feedforward and feedback pathways in shaping these responses in the primary sensory cortices. Therefore, much research is still needed to understand why these cross-modal context effects exist even in the primary sensory cortical areas of the human brain.

1.4. Theories to explain cross-modal processing in unisensory cortical areas

The literature discussed to this point has revealed neurons even in the primary sensory cortical areas can receive input not only via neural connections projecting stimulus-related information via feedforward pathways (e.g. Lamme et al., 1998), but also via feedback and lateral connections which convey contextual information. These feedback and lateral pathways can shape information processing both within a sensory modality (e.g. the context of different visual scenes can be discriminated in non-stimulated regions of early visual cortex; Smith & Muckli, 2010), and via feedback *across* modality connections (e.g. the tactile content of different familiar visual objects can be discriminated in early somatosensory cortex; Smith & Goodale, 2015). The uniform structure of these bi-directional connections across the entire cortex (Felleman & Van Essen, 1991; Maunsell & Van Essen, 1983) suggests a common computation to the function of the brain must be at work here. Therefore, the key theoretical frameworks which help to explain how and why context may shape processing in the primary sensory cortical areas will now be reviewed, with reference to Bayesian inference and predictive coding.

1.4.1. Bayesian inference.

Bayesian inference is a powerful statistical formula that is used to predict the likelihood of a given hypothesis by assigning probabilities based on all available information previously stored about the hypothesis. The weights of these probabilities can be updated when given new information, and this formula is an increasingly popular theory for understanding how the human brain functions. Theories about the Bayesian brain propose the brain has an internal model of the world, whereby incoming sensory information is represented in the brain by computing the likelihood of how such information should be encoded based on prior experience with the situation; it suggests the brain actively constructs an explanation for understanding the world that it is in. When receiving new information which was not previously stored, it is thought that the brain can use Bayesian statistics to store the information in its internal model in the most statistically optimal way, thus the model can be continuously updated based on our experiences with the world. This entire process is called Bayesian inference (Brenner, 2015). Lee and Mumford (2003) assigned Bayesian theories to information processing in visual cortex. They suggested the feedforward and feedback connections in the brain implement Bayesian inference in the visual processing hierarchy, whereby high-level visual areas guide low-level visual areas to aid sensory processing. The idea here is that the brain will find the most optimal way to integrate bottom-up sensory signals with top-down expectations based on prior experience.

Many years of classic work by Friston (2005, 2009, 2010, 2012) further proposes a unified brain theory building on Bayesian inference, suggesting the brain minimises free energy, or the “surprise”, of the internal models of probabilities generated. This means the brain not only computes probabilities about what is likely to happen, but also minimises the states that are unlikely, thus maximising the accuracy of our perceptual representations.

Much empirical research supports the theory that the brain is Bayesian, dating back to behavioural work such as that of Palmer (1975), who found objects can be perceived faster when preceded by an appropriate context. This means a visual stimulus was more readily perceived when the outcome matched what would typically be expected, based on prior experience. This research therefore suggests prior experiences with a certain event may be combined with feedforward sensory

visual input in a statistically optimal way to produce expectations and probabilities about the likely outcome. Furthermore, research has used a visual contrast detection task to find the higher the probability of a visual event occurring, the increased likelihood of reporting the presence of a visual signal (Wyart, Nobre, & Summerfield, 2012), or used pattern classification to find more weight assigned to expected visual input in visual cortex (Kok, Jehee, & de Lange, 2012). This research suggests prior expectations of visual input can influence bottom-up sensory processing, thus integrating both types of information in a statistically optimal way.

Whilst the studies discussed above are predominantly focused on Bayesian processing within an independent sensory area (e.g. visual cortex), it is important to note, as mentioned previously, that the brain constantly receives input from multiple independent sensory sources in the real world. Therefore, Bayesian statistics can also be used to help explain how the brain can integrate multiple sensory signals and determine whether such signals belong to the same or different events (Kording et al., 2007; Rohe & Noppeney, 2015). Bayesian theories suggest the brain combines the noisy information from independent senses and makes probabilistic assumptions of a common source (Kayser & Shams, 2015). For example, when hearing and seeing a person speaking (whereby vision and audition comprise independent sensory information), the brain can make probabilistic assumptions as to whether the auditory and visual input belong to the same person (the common source).

A classic study investigating Bayesian inference for multisensory processing across the two senses of vision and touch was conducted by Ernst and Banks (2002), who proposed the brain uses a rule of maximum-likelihood estimation, since they found visual and haptic information is integrated in the brain in a statistically optimal fashion. In their research, they first determined participants' reliability of discriminating the size of an object based on either visual or haptic information alone. Crucially, Ernst and Banks manipulated the reliability of discriminating the visual stimulus by adding noise to the visual display. The participants' discrimination reliability was then used to make Bayesian predictions about the amount of weight which would likely be given to visual or tactile information *alone*, when asked to determine the size of an object when conducting a multisensory discrimination task of visual and haptic information *combined*. They found the more visual noise added to the multisensory discrimination task, the more weight of probability was added to the haptic dimension. This study suggests the human brain

optimally weights signals arriving from independent sensory modalities according to Bayesian inference, since more weight was applied to the haptic domain when the visual domain was compromised.

Further research has explored the underlying neural mechanisms of Bayesian inference by suggesting the brain integrates sensory signals from a common source whilst segregating sensory information from independent sources via a neural hierarchy of multisensory processing in the brain (Rohe, Ehlis, & Noppeney, 2019; Rohe & Noppeney, 2015, 2016). This series of research has used various multisensory Bayesian modelling with cross-validation procedures to demonstrate that only high-level cortical regions integrate sensory signals from a common source, with the highest-level regions taking in to account the uncertainty of a signal based on Bayesian inference. On the other hand, the low-level primary cortical areas represent the segregation of signals from independent sources. Taken together, this series of research has provided insight into the differing computational operations across the cortical hierarchy during multisensory interactions.

Finally, Bayesian theories together with Friston's (2005, 2009, 2010, 2012) free energy principle can also explain the reason behind the plasticity of the neural connections between the sensory areas in the brain. As mentioned in Section 1.3.2., the brain can alter neural connections between brain areas based on experience. For example, two neurons that fire consistently will eventually develop a stronger connection compared to two neurons which rarely fire together (Hebb, 1949). In line with Bayesian theories and the free energy principle, if a given neuron is stimulated via one sense, such as vision, and that neuron expects another neuron in an entirely independent region to respond, such as a neuron in S1, and this expectation is met, the connection between the two areas should be increased. Conversely, if the expectation is wrong and the neuron in S1 does not respond, the strength of the connection would be reduced in order to minimise the free energy of the unexpected stimulus (Friston, 2010; Friston & Stephan, 2007; Huang, 2008).

Overall, Bayesian inference theories provide a robust explanation as to how multisensory integration may occur in the brain based on rules of probability. The theory acknowledges the fact that feedforward, feedback, and lateral pathways all contribute to sensory processing, and suggests probabilistic inference is generated based on the feedforward observations together with the contextual information sent via feedback or lateral pathways. However, Aitchison and Lengyel (2017) note that

whilst Bayesian inference provides a strong statistical method for how predictions are computed in the brain based on probabilities, it fails to specify the underlying neural computation of such predictions. Furthermore, as mentioned in a review by Friston (2012), Bayesian inference is only a description of optimal behaviour, and does not propose *how* the brain optimises events such as perception or multisensory integration under conditions of uncertainty. As such, the predictive coding theory will now be introduced, which provides one very prominent explanation for how Bayesian inference applies to human brain function at a computational level.

1.4.2. Predictive coding.

The theory of predictive coding is an increasingly popular framework in cognitive neuroscience which helps to explain *how* Bayesian inference can be implemented in the human brain in a neurally plausible manner. The key principle of predictive coding states that the brain builds internal models about the world, and generates predictions about likely upcoming events based on prior experience and the current context, continuously testing these predictions against what actually happened in real time (de Lange, Heilbron, & Kok, 2018). In relation to the primary sensory cortical areas, predictive coding suggests these areas are continuously making low-level predictions about what they will expect to see, feel, or hear, during any given situation, based on all previous experiences with the situation (for a review, see Clark, 2013). With this in mind, the idea is that the brain actively generates expectations and predictions to help shape sensory processing, as opposed to passively registering the sensory information entering the brain from the outside world (Clark, 2013; de Lange et al., 2018; Kok et al., 2012). It is theorised that the predictions that the brain generates can be updated using rules of probability in a Bayesian manner (Friston, 2009). Although theories of prediction had been hypothesised for a while (Mumford, 1991, 1992), researchers in more recent years have further organised these hypothesised ideas into one coherent theoretical predictive coding framework (for a review, see Kok & De Lange, 2015).

To explain in more detail, the framework suggests each cortical brain region contains two neuronal populations: prediction units, and prediction error units. Whilst prediction units represent the hypothesis best explained by incoming sensory information, prediction error units represent any unexplained sensory input, hence,

the difference between the actual input and the predicted input (Kok, 2016). Kok and De Lange (2015) suggest it is these prediction error units that project up the cortical hierarchy, whereby the next high-level region receives this error unit and finds a new hypothesis that best explains the input it has received. This high-level region then sends the new prediction back down to the low-level region, which compares the prediction to the low-level region's hypothesis. Any further mismatch represents another prediction error, which is sent back up the cortical hierarchy for the high-level region to match it to a new hypothesis. This efficient recurrent cycle of hierarchical cortical processing continues until all prediction error units cease to fire, and a reconstructed, precise, and current version of the world is represented. In sum, the key idea is that any given cortical area is actively building an internal model of the likely forthcoming stimulation, and is continuously comparing this expectation with the actual sensory input received until all information is explained. Figure 1.7 provides a visual diagram of this cortical processing hierarchy.

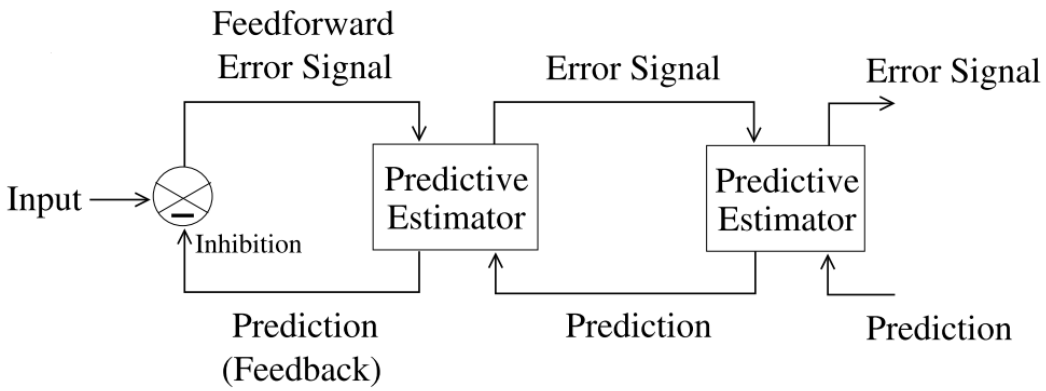

Figure 1.7: A diagram to visually represent the predictive process that occurs in human cortex. Taken from Rao and Ballard (1999).

This hierarchical prediction cycle, as stated by Kok and De Lange (2015), is suggested to have two main functions in the brain. First, prediction errors allow unexpected and potentially highly relevant stimuli to be more salient. Second, a correct prediction enables the neural *representation* of expected stimuli to be enhanced or 'sharpened'. These two functions can be empirically tested with fMRI when measuring the amplitude of the neural response in a given cortical area using univariate analysis, and the representational content of the information in that cortical area using MVPA classification techniques.

In terms of the neural response, cancellation theories suggest we prioritise unexpected events (prediction errors) by suppressing the neural response of expected input (predictions). Indeed, a renowned study by Kok et al. (2012) used a paradigm which manipulated the expectation of viewing certain orientations of different visual gratings in an fMRI scanner. They found that correctly predicted visual gratings resulted in less neural activity in V1. This result agrees with the idea that an accurate prediction leads to a dampened neural response with less firing of prediction errors, whilst unexpected stimuli leads to enhanced neuronal firing of prediction errors, enabling the stimuli to be more salient. Other studies have also found evidence of neural suppression for a correctly predicted event (Alink, Schwiedrzik, Kohler, Singer, & Muckli, 2010; Bays, Flanagan, & Wolpert, 2006; Bays & Wolpert, 2007; Blakemore, Wolpert, & Frith, 1998; Kikuchi et al., 2019; Lee & Mumford, 2003; Limanowski, Sarasso, & Blankenburg, 2018; Murray, Kersten, Olshausen, Schrater, & Woods, 2002; Richter, Ekman, & de Lange, 2018).

Whilst a correctly predicted visual grating resulted in less neural activity in V1, Kok et al. (2012) used MVPA techniques to reveal the *representation* of expected gratings was enhanced in V1, meaning the pattern classifier could better decode an expected compared to an unexpected stimulus (see also Kok & De Lange, 2015). As such, de Lange et al. (2018) alternatively suggest neural suppression for an expected event may not merely be a reflection of a dampened response, but may actually reflect an active 'sharpening' of the underlying representation of the stimulus (see also Friston, 2005; Kok, Mostert, & De Lange, 2017; Lee & Mumford, 2003). Such a theory is in line with Bayesian models that suggest cortical regions may assign more weight on sensory channels to an *expected* event, since this could help to enhance the perception of that event (see also Kaiser, Quek, Cichy, & Peelen, 2019). Indeed, Kok et al. (2012) found the reduced neural amplitude in V1 for an expected visual grating was more suppressed in neurons which preferred the *non*-presented orientation. More recently, a study by Yon, Gilbert, de Lange, and Press (2018) asked participants to perform hand actions in an fMRI scanner whilst viewing an avatar hand which would simultaneously execute an action that was either congruent or incongruent with the hand action they physically made. Results found congruent visual stimuli were better decoded in occipital cortical regions, which was complimented by a suppressed neural response only for the voxels tuned *away* from, not towards, the expected visual stimulus. These studies hence suggest that more

weight may actually be added to a predicted event by dampening the response in specific voxels which prefer alternative stimuli (see also Den Ouden, Friston, Daw, McIntosh, & Stephan, 2009; Summerfield & De Lange, 2014). In turn, this suggests a more selective population of neurons tuned to the expected event may be pre-activated in low-level cortical regions *before* the input has even been received, suppressing any unexpected features and resulting in a sharp, accurate representation of the input if the prediction is met (Press, Kok, & Yon, 2020).

The neuronal process by which predictions and prediction errors are transported through the cortical hierarchies ties back in with Section 1.2.2., whereby feedforward and feedback pathways were introduced as having different functional roles in projecting information to and receiving information from the six different layers in the cortex (Rockland & Pandya, 1979). Predictive coding theories explain the functional significance behind feedforward and feedback pathways, in turn providing an explanation as to how information is transmitted amongst the six layers of cortex. As described by Rao and Ballard (1999) when examining encoding of natural images in the visual system, a model of the feedforward pathway suggested prediction errors travel up the visual cortical hierarchy, whereas feedback pathways carry predictions from high-level visual areas back down to the low-level visual regions. Rao and Sejnowski (2002) further suggested prediction errors sent up the cortical hierarchy via such feedforward pathways are sent from superficial layers to middle layer IV of the next cortical region, whereas predictions sent via feedback pathways originate in deep layer neurons. Indeed, more recent work has investigated how predictive processing occurs in the brain using 7-Tesla fMRI to explore feedforward and feedback pathways at the layer-specific level. As mentioned briefly in Section 1.2.2., Yu et al. (2019) used layer-specific fMRI to investigate the laminar architecture of human S1 when participants either physically perceived tactile stimulation, predicted to receive tactile stimulation, or did not expect to receive tactile stimulation. By investigating sensory input and predictive feedback in S1 in this way, they found that sensory tactile input from thalamic afferents along the feedforward pathway preferentially activated middle layers, whereas tasks involving predictive feedback (that is, the participants predicted to receive tactile stimulation, but did not actually receive any stimulation) only engaged the superficial or deep layers of S1. Furthermore, this activation was significantly stronger than a control condition whereby the tactile stimulation was unpredictable. This finding provides

strong evidence for predictive processing at the submillimetre level across the different layers of cortex in S1.

Much additional empirical research has been conducted over the years which supports the theory of predictive coding. For example, Murray, Kersten, Olshausen, Schrater, and Woods (2002) showed participants either coherent or random shapes in an fMRI study, and found that activity in V1 was reduced when participants viewed the coherent shapes compared to the random shapes. This finding agrees with predictive coding theories, since predictive coding would suggest there are less prediction errors in the coherent shape condition due to the fact the information can be explained by high-level areas, thus explaining why there is less neural activity in this case. Furthermore, Alink, Schwiedrzik, Kohler, Singer, and Muckli (2010) used a visual apparent motion paradigm to find that responses to expected flashes based on the spatiotemporal context of the apparent motion pathway resulted in less signal in V1 when compared to an 'unexpected' flash which was not on the path trajectory. This finding is important as the weaker neural responses in V1 can be explained as being due to high-level regions expecting or predicting the input along the apparent pathway, since participants were completely naïve to the fact the intention of the task was to perceive an apparent motion illusion.

Overall, predictive coding theories provide an elegant explanation as to how Bayesian inference is implemented in the human brain at a representational level. The theory suggests the common goal of a given brain area is to minimise prediction errors, which is accomplished via high-level regions sending predictions about the likely upcoming input down the cortical hierarchy to the low-level cortical region in a continuous cycle until all sensory input has been explained. This can hence explain why content-specific information about a certain stimulus can be detected in a primary cortical area independent to that of stimulus presentation if the stimulus implies features representative of that modality (see Section 1.3.3.), since the theory suggests the primary sensory cortices may be actively predicting forthcoming stimulation based on prior experience. The idea here is that predictions may be transmitted from high-level cortical regions down to the primary sensory cortices, pre-activating these areas in anticipation of the expected upcoming event. Furthermore, such predictions and prediction errors explain the functional significance behind the six different cortical layers. It is important to highlight here that the idea that the laminar structure of the six layers in the cortex comprises a

common computational algorithm is not new (see Edelman & Mountcastle, 1978), rather only later did researchers suggest this common computation, and primary function of the cortex, is prediction. In turn, the predictive coding theory has helped to provide a general account of computational brain processing across perception, cognition, and action in the human brain (Clark, 2013).

1.5. The primary somatosensory cortex

The literature reviewed to this point has discussed the neural processes and overall theories underlying how the brain processes sensory information, however this section of the thesis will now focus specifically on information processing within the primary somatosensory cortex (S1). This is because the primary focus of the present thesis is to examine the neural mechanisms underlying how and why content-specific information can be sent to S1 and surrounding sensorimotor areas when information begins from an independent sensory stimulus, such as audition or vision. This section will first detail the structure and function of S1 and will proceed to explain why it is important to focus explicitly on how context and prior experience can influence the underlying neural computations within and around S1 in the human brain.

1.5.1. Structure and function of the primary somatosensory cortex.

The primary somatosensory cortex (S1) processes tactile and proprioceptive information and is located in the post-central gyrus (PCG), posterior to the central sulcus. It is further sub-divided in to four anatomically distinct areas defined by Brodmann as areas BA3a, BA3b, BA1, and BA2 (Brodmann, 1994; Brodmann & Garey, 2006). These areas can be seen in Figure 1.8, which depicts the anatomical locations of the four Brodmann's areas around the central sulcus and post-central sulcus. BA3a and BA3b are known to receive the most input from the thalamus, and deal primarily with processing proprioceptive and tactile information respectively (Chaudhuri, 2011). BA1 and BA2 receive input from BA3a and BA3b, thus are situated at a higher level in the cortical hierarchy and are involved in more high-level information processing (Eskenasy & Clarke, 2000). Whilst BA1 receives the next

higher level of tactile information, BA2 combines both tactile and proprioceptive information at the next higher-level region in the cortical hierarchy.

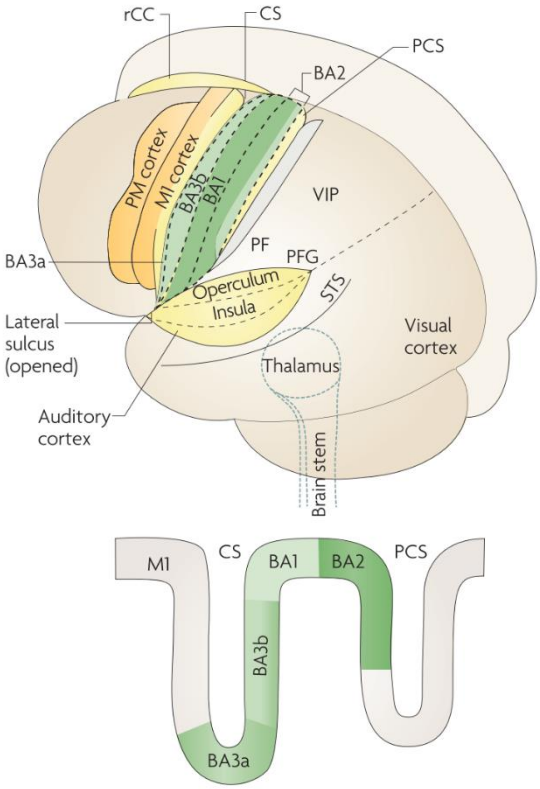

Figure 1.8: The four anatomical sub-divisions of the primary somatosensory cortex. The boundaries are around the central sulcus (CS) and post-central sulcus (PCS). Taken from Keysers, Kaas, and Gazzola (Keysers et al., 2010).

As briefly mentioned in Section 1.2.1., different areas of the surface of the skin send information to specific regions in S1 which results in a measurable topographic map. This topographic map was first discovered by Penfield and colleagues (Penfield & Boldrey, 1937; Penfield & Rasmussen, 1950, 1952), who found that when applying small electric currents to different areas of the PCG in human participants undergoing brain surgery, there was a systematic representation of the neurons to corresponding parts of the body. From this, Penfield was able to create a somatotopic map, known as the somatosensory homunculus. As can be seen in Figure 1.9, each part of the body is represented in the somatosensory homunculus in proportion to its relative importance and/or use. For example, body parts which are used often such as the hands obtain a larger mass of cortical tissue in the PCG, in

which the individual fingers are even represented in an ordered sequence (Penfield & Boldrey, 1937; Schweizer, Voit, & Frahm, 2008). In contrast, body parts used less often, such as the elbow, obtain a smaller mass of cortical tissue. This somatotopic representation in S1 has also been confirmed in research on monkeys (Kaas, Nelson, Sur, Lin, & Merzenich, 1979). Furthermore, given the extensive literature reviewed on neural plasticity in the brain (see Section 1.3.2. above), it is not surprising that this topographical map is not hardwired. For example, plastic alterations have been found in the cortical area which represents the hands in musicians, whereby the area is not only more enlarged, but the increase is specific to the fingers which are frequently used in comparison to the musically untrained (Elbert, Pantev, Wienbruch, Rockstroh, & Taub, 1995; Pantev et al., 1998).

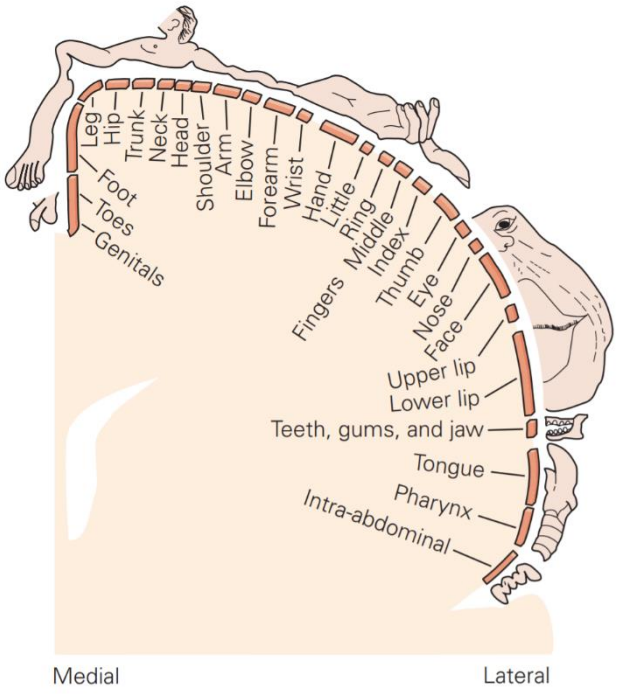

Figure 1.9: The somatosensory homunculus. Taken from Amaral (2000) and adapted from Penfield and Rasmussen (1950).

In terms of the representation of the hands in the segregated areas (e.g. BA3a, BA3b, BA1, and BA2), neuroimaging studies have found that the somatotopic distribution of the fingers is represented in BA3b and BA1 (Nelson & Chen, 2008); the two areas which receive their dominant input from tactile information (Sur, Merzenich, & Kaas, 1980). It is important to note that a study investigating

ipsilateral and contralateral responses in S1 following stimulation to the median nerve found that ipsilateral responses were significantly more posterior in the right hemisphere compared to contralateral stimulation, corresponding to BA2 (Nihashi et al., 2005). Since BA2 is suggested to be a high-level area, this suggests ipsilateral activation to posterior regions of right S1 corresponds to high-level information processes, whereas contralateral activation corresponds more to traditional feedforward input in more anterior regions of S1. This is because it has been known for some time that incoming tactile information is projected to the contralateral side of the brain, such that somatosensory signals from the right side of the body are sent to the left hemispheres S1 and vice versa (Chaudhuri, 2011). Therefore, information in ipsilateral S1 can be argued to be a result of a potentially higher level of information processing.

1.5.2. Why it is important to study the primary somatosensory cortex.

The reason that the current thesis is focusing specifically on neural processing within S1 is due to the fact that, despite an abundance of research investigating cross-modal context effects over recent years, very few studies have focused on how S1 can receive content-specific information from visual, and especially auditory, sources (Ghazanfar & Schroeder, 2006). Furthermore, the majority of research which has investigated general cortical function has focused on processing within the visual cortex (e.g. Carandini et al., 2005; David & Gallant, 2005; Masland & Martin, 2007; Maunsell & Van Essen, 1983; Rockland & Pandya, 1979). This is not surprising since it is widely considered to be the most dominant primary sensory modality (Colavita, 1974; Howard & Templeton, 1966; Welch & Warren, 1986), and comprises at least double the amount of cells compared to any other cortical region (Mumford, 1991). Therefore, there is a gap in the literature in understanding the basic cortical processes involved in other sensory modalities, such as S1.

1.6. Aims and objectives of this thesis

The literature reviewed in this thesis chapter has detailed the transition of how we currently understand the neural computations involved in the primary

sensory cortical regions of the human brain. To briefly summarise, research in recent years has established that the majority of the input to neurons, even within the primary sensory cortical brain areas, comes from other cortical sources via lateral and feedback connections in the brain (e.g. see Muckli & Petro, 2013). A prominent account suggests this is due to the fact the brain predicts upcoming sensory input, thus sends predictions of what it expects to experience in the real world to the relative primary sensory cortical brain regions (see Clark, 2013), essentially pre-activating the cortical area in the event of subsequent input. With this in mind, research has found that the primary sensory cortical brain regions are subject to contextual influences both *within* and *across* the primary sensory modalities (for reviews, see Driver & Noesselt, 2008; Ghazanfar & Schroeder, 2006). Three key questions regarding such contextual information processing that we do not know, however, have been addressed in the present thesis.

First, whilst research has found different familiar visual stimuli which imply haptic information can be discriminated in S1 (Meyer et al., 2011; Smith & Goodale, 2015), different visual stimuli which imply auditory information can be distinguished in A1 (Meyer et al., 2010), and different auditory stimuli which imply visual information can be discriminated in V1 (Vetter et al., 2014), no research to date has investigated whether content-specific information can be sent to S1 when beginning from an auditory source. Answering this question is important in order to establish whether the mechanisms for transmitting content-specific information exist across all pairs of sensory modalities. If we do indeed find information specific to the tactile content of different auditory stimuli can be discriminated in S1, this can determine whether the dominant sense of vision (Colavita, 1974; Mumford, 1991) is needed in order to observe such cross-sensory effects.

Second, no research to date has established whether content-specific information can be detected in an area of cortex independent to that of stimulus presentation using techniques other than fMRI. As such, investigating whether such information can be detected using a different technique, such as EEG, could help establish corroboration of these results across other key neuroimaging methods used in cognitive neuroscience. This is an important area of study since the previous fMRI studies can only confirm which areas in the brain can receive this cross-modal information. However, if we can corroborate these studies using EEG, we can determine the potential timing of these effects at a millisecond level. Furthermore,

establishing similar effects using EEG could open an avenue for quick advances in this field of cognitive neuroscience, since such studies are cheaper and more accessible than fMRI.

Third, to date we do not know for certain whether the primary function of the cross-modal influences detected is a likely result of predictive coding in the brain. This is because previous research can only speculate as to why the cross-modal effects observed actually exist. As such, a study investigating cross-modal influences which can also directly test the assumptions of predictive coding, rather than simply being consistent with the theory, is needed. Understanding the underlying reason as to *why* we observe these cross-modal effects is an important area of study, since it could help future research to investigate any deviations in the predictive effects we observe in neurological or psychiatric disorders.

These three questions are gaps in the literature which are important to answer in order to advance our understanding about how context and prior experience can shape the neural computations occurring in the human cerebral cortex. Specifically, these experiments aim to provide further insight into the relatively limited number of studies which have studied contextual effects within (and around) the primary somatosensory cortex (S1). In Chapter 2, fMRI was used to investigate whether simply hearing sounds that depict different familiar hand-object interactions can elicit significantly different patterns of activity in S1, despite the complete absence of external tactile stimulation. In Chapter 3, EEG was used to examine whether viewing different familiar visual object categories which participants have had a rich haptic prior experience with can be significantly discriminated in the mu rhythm oscillatory response, despite no external tactile stimulation or motor response. In Chapter 4, fMRI was used to investigate whether we could directly test the assumptions of the theory of predictive coding when asking participants to interact with real 3D objects placed directly in front of them in an MRI scanner. This thesis will now introduce each of the three experimental chapters which have aimed to answer each of these questions in turn.

CHAPTER 2

–

Decoding the sound of hand-object interactions in primary somatosensory cortex

2.1. Abstract

Neurons, even in earliest sensory regions of cortex, are subject to a great deal of contextual influences from both within and across modality connections. For example, research has shown that cross-modal connections from vision to primary somatosensory cortex (S1) transmit content-specific information about familiar, but not unfamiliar, visual object categories. As such, the present work investigated whether S1 would also contain content-specific information about sounds depicting familiar hand-object interactions (e.g. bouncing a ball). In a rapid event-related functional magnetic resonance imaging (fMRI) experiment, participants (N = 10) listened attentively to sounds from three different categories: familiar hand-object interactions, and control categories of familiar animal vocalizations and unfamiliar pure tones, while performing a one-back repetition counting task. Multi-voxel pattern analysis revealed significantly above chance decoding for the hand-object interactions within pooled S1 (i.e. post-central gyrus; PCG), whilst no significantly above chance decoding was found for either control category. Crucially, when running analyses in the top 100 hand-sensitive voxels in each participant, defined from an independent tactile localiser, decoding accuracies were significantly higher for hand-object interaction sounds when compared to both control categories in left S1. On the other hand, univariate results revealed no significant differences between categories except for primary auditory cortex. These findings indicate that hearing sounds depicting familiar hand-object interactions elicit different patterns of activity in S1, despite the complete absence of external tactile stimulation. Therefore, this suggests cross-modal connections from audition to S1 may transmit content-specific information about sounds depicting familiar hand-object interactions.

Keywords*:* cortical feedback, cross-modal, multi-voxel pattern analysis, multisensory, S1. (5)

2.2. Introduction

Much traditional neuroscientific research has typically investigated the function of the primary sensory cortical brain areas (e.g. primary visual, auditory, and somatosensory cortices) with respect to how sensory input is processed within its corresponding primary sensory modality. For example, research has explored how the primary visual cortex (V1) processes incoming visual information (for a review, see Carandini et al., 2005), or how the primary auditory cortex (A1) processes incoming sound frequencies (see Brewer & Barton, 2016 for a review). However, it is well-known that most input to neurons, even in the primary sensory cortices, is actually received from contextual cortical sources, via local or long-range internal neural connections (for a review of the visual system, see Muckli & Petro, 2013). This has been predominantly illustrated in the visual system. For example, previous research has revealed when viewing displays of different natural visual scenes, non-visually stimulated regions of early visual cortex contained distinct information about each scenes' surrounding context (Muckli et al., 2015; Smith & Muckli, 2010). This is just one of many examples that has demonstrated how the primary sensory cortices can receive contextual input that does not derive from external stimulation (see also Lee & Nguyen, 2001; Muckli, Kohler, Kriegeskorte, & Singer, 2005; Murray, Boyaci, & Kersten, 2006).

Knowing that the primary sensory cortices can receive contextual information *within* their respective sensory modality has led researchers to investigate whether the primary sensory cortices can receive contextual information via *across* modality connections (for reviews, see Driver & Noesselt, 2008; Ghazanfar & Schroeder, 2006). This is plausible since classic multisensory studies have already shown that the primary sensory cortices are subject to modulatory influences from other sensory modalities (Calvert, 1997; Fu et al., 2003; Kayser et al., 2005; Kayser & Logothetis, 2007; Liang et al., 2013; McIntosh et al., 1998; Zhou & Fuster, 1997, 2000, 2004). However, more recent research has used pattern classification algorithms to reveal the content of this cross-modal information can be reliably discriminated in such regions. For example, research has found the primary somatosensory cortex (S1), known to process tactile information, can receive information related to the content of still images of different familiar, but not unfamiliar, object categories (Smith & Goodale, 2015), or different videos of hand-

object interactions (Meyer et al., 2011), despite the absence of any tactile stimulation during the experiment. Furthermore, Meyer et al. (2010) showed that simply viewing different silent yet sound-implying video clips transmits discriminable information to A1 in the absence of external auditory stimulation. Additionally, when hearing different sounds of rich visual scenes, information specific to the content of the different scenes can be discriminated in early visual cortex, particularly in regions representing the periphery of visual space (Vetter et al., 2014). Taken together, these studies have shown that information specific to the content of a certain stimulus can be reliably discriminated in an entirely independent primary sensory modality, providing the stimulus implies features representative of that modality. One area that has not been addressed to date, however, is whether the sound of different types of haptic-implying information can be discriminated in S1. Therefore, in the present study, we aimed to examine whether simply hearing the sound of different hand-object interactions (e.g. the sound of typing on a keyboard) could send content-specific information cross-modally to S1. We would expect this to be possible due to pre-existing associative links that are formed from prior experience of both sensory aspects of such an object interaction (e.g., the sound and tactile stimulation elicited from typing on a keyboard; see Meyer & Damasio, 2009).

There are several ideas for the neural network by which these sensory signals travel along in order to be discriminated cross-modally in supposedly entirely independent sensory-specific cortices. For example, research has suggested high-level association brain areas, such as posterior superior temporal sulcus (pSTS), pre-motor cortex (PMC), or posterior parietal cortex (PPC; Driver & Noesselt, 2008), may receive information from multiple sensory sources, in turn forming multisensory convergence zones in the brain before feeding contextual information back to any associated sensory-specific areas (Ghazanfar & Schroeder, 2006). This is likely since research has found evidence for strong bidirectional neural connections between each primary sensory cortical area and such high-level multisensory convergence zones (Jones & Powell, 1970). Preferences for certain pairings of sensory modalities in these convergence zones have been indicated based on their proximity to one another. For instance, visual-auditory convergence, and visual-somatosensory convergence, is suggested to occur in pSTS and PPC respectively, given these regions are located between the two sensory-specific cortices (Ghazanfar & Schroeder, 2006; Smith & Goodale, 2015; Wallace et al., 2004). However, since

somatosensory input has also been detected in pSTS (Hikosaka, 1993; Kassuba, Menz, Röder, & Siebner, 2013; Schroeder & Foxe, 2002), thus violating this proximity rule, it may be the case that these identified multisensory convergence zones do not have proximity preferences, but rather could receive input from any combination of these senses.

Since the literature investigating multisensory convergences zones indicates a preference for visual-auditory, and visual-somatosensory convergence (Driver & Noesselt, 2008; Ghazanfar & Schroeder, 2006), it is important to examine whether evidence for convergence between auditory-tactile information can also be found. Specifically, the present study aims to investigate whether information which implies different rich tactile (and motor) information with the hands can be discriminated in S1 when beginning from an auditory source. It is important to address this question since to date is it not clear whether discriminable patterns of information can be sent between all pairs of primary sensory modalities, especially when the dominant sense of vision (Colavita, 1974; Mumford, 1991) is taken out of the equation. The reason why we expect to find such cross-modal effects for this pair of modalities is due to the overall theory of *why* information entering the cortex via one sense can be detected in a supposedly entirely independent sensory modality with any pairing. It is speculated that predictive coding theories of brain function provide a plausible explanation as to why this may be the case. The theory of predictive coding (see Chapter 1, Section 1.4.2. for a review) suggests that the brain actively generates expectations and predictions about likely upcoming input to help shape sensory processing (Clark, 2013; Friston et al., 2009). As such, it may be the case that simply viewing a familiar object may lead to content-specific activity in S1 (Meyer et al., 2011; Smith & Goodale, 2015) since it is useful information in the event of a potential future interaction with the object. If this is the case, it would be reasonable to assume the same cross-modal effects can be detected when hearing sounds that imply tactile information, such as the sounds of familiar hand-object interactions, since such information could aid future or concurrent interaction with the object.

A few human studies have previously investigated links between audition and tactile information in the brain. For example, research has used an fMRI paradigm with MVPA to find the classifier could accurately determine whether a person executed a hand or mouth action based on activation patterns elicited in PMC when simply hearing the same action (Etzel, Gazzola, & Keysers, 2008).

Furthermore, auditory stimuli of the hands crumpling different types of material have been found to show greater neural activity in the inferior parietal lobe (IPL) relative to scrambled material sounds and non-human vocalizations (Arnott, Cant, Dutton, & Goodale, 2008). Liang, Mouraux, Hu, and Iannetti (2013) also used fMRI with MVPA to show patterns between two independent stimulated modalities could be decoded in a non-stimulated early sensory region (e.g. audition vs vision could be decoded in S1). However, no studies to date have specifically tested whether content-specific information about different types of tactile-implying auditory stimuli can be discriminated cross-modally in the *primary* sensory cortex of S1.

In order to examine whether haptic-implying auditory information can be discriminated in S1, auditory sounds which convey different types of tactile stimulation would be necessary, such as sounds of the hands interacting with different types of objects. Previous research investigating the neural representation of object processing has tended to focus on the integration of visual-auditory or visual-somatosensory object information (Amedi, Von Kriegstein, Van Atteveldt, Beauchamp, & Naumer, 2005; Beauchamp, 2005), with limited research investigating object specific knowledge from the angle of audio-tactile integration. One study by Kassuba et al. (2013) has previously found semantically coherent auditory and haptic object features activated the fusiform gyrus, thus suggesting this may be a convergence zone for conceptual object knowledge. A more recent study revealed when hearing sounds of different object materials being manipulated, the different materials were better decoded in inferior frontal cortex when participants were asked to identify the material, compared to when they were asked to identify the action (Hjortkjær, Kassuba, Madsen, Skov, & Siebner, 2018). This suggests higher-order regions, such as inferior frontal cortex, may process elements of auditory information that are separated from the pure acoustic properties of the stimulus. With this in mind, we can assume that such high-level cortical regions could subsequently project information regarding the tactile properties of the sound to S1 via feedback pathways in the brain.

Based on the literature discussed, we have good reason to believe that simply hearing different sounds depicting object interactions with the hands could send discriminable information to S1. We are specifically interested in exploring whether discriminable activity can be detected cross-modally in the *primary* cortical region of S1 since previous research has found evidence for comparable cross-modal effects

between other pairs of primary sensory modalities (Meyer et al., 2010, 2011; Smith & Goodale, 2015; Vetter et al., 2014). However, it is important to note that information specific to the tactile content of the different hand-object interaction sounds could also be discriminated in pre-motor and motor cortical areas, since prior research has found evidence for distinguishable information in such areas about hand-action sounds (Etzel et al., 2008). Furthermore, since sounds which convey different types of tactile information will inevitably contain dynamic action-related components in addition to tactile sensations, activity in pre-motor and motor areas would be expected.

Therefore, the present study investigated, for the first time, whether content-specific information can be sent cross-modally to S1 when beginning from the auditory domain. Specifically, this study tested whether such cross-modal effects found in the previous literature exist when participants are presented with sounds depicting familiar hand-object interactions. As such, participants were presented with different sound clips of familiar hand-object interactions (e.g. bouncing a ball, typing on a keyboard), in addition to two control categories (familiar animal vocalizations, and unfamiliar pure tones), in an event-related functional magnetic resonance imaging (fMRI) experiment. We predicted that MVPA would show significant decoding of sound identity for the hand-object interaction sounds in S1, but not for the two control categories since no rich familiar tactile information would be implied with these sounds. Specifically, we also expected to find stronger decoding in independently localised hand-sensitive voxels of S1, since they should arguably contain maximal sensitivity to the hands and not include unrelated voxels such as those corresponding to other parts of the body. Finally, we also expected to find similar patterns of activation for the hand-object interaction sounds in pre-motor and motor areas, given the dynamic action-related content of the sounds.

2.3. Methods

2.3.1. Participants.

Self-reported right handed healthy participants (N = 10; 3 male), with an age range of 18-25 years (M = 22.7, SD = 2.41), participated in this experiment. All participants reported normal or corrected-to-normal vision, and normal hearing, and

were deemed eligible after meeting MRI screening criteria, approved by the Scannexus MRI centre in Maastricht. Written consent was obtained in accordance with approval from the Research Ethics Committee of the School of Psychology at the University of East Anglia. Participants received €24 euros (equivalent to £20 sterling British pounds) for their time.

2.3.2. Stimuli and design.

Three different categories of auditory stimuli were used in a rapid event-related fMRI design: sounds depicting hand-object interactions, animal vocalizations, and pure tones. There were five different sub-categories within each of these categories, with two exemplars of each sub-category, thus resulting in 30 individual stimuli in total. The five hand-object interaction sub-categories consisted of bouncing a basketball, knocking on a door, typing on a keyboard, crushing paper, and sawing wood. These were chosen for the reason that participants should have previously either directly experienced rich haptic interactions with such objects, or observed such interactions. Two control categories were also used to serve the purpose of controlling for familiarity and semantic richness effects. First, animal vocalizations were used as familiar sounds not directly involving interactions with the hands. These consisted of birds chirping, a dog barking, a fly buzzing, a frog croaking, and a rooster crowing. An independent ratings experiment confirmed these sounds were matched to the hand-object interactions for familiarity (see Appendix A, Table A1 and A2). Sounds from these two categories were downloaded from SoundSnap.com, YouTube.com, and a sound database taken from Giordano, McDonnell, and McAdams (2010). The second control category were non-meaningful sounds, defined as pure tones. These consisted of pure tones of five different frequencies (400Hz, 800Hz, 1600Hz, 3200Hz, and 6400Hz), created in MATLAB (The MathWorks, USA). All sounds were stored in WAV format, and were cut to exactly 2000ms using Audacity 2.1.2, with sound filling the entire duration. Finally, all sounds were normalised to the root mean square (RMS) level (Giordano, McAdams, Zatorre, Kriegeskorte, & Belin, 2013). More information regarding how these sounds were selected, including pilot experiments and ratings for the sounds, can be seen in Appendix A.

2.3.3. Procedure.

After signing informed consent, each participant was trained on the experimental procedure on a trial set of stimuli not included in the main experiment, before entering the scan room. Participants were instructed to fixate on a black and white central fixation cross presented against a grey background whilst listening carefully to the sounds, which were played at a self-reported comfortable level (as in Leaver & Rauschecker, 2010; Man, Damasio, Meyer, & Kaplan, 2015; Man, Kaplan, Damasio, & Meyer, 2012; Meyer et al., 2010). Using a custom built script in MATLAB (The MathWorks, USA, 2010a) and the Psychophysics Toolbox (Brainard, 1997), each run began and ended with 12s silent blocks of fixation. After the initial 12s fixation, 60 individual stimuli were played, with each unique sound presented twice per run. Stimuli were played in a pseudo-randomly allocated order at 2s duration with a 3s ISI (5s trial duration). At random intervals, 15 null trials (duration 5s) were interspersed where no sound was played. This resulted in a total run time of 399s.

During each run, participants performed a one-back repetition counting task, and hence counted the number of times they heard a sound repeated twice in a row, for example, two sounds each of a dog barking (randomly allocated from 2 to 6 per run). We chose this task as it was important that no explicit motor action such as pressing a button was required, to prevent a possible confound in somatosensory cortex activity (see Smith & Goodale, 2015). Thus, participants verbally stated the number of counted repetitions they heard at the end of each run, and they were explicitly asked to not make any movements in the scanner unless necessary. Participants completed either 8 (N = 3) or 9 (N = 6) runs, with the exception of one participant, who completed 7, thus, participants were exposed to approximately 32-36 repetitions per sub-category stimulus, and 16-18 repetitions per unique sound.

After the main experiment, participants took part in a somatosensory localisation experiment, whereby a vibro-tactile stimulation device was used to localise the hand region in the somatosensory cortex (see Smith & Goodale, 2015). Participants were not informed about this part of the experiment until all main experimental runs had been completed. Piezo-electric Stimulator pads (Dancer Design, UK) were placed against the participant's index finger, ring finger, and palm of each hand using Velcro (six pads total, three per hand; see Appendix B, Figure B-

1 for a visual example on one hand). Each pad contained a 6mm diameter disk centred in an 8 mm diameter static aperture. The disks stimulated both hands simultaneously with a 25 Hz vibration in a direction normal to the surface of the disk and skin, at an amplitude within the range of ±0.5mm. The somatosensory localiser runs consisted of 15 stimulation blocks and 15 baseline blocks (block design, 12s on, 12s off, 366s total run time). Note that for the first two participants, a slightly modified timing was employed (block design, 30s on, 30s off; 10 stimulation blocks, 9 baseline blocks). Each participant completed 1 (N = 2) or 2 (N = 8) somatosensory mapping runs, and kept their eyes fixated on a black and white central fixation cross presented against a grey background for the duration of each run. Participants were debriefed after completion of all scanning sessions.

2.3.4. MRI data acquisition.

Structural and functional MRI data was collected using a high-field 3-Tesla MRI scanner (Siemens Prisma, 64 channel head coil, Scannexus, Maastricht, the Netherlands). High resolution T1 weighted anatomical images of the entire brain were obtained with a three-dimensional magnetization-prepared rapid-acquisition gradient echo (3D MPRAGE) sequence (192 volumes, 1mm isotropic). Blood-oxygen level dependent (BOLD) signals were recorded using a multiband echo-planar imaging (EPI) sequence: (400 volumes, TR = 1000ms; TE = 30ms; flip angle 77; 36 oblique slices, matrix 78 x 78; voxel size = 2.5mm^3; slice thickness 2.5mm; interslice gap 2.5mm; field of view 196; multiband factor 2). A short five volume posterior-anterior opposite phase encoding direction scan was acquired before the main functional scans, to allow for subsequent EPI distortion correction (Fritz et al., 2014; Jezzard & Balaban, 1995). Slices were positioned to cover somatosensory, auditory, visual, and frontal cortex. Sounds were presented via an in-ear hi-fi audio system (Sensimetrics, Woburn MA, USA), and the visual display was rear projected onto a screen behind the participant via an LCD projector. Finally, a miniature Piezo Tactile Stimulator (mini-PTS; developed by Dancer Design, UK) was used to deliver vibro-tactile stimulation to the hands, using the same fMRI sequence with a modified number of volumes (366s for the majority, slightly longer for the first two participants due to slightly different design – see Section 2.3.3. above).

2.3.5. MRI data pre-processing.

Functional data for each main experimental run, in addition to somatosensory localiser runs, was pre-processed in Brain Voyager 20.4 (Brain Innovation, Maastricht, The Netherlands; Goebel, Esposito, & Formisano, 2006), using defaults for slice scan time correction, 3D rigid body motion correction, and temporal filtering. Functional data were intra-session aligned to the pre-processed functional run closest to the anatomical scan of each participant. Distortion correction was applied using COPE 1.0 (Fritz et al., 2014), using the 5 volume scan acquired in the opposite phase encode direction (posterior to anterior) for each participant. Voxel displacement maps (VDM)'s were created for each participant, which were applied for EPI distortion correction to each run in turn. Functional data were then coregistered to the participant's ACPC anatomical scan. Note no Talairach transformations were applied, since such a transformation would remove valuable fine-grained pattern information from the data that may be useful for MVPA analysis (Argall, Saad, & Beauchamp, 2006; Fischl, Sereno, Tootell, & Dale, 1999; Goebel et al., 2006; Kriegeskorte & Bandettini, 2007).

2.3.6. Regions of interest.

2.3.6.1. Anatomical mask of Post-Central Gyri ($S1_{mask}$).

In order to accurately capture the potential contribution from each sub-region of S1 (e.g. area 3a, 3b, 1 or 2; see Chapter 1, Section 1.5.1. for more information), hand-drawn masks of the post-central gyrus (PCG) were created in each individual participant. Drawing the anatomical masks enabled a more detailed parcellation on the brain of each participant following previous practice in the field (Meyer et al., 2011; Smith & Goodale, 2015). In doing so, this allowed us to include all the tactile and proprioceptive information potentially available in S1 for the pattern classification algorithms, thus isolating more precisely the contribution of PCG to the spatial fMRI response patterns (see Smith & Goodale, 2015 for further information).

The anatomical masks were created using MRIcron 6 (Rorden, Karnath, & Bonilha, 2007) using each participant's anatomical MRI scan in ACPC space. As in

Meyer et al. (2011) and Smith and Goodale (2015), the latero-inferior border was taken to be the last axial slice where the corpus callosum was not visible. From anterior to posterior the masks were defined by the floors of the central and post-central sulci. Furthermore, masks did not extend to the medial wall in either hemisphere. This resulted in an average of 41 slices (total range 39 to 46) for each hemisphere per participant (see Figure 2.1A and 2.1B for an example in one participant). The average voxel count was 1969 (*SD* = 229) for the right PCG, and 2106 (*SD* = 215) for the left PCG, which did not significantly differ from one another ($p = .084$). The size of each mask per participant is reported in Appendix C, Table C1. See also Appendix C, Figure C-1 for visual examples of the hand-drawn masks in each participant. The masks defined here from this point onwards will now be referred to as $S1_{mask}$.

2.3.6.2. Hand sensitive voxels in Post-Central Gyri ($S1_{localiser}$)

We also created a localised region of interest (ROI) from the somatosensory localiser which comprised a subset of 100 voxels within each participant's anatomically defined $S1_{mask}$ (see Section 2.3.6.1. above). These voxels were the most responsive to stimulation of both hands in each participant (see Section 2.3.7.3. below for more information). This subset ROI is shown in the yellow voxels overlaid on the $S1_{mask}$ in the inflated brain of one participant in Figure 2.1B. From this point onwards, this ROI will be referred to as $S1_{localiser}$. To see both the hand-drawn masks and the hand-sensitive voxels on each individual participants ACPC brains, see Appendix C, Figure C-1.

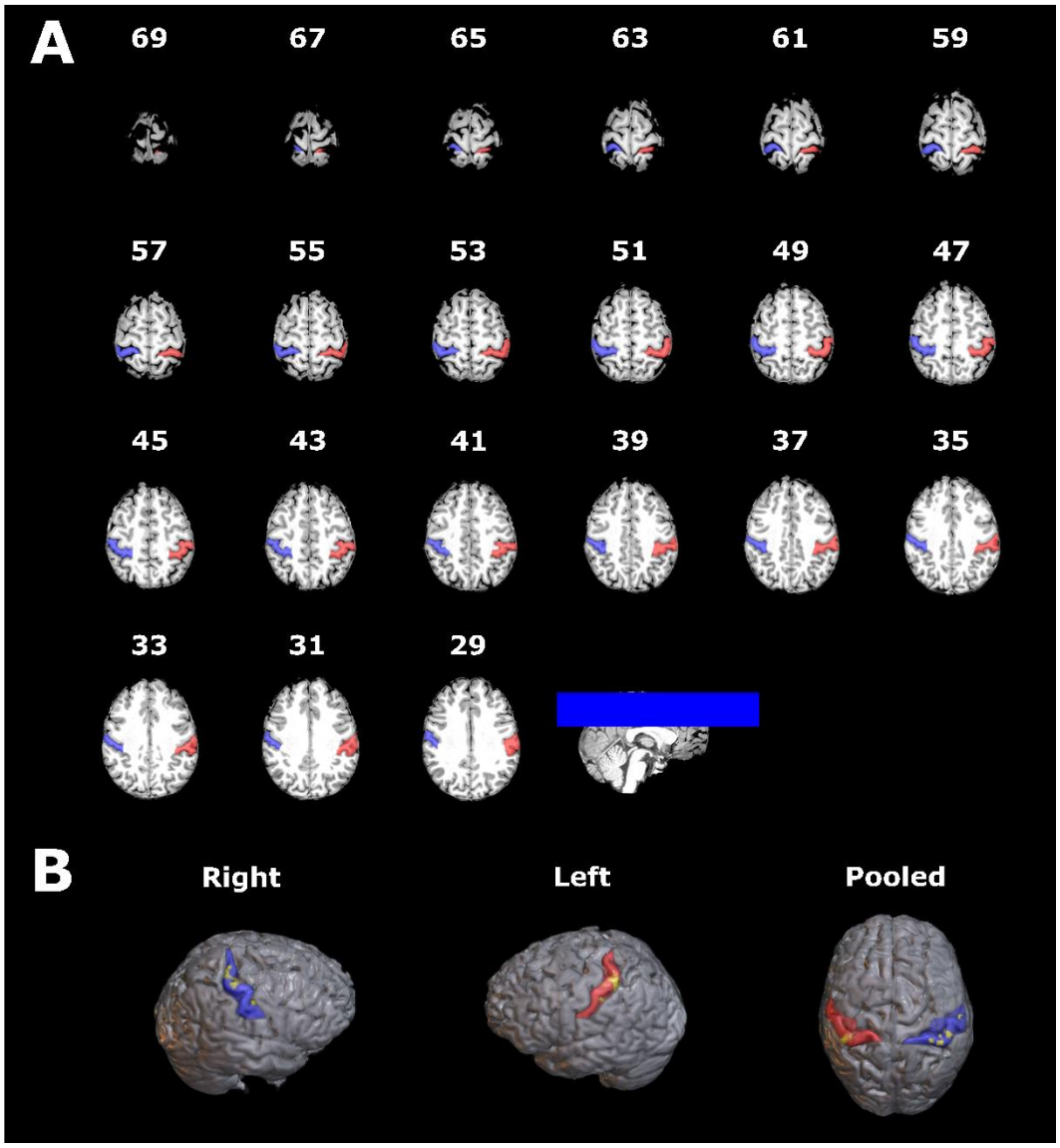

Figure 2.1: Anatomical masks of the lateral post-central gyrus (PCG) for a representative participant. (A) Raw hand-drawn masks in axial display. The numbers in white refer to slices through the Z plane. The box in the lower right image depicts the slices of the brain on which the PCG was marked (see Section 2.3.6.1). (B) As in A, but a 3D rendered version showing right (blue), left (red) and pooled hemispheres. Voxels in yellow indicate the hand-sensitive voxels (see Section 2.3.6.2. for more information).

2.3.6.3. Additional regions of interest.

Additional ROI's were created using the Jüelich Anatomy toolbox (Eickhoff et al., 2005) as in Smith and Goodale (2015). Regions included Primary Auditory Cortex (A1; Morosan et al., 2001; Rademacher et al., 2001), Pre-Motor Cortex

(PMC; Geyer, 2003), Primary Motor Cortex (M1; Geyer et al., 1996), and Primary Visual Cortex (V1; Amunts, Malikovic, Mohlberg, Schormann, & Zilles, 2000). All additional ROI's were transformed into each participants ACPC brain, and we used the 30% probability cut-off for each map as this produces a roughly comparable number of voxels as in $S1_{mask}$ (Smith & Goodale, 2015; Eickhoff et al., 2005). See Appendix D, Figure D-1 for examples of the anatomical masks for the additional ROI's.

2.3.7. Data analysis.

2.3.7.1. Multi-voxel pattern analysis.

For the multi-voxel pattern analysis (MVPA; e.g. Haynes, 2015), a GLM was created from each participant's unsmoothed and undistorted functional run in ACPC space, with a different predictor coding stimulus onset for each stimulus presentation (60 predictors), convolved with a standard double gamma model of the haemodynamic response function (see Greening, Mitchell, & Smith, 2018; Smith & Muckli, 2010). The resulting beta-weight estimates are the input to the pattern classification algorithm. We trained a linear support vector machine (LIBSVM 3.20 toolbox; C. Chang & Lin, 2011) to learn the mapping between the spatial patterns of brain activation generated in response to each of the five different sub-categories of sound within a particular sound category (for example: for hand-object interactions, the classifier was trained on a five way discrimination between each relevant sub-category: typing on a keyboard, knocking on a door, crushing paper and so on; Greening et al., 2018; Smith & Goodale, 2015; Smith & Muckli, 2010; Vetter et al., 2014). The classifier was trained and tested on independent data, using a leave one run out cross-validation procedure (Smith & Goodale, 2015; Smith & Muckli, 2010). The input to the classifier was always single trial brain activity patterns (beta weights) from a particular ROI, while the independent test data consisted of an average activity pattern taken across the repetitions of specific exemplars in the left out run (e.g. the single trial beta weights of the four presentations of 'bouncing a ball' in the left out run were averaged). We have used this approach successfully in previous studies, as averaging effectively increases the signal to noise of the patterns (Muckli et al., 2015; Smith & Muckli, 2010; Vetter et al., 2014). For similar

approaches applied to EEG and MEG data, see Smith and Smith (2019) and Grootswagers, Wardle, and Carlson (2017) respectively.

Finally, we used the LIBSVM toolbox (C. Chang & Lin, 2011) to implement the linear SVM algorithm, using default parameters (C = 1). The activity pattern estimates (beta weights) within each voxel in the training data was normalised within a range of -1 to 1, prior to input to the SVM. The test data were also normalised using the same parameters as in the training set, in order to optimise classification performance. To test whether group level decoding accuracy was significantly above chance, we performed non-parametric Wilcoxon signed-rank tests using exact method on all MVPA analyses, against the expected chance level of 1/5 (E Formisano, De Martino, Bonte, & Goebel, 2008; Greening et al., 2018), with all significance values reported two-tailed. Effect sizes for the Wilcoxon tests are calculated as $r = Z / \sqrt{N}$, when N = number of observations (Rosenthal, 1991), to be identified as small (> .1), moderate (> .3), and large (> .5), according to Cohen's (1988) classification of effect sizes. Finally, to control multiple comparisons, a false discovery rate (FDR) correction was implemented. The adjusted q-value at ≤ .05 resulted in a corrected significance value of FDR $p \leq .012$ for all decoding results (Benjamini & Yekutieli, 2001).

2.3.7.2. Univariate deconvolution analysis.

Deconvolution analysis was also conducted to ensure an accurate model of the hemodynamic response function (HRF) in each category (hand-object interactions, animal vocalizations, and pure tones). A general linear model (GLM) was created from each participants unsmoothed and undistorted functional run in ACPC space with 20 predictors per category to fully model the HRF (Uludag, Ugurbil, & Berliner, 2015). This resulted in a total of 60 predictors used to fully model the HRF for each category and participant. Each predictor was modelled as a series of delta (stick) functions coding stimulus onset. The peak amplitude of the neural response for each category was then estimated by applying the resulting design matrix file to each ROI and extracting the beta weights accordingly; see Section 2.3.6. above for more information on each ROI. The data from volumes 6 and 7 after trial onset were extracted and averaged together. This corresponded to 6s and 7s after trial onset as being the peak of the HRF, and these values were used to

calculate the peak amplitude in response to hand-object interactions, animal vocalisations, and pure tones for each participant.

A 2-way repeated measures ANOVA was conducted on the beta weights extracted independently from each ROI with the following parameters: hemisphere (right, left, pooled) and category (hand-object interactions, animal vocalizations, pure tones). We used parametric ANOVA's in order to be able to detect any interactions between the two factors in each of our ROI's (Toothaker & Newman, 1994). All univariate statistical tests are Greenhouse-Geisser corrected, and all post-hoc paired *t*-tests are reported as two-tailed at the $p < .05$ level with Bonferroni corrections applied.

2.3.7.3. Univariate analysis of somatosensory localiser.

An additional univariate analysis was conducted for the somatosensory localiser data using a GLM approach, with one predictor defining stimulation onset convolved with the standard double gamma model of the HRF. The *t*-values were defined from the localiser by taking the contrast of stimulation vs baseline in each participant. This allowed us to define the 100 voxels showing the strongest hand-related response in each participants $S1_{mask}$. Univariate neural responses to tactile stimulation were extracted by applying the somatosensory localiser GLM to the ROI of each participants $S1_{mask}$, in addition to the ROI defined from the top 100 hand-sensitive voxels ($S1_{localiser}$). As the primary somatosensory cortex is located in the post-central gyrus, and the primary motor (M1) / pre-motor cortices (PMC) are located in and around the pre-central gyrus, we checked for any signs of significant neural activity in both M1 and PMC in response to the somatosensory localiser. This was done in order to check for any signs of contamination of tactile responses across the borders of these adjacent anatomical areas.

A 2-way repeated measures ANOVA was conducted with the following parameters: hemisphere (right, left, pooled) and ROI ($S1_{mask}$, $S1_{localiser}$, PMC, M1). We used parametric ANOVA's in order to be able to detect any interactions between these two parameters (Toothaker & Newman, 1994). All univariate statistical tests are Greenhouse-Geisser corrected, and all post-hoc paired *t*-tests are reported as two-tailed at the $p < .05$ level with Bonferroni corrections applied.

2.4. Results

2.4.1. Multi-voxel pattern analysis.

For the MVPA, we computed cross-validated decoding performance of sound identity for each sound category (familiar hand-object interactions, animal vocalizations, and pure tones) independently in right, left and pooled $S1_{mask}$ and $S1_{localiser}$, and also in our additional ROI's. Control for repeated tests was implemented by use of the false discovery rate ($q < .05$).

2.4.1.1. Primary somatosensory cortex ($S1_{mask}$).

As predicted, significantly above-chance decoding was found for hand-object interaction sounds in pooled S1 (Med = 28.75%; Z = -2.490, p = .012, r = .557); signed rank, two-tailed test, chance = 20% (see Figure 2.2A). Whilst right and left S1 alone did reveal above chance decoding, this did not pass FDR correction (right S1: Med = 23.65%; Z = -2.199, p = .025, r = .492; left S1: Med = 30.56%; Z = -2.383, p = .016, r = .533). Crucially however, the same analyses for our two control categories of familiar animal vocalizations and unfamiliar pure tones did not show any significant above chance decoding in right, left, or pooled S1 (all p's > .4). Further pairwise comparisons revealed decoding performance for hand-object interactions was significantly higher than pure tones in pooled S1 (Z = -2.380, p = .016, r = .532). Decoding accuracies across the right and left hemisphere were not significantly different from one another for hand-object interaction sounds (p = .105). Thus, the S1 carries content-specific information only for the familiar hand-object interaction sounds which convey haptic properties with the hands when pooling across hemispheres.

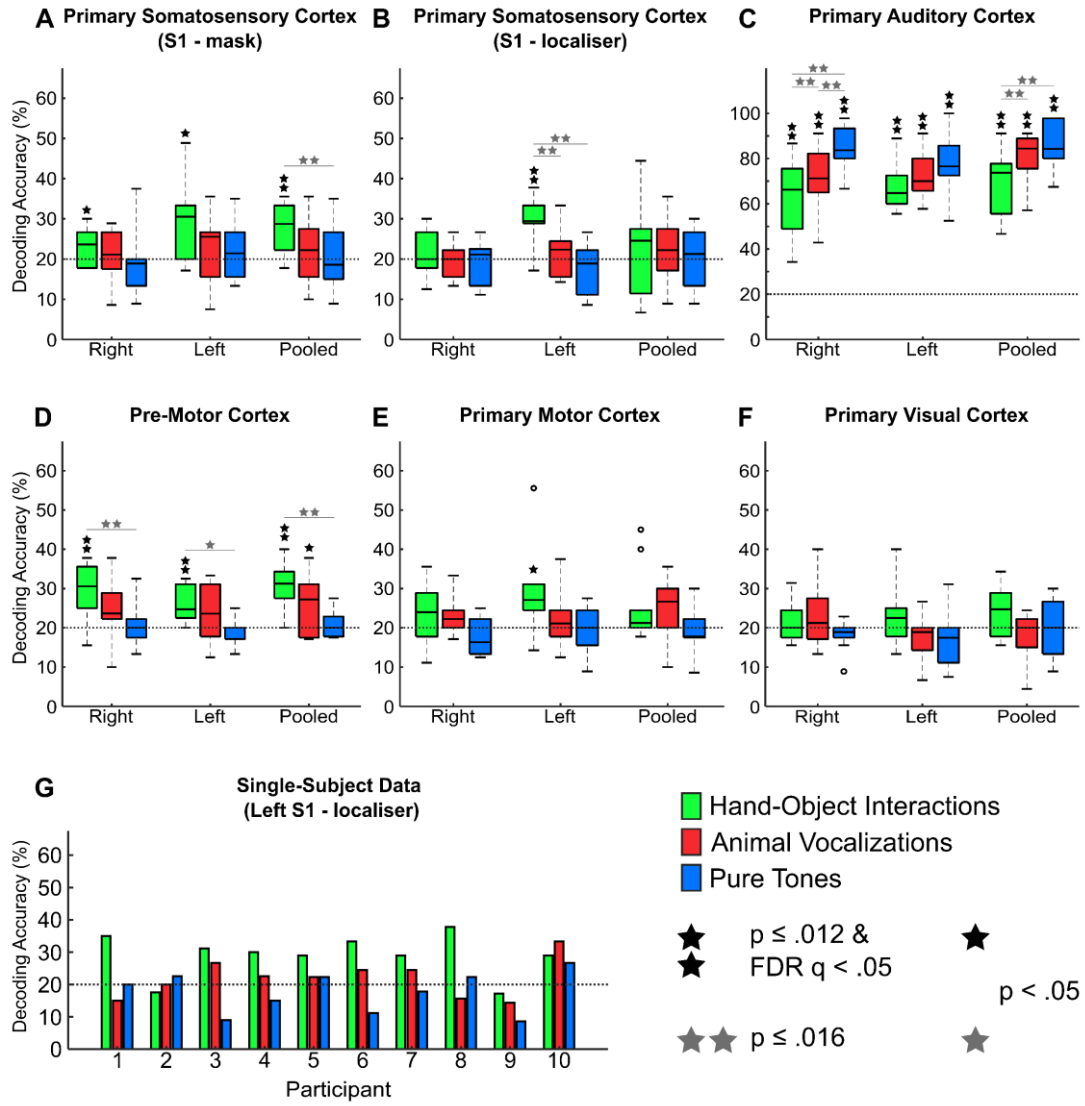

Figure 2.2: Decoding of sound identity. (A) Cross-validated 5 automatic forced choice decoding performance for each stimulus category (hand-object interactions, animal vocalizations and pure tones) for right and left S1 (post-central gyri) independently and pooled across hemispheres. Double stars: $p \leq .012$ & FDR $q < .05$. Single star: $p < 0.05$. (B) As in A but for the top 100 voxels that were responsive to tactile stimulation of the hands in an independent localiser session. (C–F) As in A but for several additional, anatomically defined, regions of interest. (G) As in B left S1 (post-central gyri), but single participant data.

2.4.1.2. Primary somatosensory cortex ($S1_{localiser}$).

When selecting the top 100 most active voxels in S1 from the somatosensory hand localiser, significant decoding for hand-object interactions was found only in left S1 (Med = 29.45%; Z = -2.504, p = .008, r = .560); signed rank, two-tailed test,

chance = 20% (see Figure 2.2B; see also Figure 2.2G for single participant data). Critically, further post-hoc comparisons revealed decoding accuracies for hand-object interactions in left S1 were significantly higher than both control categories (Hands vs Animals: Z = -2.346, p = .016, r = .525; Hands vs Tones: Z = -2.603, p = .006, r = .582). In addition, decoding of hand-object interactions was significantly higher in the left than the right S1 (Z = -2.199, p = .027, r = .492). These results show the classifier could reliably decode hand-object interaction sounds above chance when constrained to the hand-sensitive voxels in left S1, which were significantly higher than both control categories. Thus, sound identity was reliably decoded above chance when restricting the MVPA analysis to voxels with high responses to tactile stimulation of the right, but not left, hand.

2.4.1.3. Primary auditory cortex.

As would be expected, decoding in primary auditory cortex (A1) was robustly significant for all sound categories (all Meds ≥ 64.72%, all Z's ≤ -2.601, all p's ≤ .002, all r's ≥ .627; signed rank, two-tailed test, chance = 20%; see Figure 2.2C). Further pairwise comparisons showed in right A1, decoding of pure tones (Med = 83.65%) was significantly higher than both animal vocalizations (Med = 71.25%, Z = -2.431, p = .012, r = .544) and hand-object interactions (Med = 66.25%, Z = -2.666, p = .004, r = .596), in addition to animal vocalizations being significantly higher than hand-object interactions (Z = -2.668, p = .004, r = .597). In pooled A1, pure tones (Med = 84.29%) were decoded significantly better than hand-object interactions (Med = 73.75%, Z = -2.552, p =.008, r = .571), and animal vocalizations (Med = 84.45%) were decoded significantly better than hand-object interactions (Z = -2.243, p = .023, r = .502). Thus in A1, all sound categories were highly discriminated with the specific pattern of decoding performance being the opposite to that in S1, with better decoding of pure tones, followed by animal vocalizations, then hand-object interaction sounds.

2.4.1.4. Pre-motor cortex.

In pre-motor cortex (PMC), significantly above chance decoding was found for hand-object interactions in right PMC (Med = 30.56%; Z = -2.601, p = .006, r =

.582), left PMC (Med = 24.72%, Z -2.527, p = .008, r = .565) and pooled PMC (Med = 31.25%, Z = -2.666, p = .004, r = .596); signed rank, two-tailed test, chance = 20% (see Figure 2.2D). Interestingly, further tests showed decoding for hand-object interactions was significantly higher than pure tones in right PMC (Z = -2.449, p = .012, r = .548), left PMC (Z = -2.197, p = .031, r = .491), and pooled PMC (Z = -2.807, p = .002, r = .628). Finally, above chance decoding of animal vocalizations was found in pooled PMC, which did not survive FDR corrections (Med = 27.22%, Z = -1.963, p = .047, r = .439). Thus, overall it appears that PMC may contain a degree of information about both types of familiar sound, but not the pure tone control category.

2.4.1.5. Primary motor cortex.

Decoding accuracies in primary motor cortex (M1) revealed above chance decoding for hand-object interactions only in left M1 (Med = 27.09, Z = -2.245, p = .021, r = .502; signed rank, two-tailed, chance = 20%; see Figure 2.2E), however this did not survive FDR corrections. There were no reliable differences in decoding across categories or hemispheres.

2.4.1.6. Primary visual cortex.

Decoding accuracies in primary visual cortex (V1) revealed no significant above chance decoding (see Figure 2.2F).

2.4.2. Univariate deconvolution analysis.

Results from the univariate deconvolution analysis can be seen in Figure 2.3. Interestingly, the only significant differences revealed from the ANOVAs were found in primary auditory cortex (A1). Here, the ANOVA revealed a significant main effect of sound category in A1: $F_{1.630,\ 14.672}$ = 14.061, p = .001, η_p^2 = .610 (see Figure 2.3C). Post-hoc pairwise comparisons revealed the highest neural amplitude to be animal vocalizations (M = .421), followed by hand-object interactions (M = .373), then pure tones (M = .327). All these means were significantly different from each other (all p's $\leq$ .018), except for the difference between hand-object interactions

and pure tones (p = .165). No significant main effect was found of hemisphere (p = .818). Furthermore, a significant interaction was found between sound category and hemisphere in A1: $F_{1.579, 14.212}$ = 9.319, p = .004, η_p^2 = .509. Further pairwise comparisons revealed each sound to be significantly different from one another in each hemisphere of A1 (p's ≤ .025), with the exception of hand-object interactions and pure tones not being significantly different from one another in left and pooled A1 (p's = 1.000 and .154 respectively), nor animal vocalizations and hand-object interactions being significantly different from one another in right A1 (p = .167). A table of all the results from the univariate deconvolution ANOVA in each ROI can be seen in Appendix E, Table E1.

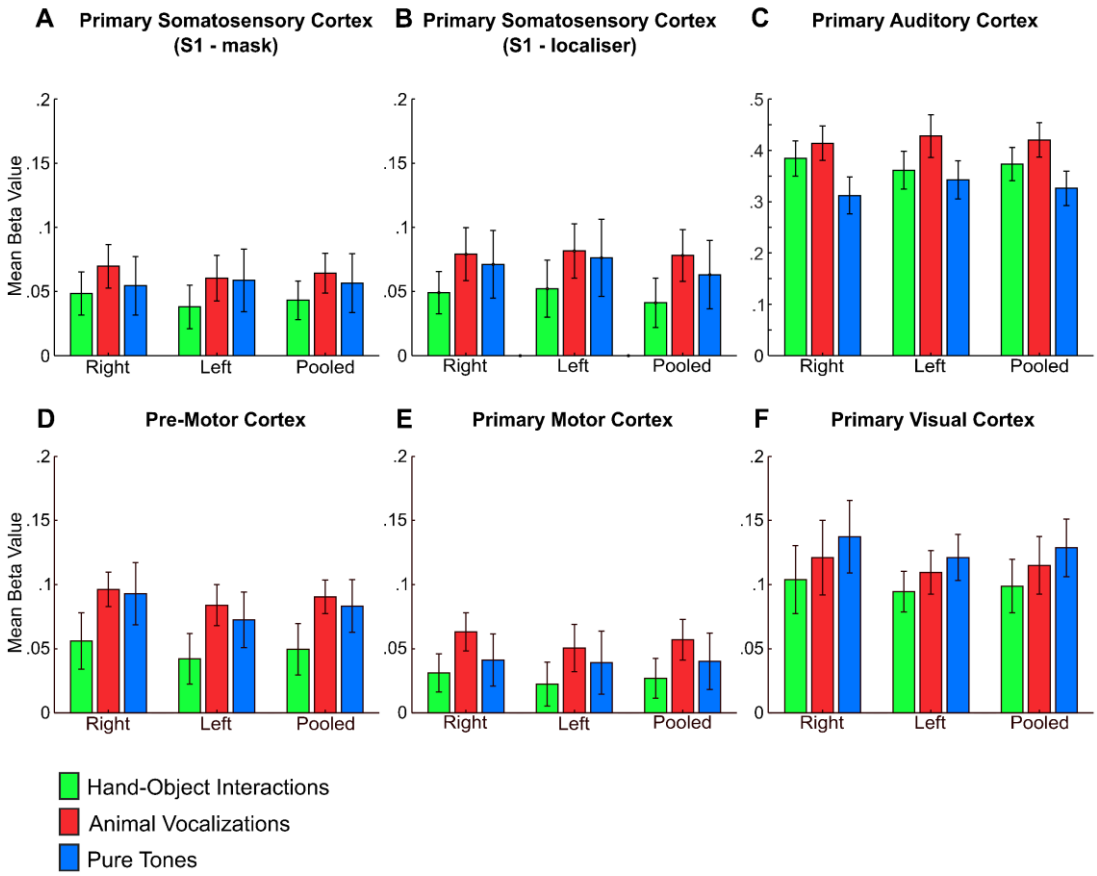

Figure 2.3: Univariate deconvolution results. (A) Mean beta values for each stimulus category (hand-object interactions, animal vocalizations and pure tones) for right and left S1 (post-central gyri), and pooled across hemispheres. (B) As in A but for the top 100 voxels that were most responsive to tactile stimulation of the hands in an independent localiser session. (C–F) As in A but for several additional, anatomically defined, regions of interest.

2.4.3. Univariate analysis of somatosensory localiser.

Univariate analysis of the somatosensory localiser data checked for differences in the neural amplitude in response to tactile stimulation on the participant's hands. Results revealed a significant main effect of ROI $F_{1.279,\ 11.511} = 85.536$, $p < .001$, $\eta_p^2 = .905$ (see Figure 2.4). Post-hoc pairwise comparisons revealed the peak neural amplitude was significantly higher in $S1_{localiser}$ when compared to all other ROI's (all *p's* < .001). Furthermore, the neural amplitude was significantly higher in $S1_{mask}$ compared to PMC and M1. There were no significant differences in the neural amplitude between PMC and M1. Additionally, there was no significant main effect of hemisphere ($p = .430$), nor was there a significant interaction between ROI and hemisphere ($p = .300$). Thus, there appears to be no indication of contamination of tactile responses in nearby regions at this level of analysis. However, given the vastly different number of voxels between $S1_{mask}$ and $S1_{localiser}$, further detailed analysis is required to confirm this suggestion.

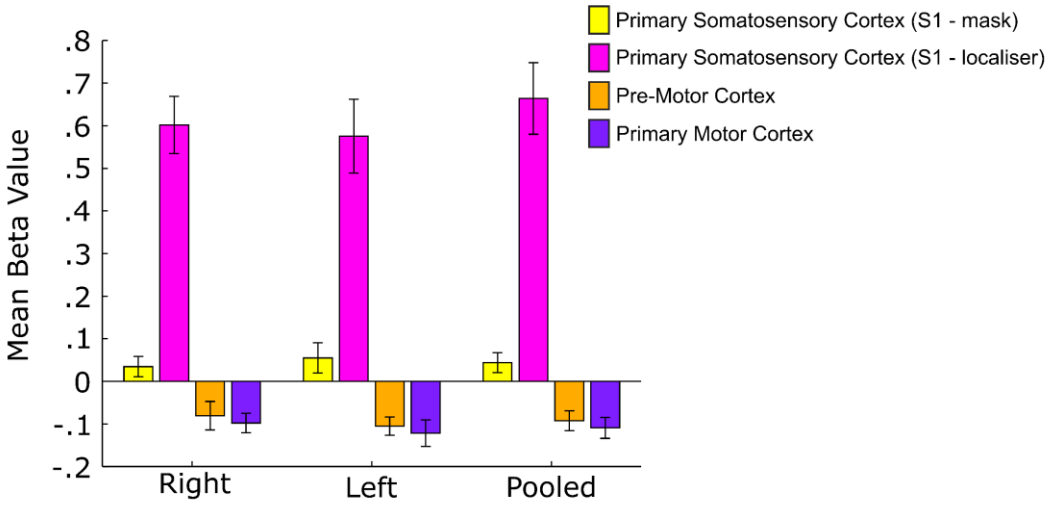

Figure 2.4: Univariate results from the somatosensory localiser. Bar chart reveals the mean beta values in response to tactile stimulation of the hands when compared to baseline in the entire mask of S1, the localised subset region of S1, pre-motor, and primary motor cortices.

2.5. Discussion

The results from the present study show, for the first time, that simply hearing sounds that depict familiar hand-object interactions can elicit significantly different patterns of activity in primary somatosensory cortex (S1), despite the complete absence of external tactile stimulation. Crucially, the same effects were not found for the two control categories of familiar animal vocalizations, and unfamiliar pure tones. Furthermore, when restricting the S1 analysis to the top 100 voxels which were most sensitive to tactile stimulation on the hands, decoding accuracies for the hand-object interaction sounds were significantly higher than both control categories. These results suggest that cross-modal connections in the brain may transmit the content of auditory information to S1, providing the sound conveys rich tactile information. Furthermore, the results show that pre-motor cortex (PMC) contains information specific to the content of the sounds of hand-object interactions, as well as weaker evidence of a similar effect for the sounds of animal vocalizations.

2.5.1. Cross-modal connections transmit the tactile related content of auditory information to S1.

The present study agrees with a set of studies that have shown supposedly sensory-specific cortices contain information related to that sensory modality even if external stimulation did not begin from that sensory domain (Meyer et al., 2010, 2011; Vetter et al., 2014; Smith & Goodale, 2015). Our results significantly extend this previous body of work by demonstrating, for the first time, that information related to the tactile component of the sound of different hand-object interactions can be found in S1, even though external stimulation arrived from the auditory domain. Specifically, these results have expanded on Smith and Goodale (2015), and Meyer et al. (2011), who were particularly interested in investigating cross-modal connections between vision and S1. They found information about the tactile content of different familiar visual objects (Smith & Goodale, 2015), or videos of different hand-object interactions (Meyer et al., 2011), could be discriminated in S1. Here, this study has shown hearing sounds related to different hand-object interactions can also trigger content-specific activity in S1. Similar to Smith & Goodale (2015), these results demonstrate that such effects are not present for all sound categories, but only

for specific sounds which convey tactile properties with the hands. Crucially, both the current study and Smith & Goodale (2015) demonstrate that these effects are strongest when the analyses are limited to independently-localised hand-(or finger-) sensitive voxels in S1, with the decoding effects being significantly higher for the tactile related stimuli when compared to the appropriate control categories. Hence, this highlights how not just any sound, or even any familiar sound, can transmit the same cross-modal information. Overall, since only *hand*-object interaction sounds were found to activate S1 where *hand*-sensitive voxels are located, this demonstrates some associative links may have been formed between the two sensory modalities from prior experience of interacting with such objects.

We have strong evidence to suggest that the results in S1 reflect high-level information about the tactile component of the different hand-object sounds being discriminated in this region, as opposed to passive relay of low-level acoustic features from auditory cortex, for two reasons. First, the pattern of decoding performance in A1 was the exact opposite to the decoding performance found in S1, whereby pure tones showed the highest decoding accuracies, followed by animal vocalizations, then hand-object interactions, particularly in right A1. Second, since the decoding for hand-object interaction sounds was stronger when restricting the analysis to the hand-sensitive voxels, and the univariate analysis from the somatosensory vibro-tactile localiser revealed a neural response only in $S1_{mask}$ and $S1_{localiser}$, this suggests the results for hand-object interaction sounds are driven by cortical regions that process tactile-related information.

It is not surprising that the pattern classification results in A1 revealed higher decoding effects for pure tones, since A1 comprises a tonotopic organization (Humphries, Liebenthal, & Binder, 2010) which is narrowly tuned to different frequency patterns (Rauschecker, Tian, Pons, & Mishkin, 1996; Wessinger et al., 2000). Furthermore, recent research in humans found neurons in auditory cortex are robust in distinguishing different frequencies of pure tone (Zhu, Liu, Li, & Yuan, 2019). The fact animal vocalizations show higher decoding accuracies compared to hand-object interactions in A1 may also be expected given voice-selective areas exist in human auditory cortex (Belin, Zatorre, Lafaille, Ahad, & Pike, 2000), and such complex sounds are important to identify in order to interact with our environment appropriately, such as when visual information is lacking (Altmann, Doehrmann, & Kaiser, 2007). Furthermore, Lewis et al. (2005) suggested processing of animal

vocalization sounds may occur closer to A1 for compactness of cortical wiring, given the probability that fewer multimodal associations should be made with such sounds (e.g. in contrast to lip reading whilst listening to speech; Calvert, 1997). Whilst no significant univariate differences in the neural signal were found in our S1 ROI's, significant differences between sound categories were found in A1. Here, animal vocalizations produced the strongest neural signal, followed by hand-object interactions, then pure tones. This could be explained by research which has found stronger activation in auditory cortices for living versus non-living sounds (Engel, Frum, Puce, Walker, & Lewis, 2009; Giordano et al., 2013; Lewis et al., 2004). Furthermore, categorising animal vocalisations has previously been found to show preferential activation in A1 and bilateral middle superior temporal gyrus (mSTG) when compared to hand-manipulated tool sounds (Lewis, Brefczynski, Phinney, Janik, & DeYoe, 2005). Overall, these results highlight the important difference between analysing data at the spatially distributed pattern level, or at the conventional univariate level, to answer separate unique questions about neural activity in the brain.

These results have expanded on the auditory literature by revealing that S1, specifically the hand-sensitive region of S1, displays a functional preference for sounds that depict hand-object interactions. Research has previously suggested evidence for cross-modal processing from audition to S1. For example, Zhou and Fuster (2004) showed that neurons in somatosensory cortex activate in response to auditory cues if they are associated with tactile information. Furthermore, Lemus, Hernández, Luna, Zainos, and Romo (2010) found neurons in somatosensory cortex that responded to acoustic stimuli, however were unable to find evidence for discriminating the identity of the sound stimuli they presented. Liang et al. (2013) were able to find stimulus modality could be decoded in S1, however they only compared stimulus pairings. For example, auditory versus visual information could be decoded in S1. As such, our results have expanded on this literature by finding, for the first time, that the specific content of auditory information which is sent to S1 is selective for hand-object sounds when limiting the analyses to the hand-sensitive voxels of S1. We note that such decoding effects were not significantly higher than our two control categories when running the analysis in the entire mask of S1, which may be due to the fact such a mask will undoubtedly comprise the entire topographic map of different areas of the surface of the skin (Penfield & Boldrey, 1937; Penfield

& Rasmussen, 1950, 1952). To expand on our findings, it could be interesting for future research to test another tactile-implying sound which involves a different area of the body, such as the mouth or feet, to test whether decoding of the sound of different haptic-implying object interactions is localised to the body regions which would be used to interact with the object.

In terms of the functional significance behind *why* this cross-sensory information has been observed in S1, it is possible that these findings can be explained by predictive coding theories of human brain function (Clark, 2013; Friston et al., 2009). Here, it may be the case that when hearing the sounds associated with a familiar hand-object interaction, information related to the tactile content of the stimuli is sent to S1 since it is information which may be useful for future (or concurrent) interaction with the specific object. If this is the case, predictive coding would assume the brain is predicting the tactile content of the hand-object interaction sounds based on prior experience of interacting with such objects. With this in mind, it could be possible for future research to directly test this theory by using appropriately designed paradigms where specific sensory cues (e.g. visual or auditory) predict forthcoming 3D objects (see for example Rossit, McAdam, Mclean, Goodale, & Culham, 2013) in a target modality such as the primary somatosensory cortex (see Kok, Jehee, & de Lange, 2012; see also Zhou & Fuster, 2000).

Alternatively, it might be the case that the pattern of activity present in S1 for hand-object interaction sounds is not useful for future object interaction, but rather the decoded information reflects a broader representation of stored object knowledge in the haptic domain (e.g. Man et al., 2012; Martin, 2016; Meyer & Damasio, 2009). These theories propose that the representation of object concepts is distributed across a network of the perceptual, action and emotion systems in the brain (Martin, 2016), and that conceptual processing involves neural re-use of the same brain areas used to represent that information during perception and action (Anderson, 2010; Barsalou, 2016). The idea here is that object knowledge, such as knowledge about a keyboard, is stored within the entire processing stream which was active at the time information was acquired or updated (Martin, 2016). With this in mind, the decoding effects we observe about the hand-object interaction sounds could be argued to be a representation of the neural re-use of brain areas which would have been utilised when the knowledge about that object was acquired. For example, when you hear the

sound of typing on a keyboard, S1 and PMC become activated since they comprise part of the same neural network that was active when information about a keyboard was first acquired. While these accounts do not generally invoke the primary sensory cortices as being involved in the representation of object knowledge, Martin's (2016) account, for example, proposes that these regions could become involved under specific task conditions. Therefore, we could expect that representation of object knowledge accounts would predict that the effects we observe in S1, or even PMC, may be modified as a function of task constraints. For example, we may expect to observe stronger decoding effects for tasks where somatosensory properties of objects and/or actions are more versus less prominent. Indeed, previous research has found evidence that attentional modulations influence perception of sensory information in S1 (Puckett, Bollmann, Barth, & Cunnington, 2017). As such, it would be interesting to see how decoding accuracies differ as a function of the experimental task in future experiments.

There are several possible neural routes which can explain how information related to the tactile content of auditory stimuli can be discriminated in S1. First, information may enter high-level multisensory convergence zones, such as posterior superior temporal sulcus (pSTS) or posterior parietal cortex (Driver & Noesselt, 2008; see also Chapter 1, Section 1.3.1. for more information), which may receive the information from the auditory source before sending the related tactile information to S1 via feedback pathways in the brain. This is highly plausible since all sensory pathways have been found to convergence in the depths of the pSTS, displaying strong bidirectional connections from this convergence zone to each primary sensory cortex (Jones & Powell, 1970). Another possibility is the fusiform gyrus, since Kassuba et al. (2013) found semantically coherent auditory and haptic object features activated this area. Second, auditory information could have been directly projected to S1, since previous research on animals has found evidence for direct cortico-cortical connections between primary auditory and primary somatosensory cortex in both directions (Budinger et al., 2006; Henschke et al., 2015; see also Cappe & Barone, 2005). However, such direct connections are relatively sparse as opposed to the amount of feedback arriving from higher multisensory areas (Driver & Noesselt, 2008), meaning it is unlikely to be a dominant route in transmitting this information. Finally, a third possibility is the involvement of lower tier multisensory regions (Driver & Noesselt, 2008) that are

anatomically located next to primary sensory cortical areas. For instance, auditory regions located close to secondary somatosensory cortex (S2) may be bimodal responding to both auditory and tactile information (see for example Cappe & Barone, 2005; Wallace, Ramachandran, & Stein, 2004). This is supported in recent studies which have indicated the presence of auditory frequency information in S2 and the parietal operculum subdivision OP4 (Pérez-Bellido, Anne Barnes, Crommett, & Yau, 2018), paired with the fact auditory information presented at very fast time-scales has been found to converge in S1, arising from the early stages of the feedforward pathway (Sugiyama, Takeuchi, Inui, Nishihara, & Shioiri, 2018).

2.5.2. Hemispheric differences between auditory and visually triggered cross-sensory information in S1.

It is important to note that both Smith and Goodale (2015) and Meyer et al. (2011) used visual stimuli (either images of familiar graspable objects, or videos depicting the hands exploring different objects, respectively) and found stronger decoding accuracies in the right hemisphere of S1, whereas in the present study with auditory stimuli stronger decoding was found in the left hemisphere of S1. There are several potential reasons for the greater involvement of hand-sensitive voxels in left S1 in the present study. First, some of the sounds used depict bimanual actions (e.g. typing on a keyboard) and previous studies have found greater activation in the left hemisphere for bimanual action sounds (Aziz-Zadeh, Iacoboni, Zaidel, Wilson, & Mazziotta, 2004). In addition, much research concerning the neural processing of tools has reported a strong left lateralization of the tool network in right-handed participants (as our participants were; Ishibashi, Pobric, Saito, & Lambon Ralph, 2016; Lewis, Brefczynski, Phinney, Janik, & DeYoe, 2005; Lewis, Phinney, Brefczynski-Lewis, & DeYoe, 2006) although this would suggest left-lateralization for both sounds and images/videos, which was not the case when comparing the results of this study to Smith and Goodale (2015), and Meyer et al. (2011). However, it may be the case that the left hemisphere lateralization observed in this study depends upon the object directed action content being strongly emphasized, as was the case in the current study due to the use of rich sounds. Finally, one further important difference between Smith and Goodale (2015) and the present study is that Smith and Goodale localised the finger sensitive voxels in S1 for each participants

hand independently, which permitted considering the relative influence of contra- and ipsi-lateral influences, whereas in the present study both hands were mapped simultaneously. Hence, in the present study, the selected voxels may have reflected a stronger contra-lateral bias, and therefore reflect the relatively earlier sub-regions of S1, such as area 3b (Keysers, Kaas, & Gazzola, 2010). To determine whether this is the case, future research would ideally run the localisers on each hand independently to determine the relative role of hand sensitive voxels in left and right S1 to either visually or auditory triggered information.

2.5.3. Decoding action related information in pre-motor cortices.

In pre-motor cortex (PMC), reliable decoding of hand-object interaction sounds was found in both the left and right hemisphere, which was significantly greater compared to the decoding of pure tones. Traces of evidence for decoding of animal vocalizations was also found in PMC when pooling across hemispheres, which notably did not survive FDR correction. Overall, these decoding effects are not surprising, since PMC is known to play a large role in processing action related information (Gallese, Fadiga, Fogassi, & Rizzolatti, 1996). For instance, PMC has been found to be preferentially activated for object-related hand actions and non-object-related mouth actions (Buccino et al., 2001). Since both the familiar sounds of hand-object interactions and animal vocalizations imply such an action, it would seem reasonable for the sounds to be discriminated in pre-motor areas.

Decoding in PMC for both hand-object interactions and (albeit weak evidence) for animal vocalizations could also be part of a somatotopic auditory mirror neuron system, since PMC has previously been found to be active in response to both performing an action and hearing the corresponding action sound (Kohler et al., 2002). PMC has also been found to be able to reliably discriminate between whether a person executed a hand or mouth action based on activation patterns elicited in PMC when hearing the same action (Etzel et al., 2008). Furthermore, Gazzola, Aziz-Zadeh, and Keysers (2006) found overlap at the voxel level between left PMC activation when human participants executed a motor action, or listened to the sound of the action. Crucially, they found a somatotopic pattern, whereby a dorsal cluster within PMC was involved in listening to and executing hand actions, and a ventral cluster within PMC was involved in listening to and executing mouth

actions. Therefore, both hand- and mouth-specific clusters within PMC may contribute to the decoding found in the present experiment. We would predict no significant decoding for the hand-object sounds if PMC analyses were limited to mouth-sensitive voxels in PMC, and likewise for animal vocalizations in hand-sensitive voxels in PMC. Hence in future work it would be optimal to include an additional mouth and hand movement localiser to test these predictions. Overall, the decoding effects observed for action-related information in PMC (and also M1, although not surviving FDR correction) suggest these regions also receive content-specific information regarding the action properties of familiar hand-object interaction sounds (with weaker evidence of an effect for animal vocalizations).

Finally, as mentioned previously in Chapter 1, Section 1.3.1., pre-motor cortical regions are known to be involved in multisensory processing (Driver & Noesselt, 2008). Specifically, research has found ventral PMC contains representations about both the sight and sound of different actions (Kaplan & Iacoboni, 2007). Additionally, a variety of research has found evidence for PMC being part of the auditory dorsal stream, which is thought to be involved in linking sound and action (Brown et al., 2013; Brown, Zatorre, & Penhune, 2015; J. L. Chen, Penhune, & Zatorre, 2009; J. L. Chen, Rae, & Watkins, 2012; Hickok & Poeppel, 2004; Lega, Stephan, Zatorre, & Penhune, 2016; Zatorre, Chen, & Penhune, 2007). Therefore, another possibility is that we found evidence for decoding the sound of hand-object interactions in PMC since such sounds include an action, and PMC may have played a crucial role in linking the hand-object sound with the individual representation of the action.

2.6. Conclusion

Overall, this study has shown, for the first time, that the identity of different familiar hand-object interaction sounds can be discriminated in hand-sensitive areas of S1, in the absence of any external tactile stimulation. Such decoding effects were not found for the two control categories of familiar animal vocalizations, and unfamiliar pure tones, thus suggesting not just any sound, or even any familiar sound, can produce the same effects. Therefore, since only *hand*-object interaction sounds were found to be discriminated in S1 where *hand*-sensitive voxels are located, we suggest cross-modal connections from audition to S1 may transmit

content-specific information only about familiar sounds that involve a tactile component. This work provides converging evidence that activity in supposedly modality-specific primary sensory cortical areas can be shaped in a content-specific manner by relevant contextual information transmitted across sensory modalities. This effect is in keeping with the rich range of contextual effects expected in primary sensory cortical areas under the predictive coding framework.

CHAPTER 3

–

Decoding the content of familiar visual object categories in the mu rhythm oscillatory response

3.1. Abstract

Recently we have used fMRI to show that cross-modal connections from vision to primary somatosensory cortex can transmit information specific to the content of different familiar, but not unfamiliar, visual object categories, despite the complete absence of tactile stimulation. Here we sought to corroborate and extend our fMRI results using high temporal resolution neuroimaging (EEG), specifically by investigating whether the mu rhythm, thought to reflect sensorimotor processing, could also discriminate between such different familiar, but not unfamiliar, visual objects categories. Therefore, in the present study, right-handed participants (N=27) viewed images of both familiar (apple, wine glass) and unfamiliar (cubie, smoothie) objects, whilst detecting colour changes in a central fixation cross. Multivariate pattern analysis (MVPA) revealed significant decoding of familiar, but not unfamiliar, visual object categories in the mu rhythm oscillatory response. Thus, we suggest that connections between vision and sensorimotor areas may transmit information specific to the tactile (or motor) component of only familiar visual objects, even when no action or motor response is either executed or implied – corroborating our previous fMRI study. In addition, we report significant attenuation in the central beta band for both familiar and unfamiliar visual objects, but not in the mu rhythm. This finding highlights how analysing two different aspects of the oscillatory response – either attenuation or the representation of information content – provide complementary views on the role of the mu rhythm in response to viewing different visual object categories.

Keywords: alpha, EEG, multisensory, multivariate pattern analysis, mu rhythm. (5)

3.2. Introduction

Over the past decade, research has found multisensory integration occurs even in the primary sensory cortices of the human brain (see Driver & Noesselt, 2008; Ghazanfar & Schroeder, 2006 for reviews). More recently, research has used fMRI with multi-voxel pattern analysis (MVPA) to find that the content of information presented via one sense can actually be discriminated in an entirely independent primary sensory modality if the stimulus implies features representative of that modality. For example, Smith and Goodale (2015) have recently shown cross-modal connections from vision to primary somatosensory cortex (S1) transmit information specific to the content of familiar, but not unfamiliar, visual object categories in the absence of tactile stimulation. Furthermore, Chapter 2 revealed cross-modal connections between audition and S1 transmit information specific to the content of different sounds which convey object interactions with the hands (see also Bailey, Giordano, Kaas, & Smith, 2019). In the present study, we sought to corroborate these previous findings using electroencephalography (EEG). Specifically, EEG was used to investigate whether presenting a visual stimulus of a familiar object which implies rich haptic information could produce a distinct oscillatory pattern over sensorimotor cortex, namely the mu rhythm (Berger, 1929), despite the complete absence of tactile stimulation or a motor response when viewing the familiar visual objects.

The mu rhythm is a movement related neural oscillation in the 8-13 Hz frequency range measured over sensorimotor cortex (Berger, 1929). It is a resting oscillation, meaning it can be measured when no active processing is occurring (Kuhlman, 1978; Pfurtscheller, Neuper, Andrew, & Edlinger, 1997). As such, attenuation of the mu rhythm, also known as event-related desynchronization (ERD), can be interpreted as an electrophysiological correlate of an *active* sensorimotor cortex, since oscillatory power decreases are presumably due to desynchronization of neurons in a local patch of cortex (Pfurtscheller, 1997; Pfurtscheller, Stancák, & Neuper, 1996; Steriade & Llinás, 1988). A vast amount of research has found mu rhythm desynchronization when executing an action, observing an action, or even when one merely has the intention to act (Fox et al., 2016; Muthukumaraswamy & Johnson, 2004; Pfurtscheller et al., 1997; Pineda, 2005). For this reason, the mu

rhythm has often been considered to be an index of mirror neuron activity (Fox et al., 2016; Muthukumaraswamy, Johnson, & McNair, 2004).

However, a recent review by Hobson and Bishop (2016) suggests whilst mu rhythm suppression can be used to measure mirror neuron activity, the observed effects are weak and unreliable, hence making one question whether the mu rhythm is truly a reflection of the human mirror neuron system. In fact, some research has suggested that the mu rhythm actually primarily reflects the somatosensory features of actions, such as the texture of an object being picked up during an action, rather than the action itself (Coll, Bird, Catmur, & Press, 2015; Coll, Press, Hobson, Catmur, & Bird, 2017; Quandt, Marshall, Bouquet, & Shipley, 2013; Ritter, Moosmann, & Villringer, 2009). The idea that the mu rhythm may reflect tactile stimulation in addition to executed and observed motor activity is not new. For example, Cheyne et al. (2003) used MEG to find tactile stimulation during a finger brushing task produced a brief suppression of the mu rhythm, in addition to the central beta rhythm (15-25 Hz over sensorimotor cortex) which has also previously been shown to be involved in action related processes such as motor imagery, passive movement, and action observation (Zaepffel, Trachel, Kilavik, & Brochier, 2013). From this study, Cheyne et al. attributed the suppression of the mu rhythm to tactile activity in S1, and suppression of the central beta rhythm to motor activity in primary motor cortex (M1); see also Cheyne (2013) for a review. Further research also supports the idea that the mu rhythm reflects tactile information processes (Arnstein, Cui, Keysers, Maurits, & Gazzola, 2011; Cannon et al., 2014).

The research to this point has suggested that the mu rhythm oscillatory response may be an index of somatosensory features of actions in addition to the motoric components of actions themselves. In fact, suppression of the mu rhythm has even been found when participants simply viewed still images of manipulable objects (Proverbio, 2012). Proverbio suggested the observed suppression was a reflection of somatosensory regions representing object affordance of tool manipulability. However, based on our previous work (Bailey et al., 2019; Smith & Goodale, 2015; see also Chapter 2), we believe that observing such effects when viewing still images of manipulable objects may also reflect information about the tactile features of the object being projected to S1 via feedback connections in the brain. Whilst this could explain how object affordance is implemented in S1, another

theory is that these effects may be a reflection of predictions about the tactile features of objects being sent to S1 in anticipation of a potential subsequent interaction with the object, in line with predictive coding theories of human brain function (Clark, 2013). If this is the case, we may expect to not only observe a suppression of activity in the mu rhythm when viewing familiar objects, but actually find information specific to the content of different familiar visual objects can be discriminated in the mu rhythm, based on learned differences about their tactile (or motor) properties. Whilst this cannot directly confirm whether predictive coding is indeed the reason behind these effects, such results would provide convincing support for the theory.

The reason why we expect such discriminable information may be present specifically within the mu rhythm is due to the fact a recent study by Coll et al. (2017) found the mu rhythm shows specificity to somatosensory features of actions. In their research, they asked participants to either observe or execute different action types with or without concurrent tactile stimulation, and with a real object or a pantomime action. In doing this, they could ascertain whether decoding accuracies differed as a function of action type, tactile stimulation, or object use. Interestingly, MVPA only revealed such specificity for concurrent tactile stimulation and object use, and *not* for different action types. This suggests the mu rhythm shows specificity to somatosensory, and not motor, features of actions.

Furthermore, we have reason to believe we will find discriminable information about different familiar visual objects within the mu rhythm despite the complete absence of tactile stimulation or a motor response for two reasons. First, such cross-modal context effects have already been found with fMRI, since Smith and Goodale (2015) found information about the exact same different familiar visual objects could be discriminated in S1, in which the mu rhythm is thought to originate from (Cheyne, 2013; Cheyne et al., 2003). Second, previous research investigating feedforward and feedback processing in the macaque visual cortex found causal evidence to suggest low-frequency oscillations, such as alpha, propagate in a feedback direction, whereas high-frequency oscillations, such as gamma (40-80 Hz) convey feedforward information (Van Kerkoerle et al., 2014). Since the mu rhythm oscillates in the alpha frequency range, it is therefore considered to convey feedback

related information thus is the likely oscillatory frequency for transmitting feedback contextual information across sensory modalities.

Building on this, the laminar architecture of this coordinated activity has been investigated by Bonaiuto et al. (2018), who found low-frequency alpha activity originated in deep cortical laminae (see also Buffalo, Fries, Landman, Buschman, & Desimone, 2011; L. R. Silva, Amitai, & Connors, 1991; W. Sun & Dan, 2009). Hence, this further suggests the alpha oscillation may play a pivotal role in coordinating feedback information, since information projected via feedback connections is known to originate from deep layers of cortex (Felleman & Van Essen, 1991; Rockland & Pandya, 1979). Furthermore, forming predictions about when a stimulus may appear has been found to bias the phase of alpha oscillations (Samaha, Bauer, Cimaroli, & Postle, 2015), thus predictions have been suggested to be coordinated at this oscillatory rate (Bastos et al., 2012). Therefore, if the cross-modal context effects found by Smith and Goodale (2015) are a result of predictive processes occurring in the cortex, we can assume such predictions will be detected in the mu rhythm response. This is further supported by the fact Rao and Sejnowski (2002) found convincing evidence to suggest predictions are implemented in deep layers of cortex (where alpha originates; Bonaiuto et al., 2018), especially in S1 (Yu et al., 2019).

It is important to note here that whilst the oscillatory rate of feedforward and feedback connections has been investigated *within* a modality (e.g. how information is communicated between high-level visual areas, such as V4, and low-level visual areas, such as V1; Van Kerkoerle et al., 2014), it is not clear how this coordination may be implemented *across* modalities in the brain. This is because, to the best of our knowledge, this has not yet been explored. However, the literature to date gives us a strong reason to assume any discriminable information about the familiar visual objects found in the mu rhythm oscillatory response may be a result of feedback coordination, and potentially predictions, in the brain (see also Scheeringa & Fries, 2019 for a recent review).

Finally, the central beta oscillation may also be of interest, since Cheyne (2013) suggested the exact functional roles of the mu rhythm and central beta oscillations are not well understood. The beta oscillation has also been suggested to originate from deep layers of cortex, thus it may also reflect feedback processes

(Bastos et al., 2015; Michalareas et al., 2016). One interesting difference between the mu rhythm and the central beta oscillation, however, is the fact that Cheyne (2013) suggested the mu rhythm reflects activity in S1, and the central beta rhythm reflects activity in M1. Therefore, we may only expect to find discriminable information within the mu rhythm, since this is the oscillation which has been suggested to best reflect underlying activity in S1 – our key region of interest which we would expect to find information related to the tactile features of viewing images of familiar objects, especially since Smith and Goodale (2015) did not find discriminable patterns of information in M1 when participants viewed the same familiar visual objects.

As such, in the present study, we used MVPA cross-classification methods to examine the oscillatory activity underlying content specific transfer of information from vision to sensorimotor areas. To do this, we investigate whether information specific to the content of simply viewing familiar, but not unfamiliar, visual object categories can be discriminated in the mu rhythm oscillation. We investigated familiarity with objects to determine whether experience with the haptic interactions of the object is necessary to observe such effects in the neurophysiological responses. Since such links have already been found between vision and S1 when viewing these objects which convey this rich tactile and motor related information (Smith & Goodale, 2015; see also Meyer & Damasio, 2009), we expect the same underlying neuronal processes can be detected using EEG. We also investigated whether such effects could be detected in the beta (15-25 Hz) frequency band (as in Coll et al., 2017), since the central beta band has previously been shown to be involved in action related processes such as motor imagery, passive movement, and action observation (Zaepffel et al., 2013). Finally, analyses were also performed in the occipital alpha band as a control analysis to rule out potential confounds by changes in attentional engagement (Hobson & Bishop, 2016). Furthermore, this analysis was performed since research has shown occipital alpha reflects neuronal top-down influences on perception (M. T. Sherman, Kanai, Seth, & Van Rullen, 2016), therefore investigating differences in this frequency band in relation to familiarity and prior experience with the objects was also of interest. This study focused on MVPA as the main analysis technique since it indicates the representational content from the task (Mur, Bandettini, & Kriegeskorte, 2009), as

opposed to univariate analysis which can only investigate overall involvement in a task based on changes in synchronisation in a given region. We expect, based on the literature reviewed, to find discriminable patterns of information related to the different familiar, but not unfamiliar, visual object categories in the mu rhythm oscillatory response.

3.3. Methods

3.3.1. Participants.

Participants (N = 27; 13 male) were right handed (Oldfield, 1971), with an age range of 18-34 years (M = 21.19, SD = 3.35). All participants reported normal or corrected-to-normal vision and no history of neurological disorders. Written consent was obtained in accordance with approval from the Research Ethics Committee of the School of Psychology at the University of East Anglia. Participants were recruited through an online system and awarded partial course credit, or through a paid participant panel, receiving £16 for their participation.

3.3.2. Stimuli and design.

Two different conditions of full colour visual object stimuli were used in a block design: familiar or unfamiliar objects. Familiar objects consisted of apples and wine glasses (Smith & Goodale, 2015; see Figures 3.1A and 3.1B), and unfamiliar objects consisted of cubies and smoothies (Op de Beeck, Torfs, & Wagemans, 2008; see Figures 3.1C and 3.1D). There were three exemplars of each visual object, resulting in 12 individual stimuli total. Familiar objects were chosen based on the assumption that participants would have a rich haptic experience with such objects (as in Smith & Goodale, 2015). All images were 400 x 400 pixels, displayed against a white background in the centre of a 24” monitor screen (resolution 1920 x 1080 pixels) using E-Prime 2.0. A black and white fixation cross with a black border (28 x 28 pixels), and a red and green fixation cross with a black border (28 x 28 pixels), was also used. A viewing distance of 45cm was maintained for a visual angle height of 14° for the stimuli, as in Smith and Goodale (2015).

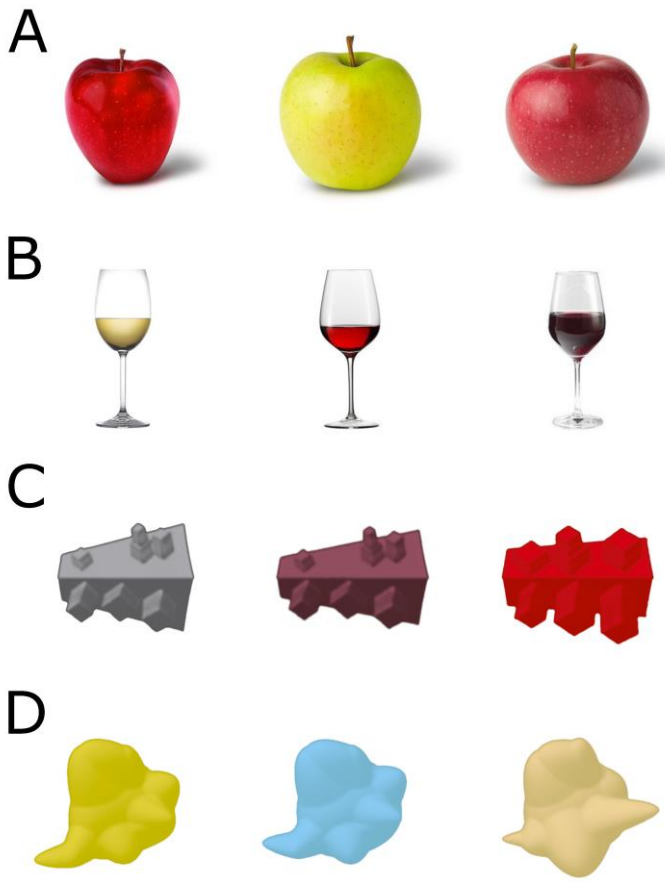

Figure 3.1: Familiar visual object categories; (A) three exemplars of an apple, (B) three exemplars of a wine glass. Unfamiliar visual object categories; (C) three exemplars of a cubie, (D) three exemplars of a smoothie. All stimuli taken from Smith and Goodale (2015), and modified from Op de Beeck, Torfs, and Wagemans (2008).

3.3.3. Apparatus and materials.

A 64-channel slim active electrode system (Brain Products GmbH: BrainVision actiCAP) with a BrainAmp MR64 PLUS amplifier was used for the EEG data acquisition (see Section 3.3.5. below for more information). The Karolinska Sleepiness Scale (KSS; Akerstedt, Anund, Axelsson, & Kecklund, 2014; Åkerstedt & Gillberg, 1990) was used to measure participant's sleepiness during the five minutes prior to the end of the experiment. This scale is rated on a Likert scale from 1-9 with the following options: 1) extremely alert, 2) very alert, 3) alert, 4) rather alert, 5) neither alert nor sleepy, 6) some signs of sleepiness, 7) sleepy, but no

effort to keep awake, 8) sleepy, some effort to keep awake, and 9) very sleepy, great effort to keep awake, fighting sleep. We included this scale to test whether participants attention and/or drowsiness correlated with overall levels of occipital alpha activity (Niedermeyer & da Silva, 2005).

3.3.4. Procedure.

Upon arrival, participants signed informed consent and the EEG cap was mounted. Once the cap was installed, participants received both verbal and written instructions for the task and were trained via practice trials. Before beginning the experiment, each participant was shown their eye blinks and muscle artifacts (e.g. teeth grinding) on the EEG monitor to emphasize the importance of remaining still during EEG recording, and was asked to blink between trials where possible. During the experiment, participants sat in a dimly lit room. A black and white fixation cross with a black border remained in the centre of the screen throughout the entirety of a block, and each block began and ended with 2000ms of fixation against a white background. After the initial 2000ms fixation, 12 individual stimuli were displayed in a randomly allocated order, meaning each unique stimulus was presented once per block. Each stimulus trial began with 1000ms of fixation, followed by a stimulus presentation of 1000ms whereby the fixation remained on the screen. Each stimulus offset followed a variable delay of fixation for 1500-1900ms. There were 50 blocks in total, however 10 of which were catch blocks. In a catch block, a red and green fixation cross with a black border (28 x 28 pixels) was displayed over one of the stimuli at random.

Participants were instructed to remain fixated on the central fixation cross in order to detect whether there was a colour change in the fixation cross during a block. Participants were asked to pay attention to the stimuli which would appear behind the fixation cross, but to remain fixated at all times. At the end of an experimental block, a question screen appeared which asked participants whether they had detected a red and green fixation cross. Participants were instructed to press one of two buttons on a four-button response device with their right hand in order to answer yes or no, thus eliminating the need for a motor response during experimental trials (see also Smith & Goodale, 2015 for a similar approach). Participants would receive a break screen after their response, enabling them to take a break before the

next block if they wished to do so. Every 10 blocks, participants received a longer break in which the screen offset was controlled by the experimenter. During this break, the participant was checked on by the experimenter and offered water to aid alertness during the experiment. In total, each participant was exposed to 40 repetitions of each unique stimulus, resulting in 240 familiar visual objects, and 240 unfamiliar visual objects after removing the catch blocks. The main experiment lasted approximately 40-50 minutes.

At the end of the main experiment, participants were asked to complete the KSS (see Section 3.3.3. above) to indicate their sleepiness on a scale from 1 (extremely alert) to 9 (very sleepy, great effort to keep awake, fighting sleep) during the five minutes before completing the rating. This was included since attention and/or drowsiness has previously been found to correlate with overall levels of occipital alpha activity (Niedermeyer & da Silva, 2005). Then, since a key feature of mu suppression is its occurrence both when an individual observes or executes an action (Pfurtscheller et al., 1996), participants were asked to complete a voluntary motor response task in order to map the mu rhythm in relation to a physical motor response. In this experiment, a central black and white fixation cross with a black border remained in the centre of the screen with a white background throughout the entire block. Participants were instructed to fixate on the black and white central fixation cross and press one button from a four-button response device with their right index finger approximately every six seconds. The fixation cross was included to ensure task engagement when making button responses. Each participant was encouraged not to count in their head to avoid alpha contamination (Hobson & Bishop, 2016). Participants completed 40 trials of the button pressing, separated in to four blocks of 10 trials which lasted approximately 5-10 minutes total. On completion of the voluntary motor response task, the EEG cap was dismounted and hair washing facilities were offered to all participants. Participants were debriefed before leaving the room. The entire session lasted no more than two hours per participant.

3.3.5. EEG data acquisition.

The electroencephalogram (EEG) was recorded with a 64-channel slim active electrode system (Brain Products GmbH: BrainVision actiCAP) embedded in a

nylon cap (international 10/20 localisation system), with a BrainAmp MR64 PLUS amplifier. One electrode (FT9) was removed from the cap and placed diagonally below and away from the outer canthus of the left eye in order to monitor vertical eye movements (lower EOG). The reference electrode was placed on the tip of the participant's nose (as in Pfurtscheller, Neuper, Andrew, & Edlinger, 1997), and electrode FT10 was moved to the location of FCz, in order to record from the position where the reference electrode is usually embedded in this cap. The ground electrode was located in the position of FPz. The continuous EEG signal was acquired at a high sampling rate of 1000 Hz. Impedance was kept equal to or less than 50kΩ before recording started.

3.3.6. EEG data pre-processing.

All EEG data pre-processing was performed using the open toolbox EEGLAB (Delorme & Makeig, 2004), used within MATLAB (The MathWorks, USA, 2017b). Raw data from both the main experiment and voluntary motor response task were pre-processed according to the following steps. First, imported data were and high- and low-pass filtered between 0.1 Hz and 50 Hz to remove low-frequency drifts and high-frequency noise respectively. All practice trials, catch blocks, and break periods were then manually removed from the continuous data. A 50 Hz notch filter was also applied to reduce electrical noise. A vertical EOG (VEOG) was reconstructed offline by subtracting the lower EOG from FP1 activity. A horizontal EOG (HEOG) was also constructed by subtracting F7 from F8 activity (Renoult et al., 2015). Independent component analysis (ICA) was then ran on the data to detect eye blink artifacts, which were clearly identified and removed when inspecting components and scalp maps. Finally, data was cleaned using the artifact subspace reconstruction (ASR) plugin developed by Kothe and Jung (2016; Patent No. 14/895,440). See also Chang, Hsu, Pion-Tonachini, and Jung (2018) and Mullen et al. (2013). The ASR interpolated artifact bursts with a variance of more than 5 standard deviations different from the automatically detected clean data (see Gabard-Durnam, Mendez Leal, Wilkinson, & Levin, 2018; Grummett et al., 2014). Data segments post-ASR were then rejected with a time-window rejection criterion of 0.25, meaning the segment was rejected if more than 0.25 of channels were marked as bad. Any channels marked as bad in this process were interpolated, and any

remaining noisy electrodes were interpolated based on computing kurtosis with a threshold of 5 using spherical method (Bigdely-Shamlo, Mullen, Kothe, Su, & Robbins, 2015). This resulted in an average of 2.59 electrodes interpolated (*SD* = 1.72, range 0-5). The cleaned data was then epoched from -1000ms to 1500ms, time-locked to stimulus onset (or time-locked to the button press if the voluntary motor response task), with a baseline correction of -1000ms. Finally, step-like artifact detection was carried out on all electrodes on the epoched data (with the exception of the lower EOG electrode) using a threshold of 100μV and moving window of 200ms in 50ms steps (see Luck, 2005). An average of 0.39% (*SD* = .01, range 0 – 5.21%) of trials were rejected during the entire cleaning process.

3.3.7. Regions of interest.

Two regions of interest (ROI)'s were created for both the univariate and multivariate pattern analysis (MVPA). In line with Coll et al. (2017), ten central electrodes were selected for the central ROI (C1-2-3-4-z, CP1-2-3-4-z). Furthermore, eight occipital electrodes were selected for the occipital ROI (PO3-4-7-8-z, O1-2-z). The central ROI was created to compare the effects of mu rhythm suppression and content specificity to the different visual object categories in each condition (familiar, or unfamiliar visual objects). The occipital ROI was created as a control region to rule out potential confounds by changes in attentional engagement from occipital alpha activity (see Hobson & Bishop, 2016).

3.3.8. Data analysis.

3.3.8.1. Behavioural analysis.

Behavioural data for the main experiment was analysed based on correct detection of a red and green fixation cross, or correct rejection of no colour change during a block. Any failures to detect a colour change, or detection of an absent red and green fixation cross was classified as an incorrect response. An average accuracy was calculated for each participant.

3.3.8.2. Univariate cluster-based analysis.

Univariate time-frequency analysis was conducted at the channel level by computing the power of event-related desynchronization/synchronization (ERD/ERS) using event-related spectral perturbations (ERSP)'s. The ERSP is a known measure of average dynamic changes in amplitude of the specified broad band EEG frequency spectrum, as a function of time relative to an experimental event (Cuellar & Toro, 2017; Makeig, 1993; Pfurtscheller & Lopes, 1999). To obtain the time-frequency data, a short-time Fourier transform was computed across the averaged baseline-corrected trials by extracting 200 time points in steps of 10ms, using a Hanning-tapered sliding time window with a fixed length of 500ms, covering the entire epoch from -1000ms to 1500ms. Here, a divisive baseline was used relative to the -1000ms to 0ms time period (Ciuparu & Mureşan, 2016; Marini et al., 2019). Power was calculated from 1-30 Hz in steps of exactly 1 Hz. Such analyses were conducted in both central and occipital ROIs and applied to both conditions of familiar and unfamiliar visual object categories, in addition to the voluntary motor response task. Mean changes in spectral power are expressed in decibels (dB).

To avoid circular inference (see Kriegeskorte, Lindquist, Nichols, Poldrack, & Vul, 2010; Kriegeskorte, Simmons, Bellgowan, & Baker, 2009), oscillation clusters were then identified by selecting all pixels across the time-frequency plots during stimulus duration (0-30 Hz, 100 time points corresponding to 0-1000ms) in both the central and occipital ROIs which were statistically significant based on the average ERSP data of *all conditions* (M. Cohen, 2014), at a significance level of 0.01. Once the precise boundaries of the significant clusters had been defined, the cluster masks were applied separately to each condition (familiar and unfamiliar visual objects) and ROI (central and occipital). The data from each mask and each participant was then extracted and averaged. The average ERSP data was also extracted from the voluntary motor response task by identifying significant clusters based on the ERSP data from the button press.

Overall, a single averaged ERSP value was extracted in each ROI and condition from the mask created from each significant cluster. Paired-sample parametric *t*-tests were then conducted to compare differences between ERSP data for familiar and unfamiliar visual objects. A single ERSP value was also extracted

from each cluster and ROI from the voluntary motor response task for each participant. Effect sizes for all *t*-tests are calculated as Cohen's $d = t / \sqrt{N}$ (Lakens, 2013).

3.3.8.3. Univariate time-frequency window analysis.

The univariate ERSP data from the main experiment (see Section 3.3.8.2. above for information on how this data was extracted) was also analysed for significant desynchronization within strictly selected alpha and beta frequency bands for each ROI (central and occipital) averaged over stimulus duration (0-1000ms time-locked to stimulus onset). The frequencies selected were between 8-13 Hz for alpha, and 15-25 Hz for beta (Coll et al., 2017). This additional analysis was done in order to match the univariate desynchronization data exactly to the frequency bands selected for the MVPA (see Section 3.3.8.5. below for comparison to MVPA). To test whether the ERSP data showed significant synchronization/desynchronization, we performed one-sample parametric *t*-tests against zero (baseline). All paired *t*-tests are reported as two-tailed at the $p < .05$ level with Bonferroni corrections applied. Effect sizes for all *t*-tests are calculated as Cohen's $d = t / \sqrt{N}$.

3.3.8.4. Correlation analysis.

In order to examine whether participants subjective ratings of sleepiness correlated with occipital alpha activity (Niedermeyer & da Silva, 2005), a correlation analysis was ran using participants scores from the KSS (see Section 3.3.3. above) against all conditions and ROIs.

3.3.8.5. Multivariate pattern analysis.

The MVPA was trained on single-trial ERSP data using a linear support vector machine (LIBSVM 3.20 toolbox; C. Chang & Lin, 2011) and tested against the average pattern from each visual object category (see Smith & Smith, 2019). The pattern classifiers were trained to discriminate between object identity within our two conditions: familiar or unfamiliar visual object categories. For example, in the familiar object condition, the classifier was trained to discriminate between an apple

and a wine glass. A k-fold cross validation approach was used to estimate this performance, whereby the model was built from k – 1 subsamples (70% of trials) and tested on the average of the remaining independent k subsample (30% of trials). Therefore, the classifier was trained with 168 single trials (84 trials for each visual object category; e.g. apples and wine glasses), and tested on decoding performance against the average of 72 trials (36 for each visual object category) in each condition. This was carried out in both the alpha (8-13 Hz) and beta (15-25 Hz) frequency bands (see Coll et al., 2017; Cuellar & Toro, 2017), in both the central and occipital ROI's, to test whether discriminable patterns of information could be detected for different familiar or unfamiliar visual objects in each ROI and frequency band. This analysis was performed on 20 randomly partitioned training test set iterations across the entire 1000ms stimulus duration time window. Overall, one decoding accuracy was obtained for each condition, separated by ROI and frequency band for each participant.

To test whether group level decoding accuracy was significantly above chance, we performed one-sample parametric *t*-tests on all MVPA analyses, against the chance level of 1/2 (50%). Significance values are reported as one-tailed due to prior expectations of the direction of the results. To control for multiple comparisons, all decoding accuracies are corrected using false discovery rate (FDR). The adjusted q-value at ≤ .05 resulted in a significance value of FDR $p \leq .016$ for all results (Benjamini & Yekutieli, 2001). Effect sizes for all *t*-tests are calculated as Cohen's $d = t / \sqrt{N}$. All effect sizes are to be identified as small (> .2), medium (> .5), and large (> .8) according to Cohen's (1988) classification of effect sizes.

3.4. Results

3.4.1. Behavioural accuracy.

The mean accuracy of catch trial detection was 99.56% (*SD* = 1.01%, range = 96% - 100%), thus indicating that participants were very good at detecting the absence or presence of a red and green fixation cross during a block. Participants sleepiness ratings covered the full scale, with an average of 5.74 (*SD* = 2.03, range 1 - 9). Average response times for the voluntary motor response task were 6838ms (*SD* = 933ms, range 5497 – 7244ms).

3.4.2. Univariate results: Cluster-based analysis.

For the univariate analysis, significant clusters were first identified via a data-driven approach, to investigate where there were significant differences in power across the 1-30 Hz frequencies. The purpose of this analysis was to determine whether a mu rhythm desynchronization could be detected from merely viewing the familiar graspable objects. We also tested whether a mu rhythm desynchronization could be detected in the voluntary motor response task.

3.4.2.1. Main experiment central ROI.

When examining the significant clusters of both conditions averaged together in the central ROI, we observed significant synchronization over the delta/theta band covering stimulus duration and peaking around 100-400ms post stimulus onset, and significant desynchronization covering the beta band, also spanning stimulus duration and peaking over 200-600ms (see Figure 3.2A). Data from these clusters were then extracted separately for each condition (familiar or unfamiliar object categories; see Figure 3.2A). Note that the actual significant pixels for familiar and unfamiliar visual objects are displayed in Appendix F, Figure F-1, however to keep the number of pixels matched across both conditions and avoid circular inference, the masks based on the average of both conditions were used to extract the data (Figure 3.2A). The synchronization over the delta/theta band was found to be strongly significant for both familiar (M = .454, t_{26} = 7.918, p < .001, d = 1.524) and unfamiliar (M = .463, t_{26} = 6.174, p < .001, d = 1.188) visual object categories. Further pairwise comparisons revealed these were not significantly different from one another (t_{26} = .157, p = .876). The desynchronization from the beta band was also strongly significant for both familiar (M = -.272, t_{26} = -5.333, p < .001, d = -1.026) and unfamiliar (M = -.309, t_{26} = -6.252, p < .001, d = -1.203) visual object categories. Once again, further pairwise comparisons revealed these were not significantly different from one another (t_{26} = -1.207, p = .238). A bar chart displaying the averaged ERSP values can be seen in Figure 3.2B. Taken together, the results from the central ROI show that observation of graspable objects, regardless of familiarity with the object, causes desynchronization in the beta frequency band. In

contrast to our expectations, there were no such significant effects found within the mu rhythm in these analyses.

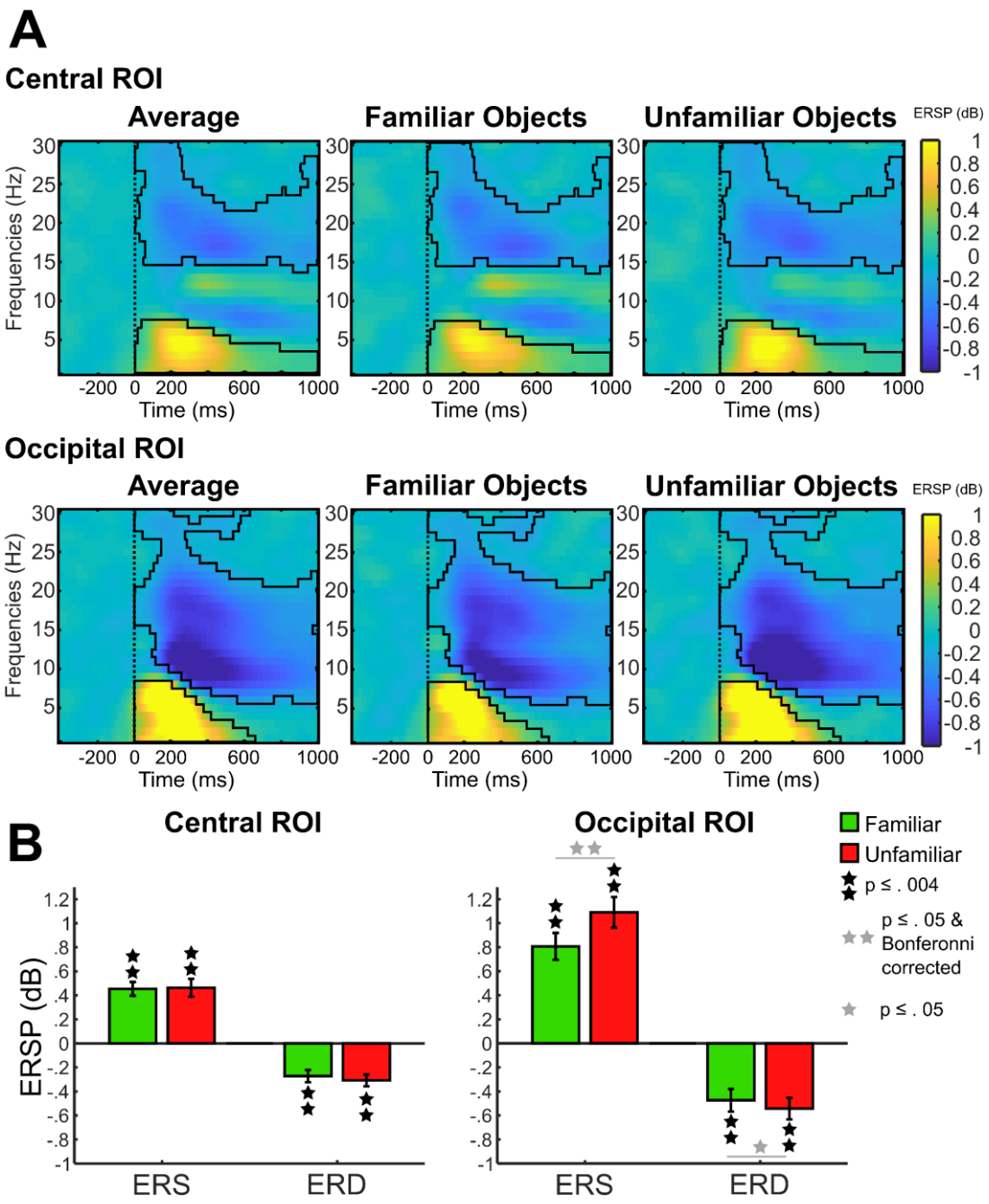

Figure 3.2: Univariate results from the cluster analysis. (A) The significant pixels taken from the average ERSP data from both familiar and unfamiliar objects, in both central and occipital ROIs. The raw ERSP data taken from this mask is visually shown for both conditions of familiar and unfamiliar visual objects. (B) Average ERSP values in each significant cluster for both central and occipital ROIs. Significant differences between conditions are shown.

3.4.2.2. Main experiment occipital ROI.

When we examined the significant clusters of both conditions averaged together in the occipital ROI, we observed significant synchronization over the delta/theta band from 0-600ms and peaking between 0-400ms post stimulus onset, and significant desynchronization covering the alpha/beta band, spanning stimulus duration and peaking between 200-600ms (see Figure 3.2A). Data from these clusters were then extracted separately for each condition (familiar or unfamiliar object categories; see Figure 3.2A). Note that the actual significant pixels for familiar and unfamiliar visual objects are displayed in Appendix F, Figure F-1, however to keep the number of pixels matched across both conditions and avoid circular inference, the masks based on the average of both conditions were used to extract the data (Figure 3.2A). The significant synchronization covering the delta/ theta combined frequency bands was significant for both familiar (M = .807, t_{26} = 7.230, p < .001, d = .1.391) and unfamiliar (M = 1.090, t_{26} = 8.547, p < .001, d = 1.645) visual object categories. Here, mean synchronization for familiar and unfamiliar visual object categories were significantly different from one another (t_{26} = 3.298, p = .003, d = .635). The significant desynchronization covering the alpha and beta combined frequency bands was significant for familiar (M = -.474, t_{26} = -4.985, p < .001, d = -.959) and unfamiliar (M = -.543, t_{26} = -6.057, p < .001, d = -1.166) visual object categories. Further pairwise comparisons revealed the mean desynchronization for familiar and unfamiliar visual object categories were different from one another (t_{26} = -2.177, p = .039, d = -.419), however, this result did not survive Bonferroni correction at a corrected p value of .013. A bar chart displaying the exact averaged ERSP values can be seen in Figure 3.2B. The results in the occipital ROI suggest a strong desynchronization can be found over both the alpha and beta frequency bands in response to viewing both the familiar and the unfamiliar visual object categories, in which the suppression appears to be slightly stronger for viewing unfamiliar visual objects compared to familiar.

3.4.2.3. Voluntary motor response task central ROI.

Three significant clusters were identified in the central ROI for the voluntary motor response task, as seen in Figure 3.3A. A significant desynchronization was

found over the alpha band central electrodes (the mu rhythm), beginning at the onset of button press and lasting approximately 1000ms, with the peak around 400-800ms (M = -.712, t_{26} = -5.297, p < .001, d = -1.019). Another significant desynchronization was found over the beta frequency band, spanning around -100ms to 200ms time-locked to the button press, with the peak around 0-200ms (M = -.457, t_{26} = -6.419, p < .001, d = -1.235). Finally, significant synchronization was found over the beta frequency band, spanning around 500-1000ms post-button press, peaking around 700-1000ms (M = .590, t_{26} = 4.517, p < .001, d = .869). These results show a strong mu rhythm desynchronization can be found when participants completed a simple button-press experiment, demonstrating the mu rhythm can easily be detected when participants execute a physical motor response.

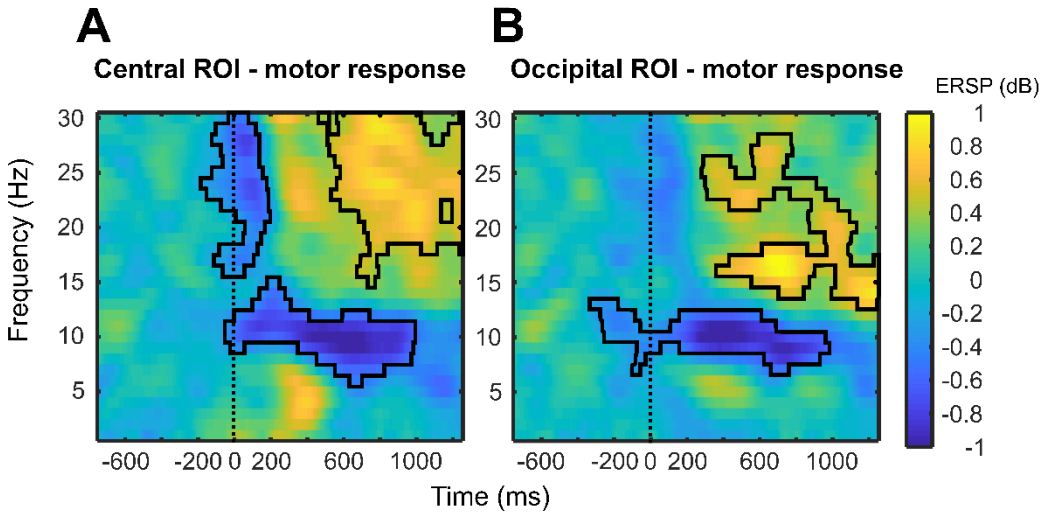

Figure 3.3: Univariate results from the cluster analysis. The significant pixels corresponding to the ERSP data from the voluntary motor response task are outlined in both central and occipital ROIs.

3.4.2.4. Voluntary motor response task occipital ROI.

Two significant clusters were revealed in the occipital ROI for the voluntary motor response task (see Figure 3.3B). Significant desynchronization was found in the alpha frequency band from around -200ms to 1000ms time-locked to button press, and peaking around 200-600ms (M = -.653, t_{26} = -4.502, p < .001, d = -.866). Significant synchronization was also found in the beta frequency band, lasting from

around 300-1000ms post-button press, and peaking around 600-800ms (M = .572, t_{26} = 4.469, p < .001, d = .860). These results show that the alpha band also attenuates in the occipital ROI in response to execution of a button press.

3.4.3. Univariate results: Alpha- and beta-band analysis.

The univariate data was also analysed within strictly selected alpha and beta frequency bands for each ROI (central and occipital) averaged over stimulus duration (0-1000ms time-locked to stimulus onset), in order to match the univariate desynchronization data exactly to the frequency bands selected for the MVPA.

3.4.3.1. Main experiment central ROI.

When restricted to the 8-13 Hz frequency band, no significant desynchronization was found for either familiar (t_{26} = -.042, p = .967) or unfamiliar (t_{26} = -1.160, p = .257) visual object categories. Similar to the cluster-based analysis, the beta (15-25 Hz) frequency band revealed significant desynchronization for both the familiar (M = -.251, t_{26} = -4.630, p < .001, d = -.891) and unfamiliar (M = -.284, t_{26} = -5.296, p < .001, d = -1.019) visual object categories. Further pairwise comparisons revealed there were not significantly different from one another within the beta band (t_{26} = 1.001, p = .326). These results (see Figure 3.4) compliment the cluster-based analysis, suggesting no significant desynchronization within the mu rhythm frequency band, yet significant desynchronization for both visual object categories in the beta frequency band.

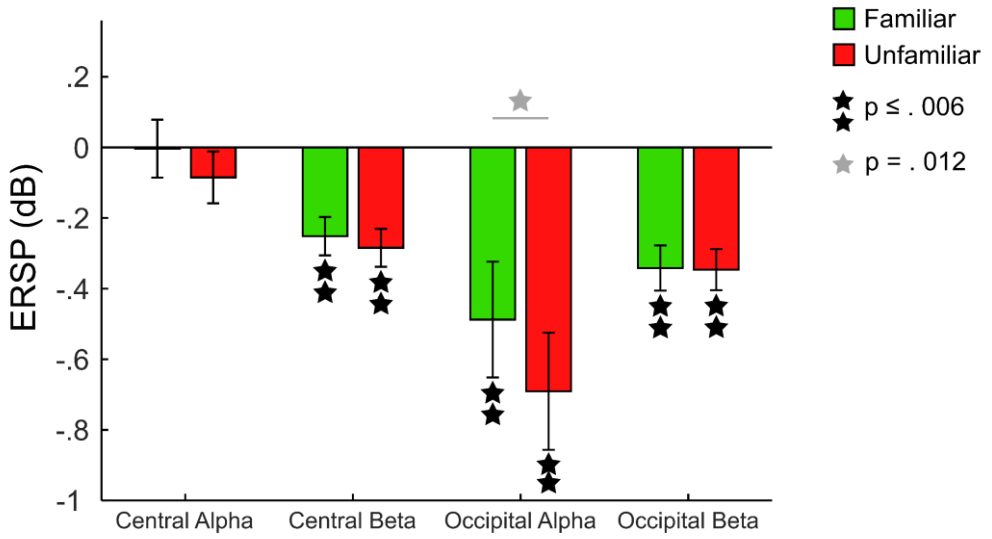

Figure 3.4: Univariate results from the alpha- and beta-band analysis. Figure shows the ERSP data in response to viewing both familiar and unfamiliar objects, in both central and occipital ROIs.

3.4.3.2. Main experiment occipital ROI.

The 8-13 Hz frequency band in the occipital ROI revealed significant desynchronization for familiar (M = -.488, t_{26} = -2.972, p = .006, d = -.572) and unfamiliar (M = -.691, t_{26} = -4.161, p < .001, d = .801) visual object categories. Further pairwise comparisons revealed these to be significantly different from one another (t_{26} = 2.711, p = .012, d = .522). In the beta (15-25 Hz) frequency band, significant desynchronization was also found for both familiar (M = -.342, t_{26} = -5.336, p < .001, d = -1.027) and unfamiliar (M = -.346, t_{26} = -5.949, p < .001, d = -1.145) visual object categories. Further pairwise comparisons revealed these were not significantly different from one another (t_{26} = .164, p = .871). These results (see Figure 3.4) compliment the cluster-based analysis, showing alpha and beta desynchronization for both visual object categories. Interestingly, when separating the alpha and beta band rather than looking at the combined cluster, we find the alpha band shows significant differences in desynchronization for the familiar and unfamiliar visual objects, with stronger attenuation for viewing the unfamiliar objects compared to the familiar objects.

3.4.4. Correlation analysis.

The results from the correlation analysis revealed no significant correlations between each participant's subjective sleepiness ratings and any alpha activity across all conditions and ROI's (all *p*'s ≥ .321). As such, we can assume participants feelings of drowsiness throughout the experiment did not influence any of the alpha desynchronizations that we observe.

3.4.5. Multivariate pattern analysis results.

In order to determine whether content-specific information regarding the familiar visual objects could be decoded from the mu rhythm frequency band, we computed cross-validated decoding performance of visual object category independently for each condition (familiar and unfamiliar visual objects) in the central and occipital ROI, for both the alpha (8-13 Hz) and beta (15-25 Hz) frequency bands. The analysis was conducted across stimulus duration (0-1000ms time-locked to stimulus onset). Therefore, this analysis matched the univariate alpha- and beta-band analysis (see Section 3.4.3. above).

3.4.5.1. Central ROI.

Remarkably, significantly above chance decoding was found for the familiar visual object categories in the central alpha (mu rhythm) frequency band (M = 57.31%, t_{26} = 2.268, p = .016, d = .436; see Figure 3.5). Conversely, such decoding effects were not found for the unfamiliar object categories (t_{26} = .670, p = .509). Further paired samples tests showed these decoding accuracies were not significantly different from one another (t_{26} = .921, p = .366). Interestingly, no significant decoding was found for either familiar (t_{26} = -.746, p = .462) or unfamiliar (t_{26} = .026, p = .980) visual object categories in the central beta frequency band. These results show, despite a lack of desynchronization in the mu rhythm in the univariate analysis, discriminable information regarding the familiar, but not unfamiliar, visual object categories can be found in the mu rhythm oscillatory response.

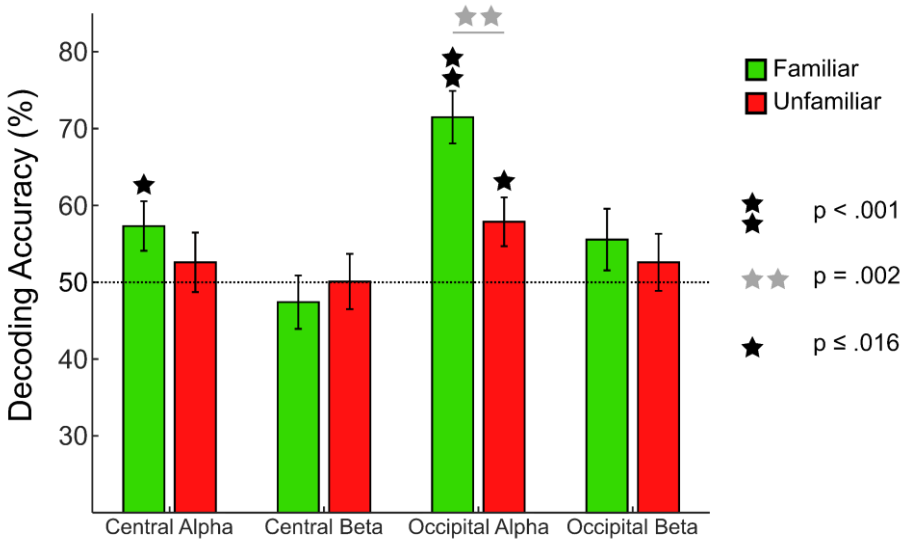

Figure 3.5: Decoding of object identity within each visual object category. Cross-validated two automatic forced choice decoding performance for each stimulus category (familiar and unfamiliar objects) for each frequency band and ROI.

3.4.5.2. Occipital ROI.

As can be seen in Figure 3.5, strong significant decoding was found for familiar visual object categories in the occipital alpha frequency band (M = 71.48%, t_{26} = 6.284, p < .001, d = 1.209). Significant decoding was also found for unfamiliar object categories (M = 57.87%, t_{26} = 2.478, p = .010, d = .477). Interestingly, further comparisons revealed decoding for familiar visual object categories to be significantly higher than decoding for unfamiliar visual object categories (t_{26} = 3.124, p = .002, d = .601). No significant decoding was found for either familiar (t_{26} = 1.385, p = .178) or unfamiliar (t_{26} = .699, p = .491) visual object categories in the occipital beta frequency band. These results show discriminable information for both conditions of familiar and unfamiliar visual object categories in the alpha frequency band, which compliments the desynchronization results in the univariate analysis. However, interestingly the familiar visual objects are significantly more discriminable than the unfamiliar visual objects, which is in contrast to the univariate analysis which reveals stronger desynchronization for the unfamiliar objects in the occipital alpha frequency band. Decoding was not significant for either object

category in the beta frequency band, which is interesting given strong significant desynchronization was found within the beta band in the univariate analysis.

3.5. Discussion

The present study revealed viewing different familiar visual objects which participants have had a rich haptic prior experience with can be significantly discriminated in the mu rhythm oscillatory response, despite no tactile stimulation or motor response during the experiment. Interestingly, no reliable information related to viewing different images of unfamiliar visual object categories was found in the mu rhythm. These results thus suggest connections from vision to sensorimotor areas may transmit content-specific information about familiar, but not unfamiliar, visual object categories, in which this information can be detected in the alpha frequency patterns generated by clusters of neurons in sensorimotor areas. Furthermore, univariate analysis investigating changes in event related spectral power revealed significant attenuation in the central beta frequency band when viewing both familiar and unfamiliar objects, whilst no such attenuation was found in the mu rhythm. These findings suggest content specific information from vision to sensorimotor areas may occur in specific oscillation frequencies, and highlight how the analysis technique employed can answer different questions about the role of the mu rhythm in response to viewing different visual object categories.

3.5.1. Connections from vision to sensorimotor areas trigger content specific information in the mu rhythm oscillatory response.

The findings from the current study corroborate that of Smith and Goodale (2015), who found content-specific information about different familiar visual objects could be sent from vision to S1 when participants viewed the same stimuli. Here we have expanded on Smith and Goodale's study by finding a likely oscillatory marker for such cross-modal processes that dominates the alpha, and not beta, frequency band. This is because content-specific information could be decoded in the mu rhythm oscillatory response when participants viewed the different familiar, but not the unfamiliar, visual objects. Since both the present study and Smith and Goodale found no such decoding for the unfamiliar visual objects, this suggests a

rich prior haptic experience with the object is necessary to produce such effects. If the underlying effect is originating from S1, then these results are in line with a variety of previous research which has also found content-specific information belonging to supposedly unisensory modalities can be sent cross-modally to an entirely independent sense (Bailey et al., 2019; Meyer et al., 2011, 2010; Vetter et al., 2014; see also Chapter 2). We expand on this literature by showing, for the first time, that EEG can be used to find information specific to the content of different familiar visual objects can be sent from vision to sensorimotor areas when simply viewing them, despite the fact the mu rhythm is functionally related to motor and tactile related activity in sensorimotor cortex (for a review, see Pineda, 2005; see also Cheyne, 2013). As such, we suggest electrophysiological connections from vision to S1 may transmit content-specific information only about different familiar visual objects that convey rich tactile information.

It is important to note that due to the weak spatial resolution of EEG it may be the case that the significant decoding we observe in the mu rhythm oscillation could be originating from M1, especially since we found weak evidence for a degree of information about hearing the sound of familiar hand-object interactions in M1 (see Chapter 2; see also Bailey et al., 2019). However, since Cheyne et al. (2003) attributed the suppression of the mu rhythm to activity in S1, and suppression of the central beta rhythm to activity in primary motor cortex (M1), and Smith and Goodale (2015) found decoding for viewing familiar visual objects only in S1, and not M1, we have reason to believe the effects we observe originate from S1.

These results have provided a valuable contribution to understanding the role of the mu rhythm oscillatory response, building upon previous research such as that of Coll et al. (2017) who suggested the mu rhythm contains specificity to the somatosensory features of observed and executed actions. Interestingly, they only found such specificity for tactile stimulation and real object use in mu rhythm activity when using *cross-modal* MVPA methods (e.g. trained on observation of actions, tested on execution of actions). It is important to note here that cross-modal classification would not have been possible in the present experiment since participant passively viewed still images of object stimuli and no action execution task was required. Interestingly however, when Coll et al. used *uni-modal* MVPA (e.g. trained on observation of actions, tested on observation of actions), such as in

the present study, little specificity for somatosensory features of actions was found, since widespread above-chance decoding was found for all conditions. This finding supports the meta-analysis by Foxe et al. (2016) who suggested the specificity of the mu rhythm is insensitive to differences between conditions. We on the other hand provide some support for the specific content of information in the mu rhythm oscillation by finding different familiar visual objects can be reliably discriminated when using uni-modal MVPA methods (e.g. trained and tested on the observation of an object). We suggest that familiarity with the tactile (or motor) features of an object may be a critical component for specificity, since discriminable information between the different unfamiliar visual objects could not be detected. However, it is important to note that this claim must be interpreted with caution, since the significant decoding for the familiar visual objects was not significantly higher than the non-significant decoding of the unfamiliar visual objects. Furthermore, we show such discriminable information is present when no action is performed. Whilst previous research has found significant attenuation within the mu rhythm when viewing images of tools which elicit motor affordances (see for example Proverbio, 2012), this is the first study to find the content of such information can be discriminated in the mu rhythm when viewing static images of familiar objects. Taken together, these results strongly suggest the mu rhythm oscillation receives information about the tactile and/or motor components of objects which participants have had a rich haptic prior experience with.

The fact we find discriminable information in the mu rhythm specific to the content of static images of familiar graspable objects challenges previous research which suggests the mu rhythm is simply a measure of mirror neuron activity. To reiterate, a review by Hobson and Bishop (2016) suggests that whilst mu suppression can be used to measure mirror neuron activity, the observed effects are weak and unreliable when observing actions compared to the strong effects observed from executing actions. We do not argue against the notion that mu suppression can be used to measure the mirror neuron system, as numerous research has indeed found firing of cells over sensorimotor cortex are desynchronised during performance of, observation of, or imagining to perform an action (see for example Arnstein et al., 2011; Fox et al., 2016; Muthukumaraswamy et al., 2004; Pfurtscheller et al., 1997). Rather, we emphasize the fact that the mu rhythm can be used to answer more

questions beyond the function of the mirror neuron system, specifically highlighting how different analysis methods can provide new insights into the key function of the mu rhythm oscillatory response.

For example, our research suggests the content of information which is likely being sent to sensorimotor cortex via feedback connections from a distal area of cortex, in our case, visual cortex or high-level multisensory convergence zones, can be measured in the mu rhythm when using multivariate pattern analysis techniques which cannot be detected in simple univariate responses. Most previous research has analysed mu rhythm attenuation to measure sensorimotor cortex activation. To directly compare this to our results would suggest viewing and executing actions, or receiving tactile stimulation, is pivotal to detect a mu rhythm response. This is because no significant attenuation was found in the mu rhythm when viewing either different familiar or unfamiliar object categories in the present study, whereas we find strong significant attenuation when participants performed a voluntary motor response task. However, a crucial finding is the fact discriminable information about the different familiar visual objects can be detected in the mu rhythm when analysing the data at the multivariate level. This result highlights how research should consider adopting a strong focus on multivariate classification techniques to further understand the role of the mu rhythm (see also Coll et al., 2017), since this method has higher sensitivity and power to detect fine-grained differences in the representational content of the data (see Norman et al., 2006).

The reason why we find information specific to the content of only familiar, and not unfamiliar, visual object categories in the mu rhythm may be reflective of predictive coding processes in the brain (see Clark, 2013 for a review; see also Chapter 1, Section 1.4.2.). The predictive coding account suggests high-level areas in the brain predict expected incoming sensory inputs, in turn projecting these predictions down to low-level areas via feedback connections (see Kok & De Lange, 2015). Of interest is the fact that previous research has suggested low-frequency oscillations, such as alpha, conveys feedback related information (Bonaiuto et al., 2018). Furthermore, alpha activity has been found to originate in deep cortical laminae known to convey feedback information (Bonaiuto et al., 2018), such as from pyramidal cells in layer V of cortex (Buffalo et al., 2011; L. R. Silva et al., 1991; W. Sun & Dan, 2009), with further research suggesting cells in layer V are the cortical

origin of the alpha rhythm (F. L. Da Silva & Van Leeuwen, 1977). Research has previously found convincing evidence that predictions are implemented in such deep cortical layers (Rao & Sejnowski, 2002), specifically in S1 (Yu et al., 2019). Therefore, it is possible that the decoding we see in the mu rhythm reflects predictions being sent from high-level cortical areas about the tactile and/or motor features of the different familiar objects based on predictive coding theories of brain function (Clark, 2013). Future research could consider replicating Smith and Goodale's (2015) research at 7-Tesla fMRI to determine which layers of S1 receive content-specific information about the different familiar visual objects, to see whether the content within each layer correlates with mu rhythm activity. If the same participants were tested from the EEG and 7-Tesla fMRI study, we may expect to find information specific to the content of different familiar visual objects in the mu rhythm oscillatory response from the EEG, which is also detectable in either the deep or superficial layers of S1 from the 7-Tesla fMRI study, since such layers have previously been found to be more engaged for cortico-cortical predictive feedback input (Yu et al., 2019).

However, our results do not uniquely support predictive coding as the reason behind the effects we have observed. Another reason why we find information specific to the content of only familiar visual objects in the mu rhythm may be due to the fact participants naturally paid more attention to an object they were familiar with rather than an unfamiliar object. However, since spectral power changes in the occipital alpha oscillation are sensitive to attentional engagement (Hobson & Bishop, 2016), and we actually found stronger desynchronization for viewing the *unfamiliar* objects compared to the familiar objects, this suggests it is unlikely that we are merely measuring engagement of attention to objects that participants are more familiar with. However, it could be interesting for future research to test participants after haptic exploration of the unfamiliar objects via 3D printing in order to determine whether experience with the objects is needed in order for these effects to emerge. In this case, we may find discriminable information for both different familiar and unfamiliar visual objects in the mu rhythm oscillation, and no differences in desynchronization, once participants have explored the haptic properties of the unfamiliar objects, when compared to participants who receive no training. Whilst this would not directly test predictive coding theories per se, it

would strongly support the importance of prior experience with the haptic and/or motor properties of the objects to observe such effects in the mu rhythm oscillation.

3.5.2. The central beta oscillatory response to observation of graspable objects.

An additional interesting finding is the significant desynchronization observed in the central beta oscillation in response to participants viewing both familiar and unfamiliar graspable objects. These responses were not significantly different from one another, suggesting no familiarity effects in the central beta band, but rather viewing any graspable object in general can elicit central beta band desynchronization. The significant attenuation is not a surprising finding given previous research has found the central beta oscillation is involved in action related processes such as motor imagery, passive movement, and action observation (Zaepffel et al., 2013). However, interestingly, whilst significant desynchronization was observed in the central beta band when viewing graspable objects, multivariate analysis revealed no above chance decoding in the same frequency band for either visual object category. We note Coll et al. (2017) found similar results in their uni-modal classification analysis, supporting the idea that the central beta oscillation lacks specificity for discriminating between different object categories. Rather, it seems the central beta oscillation can classify between an observed or executed action (Coll et al., 2017), and may even play a role in movement planning (see also Tucciarelli, Turella, Oosterhof, Weisz, & Lingnau, 2015; Turella et al., 2016), however it fails to distinguish between different action types or different tactile properties of objects. Here, these results once again highlight the importance of using different analysis techniques to answer different questions about oscillatory responses.

Another interesting finding is the clear difference of attenuation found between the main experiment and the voluntary motor response task in the central beta oscillation. Neuper, Wörtz, and Pfurtscheller (2006) found beta band suppression during preparation of movement, followed by a strong rebound beta synchronisation after movement, which occurs whilst the mu rhythm continues to desynchronise. This is exactly what we see in the voluntary motor response task and is important to highlight for two reasons. First, this directly indicates how central

alpha and beta frequency bands exhibit different dynamics (as previously suggested by Pfurtscheller, Pregenzer, & Neuper, 1994), emphasizing the importance of separating these frequency bands to answer different questions regarding cortex function. This contrasts with previous research which suggests the central alpha (mu rhythm) and central beta frequency bands are closely related to one another during action production and gesture observation (Quandt, Marshall, Shipley, Beilock, & Goldin-Meadow, 2012). Future research should consider an EEG source-based analysis or magnetoencephalography (MEG) study in order to estimate the location of neural activation found in the alpha and beta frequency bands. Indeed, previous research has found mu and beta correspond to different sources in the primary somatosensory and motor cortex (Cheyne, 2013; Cheyne et al., 2003; Hari & Salmelin, 1997). Based on our results, one might expect that the mu rhythm desynchronization corresponds to the tactile feel of the button press in S1, whereas the beta desynchronization corresponds to the motor plan of the button press in M1 or pre-motor cortex (Tucciarelli et al., 2015; Turella et al., 2016). Second, the difference in desynchronization between the main experiment and the voluntary motor response task emphasizes the importance of separating observation and execution conditions to answer different questions about the central beta oscillation, in line with Coll et al. (2017) who suggested the central beta oscillation can classify between an observed or executed action yet fails to show specificity to different action types, such as action with a real object or pantomime action.

3.5.3. Occipital alpha may reflect top-down synchronous activity when viewing graspable objects.

The results found in the occipital alpha frequency band may reflect top-down neuronal processes underlying perception of objects, since the alpha frequency has previously been suggested to play an important role in directing information flow through the brain and allocating resources to relevant regions (Haegens, Handel, & Jensen, 2011; Jensen & Mazaheri, 2010). The univariate analysis revealed significant desynchronization in the occipital alpha/beta cluster in response to viewing both familiar and unfamiliar visual object categories, in which the suppression was significantly stronger for unfamiliar objects in the alpha band when restricting the analyses to precise frequency boundaries. The overall attenuation may be a reflection

of increased blood flow to the visual cortex during perception, since Perry and Bentin (2009) have previously found a relationship between alpha suppression recorded posteriorly and BOLD responses in parietal and visual cortex. Scheeringa et al. (2011) also found alpha suppression reflects the magnitude of the MRI response in visual cortex during a visual attention task. The reason why attenuation was stronger for the unfamiliar objects in the occipital alpha band may be a result of a novelty effect, since previous research has demonstrated stronger occipital alpha desynchronization following presentation of a novel stimulus compared to a familiar expected stimulus (Harrison, 1946; Mulholland & Runnals, 1962).

We argue this difference is not simply a confound of expectation about the onset of the stimulus or attentional engagement which are known to influence alpha activity (see e.g. Hobson & Bishop, 2016; Pfurtscheller, 1992). Tight controls were adopted in this experiment to account for such confounds; for instance, maintaining constant fixation with a variable delay eliminated the risk of forming an expectation about when the stimuli might appear (Samaha et al., 2015). Furthermore, the results of the correlations between KSS scores (Akerstedt et al., 2014; Åkerstedt & Gillberg, 1990) and occipital alpha desynchronization suggest no significant relationship between feelings of sleepiness, therefore attentional engagement, and the power of attenuation in the occipital alpha frequency band. Finally, if the stronger suppression in the occipital alpha oscillation for viewing unfamiliar objects compared to familiar objects is due to stronger attention paid to these stimuli, we may expect to find a significantly stronger suppression in the mu rhythm also. This is because Hobson and Bishop (2016) argue the mu rhythm is easily confounded with occipital alpha suppression. However, we do not find the same pattern of results in the mu rhythm oscillatory response, with the strength of desynchronization between viewing familiar and unfamiliar objects not being significantly different from one another.

Interestingly, the multivariate analysis in the occipital alpha band revealed significant decoding when viewing both visual object categories, which shows a reverse effect to the univariate analysis whereby decoding is significantly stronger for viewing *familiar* visual object categories when compared to unfamiliar visual objects. We suggest this difference is due to the different analysis techniques detecting different aspects of the oscillatory response, since multivariate analysis has more power to detect fine-grained differences in the *representational* content of the

data (Norman et al., 2006). As mentioned previously, Bastos et al. (2012) suggested the alpha frequency coordinates the feedback of predictions to low-level areas, however occipital alpha in particular is known to transmit prior knowledge and expectations to visual cortex, such as in a perceptual decision making experiment (M. T. Sherman et al., 2016). As such, it may be the case that viewing familiar objects could be better read out from occipital alpha activity due feedback cortical pathways transmitting information relating to previous knowledge about the different familiar visual objects.

It is important to note that the direction of the multivariate effect in the occipital alpha band is similar to the multivariate effect in the central alpha band (mu rhythm), meaning in both cases decoding is stronger for viewing familiar compared to unfamiliar objects. Once again, decoding accuracies were significantly different from one another in the occipital alpha band, yet not in the mu rhythm, thus suggesting no occipital alpha confounds in the mu rhythm (Hobson & Bishop, 2016). Instead, the reason why the effect is similar (yet weaker) in the mu rhythm may be a case of more information being fed back to occipital cortex than sensorimotor cortex regarding the stored knowledge about the familiar objects (Martin, 2016), since feedback information is suggested to oscillate at an alpha frequency (Bastos et al., 2012). To confirm this idea, an interesting avenue for future research could consider conducting the multivariate analyses in the gamma (40-80 Hz; Seymour, Rippon, Gooding-Williams, Schoffelen, & Kessler, 2018) frequency range in both occipital and central electrodes, since information processing in this frequency is coherent with activity in superficial layers of cortex (Buffalo et al., 2011). This is important since feedforward connections predominantly arise from superficial layers of cortex (Barone, Batardiere, Knoblauch, & Kennedy, 2000; Buffalo et al., 2011). Furthermore, research has suggested gamma conveys feedforward information (Van Kerkoerle et al., 2014). Therefore, if gamma reflects feedforward processing, we would expect to find above chance decoding for both familiar and unfamiliar visual objects in the occipital gamma oscillation, yet no above chance decoding in the central gamma oscillation. Furthermore, we would expect to find no differences between decoding accuracies for familiar and unfamiliar visual objects in the occipital gamma band if this frequency reflects feedforward input, since Smith and Goodale (2015) found no significant differences in decoding between viewing

familiar and unfamiliar visual objects in V1. This idea is further supported by previous research which has found gamma activity most strongly and significantly contributed to explaining BOLD variance (Scheeringa et al., 2011) or changes in contrast (S. P. Koch, Werner, Steinbrink, Fries, & Obrig, 2009) in human visual cortex.

3.6. Conclusion

In summary, this study has shown that simply viewing still images of different familiar visual object categories which participants have had a rich haptic prior experience with can be discriminated within the mu rhythm oscillatory response. In contrast, no such decoding effects were found when participants viewed still images of different unfamiliar visual object categories. As such, this is the first known study to date to find content-specific information about different familiar visual object categories can be detected from vision to sensorimotor areas using EEG as the analysis technique. In doing this we have shown, for the first time, evidence for the precise temporal communication of information, thus a potential oscillatory marker, of cross-sensory effects from vision to sensorimotor cortex. Finally, we highlight the importance of using different analysis techniques to extract different types of information from neural oscillations. We emphasize the need for research to focus on multivariate analysis techniques which can read out fine-grained pattern information from oscillatory responses, in turn answering new questions that simple analyses on attenuation of power fail to detect.

CHAPTER 4

–

Exploring predictive coding as an account of cross-modal influences in the brain

4.1. Abstract

Over recent years, research has shown even the primary sensory cortical regions of the human brain display remarkable effects of high-level context such that, for example, primary somatosensory regions can discriminate different hand-object sounds. These effects are consistent with theories of predictive coding, which suggest the role of even the primary sensory regions is not to passively register incoming sensory stimuli, but rather to develop internal models about the world and actively test them against prior experience. Here, we used real familiar objects in a functional magnetic resonance imaging (fMRI) experiment to directly test whether predictive coding mechanisms may account for such multisensory information being present in primary somatosensory cortex (S1). In an event-related design, right-handed participants (N = 18) first viewed either a tennis ball, or a plastic cup, placed directly in front of them (the prime phase), followed by either the same or a different object (the target phase). In the target phase, participants either continued to view the object, or reached out to touch the object with their right hand. MVPA results showed that whilst S1, and other motor-related cortical regions, could significantly decode between whether the participant viewed or touched the object, no significant decoding was found for object identity for any of the trial types following FDR corrections. The pattern we observed for decoding in S1 revealed stronger decoding when the target object was incongruent with the prime object. Interestingly, when running the analysis in the finger-sensitive voxels of left S1 (defined from an independent finger-mapping localizer to the right hand), this pattern was reversed. We discuss our findings with respect to predictive processing operating across sensory modalities, but also to alternative reasons why we believe we observed such effects along with possible limitations of the study.

Keywords: cross-modal, multisensory, multi-voxel pattern analysis, predictive coding, S1. (5)

4.2. Introduction

Whilst traditional views of cortex function assume the primary sensory cortices in the brain passively register incoming sensory information which belongs to its respective modality (see Carandini et al., 2005 for such an example of the visual system), it is becoming increasingly apparent that a primary sensory cortex can receive information which was not traditionally thought to belong to that primary sensory region (see Driver & Noesselt, 2008; Ghazanfar & Schroeder, 2006 for reviews). This has been further demonstrated in studies which have found content-specific information about a specific stimulus can be transmitted to a primary sensory modality independent to that of the source of stimulus presentation (for a detailed review, see Chapter 1, Section 1.3.3.). For example, information specific to the content of a visual stimulus which implies rich tactile information can be reliably discriminated in primary somatosensory cortex (Meyer et al., 2011; Smith & Goodale, 2015). Similarly, a visual stimulus which implies auditory information can be distinguished in primary auditory cortex (Meyer et al., 2010). Furthermore, content-specific information about auditory stimuli which imply visual or haptic features have been observed in early visual cortex (Vetter et al., 2014), or primary somatosensory cortex (see Chapter 2, see also Bailey et al., 2019), respectively. What remains unclear, however, is the functional significance behind these cross-modal effects which have been observed. The present study aims to address this unanswered question, specifically by investigating whether the identified cross-modal effects are consistent with key aspects of predictive coding.

Predictive coding theories suggest that the function of any cortical region, even the primary sensory cortices, is not to passively register incoming sensory information, but rather to generate hypotheses about what is likely to happen based on prior experience with the world, and test them against the incoming sensory input, in turn actively predicting possible future stimulation (see Clark, 2013). To do this, the idea is that any given cortical region comprises two neuronal populations; prediction units and prediction error units (Friston, 2005; Kok & De Lange, 2015). It is thought that prediction units represent the hypotheses the brain has predicted based on prior experience with the situation, whereas prediction error units represent the difference between these predictions and the veridical sensory input (Kok, 2016).

This theory suggests the neural activity in the primary sensory areas underlying perception involves a combination of these neuron populations, whereby each cortical area is actively building an internal model of the likely forthcoming stimulation and continuously comparing this expectation with the actual sensory input received until all information is explained (see Chapter 1, Section 1.4.2. for a detailed review).

Functional magnetic resonance imaging (fMRI) can be used to detect and separate likely markers of predictions from prediction errors in the human brain when measuring the amplitude of the neural response in a given cortical area using univariate analysis, and the representational content of the information in that cortical area using multi-voxel pattern analysis (MVPA). When measuring a predicted or unpredicted event in terms of the amplitude of the neural response, cancellation theories suggest we prioritise unexpected events (prediction errors) by suppressing the neural response of expected input (predictions). Indeed, research has found predictable sensory inputs have been found to evoke less neural activation in the brain (Bays et al., 2006; Blakemore et al., 1998; Kikuchi et al., 2019; Limanowski et al., 2018; Richter et al., 2018). Other research has found primary cortical regions suppress predicted input, suggesting more weight is added to unexpected outcomes which may be more important to explain (Alink et al., 2010; Bays & Wolpert, 2007; Lee & Mumford, 2003; Murray et al., 2002). As a compliment to a reduced neural amplitude, a few studies have found the *representational content* of the neural response to be stronger for an expected outcome. For example, fMRI studies investigating both vision (Kok & De Lange, 2015; Kok et al., 2012) and action (Yon et al., 2018) related expectations used MVPA to find expected events were better decoded compared to unexpected events. This has been further supported in single neuron studies investigating stimulus expectations in the Macaque brain (Bell, Summerfield, Morin, Malecek, & Ungerleider, 2016). As such, the amplitude of the neural response does not necessarily relate to the representational content of the data within that cortical region (Press et al., 2020).

However, Bayesian models propose that neural processing in cortical regions may assign more weight on sensory channels to an *expected* event, since this could help to enhance the generated percept of the subsequently perceived event (de Lange

et al., 2018; Kaiser et al., 2019). If this is the case, an alternative explanation is that a neural suppression of an expected stimulus actually reflects a suppression of the unexpected *features* of that stimulus. This would thus result in a 'sharpened' percept of the event, with the neural response reflecting a more selective population of neurons tuned to the expected event, producing a lower amplitude overall (see de Lange et al., 2018; see also Yon, Zainzinger, De Lange, Eimer, & Press, 2019). Indeed, a noteworthy study found that whilst a reduced neural amplitude in primary visual cortex (V1) was apparent when participants were presented with different orientations of expected visual gratings (in line with cancellation models - see above), this reduced amplitude was actually stronger in neurons which preferred the *non-presented* orientation (Kok et al., 2012). Since voxels preferring an unexpected orientation produced a stronger suppression, this suggests more weight may actually be added to expected input by suppressing activity in the specific voxels which prefer *alternative* stimuli (Den Ouden et al., 2009; Summerfield & De Lange, 2014). Indeed, more recent research investigating prediction with real action has found a reduction in neural activity for expected hand actions only for the voxels tuned *away* from, not towards, the expected action (Yon et al., 2018). These studies agree with the suggestion that the brain may incorporate a 'sharpening' account of prediction (Friston, 2005; Lee & Mumford, 2003). The sharpening account suggests the neural representation of an expected event is not merely suppressed as redundant information, but rather reflects a sharpened response which actively enhances the representation of the stimulus (Kok et al., 2017). In other words, if sensory input is accurately predicted, the idea is that this information has pre-activated the corresponding cortical area, thus resulting in a sharp, accurate representation of the input (Press et al., 2020).

Relating predictive coding theories specifically to the cross-modal context effects identified in the previous literature (Bailey et al., 2019; Meyer et al., 2010, 2011; Smith & Goodale, 2015; Vetter et al., 2014), it may be the case that the primary sensory cortices are actively predicting their likely future stimulation before the stimulation has even happened. To take the findings from Smith and Goodale (2015) as one example, they found content-specific information could be detected in primary somatosensory cortex (S1) when participants simply viewed static images of familiar objects which implied rich tactile information, such as a wine glass. The

reason why such information could be detected may be because neurons in S1 received predictions containing information about the tactile sensation of the wine glass in the event of a possible subsequent interaction (Clark, 2013). Here, predictive coding theories provide an elegant framework to help explain *why* information specific to the content of the original source can be detected in a supposedly entirely independent primary cortical area.

Whilst the theory of predictive coding provides a convincing argument as to why such cross-modal effects have been observed, the studies introduced to date do not provide a direct test that suggests predictive coding is indeed the key component which is guiding these effects. This is a necessary area of study because there are other plausible theories which can explain why such cross-modal effects have been observed in previous research. For example, they may simply reflect activations of a broader representation of the stored knowledge of an object (see for example Martin, 2016). Martin's (2016) representation of object concepts theory suggests the neural representation of object concepts is distributed across the perceptual, action, and emotion systems in the brain. Furthermore, Barsalou (2016) suggests object perception or categorization involves a neural re-use of the same systems which were active when a person stored the initial representation of an object in the brain (see also Anderson, 2010). This could also explain why we have previously found discriminable information about certain stimuli in cortical areas independent to that of stimulus presentation.

As such, one way to test the potential involvement of *predictive coding* in this context, rather than the potential representation of object concepts in the brain, could be to develop an experiment which asks participants to physically interact with real 3D objects which may or may not be predicted based upon a visual prime of either the same or a different real 3D object. In doing this, we could determine whether a purely *visual* prime of a real 3D object can influence the neural representation of the object in *tactile*-related cortices when physically asked to subsequently interact with it. If we find any differences in the neural representation in a region such as S1 based upon either a congruent or incongruent visual prime, we could argue that the observed cross-modal effects must reflect some information processing beyond activations of a broader representation of the stored knowledge of an object (Martin, 2016). This is because in both cases, the object the participant

interacts with would be exactly the same, yet any observed differences would be based upon how the previous object influenced the expectation of interacting with the subsequent object. Furthermore, this would build on Smith and Goodale (2015) by indicating that the cross-modal context effects that have previously been observed are relevant for aiding subsequent object interactions.

To measure such an experimental paradigm would require physical interaction with real 3D objects whilst in an MRI scanner. Such an experimental set-up is a rare and novel approach, yet has been tested before when investigating how the brain responds to 3D tool use (Brandi, Wohlschlager, Sorg, & Hermsdorfer, 2014; Gallivan, McLean, Valyear, & Culham, 2013; Hermsdörfer, Terlinden, Mühlau, Goldenberg, & Wohlschläger, 2007; Imazu, Sugio, Tanaka, & Inui, 2007; Valyear, Gallivan, McLean, & Culham, 2012). Other research has also used such a set-up when investigating different types of hand actions toward artificial 3D objects (Cavina-Pratesi, Goodale, & Culham, 2007; Rossit et al., 2013), or when viewing real objects in the scanner (Snow et al., 2011). One study in particular found viewing repetitions of real 3D tools led to a reduced neural signal amplitude in parietal and pre-motor areas, thus suggesting passive viewing of tools can activate the corresponding sensorimotor areas relating to their conventional use (Valyear et al., 2012). As such, we borrowed the real action methodology from this rich line of previous studies investigating the neural correlates of acting with real 3D objects.

Following from the literature discussed, the current study aims to directly examine, for the first time, whether the cross-modal context effects which have previously been found from vision to S1 (Meyer et al., 2011; Smith & Goodale, 2015) can be explained by the assumptions of predictive coding theories of human brain function. To do this, participants were asked to view and subsequently interact with real 3D objects (either a tennis ball, or a plastic cup) placed directly in front of them in an MRI scanner. On each trial, participants were first shown an object (prime phase) and were subsequently shown a second object (target phase) which was either consistent or inconsistent with the primed object. We anticipated, based on theories of predictive coding, that interacting with objects in the target phase that were consistent with the object viewed in the prime phase would yield a suppressed neural response, complimented with a greater representation of the object in S1 (Kok et al., 2012). On the other hand, if the primed visual object is inconsistent with the

target object, we may expect a stronger neural amplitude complimented with a weaker representation of the object in S1. Note that in either case, we investigated differences in the neural amplitude and neural representation of the *exact same* object interaction in S1. For example, we aimed to examine whether the neural representation of a physical interaction with a real tennis ball would differ as a function of either a consistent visual prime of a tennis ball, or an inconsistent visual prime of a plastic cup.

4.3. Methods

4.3.1. Participants.

Right-handed healthy participants (N = 18; 9 male), with an age range of 19-29 years (M = 23.33, SD = 2.97), participated in this experiment. All participants reported normal or corrected-to-normal vision, normal hearing, and no history of neurological or psychiatric disorders. Participants were deemed eligible after meeting MRI screening criteria, approved by the radiology department at the Norfolk and Norwich University Hospital (NNUH). Written consent was obtained in accordance with approval from the Research Ethics Committee of the School of Psychology at the University of East Anglia, in addition to approval from NNUH. Participants received £10 per MRI hour, and £8 per behavioural hour for their time.

4.3.2. Design.

A 2 x 2 design was used with two factors. The first factor was the congruency of the primed object with the target object, which consisted of two levels (Valid, or Invalid). The second factor was task, which consisted of two levels (View, or Touch). As such, there were four trial types (see Figure 4.1) as follows: in a Valid-View trial, the participant saw an object (the prime), and viewed the same object again in the target phase (e.g. primed with a cup, then viewed a cup). In an Invalid-View trial, the participant was primed with an object, and subsequently viewed a different object in the target phase (e.g. primed with a cup, then viewed a ball). In a Valid-Touch trial, the participant was primed with an object, and was then asked to reach out and touch the same object in the target phase (e.g. primed with a cup, and

then asked to reach out and touch a cup). In an Invalid-Touch trial, the participant was primed with an object, and then asked to reach out and touch a different object in the target phase (e.g. primed with a cup, then asked to reach out and touch a ball). These four trial types will now be referred to as Valid-View, Invalid-View, Valid-Touch, and Invalid-Touch trials from this point onwards.

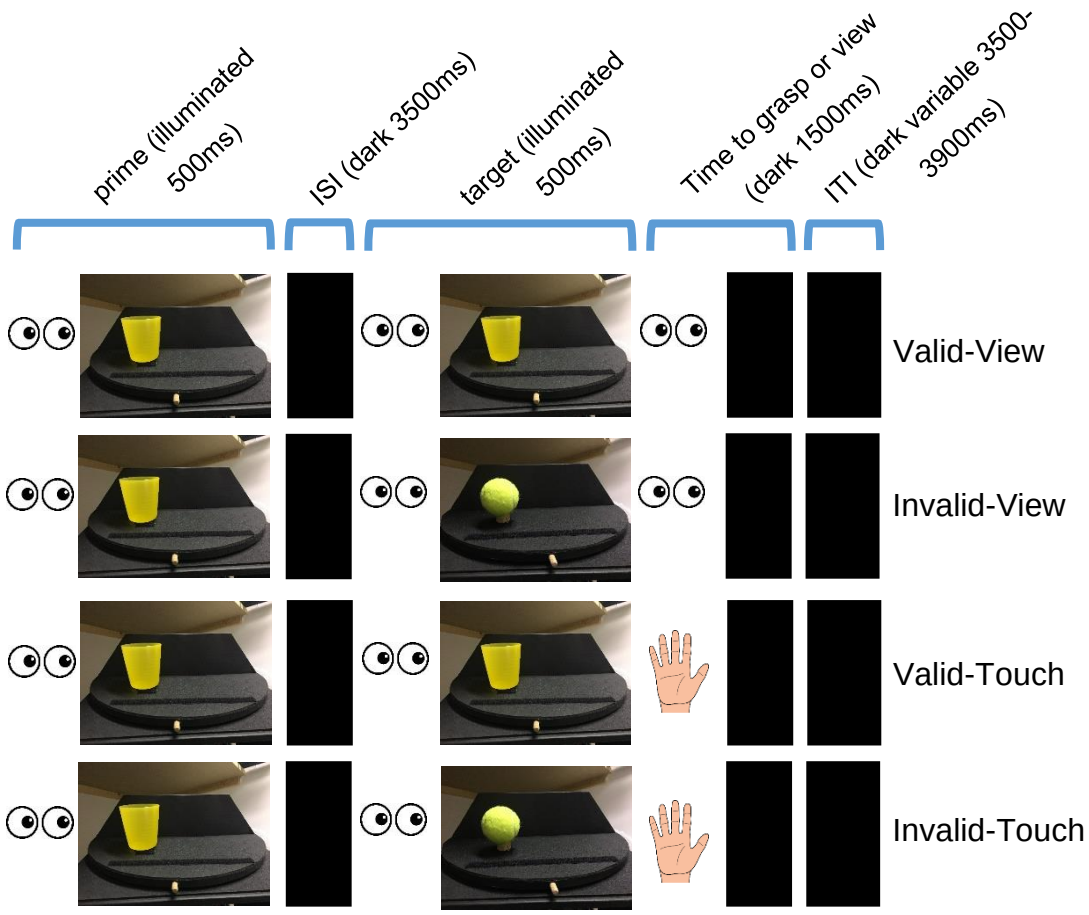

Figure 4.1: An example of the four trial types during the experiment when the cup was presented first. The participant was in complete darkness meaning the object could only be seen when illuminated. In each trial, the participant would first view the illuminated object in the prime phase. Then, the same or a different object would become briefly illuminated for a second time at the start of the target phase. The participant would hear the instruction to continue to view or to reach out and touch the object they saw the second time. The command was then executed in the dark. Each trial lasted 6000ms. Note four more trial types were used whereby the ball was presented first.

4.3.3. Stimuli.

Two different real 3D objects were used; a yellow tennis ball and a yellow plastic cup (see Figure 4.1). These objects were chosen for the reason that they comprise different tactile properties and motor functions and participants should have prior experience of interacting with both objects. The tennis ball conformed to the standard criteria for size and weight of a tennis ball, with a circumference of 21cm. The plastic cup had a 280ml capacity, with the circumference around the middle of the cup also being 21cm.

4.3.4. Apparatus and materials.

Both objects were presented on a turntable apparatus (see Figure 4.2, see also Snow et al., 2011; Valyear et al., 2012). Use of the metal-free turntable enabled direct viewing of the hand workspace without the use of mirrors. The dimensions of the turntable were set up in accordance to the dimensions of the wide bore MR scanner at NNUH. The visual workspace was 40cm width, 20cm depth, and 10cm height. A red Light Emitting Diode (LED) attached to a flexible plastic stalk (LOC-LINE; Lockwood Products, Inc., Lake Oswego, OR, USA) was positioned centrally above the visual workspace to allow for more natural viewing conditions and to avoid discomfort by viewing downwards towards the turntable apparatus (Cavina-Pratesi et al., 2007). Furthermore, as mentioned by Cavina-Pratesi et al. (2007), this allowed the objects to be presented in the participant's lower visual field which is typical of everyday situations when interacting with objects. Following a pilot session, a black square piece of cardboard was attached to the underside of the LED to ensure no reflection of the light onto the objects. A camera and infrared source (MRC Systems GmbH, Germany) were attached to the left side of the turntable, positioned behind the participants head and facing towards the object in the visual workspace. This enabled validation of the correct object being displayed, and the correct task being executed, throughout the experiment. An illuminator with white LED's was also attached to the table beside this camera, which allowed viewing of the object during a trial since the participant was situated in complete darkness. A second camera with infrared lights was attached to the head coil on the right side of the participant and angled towards the participant's right eye to enable confirmation

of stable eye movements across the experiment (see Figure 4.2 for a detailed example of the set-up).

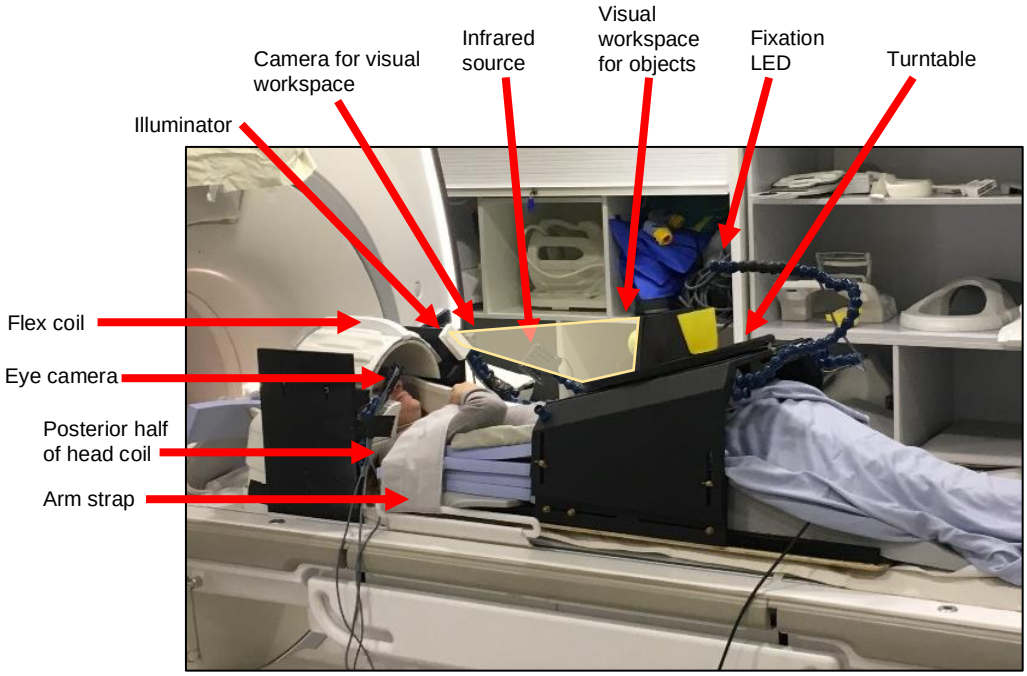

Figure 4.2: fMRI set-up for real action experiments (adapted from Rossit et al., 2013). The participant lies supine with the head tilted to enable direct viewing of real 3D objects placed on a turntable without the use of mirrors. The turntable can be rotated by the experimenter between trials to change the object in view. Here, a real 3D tennis ball is placed in front of the participant's visual field, and a real 3D plastic cup is placed on the other side of the turntable. Flexible stalks are used to position a red LED fixation point, illuminator and MR-compatible cameras to record hand and eye movements. The participant's upper arm is restrained such that movements can still be made with elbow, wrist and fingers. Between actions, the hand will rest in a comfortable home position as shown. Auditory cues regarding the tasks are presented through MR-compatible earphones. During the experiment the scanner room is completely dark and the object and workspace can only be seen when illuminated.

4.3.5. Procedure.

Participants were invited to a training session before the main scanning day to be familiarised with the equipment and briefed about what to expect during the MRI scan. On the scan day, participants signed informed consent and were screened by the radiographers at NNUH before entering the scan room. Participants were then

set up in the turntable apparatus (see Section 4.3.4 above; see also Figure 4.2). To do this, the participant was asked to lay supine on the scan bed in the turntable so that their shoulders touched the top of the bed and their head was tilted (~20-30°) with foam padding (NoMoCo Pillow, La Jolla, CA, USA) to enable direct viewing of the objects placed in front of them. Both objects were placed on the left side of the visual workspace of the turntable apparatus. The centre of the left-most edge of the object (the position where the right hand would grasp) was placed 8.5cm from the left side of the edge of the table, and the centre of the front-most edge of the object being placed 7cm from the front of the turntable. This was done in order to keep the grasping positions as similar as possible across the two objects.

Participants placed Sensimetric earphones (Sensimetrics, Woburn MA, USA) in their ears and the sound was checked until played at a self-reported comfortable level (as in Leaver & Rauschecker, 2010; Man, Damasio, Meyer, & Kaplan, 2015; Man, Kaplan, Damasio, & Meyer, 2012; Meyer et al., 2010). Foam padding was placed around the crown of the participant's head to minimise head movement, avoiding the ears to ensure no pressure on the earphones which could cause discomfort during the experiment. The squeeze ball was placed in the left hand and the left arm was placed by the participant's left side. Foam padding was used under the participant's right arm until the right elbow was in line with the height of the turntable, thus maintaining a comfortable position for grasping the objects (see Figure 4.2). The upper right arm was then secured with a Velcro^{TM} strap to restrict shoulder movements yet allow full movement of the lower arm, including the elbow and wrist (as in Rossit et al., 2013). The participants were then instructed to fold their right arm diagonally across the chest with the hand in a fist on the left side of their chest; this was the resting position which was to be maintained throughout the experiment unless instructed otherwise. Participants were asked to confirm they could see the objects at the angle their head was tilted at. Finally, participants were asked to practice reaching out and grasping the two objects by placing their four fingers behind the object and thumb in front of the object to ensure the reaching distance was optimal for their arm length. Once they had finished practicing, participants were told to maintain the same grasp on the object throughout the experiment for consistency.

During the experiment, participants were situated in complete darkness and instructed to remain fixated on the red LED fixation presented above the objects in the centre of their visual field, which remained constant throughout the entire experimental run. This ensured the participant was unaware of which object was placed in front of them when the object was not illuminated. Using a custom built script in MATLAB (The MathWorks, USA, 2010a) and the Psychophysics Toolbox (Brainard, 1997), each run began and ended with 12s silent blocks of fixation from the red LED. After the initial 12s fixation, a trial began with an object illuminated for 500ms (the prime phase), followed by a 3500ms ISI until an object was illuminated again for a subsequent 500ms (the target phase). There was then an additional 1500ms for the participant to execute the task in darkness. Therefore, the trial lasted 6000ms, followed by a 3500 - 3900ms variable ITI until the next trial. Participants were informed that on each trial they would see an object become illuminated (the prime), and when they saw the object illuminated for a second time (the target), they would simultaneously hear the verbal instruction 'View' or 'Touch'. If participants heard the word 'View', they were instructed to remain looking at the LED fixation. If participants heard the word 'Touch', they were asked to reach out and touch the object in front of them using a natural grasp whilst remaining fixated on the LED fixation. All hand movements were executed in the dark after the illumination to reduce activation due to viewing the motion of the hand (Cavina-Pratesi et al., 2007). Participants were informed they had a 2000ms time window to reach out, comfortably grasp the object, and return to resting position. In order to produce these trial types, an experimenter was positioned in the scanner room next to the turntable and would hear the commands to move the turntable appropriately through MR-compatible headphones.

During any experimental run, 40 trials were executed in a randomly allocated order, with 10 repetitions of each trial type, resulting in a total run time of 465s. Overall, most participants completed 6 runs (M = 5.67, SD = .77, range 4 - 7), thus, participants were exposed to approximately 60 repetitions per trial type (either Valid-View, Invalid-View, Valid-Touch or Invalid-Touch; see Figure 4.1).

On a separate day, a subset of participants took part in a somatosensory localiser to map the region of S1 which corresponded to the fingers on the right hand (N = 10). On entering the scanner, the participant was asked to lay on the scanner

bed whilst Piezo-electric stimulator pads (Dancer Design, UK) were placed against the participant's thumb, index finger, middle finger, and ring finger of the right hand using Velcro (four pads total; see Appendix B, Figure B-1 for an example of the equipment demonstrated from the set-up in Chapter 2). Each pad contained a 6mm diameter disk centred in an 8mm diameter static aperture. The disks stimulated the participant's right hand using a 30 Hz sine wave, with the Dancer Design amplifier set at 7. Foam padding was used under the right arm for comfort, and the participants rested their right hand on foam padding which was placed on their abdomen. During an experimental run, participants were given no instruction except to relax, avoid any movement and keep fixated on a point in the scanner. In a block design (12s on, 12s off), participants received 15 blocks of stimulation to the right hand and 15 blocks of baseline. Localiser blocks lasted approximately 348s each. On average, each participant completed 2 somatosensory mapping runs (M = 1.9, SD = .57, range 1-3), thus resulting in approximately 30 stimulation blocks of the right hand. Participants were debriefed after completion of each session.

4.3.6. MRI data acquisition.

Structural and functional MRI data was collected using a 3T MR scanner (GE Discovery 750 Wide-Bore, NNUH, Norwich, England). A combination of phased-array coils were used to achieve good signal-to-noise ratio and whole brain coverage; the posterior half of a 21-channel head neck unit (HNU) coil at the back of the head, with a small flex coil at the front (see Rossit, et al., 2013; see also Figure 4.2 above). This use of parallel channels also allows the coil to be tilted to enable direct viewing of the turntable without the use of mirrors (see Rossit et al., 2013). T1 weighted anatomical images of the whole brain were acquired using a three-dimensional BRAVO sequence (196 volumes, voxel size =1mm^3). Blood-oxygen level dependent (BOLD) signals were recorded using an echo-planar imaging (EPI) sequence: (233 volumes, TR = 2000ms, TE = 30ms, flip angle 78, 35 slices, matrix 64 x 64, voxel size 3.3mm^3, slice thickness 3.3mm, interslice gap 3.3mm, field of view 211). Sound instructions were presented via an in-ear hi-fi audio system (Sensimetrics, Woburn MA, USA).

On a separate day, a miniature Piezo Tactile Stimulator (mini-PTS; developed by Dancer Design, UK) was used to deliver vibro-tactile stimulation to

the hands. Here, data was collected using the same MR scanner with only the 21-channel HNU coil. Both anatomical and functional scans were acquired using the same sequence as the main real action experiment, with the exception that there were 174 volumes in the functional scans for the somatosensory localiser data. All MRI data acquired was routinely checked for incidental findings by the consultant radiologist at NNUH.

4.3.7. MRI data pre-processing.

All MRI data was pre-processed in Brain Voyager 20.4 (Brain Innovation, Maastricht, The Netherlands; Goebel et al., 2006). We used cubic spline slice scan time correction and 3D motion correction (sinc interpolation), with defaults for temporal filtering. Functional data for each run was then separately co-registered to each participants ACPC anatomical scan. No Talairach transformations were applied to avoid removing valuable fine-grained pattern information from the data that may be useful for MVPA analysis (see Chaper 2, also Argall, Saad, & Beauchamp, 2006; Bailey et al., 2019; Fischl, Sereno, Tootell, & Dale, 1999; Goebel et al., 2006; Kriegeskorte & Bandettini, 2007).

4.3.8. Regions of interest.

Due to time constraints, regions of interest (ROIs) for the primary somatosensory cortex (S1) were created using the anatomical masks defined in Chapter 2 (see also Bailey et al., 2019). All anatomical masks from this previous experiment were transformed into Talairach space and overlaid. A probability map with 30% cut-off was used to create a standard mask which was transformed into each participants ACPC brain, resulting in a mask which will henceforth be described as $S1_{mask}$ (see Appendix G Figure G-1). A second ROI was created for S1 from the somatosensory localiser data. Here, a $15mm^3$ cube was created around the peak voxel from each participant's tactile localiser data. This was created to localise the specific region of S1 which is sensitive to stimulation on the fingers from each participant's right hand, and will henceforth be referred to as $S1_{localiser}$. We experienced difficulty in data acquisition of one participant and failed to find activation in S1, thus $N = 9$ for the creation of $S1_{localiser}$. For a probability map of the

$S1_{localiser}$ ROI in our 9 participants, see Appendix H, Figure H-1. We note the finger-selective localisation methods differ from that of Chapter 2 and Bailey et al. (2019), which was decided for the reason that the anatomical masks of S1 would not be as accurate in this experiment since they were defined from a group average – thus, a functionally localised region within each participant would be more accurate.

All additional ROI's were created using the Jüelich Anatomy toolbox (Eickhoff et al., 2005) as in Smith and Goodale (2015) and in Chapter 2 (see also Bailey et al., 2019). Regions included Secondary Somatosensory Cortex (Grefkes, Geyer, Schormann, Roland, & Zilles, 2001), Pre-Motor Cortex (Geyer, 2003), Primary Motor Cortex (Geyer et al., 1996), and Primary Visual Cortex (Amunts et al., 2000). We used the 30% probability cut-off for each map to roughly equate the voxel size. A figure of the anatomical masks can be seen in Appendix G, Figure G-1.

4.3.9. Univariate deconvolution analysis.

Since a rapid event-related design was used, a deconvolution analysis was carried out for the univariate analysis to ensure an accurate model of the hemodynamic response function (HRF) in each condition. A general linear model (GLM) was created from each participant's unsmoothed functional run in ACPC space with 10 predictors per trial type. As we used a 2 x 2 design with the following factors: Congruency (Valid or Invalid) and Task (View or Touch), this resulted in a total of 40 predictors (4 conditions x 10 predictors to span 20s of activity for each trial) used to fully model the HRF for each trial type and participant. Each predictor was modelled as a 3 volume boxcar function relating to the 6s trial duration (as in Valyear et al., 2012; see Figure 4.3 below). We also included the six 3D head motion correction parameters (x, y, and z translation and rotation) from each run as covariates (as in Giordano, McAdams, Zatorre, Kriegeskorte, & Belin, 2013). The peak amplitude of the neural response for each condition was then estimated by applying the resulting design matrix file to each ROI and extracting the beta weights; see Section 4.3.8. above for more information on the ROI's. The data from volumes 5 and 6 after trial onset (see Figure 4.3 below) were then extracted and averaged together (see Appendix I, Figure I-1 for all data in each ROI). Therefore, the mean beta weights from 10-12s after trial onset corresponded to the peak of the HRF for

each trial, and these values were used to calculate the peak amplitude in response to the Valid-View, Invalid-View, Valid-Touch, and Invalid-Touch trials.

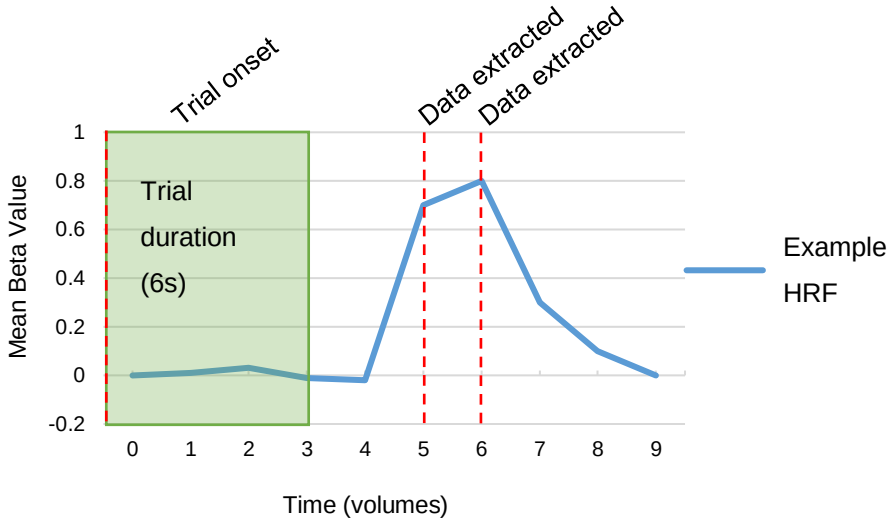

Figure 4.3: An example of the modelled deconvolved HRF during a standard trial. The data points extracted for the univariate analysis correspond to the peak of the HRF, estimated at 10-12s after trial onset.

A 3-way repeated measures ANOVA was carried out separately in each ROI with the following parameters: hemisphere (right, left, pooled), congruency (valid, invalid), and task (view, touch). All univariate statistical tests are Greenhouse-Geisser corrected, and all post-hoc paired *t*-tests are reported as two-tailed at the $p < .05$ level with Bonferroni corrections applied.

4.3.10. Multi-voxel pattern analysis.

For the multi-voxel pattern analysis (MVPA; e.g. Haynes, 2015), a separate GLM was created from each participants unsmoothed functional run in ACPC space, with a different predictor coding stimulus onset of each trial in both the prime and the target phase. Hence, predictors coded either the ball or the cup in both the prime and the target phase, separated by each of the four trial types (see Figure 4.1). Therefore, we had 16 predictors in total (2 object identities x 2 phases x 4 trial types). Predictors were convolved with a standard double gamma model of the haemodynamic response function (see Greening, Mitchell, & Smith, 2018; Smith &

Muckli, 2010). The resulting beta-weight estimates are the input to the pattern classification algorithm. We used a linear support vector machine (LIBSVM 3.20 toolbox; C. Chang & Lin, 2011) to implement the linear SVM algorithm, using default parameters ($C = 1$). The activity pattern estimates (beta weights) within each voxel in the training data was normalised within a range of -1 to 1, prior to input to the SVM. The test data were also normalised using the same parameters as in the training set, in order to optimise classification performance.

The classifier was then trained and tested on independent data, using a leave one run out cross-validation procedure (Smith & Goodale, 2015; Smith & Muckli, 2010) to learn the mapping between the spatial patterns of brain activation generated in response to each object identity (ball or cup) at the *target* phase of a trial. The input to the classifier was always single trial brain activity patterns (beta weights) while the independent test data consisted of an average activity pattern taken across the repetitions of specific exemplars in the left out run (e.g. an average of the single trial beta weights from the target phase of the five Valid-Touch trials where the ball was the target were averaged). Note this is the same approach as the classifications in Chapters 2 and 3 (see also Bailey et al., 2019). As noted previously, we have also used this approach successfully in previous studies, as averaging effectively increases the signal-to-noise of the patterns (Muckli et al., 2015; Smith & Muckli, 2010; Vetter et al., 2014). For similar approaches applied to EEG and MEG data, see Smith and Smith (2019) and Grootswagers, Wardle, and Carlson (2017) respectively (see also Chapter 3).

For example, in a Valid-Touch trial, the classifier was trained on a two way discrimination between either the cup or the ball when the participant viewed (prime) and subsequently touched (target) the same object, with the classifier discriminating information about the object from the *target* phase where they reached out and touched the object (Greening et al., 2018; Smith & Goodale, 2015; Smith & Muckli, 2010; Vetter et al., 2014). The reason why we analysed the activation patterns only from the target phase in the MVPA and not from the entire 6s trial duration (as in the univariate deconvolution analysis – see Section 4.3.9. above) was because we are interested in decoding the *representation* of the object identity in this analysis, as opposed to accurately measuring the HRF. If we ran the analysis over the entire 6s trial duration, we would be effectively averaging across activation patterns of two of

the exact same stimuli in the Valid conditions (e.g. averaging across ball prime, ball target) yet averaging across activation patterns of two different stimuli in the Invalid conditions (e.g. averaging across cup prime, ball target). If we were to do this, we would naively predict the decoding performance to always be better when averaging across two stimuli which are the same when compared to averaging across two different stimuli, since the classifier is getting more information about the representation of a certain object in a valid condition. Therefore, to run the MVPA over the 6s trial duration is methodologically suboptimal as it cannot accurately model the representation of the object in the target phase for each trial type.

Finally, to test whether group level decoding accuracy was significantly above chance, we performed one-sample *t*-tests on all MVPA analyses, against the expected chance level of 50% due to having two object identities (E Formisano et al., 2008; Greening et al., 2018). Since all decoding is testing for above chance accuracy, all significance values for the MVPA analysis are reported one-tailed (as in Bannert & Bartels, 2013; Vickery, Chun, & Lee, 2011). We used this in order to maximise power for data collected under challenging conditions (Snow et al., 2011). Effect sizes for all one-sample *t*-tests are calculated as Cohen's $d = t / \sqrt{N}$. Effect sizes are to be identified as small (> .2), medium (> .5), and large (> .8) according to Cohen's (1988) classification of effect sizes. Finally, to control multiple comparisons, a false discovery rate (FDR) correction was necessary. The adjusted q-value at ≤ .05 resulted in a corrected significance value of FDR $p \leq .010$ for all results (Benjamini & Yekutieli, 2001).

4.4. Results

4.4.1. Univariate deconvolution analysis.

Due to the use of a rapid event-related paradigm, a deconvolution analysis was conducted. Before describing the results, the task along with the expected findings will be explained again to aid understanding.

In a touch task, all trials consisted of a prime phase and a target phase. In a Valid-Touch trial, participants would see an object in the prime phase (e.g. see a ball) and would subsequently be asked to reach out and touch the *exact same* object in the target phase (e.g. touch the ball). In an Invalid-Touch trial, participants would

see an object in the prime phase (e.g. see a ball) and would subsequently be asked to reach out and touch a *completely different* object in the target phase (e.g. touch a cup). If the predictive coding account is true, we would expect to find more overall neural activity in the Invalid-Touch trial when compared to the Valid-Touch trial in touch-related cortical regions, because the prediction has been violated in the former case (Kok et al., 2012; Lee & Mumford, 2003).

In a view task, all trials would also consist of a prime phase and a target phase. In a Valid-View trial, participants would see an object in the prime phase (e.g. see a ball) and would subsequently be asked to continue to view the *exact same* object in the target phase (e.g. view the ball). In an Invalid-View trial, participants would see an object in the prime phase (e.g. see a ball) and would subsequently be asked to view a *completely different* object in the target phase (e.g. view a cup). If the predictive coding account is true, we would expect to see less overall neural activity in visual cortical brain regions for the Valid-View trial when compared to the Invalid-View trial. This is because in the former case, the prediction has been met, resulting in less overall neural activity because prediction errors are likely to have been silenced. In the latter case, the prediction has been violated, thus we would expect more prediction errors are projected through the cortical hierarchy which is reflected by means of more overall neural activity (Kok et al., 2012; Lee & Mumford, 2003). Furthermore, we may expect to find a weaker neural response in a Valid-View trial compared to an Invalid-View trial based on basic adaptation effects, since stimulus repetitions are known to produce an instant decrease in neural activity (Grill-Spector, Henson, & Martin, 2006; Koutstaal et al., 2001).

4.4.1.1. Primary somatosensory cortex.

In primary somatosensory cortex (S1), we ran analyses in two ROI's; see Section 4.3.8. above for more information on the difference between $S1_{mask}$ and $S1_{localiser}$. The 3-way ANOVA in $S1_{mask}$ revealed a significant main effect of hemisphere $F_{1.007,\ 17.115} = 25.484$, $p < .001$, $\eta_p^2 = .600$, whereby the peak amplitude was lowest for the right hemisphere ($M = .080$), followed by the pooled ($M = .209$), and left ($M = .305$) hemispheres of $S1_{mask}$, with all means being significantly different from one another (all p's $< .001$). A significant main effect of task $F_{1,\ 17} = 65.820$, $p < .001$, $\eta_p^2 = .795$ was also found, whereby the peak amplitude was higher

for touch (M = .413) compared to view (M = -.017) at p < .001. However, we found no significant main effect of congruency ($F_{1, 17}$ = 1.389, p = .255). A significant interaction was also found between hemisphere and task $F_{1.011, 17.193}$ = 78.173, p < .001, η_p^2 = .821. As would be expected, post-hoc pairwise comparisons investigating task differences revealed the peak amplitude was significantly higher in all touch tasks when compared to all view tasks in each hemisphere (p's ≤ .020). Furthermore, post-hoc comparisons on hemisphere within each task revealed the peak amplitude between each hemisphere was significantly different in every comparison (p's ≤ .042), with the exception of the difference between the right and pooled hemispheres in the view task (p = .051). All mean beta values can be seen in Figure 4.4A.

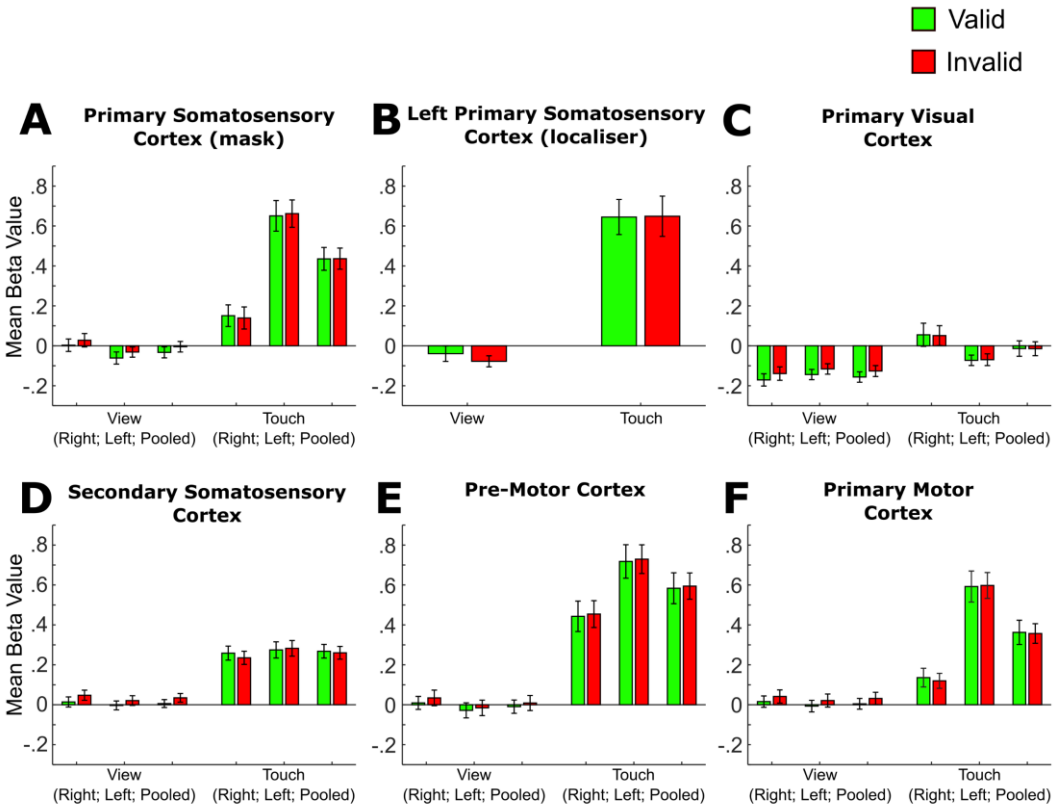

Figure 4.4: Univariate deconvolution results. (A) Mean beta values for each trial type (Valid-View, Invalid-View, Valid-Touch, Invalid-Touch) for right and left S1 (post-central gyri), and pooled across hemispheres. (B) As in A but for the top 100 voxels that were most responsive to tactile stimulation of the hands in an independent localiser session. (C–F) As in A but for several additional, anatomically defined, regions of interest.

A two-way ANOVA was also ran in the $S1_{localiser}$ ROI to reveal a significant main effect of task $F_{1, 8} = 30.129$, $p = .001$, $\eta_p^2 = .790$ (see Figure 4.4B), whereby the peak amplitude in the touch task ($M = .647$) was significantly larger than the peak amplitude in the view task ($M = -.059$). There was no significant main effect of congruency ($F_{1, 8} = .212$, $p = .657$), nor was there a significant interaction between task and congruency ($F_{1, 8} = .285$, $p = .608$).

4.4.1.2. Primary visual cortex.

In primary visual cortex (V1), a three-way repeated measure ANOVA revealed a significant main effect of task $F_{1, 17} = 16.588$, $p = .001$, $\eta_p^2 = .494$ (see Figure 4.4C), whereby the peak amplitude was significantly lower in the view task ($M = -.142$) compared to the touch task ($M = -.011$). No significant main effect was found of hemisphere ($F_{1.001, 17.022} = 3.692$, $p = .072$) or congruency ($F_{1, 17} = 1.406$, $p = .252$). A significant interaction was also found between hemisphere and task $F_{1.001, 17.020} = 16.588$, $p = .001$, $\eta_p^2 = .492$. Further post-hoc pairwise comparisons investigating task differences revealed the peak amplitude was significantly lower in the view task when compared to the touch task in each hemisphere (p's $\leq .015$). When investigating hemisphere comparisons for each task, the peak amplitude was significantly different between each hemisphere in the touch task (p's $\leq .022$), however no significant differences were found between hemispheres in the view task.

Here, it is important to note the negative signal we observe in the view task. The reason this is a negative amplitude may be due to the specific way the data has been modelled in order to incorporate the duration of the motor action. We could not accurately segregate the HRF response of the prime and target phase due to the use of a rapid event-related design with a fixed ISI in a trial. As such, the entire 6s trial duration is included (see Section 4.3.9. above for more information). In the view task, this means the majority of the modelled HRF is when the participant remained fixated on the fixation LED in the *dark*, thus a negative amplitude would be expected in this case. To confirm this speculation, we ran a standard univariate GLM analysis which revealed positive BOLD amplitudes in V1 of a viewed object in both the prime and target phase when modelled separately. However, due to the fact the data from the prime and target phase cannot be accurately segregated due to the fixed ISI,

this data has not been included. See also Appendix I, Figure I-1 for all the data in V1 from the deconvolved HRF response.

4.4.1.3. Secondary somatosensory cortex.

A significant main effect of task was found in secondary somatosensory cortex (S2) $F_{1, 17} = 105.399$, $p < .001$, $\eta_p^2 = .861$ (see Figure 4.4D), whereby the peak amplitude was significantly higher for the touch task ($M = .263$) when compared to the view task ($M = .020$). No significant main effect was found of hemisphere ($F_{1.001, 17.022} = .040$, $p = .961$) or congruency ($F_{1, 17} = 1.479$, $p = .241$). Interestingly, we also found a significant three-way interaction between hemisphere, congruency, and task $F_{1.005, 17.078} = 6.651$, $p = .019$, $\eta_p^2 = .281$. Further pairwise comparisons to investigate this interaction revealed the peak amplitude of the Invalid-View trial to be significantly higher than the peak amplitude of the Valid-View trial in the right ($p = .010$) and pooled ($p = .030$) hemispheres for the View task (see Figure 4.4D).

4.4.1.4. Pre-motor cortex.

In pre-motor cortex (PMC), a significant main effect of hemisphere was found $F_{1.002, 17.027} = 26.138$, $p < .001$, $\eta_p^2 = .606$ (see Figure 4.4E), whereby the peak amplitude was highest in left PMC ($M = .351$), followed by pooled PMC ($M = .294$), with the lowest amplitude being in right PMC ($M = .235$). These means were all highly significantly different from one another (p's $< .001$). A significant main effect of task was also found $F_{1, 17} = 76.755$, $p < .001$, $\eta_p^2 = .819$, with the peak amplitude being higher for the touch task ($M = .587$) when compared to the view task ($M = .000$) at $p < .001$. No significant effect of congruency was found ($F_{1, 17} = .985$, $p = .335$). A significant interaction was also found between hemisphere and task $F_{1.002, 17.032} = 39.725$, $p < .001$, $\eta_p^2 = .700$. Further post-hoc pairwise comparisons revealed when looking at task differences the peak amplitude was significantly higher for the touch task when compared to the view task in each hemisphere, with all p's $< .001$. When looking at hemisphere differences, the peak amplitude in the touch task was significantly higher for the left hemisphere, followed by the pooled hemisphere and the lowest being the right hemisphere (all p's $< .001$). No significant differences were found between the hemispheres in the view task (p's $\geq .111$).

4.4.1.5. Primary motor cortex.

In primary motor cortex (M1), significant main effect of hemisphere was observed $F_{1.003,\ 17.055} = 98.379$, $p < .001$, $\eta_p^2 = .853$ (see Figure 4.4F), whereby the peak amplitude was significantly higher for the left hemisphere ($M = .301$), followed by the pooled ($M = .189$) and the right ($M = .078$) hemisphere (p's $< .001$). A significant main effect of task was also found $F_{1,\ 17} = 43.402$, $p < .001$, $\eta_p^2 = .719$, with the peak amplitude being larger in the touch task ($M = .361$) when compared to the view task ($M = .018$). No main effect of congruency was found ($F_{1,\ 17} = .818$, $p = .379$). A significant interaction was also found between hemisphere and task $F_{1.003,\ 17.059} = 98.150$, $p < .001$, $\eta_p^2 = .852$. Further post-hoc pairwise comparisons investigating hemisphere differences revealed the peak amplitude in response to the touch task in each hemisphere were all significantly different from one another (all p's $< .001$), however no significant changes were found between hemispheres in the view task. When investigating task differences, the peak amplitude was found to be larger for the touch task when compared to the view task in each hemisphere (p's $\leq .011$).

4.4.2. Multi-voxel pattern analysis.

Here, cross-validated decoding performance of object identity was computed in the *target* stage of the trial. As such, the classifier was trained and tested to discriminate between object identity (either cup or ball) independently for Valid-View, Invalid-View, Valid-Touch and Invalid-Touch trials. Such decoding was computed separately in each hemisphere in each ROI. This was done in order to test whether the primed object in each trial influenced the representation of the object in the target stage of the trial. We also performed cross-validated decoding of task (either View or Touch). This was done in order to determine whether each ROI could significantly discriminate between task without taking object identity into consideration.

4.4.2.1. Decoding object identity: Valid-Touch vs Invalid-Touch.

The classifier was trained to discriminate between object identity (cup or ball) in the *target* phase of the touch task independently for each congruency condition (Valid-Touch or Invalid-Touch; see Figure 4.1). To support the predictive coding account, we would expect MVPA to reveal higher decoding in the Valid-Touch trials when compared to Invalid-Touch trials in tactile and/or motor-related cortical regions. This is because the prediction has been met in the former case, thus resulting in correct predictions causing a stronger neural representation of the object when subsequently interacting with the object (Kok et al., 2012; Lee & Mumford, 2003).

When looking in S1, MVPA analysis revealed above chance decoding in the pooled $S1_{mask}$ for the Invalid-Touch trials (M = .557, t_{17} = 2.010, p = .030, d = .474, chance = 50%; see Figure 4.5A). A similar trend was observed in left S1 which did not reach significance at p = .088. However, neither of these findings survived FDR correction. Interestingly however, when looking in $S1_{localiser}$, we observed a flip effect whereby decoding accuracies were subjectively higher for the Valid-Touch trials compared to the Invalid-Touch trials (see Figure 4.5B). This is of potential interest, however, no decoding accuracies reached significance in the $S1_{localiser}$ data. We also found above chance decoding in the Invalid-Touch trials in right (M = .549, t_{17} = 1.873, p = .039, d = .441), and left S2 (M = .561, t_{17} = 1.999, p = .031, d = .471; see Figure 4.5D) and pooled PMC (M = .565, t_{17} = 1.924, p = .036, d = .453; see Figure 4.5E). However, once again these findings did not survive FDR correction. No significantly above chance decoding was found in the Valid-Touch trials within any of these regions (all p's $\geq$ .257).

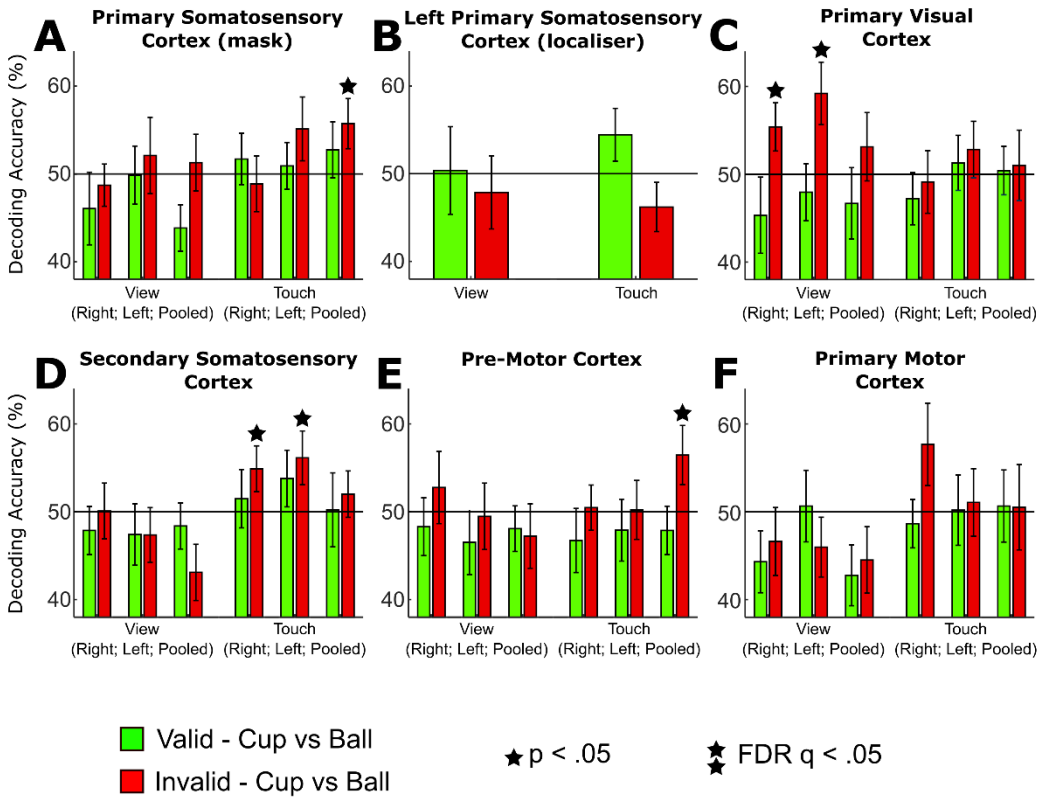

Figure 4.5: Decoding of object identity. (A) Cross-validated 2 automatic forced choice decoding performance of object identity (Cup or Ball) for right and left S1 (post-central gyri) independently and pooled across hemispheres. Decoding is separated by Valid-View, Invalid-View, Valid-Touch, and Invalid-Touch trials. Chance = 50%. (B) As in A but for the top 100 voxels that were responsive to tactile stimulation of the hands in an independent localiser session. (C–F) As in A but for several additional, anatomically defined, regions of interest.

4.4.2.2. Decoding object identity: Valid-View vs Invalid-View.

The classifier was trained to discriminate between object identity (cup or ball) in the *target* phase of the view task independently for each congruency condition (Valid-View or Invalid-View; see Figure 4.1). Here, to support the predictive coding account, we may expect MVPA to reveal higher decoding in the Valid-View trials compared to the Invalid-View trials, particularly in visual cortical regions. This is because the prediction has been met in the former case, thus resulting in correct predictions causing a stronger neural representation of the object (Kok et al., 2012; Lee & Mumford, 2003). However, in this particular pairing of conditions it

is important to note we could find stronger decoding in the Invalid-View condition if the Valid-View condition causes adaptation effects (see Section 4.4.1. above; Grill-Spector et al., 2006; Koutstaal et al., 2001). This is because previous research has found MVPA is sensitive to voxels which show a stronger univariate neural response to a stimulus (Albers, Meindertsma, Toni, & de Lange, 2018; Norman et al., 2006).

The MVPA results revealed decoding for cup vs ball was above chance in the Invalid-View trials in the right (M = .554, t17 = 1.960, p = .033, d = .462) and left (M = .592, t_{17} = 2.583, p = .019, d = .609) hemispheres of V1 (see Figure 4.5C). However, both effects did not survive FDR correction. No significant decoding was found for the Valid-View trials in V1, and no significantly above-chance decoding was found in any other ROI for either Valid-View or Invalid-View trials (all p's ≥ .511).

4.4.2.3. Decoding task: View vs Touch.

Given the results, we decided to perform cross-validated decoding of task, meaning the classifier was trained to discriminate between the View or Touch task without taking object identity or congruency into account. This was to determine whether each ROI could significantly discriminate between whether the participant had simply viewed or reached out to touch an object during a trial. As would be expected, robustly significant decoding was found following FDR corrections in all ROI's and all hemispheres for discriminating between task type (all M's range from .760 - .960, all t's range from 8.201 – 35.274, all p's < .001, all d's range from 1.933 – 8.314; see Figure 4.6). Further pairwise comparisons revealed decoding was significantly higher in the left and pooled hemispheres when compared to the right hemispheres for all ROI's except in V1 (all p's ≤ .005; see Figure 4.6).

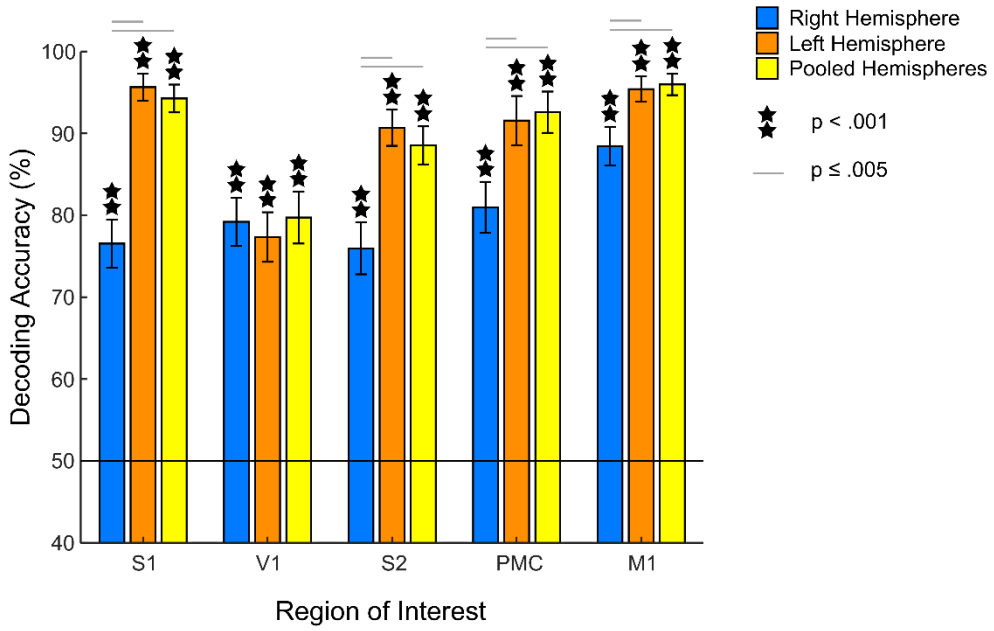

Figure 4.6: Multi-voxel pattern analysis decoding accuracies for cross-validated decoding of task (View vs Touch) in each ROI, without taking object identity or congruency into account. Chance = 50%.

4.5. Discussion

The primary aim of this study was to investigate whether we could directly test the assumptions of the theory of predictive coding when asking participants to interact with real 3D objects placed directly in front of them in an MRI scanner. Predictive coding was measured by examining whether a consistent or an inconsistent visual prime of a real 3D object could influence the neural processes in the brain when participants were asked to subsequently reach out and touch a real 3D object. We expected to find a suppressed neural amplitude complimented by a greater representation of the object in primary somatosensory cortex (S1) when participants viewed and subsequently reached out to touch the same object (Valid-Touch). Conversely, we expected a stronger neural amplitude and weaker representation of the object in S1 if the participant viewed one object and subsequently reached out to touch a different object (Invalid-Touch). We also compared such differences when participants only perceived the objects and did not

reach out to touch them (Valid-View and Invalid-View). Whilst no univariate differences were found in the neural amplitude between conditions in S1, we did find a reduced neural amplitude in right and pooled hemispheres of secondary somatosensory cortex (S2) when participants viewed an object and subsequently viewed the same object (Valid-View), compared to when they viewed an object and subsequently viewed a different object (Invalid-View). This result thus surprisingly reveals evidence for suppression of expected sensory input only during perception, and not action, in S2. Interestingly, in contrast to our expectations, we found a trend for higher decoding accuracies (albeit not surviving FDR correction) when the participants reached out to touch an object which was *inconsistent* with the visual prime (Invalid-Touch). However, due to the absence of above-chance decoding surviving any FDR corrections, the results remain inconclusive in this respect. Reasons for the non-significant decoding results are discussed along with other interesting findings outside of the main research question.

4.5.1. Predictive coding with action: The influence of a visual prime when subsequently reaching out to touch the same or a different real 3D object.

Here, we investigated whether a visual prime of a real 3D object could send predictions about the tactile features of the object to S1, thus strengthening the representation of the object upon a subsequent object interaction. We expected this would be possible since previous research has found cross-modal connections can transmit information specific to the content of different categories of familiar visual objects to S1, despite the absence of tactile stimulation during the experiment (Smith & Goodale, 2015). The results from Chapter 2 (see also Bailey et al., 2019) also revealed similar cross-modal effects whereby information specific to the content of familiar hand-object sounds could be discriminated in S1. We suggest predictive coding theories (Clark, 2013) can explain the functional significance behind such effects, since the cross-modal responses may be useful for future interaction with the object. To test this, we compared the neural responses between reaching out to touch a real 3D object when the participant was visually primed with either exactly the same object (a Valid-Touch trial), against reaching out to touch a real 3D object when the participant was visually primed with a completely different object (an Invalid-Touch trial). For reference, these two trial types can be seen in Figure 4.1.

Based on predictive coding models, we expected to find a reduced neural amplitude in S1 in the univariate analysis, complimented with a stronger representation of the object in S1 in the MVPA, for a Valid-Touch trial when compared to an Invalid-Touch trial (see Kok et al., 2012; Lee & Mumford, 2003; Yon et al., 2018). We also explored whether similar effects would be found in other somatosensory and motor related cortical regions.

The univariate results revealed no significant differences in the neural responses between the Valid-Touch and Invalid-Touch trials in any ROI, meaning a congruent versus an incongruent visual prime did not appear to influence the neural amplitude of the response to physically reaching out and touching a real 3D object. The reason why we did not find any differences here may be due to the fact the brief illumination of the object in the target phase may have been enough information for the somatosensory (and motor) cortex to predict their determined tactile sensation, thus producing comparable effects across both trial types. Furthermore, it may be the case that the perceptual prediction from the visual prime was overridden by the physical motor prediction in relation to reaching out to grasp the object in the target phase. Support for this idea comes from previous research which suggests error signals in motor systems self-suppress when eliciting physical movements (Friston, 2003), with a review by Clark (2013) suggesting a physical action becomes conceptually primary in accounts of prediction, whereby the action not only precedes sensation, but actually determines sensation. In other words, it is likely that any perceptual predictions were updated when participants made the physical motor response toward the object they saw in the target phase, rendering the object in the prime phase obsolete. This would explain why we find different effects to that of Yon et al. (2018), since participants in Yon et al. were *simultaneously* executing an action which differed from the action they saw in the visual display, thus generating detectable differences in the neural signal.

Interestingly however, the MVPA results in the present experiment revealed hints of above-chance decoding in primary and secondary somatosensory cortices, in addition to pre-motor cortices, only for the Invalid-Touch trials. This finding, despite not reaching significance after FDR corrections, is interesting since there is a clear trend in the opposite direction to our expectations. If our study is a valid measure of predictive coding mechanisms in the brain (Kok et al., 2012; Lee & Mumford,

2003), we would expect to find higher decoding accuracies when participants viewed and subsequently interacted with the same object, since we suggest the representation of the object would be stronger in this case. However, we failed to find such effects. The reason why could be due to the experimental design employed. As mentioned above, we maintained a brief flash of light at the start of the target phase of each trial regardless of the impending task. The experiment was designed in this way to prevent participants from grasping inappropriately which would create artifacts in the signal. However, due to the nature of this design, participants would view a repeated object during Valid-Touch trial before reaching out to touch the object. This means the representation may have been weaker in this case since previous research has suggested repetition results in a sparser representation of the stimulus (Desimone, 1996; Wiggs & Martin, 1998), with further research revealing decreases in classification accuracies for a repeated stimulus compared to a non-repeated stimulus (Kaliukhovich & Vogels, 2013).

Furthermore, the expectation of seeing one of the two objects throughout the experiment was at an equal chance, meaning the element of surprise may have decreased throughout the experiment. Therefore, using more objects and/or manipulating the levels of expectation in the experimental trials could be an interesting avenue for future research to investigate whether we find significantly above chance effects of prediction in this instance. Indeed, much of the previous literature has manipulated expectation in order to find predictive effects (Kok et al., 2012; Schenke, Wyer, & Bach, 2016; Yon et al., 2018).

One final interesting finding in this analysis is the difference in the decoding accuracies when running the analysis in left $S1_{mask}$ and left $S1_{localiser}$; a subset region of left S1 which was independently localised to the fingers of the right hand (see Section 4.3.8. above for more information; see also Appendix H, Figure H-1). As can be seen in Figure 4.5A and 4.5B, the decoding accuracies in $S1_{localiser}$ for Valid trials are clearly higher compared to the decoding accuracies for Valid trials in $S1_{mask}$. Conversely, decoding accuracies in $S1_{localiser}$ for Invalid trials are visibly lower when compared to decoding accuracies for Invalid trials in $S1_{mask}$. Out of curiosity, a 3-way repeated measures ANOVA was carried out with the following parameters: ROI ($S1_{mask}$, $S1_{localiser}$), congruency (valid, invalid), and task (view, touch). Interestingly, whilst no significant main effects were found, a significant

interaction was found between ROI and congruency ($F_{1, 8} = 6.067$, $p = .039$, $\eta_p^2 = .431$), whereby the decoding accuracies for Invalid trials were significantly lower in $S1_{localiser}$ when compared to $S1_{mask}$ ($p = .033$). Furthermore, in $S1_{mask}$, decoding accuracies were found to be significantly lower for Valid compared to Invalid trials ($p = .041$). This finding is interesting since it reveals hints of a sharpened representation of the stimulus specifically in the finger-sensitive voxels of S1 (Friston, 2005; Kok et al., 2012, 2017; Kok & De Lange, 2015; Lee & Mumford, 2003; Press et al., 2020; Yon et al., 2018). However, it is worth noting that the $S1_{mask}$ ROI was not entirely optimal for the analysis. Here, instead of creating hand-drawn masks of the post-central gyrus as in Chapter 2 (see also Bailey et al., 2019; Smith & Goodale, 2015), we created probability maps from the masks defined from a previous study (see Appendix G, Figure G-1). The reason why this is a problem is because the masks in the current study were not as well matched to participant-specific brain anatomy and therefore more susceptible to overlap with other nearby cortical ROI's (for example, motor and pre-motor cortices). Furthermore, the lower decoding for the Invalid-Touch trials in $S1_{localiser}$ could simply be due to the smaller sample size ($N = 9$), or the smaller voxel count. Due to these significant confounds, we cannot make any definitive conclusions from this finding. More participants are needed for the localiser session to confirm this reverse effect, in addition to normalising the number of voxels used across this comparison.

4.5.2. Predictive coding with perception: The influence of a visual prime when subsequently viewing the same or a different real 3D object.

Another area of study was to investigate whether the neural responses differed between viewing a real 3D object when the visual prime was the same object (a Valid-View trial), and viewing a real 3D object when the visual prime was a different object (an Invalid-View trial). These two trial types can be seen in Figure 4.1. The univariate results revealed a significantly higher amplitude for an Invalid-View trial when compared to a Valid-View trial in the right and pooled hemispheres of S2. No other significant differences in any other ROI were found when comparing the neural amplitude of these two trial types. The results we observe here suggest that viewing two of the exact same objects in succession, or viewing two different objects in succession, produces differences in the amplitude of neural activity in S2,

despite the fact no tactile information was present in this comparison. Interestingly however, we only found a univariate difference and did not find any above chance decoding of object identity for Valid-View or Invalid-View trials in any ROI after FDR correction. We note hints of above chance decoding in Invalid-View trials in right and left V1, however, these did not survive FDR correction.

The difference in the univariate cross-modal response from vision to S2 is noteworthy, especially since previous research has found content-specific information can be sent to S2 when viewing static images of objects (Smith & Goodale, 2015) or videos of hand-object interactions (Meyer et al., 2011). Furthermore, it may not be surprising that we have found links between vision and S2 given the anatomical connections between S2 and areas known to have visual properties (for a review, see Keysers, Kaas, & Gazzola, 2010). The reason why we find a weaker neural response for the Valid-View trials when compared to the Invalid-View trials may be explained by the fact the stimuli were predicted in the Valid-View trials, thus triggering a high-level cross-modal response to S2 which evoked less neural activation in the brain when the stimuli were predicted (Bays et al., 2006; Blakemore et al., 1998; Kikuchi et al., 2019; Limanowski et al., 2018; Richter et al., 2018), in line with a predictive coding mechanism of cortex function. The S2 results may also be detecting traces of a high-level representation of the associated sensation with the object when it is merely viewed, since this is the region where visual information is known to enter the somatosensory system (Keysers et al., 2010). Furthermore, S2 has previously been found to reliably discriminate between the rough and smooth surfaces of visual objects (H. C. Sun, Welchman, Chang, & Di Luca, 2016). This is important since we presented participants with both a rough (tennis ball) and smooth (plastic cup) surface on our two chosen objects.

Another reason why we observe more neural suppression for a Valid-View trial when compared to an Invalid-View trial in S2 may be because in the former case the stimulus has been repeated, thus we may expect a weaker neural response based on suppression effects from a repeated stimulus (Grill-Spector et al., 2006; Koutstaal et al., 2001). Repetition suppression, also known as fMRI adaptation, is a robust effect found in the fMRI literature whereby a significant reduction in the hemodynamic response is found for repetitions of identical stimuli (Grill-Spector et

al., 2006; Grill-Spector & Malach, 2001; Henson, Shallice, & Dolan, 2000; Weiner, Sayres, Vinberg, & Grill-Spector, 2010). There is a large body of research which has shown repetition suppression effects when participants are asked to view repeated images of objects. For example, a reduction in neural activity has been found in the lateral occipital complex (LOC), when repeating 2D images of objects (Kovács, Kaiser, Kaliukhovich, Zoltán, & Vogels, 2013; Sayres & Grill-Spector, 2006). Furthermore, similar results were observed in Valyear et al. (2012), who found repetition suppression in parietal and pre-motor areas when participants viewed repetitions of real 3D tools compared to non-repetitions. We expand on this by suggesting that viewing repetitions of real 3D objects which are not tools can produce a comparable effect in S2. Furthermore, it is worth noting a similar pattern across all our ROI's, despite no other comparisons revealing significant differences in the neural response.

The reason why we observe these effects in S2 yet do not find significant effects of suppression between a Valid-View and Invalid-View trial in V1 is a surprising result. As such, the univariate differences we observe in S2 must be interpreted with caution. We note that whilst the univariate effects during a Valid-View trial do indicate a trend in the direction we would expect (that is, we do indeed observe more suppression for a Valid-View trial when compared to an Invalid-View trial; see Figure 4.4C), the difference is a small trend and not significant. We speculate this may be explained by the fact we used broad anatomical masks of V1 with no retinotopy, which hence may have led to a weak isolation of regions of V1 which truly represented the response to the objects. The non-significance of these results does coincide with previous research investigating repetition suppression effects in the visual system when viewing real 3D objects in the scanner (Snow et al., 2011). Snow et al. (2011) were specifically interested in testing whether the neural mechanisms of perception measured via repetition-related changes are the same when viewing real 3D objects, or a corresponding set of 2D photographs of the same objects, both presented via a turntable apparatus in the scanner. Whilst they found robust repetition suppression along the ventral and dorsal visual processing stream when participants viewed repeated images of the 2D photographs, they found extremely weak and non-significant effects of repetition suppression when participants viewed repetitions of real 3D objects. Our findings are similar to this

research, thus we loosely support the idea from Snow et al. who suggest there may be separate neural mechanisms involved in visual processing of 2D images of 3D objects and real 3D objects in the brain. An interesting addition to our analysis would be to complete an independent LOC localiser scan for our participants, since we could determine whether the same non-existent repetition suppression effects are apparent in object-selective regions of cortex in the present study, as was the case in Snow et al. (2011). Finally, the MVPA results for the view task revealed hints of above-chance decoding only in primary visual cortex (V1) for the Invalid-View trials. As mentioned previously, the stronger decoding for an Invalid-View trial may be explained by the fact decreases in classification accuracies have previously been found for a repeated stimulus compared to a non-repeated stimulus (Kaliukhovich & Vogels, 2013). However, since no MVPA results survived FDR correction, any explanations must be interpreted with caution.

4.5.3. Task effects of vision versus touch with real 3D everyday objects.

An additional interesting finding in this study is the strong significant decoding we found for the task (Touch vs View) in each of our ROI's. We ran this analysis as a validation check to determine our data was of a high quality to be able to accurately determine when an action occurred versus when it did not occur in somatosensory and motor regions. The fact we found robust above chance decoding in all ROIs suggests our data is of a decent level of quality. Additionally, as was found in our research, Gallivan, Cavina-Pratesi, and Culham (2009) found a stronger neural response to grasping and reaching actions towards real 3D artificial objects when compared to passive viewing at the univariate level. Studies using real world objects in the fMRI literature have investigated 3D tool use (Brandi et al., 2014; Gallivan et al., 2013; Hermsdörfer et al., 2007; Imazu et al., 2007; Valyear et al., 2012), hand actions made towards artificial 3D objects (Cavina-Pratesi et al., 2007; Gallivan et al., 2009; Rossit et al., 2013), viewing real 3D objects (Snow et al., 2011; Snow, Skiba, et al., 2014), or touching real world objects without viewing (Snow, Strother, et al., 2014). Other research has also found it is possible to decode the modality of stimulus presentation from all primary sensory areas (Liang et al., 2013). Here, the robustly significant decoding of task in the present study corroborates previous literature by finding the brain can decode differences between the task of

viewing or touching real 3D familiar objects in visual, tactile, and motor related regions in the human brain. Furthermore, we find such decoding effects are stronger in the left hemisphere of the tactile and motor-related cortical regions, as would be expected since our participants were right handed, acting with their right arm (see also Gallivan et al., 2009).

It is worth noting that the decoding may be better for View vs Touch in each ROI since the univariate analysis revealed a significantly higher peak neural amplitude for the Touch task when compared to the View task in all our ROI's. The reason why the univariate response was significantly stronger for the Touch task may be due to the fact this experiment was highly vision-oriented, whereby all trials regardless of a View or Touch task began with a visual prime. Thus, a Touch task may have always produced a stronger neural response since it always involved a change in the task requirement of the participant between the prime and the target phase. As such, it would be interesting for future research to include a Touch-Touch trial, whereby the participant reaches out to touch the same object in both the prime and the target phase, or reaches out to touch two different objects in the prime and target phase. Here, we may expect to find a weaker neural response in tactile and motor-related cortical regions since the task in the prime and target phase would be repeated, as is the case in a View task. Furthermore, including a Touch-Touch trial would enable a more accurate comparison between the View and the Touch task.

4.6. Conclusion

The present study aimed to directly examine whether the cross-modal context effects found in previous research have the functional role of prediction by asking participants to physically interact with real 3D objects placed directly in front of them in the MRI scanner. Whilst our results failed to find a significant result for predictive effects, corroborating previous studies we found that the brain can decode differences between the task of viewing, and reaching out to touch, real familiar 3D objects placed directly in front of them in the scanner using a rapid-event related design. Therefore, our results have uncovered the plausibility of using rapid-event related designs in the real-action literature. Furthermore, this study has provided a guide for informing future research how predictive effects from vision to somatosensory and motor regions could be investigated in the brain.

CHAPTER 5

–

General Discussion

5.1. Chapter overview

The research conducted in this thesis used fMRI and EEG to examine how context and prior experience can shape the neural computations occurring in the primary somatosensory (and sensorimotor) cortex of the human brain, specifically by using pattern classification analysis to decode the content of cross-modal influences in the brain. The experiment in Chapter 2 used fMRI to investigate whether hearing different familiar sounds depicting object interactions with the hands can be discriminated in primary somatosensory cortex (S1), even though stimulus presentation occurred in the auditory domain. Chapter 3 aimed to corroborate the cross-modal effects found in the previous fMRI literature using a high temporal resolution neuroimaging technique: EEG. Specifically, EEG was used to explore whether viewing images of different familiar visual objects which imply rich haptic information could be identified from sensorimotor-related oscillatory responses, even though input was purely from a visual source. Chapter 4 involved an interactive paradigm using real 3D objects in an fMRI experiment to test whether predictive coding theories can explain the functional significance behind the cross-modal effects we observed in Chapters 2 and 3. The results from each experimental chapter will now be briefly summarised. Theoretical implications, real world applications, limitations, and future directions from the experiments conducted in this thesis will also be discussed.

5.2. Summary of results

5.2.1. Summary of Chapter 2 results.

The motivation behind the research conducted in Chapter 2 was to determine whether the cross-modal effects observed in the previous literature are present between all pairs of primary sensory modalities. Previous research investigating cross-modal effects has found that if a stimulus presented via one sense implies features representative of an independent sensory modality, information related to the content of the stimulus can be detected in that independent primary sensory modality. For example, research has found visual stimuli which imply haptic information can be discriminated in S1 (Meyer et al., 2011; Smith & Goodale, 2015),

visual stimuli which imply auditory information can be distinguished in A1 (Meyer et al., 2010), and auditory stimuli which imply visual information can be discriminated in V1 (Vetter et al., 2014). All of these studies found information related to the content of the stimulus could be detected in a primary sensory cortex which was entirely independent to that of stimulus presentation. What had not been shown, however, was whether haptic-implying auditory information could be detected in S1. This was an important area of study because we have previously found haptic-implying visual information can be discriminated in S1 (Smith & Goodale, 2015), and since sound is another form of input that could help to predict future interaction with objects, this research can help determine whether the cross-modal effects observed are apparent between all pairs of sensory modalities. Furthermore, investigating this particular pair of modalities could determine whether the dominant sense of vision (Colavita, 1974; Mumford, 1991) is needed in order to observe such cross-sensory effects.

The results of this study found, for the first time, that sounds which depicted familiar hand-object interactions could be reliably detected in S1, even in the absence of any external tactile stimulation during the experiment. Specifically, when limiting our analyses to the hand-sensitive areas of S1 (determined from a vibro-tactile localiser), we found decoding of hand-object interaction sounds to be significantly better in the left hemisphere when compared to our two control categories of the sounds of familiar animal vocalizations, and unfamiliar pure tones. This result suggests it is not simply the content of any familiar sound, or any unfamiliar sound, which can be reliably discriminated in S1, but specifically sounds which imply haptic interactions with the hands. Furthermore, the results we found in A1 strongly suggest the results in S1 reflect high-level information about the tactile component of the hand-object sounds, and not passive relay of low-level acoustic features from auditory cortex, since decoding in A1 revealed the exact opposite pattern of effects. Therefore, we suggest from the results in this study that cross-modal connections from audition to hand-sensitive areas of S1 transmit content-specific information about familiar sounds which convey object interactions with the hands.

5.2.2. Summary of Chapter 3 results.

The primary aim of the study in Chapter 3 was to determine whether the cross-modal effects which have been observed in the previous literature (Bailey et al., 2019; Meyer et al., 2011, 2010; Smith & Goodale, 2015; Vetter et al., 2014; see also Chapter 2) could be corroborated using a different method of data collection. Therefore, we used EEG to investigate whether presenting a stimulus via one sense, such as vision, which implied features representative of another sense, such as touch, could produce a distinct oscillatory response over the associated, yet non-stimulated, sensorimotor cortical area. Specifically, we investigated whether neural oscillations detected over sensorimotor cortex (the mu rhythm; Berger, 1929), would carry information related to images of familiar visual objects which implied rich tactile information when compared to unfamiliar visual objects which also imply rich tactile information (see also Smith & Goodale, 2015), despite no requirement for a motor movement or tactile sensation when viewing the stimuli. This was an important area of study for two reasons. First, no studies to date have used a technique other than fMRI to test whether information specific to the content of a stimulus can be reliably discriminated in/over a primary sensory or sensorimotor cortical area independent to that of stimulus presentation. Having only found such effects with fMRI is a constraint since such studies can only confirm which areas in the brain can receive this cross-modal information. However, if we can corroborate these studies using EEG, we can potentially determine the timing of the effects at a millisecond level. Secondly, as EEG is a cheap method of data collection, finding a corroborating result could open an avenue for quick advances in this field of cognitive neuroscience since such studies are more accessible than fMRI.

The results of this study found, for the first time, that when participants simply viewed still images of familiar visual objects which implied rich haptic information, multivariate pattern analysis could significantly discriminate between the different familiar visual object categories based on information extracted from the mu rhythm oscillatory response. This was found despite the fact the mu rhythm is a sensorimotor neural oscillation detected over central electrodes (Berger, 1929), known to respond to an execution of an action, observation of an action, the intention to act, or the texture of an object being picked up during an action (Coll et al., 2015, 2017; Muthukumaraswamy & Johnson, 2004; Pfurtscheller et al., 1997; Pineda,

2005; Quandt et al., 2013; Ritter et al., 2009). In contrast, we did not find any reliable information in the mu rhythm oscillatory response related to viewing images of the unfamiliar visual object categories. As such, we corroborated and strengthened the results of Smith and Goodale (2015), by finding that information likely related to the tactile component of *only* familiar visual objects could be detected in a sensorimotor-related oscillatory response (the mu rhythm), even though no tactile stimulation or motor response was either executed or implied. Whilst we cannot rule out the idea that these effects could be originating from primary motor cortex (M1), we have reason to believe the effects we observe originate from S1 since this study is a corroboration of Smith and Goodale, who only found such discriminable information in S1, and not M1. Therefore, we suggest, similar to Smith and Goodale (2015), that information about a visual objects tactile (or motor) properties can be sent to sensorimotor related cortices even in the absence of explicit haptic interaction, and that a rich prior haptic experience with the objects is necessary to observe such effects. Whilst we did not find decoding for the familiar visual objects to be significantly higher than the non-significant decoding of unfamiliar visual objects, we provide evidence for the oscillatory frequency of these cross-modal effects and show promising developments for using cheaper methods of data collection in the cross-modal literature.

5.2.3. Summary of Chapter 4 results.

The aim of the study conducted in Chapter 4 was to test whether the identified cross-modal effects observed in the previous literature (Bailey et al., 2019; Meyer et al., 2011, 2010; Smith & Goodale, 2015; Vetter et al., 2014; see also Chapter 2) have the functional role of predictive processing (Clark, 2013). This was an important study since this previous research can only speculate as to why the cross-modal effects observed actually exist. Therefore, we used fMRI to investigate whether predictive processing may underlie why S1 has been found to contain information triggered from distal sensory modalities, such as from vision (Meyer et al., 2011; Smith & Goodale, 2015) or audition (Bailey et al., 2019; see also Chapter 2). To do this, we presented participants with real familiar 3D objects (either a tennis ball, or a plastic cup) in the MRI scanner. Each trial consisted of a prime and target phase, in which the primed object was either congruent or incongruent with the

target object. The participant would always see the object in the prime phase, and was asked to either continue viewing, or to reach out and touch, the object in the target phase. To test predictive processing, we investigated whether a congruent visual prime would aid subsequent interaction with the object by leading to a decreased neural response complimented with a better representation of the object in S1 (Kok et al., 2012; Kok & De Lange, 2015). In contrast, we expected an amplified neural response complimented with a weaker representation of the object in S1 if the visual prime was inconsistent with the target.

Interestingly, the results in this study found the opposite to our expectations in S1, whereby we observed a trend only for above chance classification, thus better representation, of object identity when the visual prime was *incongruent* with the target object that the participant was asked to reach out and touch. The same pattern was found in additional regions of interest, such as left secondary somatosensory cortex (S2) and pooled pre-motor cortex (PMC). We also investigated a subset region of S1 which was specifically localised to the right hand, defined by an independent vibro-tactile localiser to the fingers and thumb of the participants' right hand. Curiously, in this analysis the pattern indicated a potential reverse effect, whereby decoding for incongruent trials was lower than decoding for the congruent trials. Speculating on the basis of these trends, we suggest that running the analysis in hand-sensitive voxels may have 'sharpened' the representation of the object, since we were analysing the data in a more selective population of neurons tuned to the task (de Lange et al., 2018). If this is the case, this follows previous suggestions that voxels tuned to the task produce a stronger representation of the stimulus (Kok et al., 2012; Kok & De Lange, 2015; Yon et al., 2018). However, due to the lack of significant findings after controlling for the false discovery rate (FDR; Benjamini & Hochberg, 1995; Benjamini & Yekutieli, 2001), these findings must be interpreted with significant caution.

5.3. Theoretical implications

5.3.1. Predictive coding as a theoretical mechanism for decoding high-level influences in the primary sensory cortices.

The results from Chapter 2 support the increasingly popular predictive coding, also known as predictive processing, theory of human brain function (Clark, 2013), as we can find high-level influences in a primary somatosensory cortical area which is independent to the source of stimulus presentation. This would not be possible if the primary sensory cortical areas of the human brain passively registered incoming sensory information (e.g. if incoming visual information is only passively registered in the primary visual cortex). Rather, it is likely that predictive coding models can explain why we observe cross-modal context effects in such primary sensory areas. Predictive coding (see Chapter 1, Section 1.4.2. for a detailed review) suggests the brain builds internal models about the world through experience, and uses contextual information from prior experience and the current context to generate predictions about likely upcoming sensory events, continuously testing these predictions against what actually happened in real time (de Lange et al., 2018). With this theoretical account, it is likely that the primary sensory cortices actively predict forthcoming stimulation, with predictions being sent from high-level areas down the cortical hierarchy towards the primary sensory areas, whereby the predictions are compared against the veridical input in a continuous cycle until all sensory input has been explained (Clark, 2013; Kok & De Lange, 2015).

In relation to the results we see in Chapter 2, the brain has likely built internal models about interacting with a familiar object, such as a keyboard, meaning associative links have been formed in the brain from prior experience of all sensory aspects involved when interacting with the object (e.g. the sound and tactile sensation of typing on the keys). If this is the case, when hearing only the sound of a familiar hand-object interaction, such as typing on a keyboard, information related to the tactile and/or motor content of the stimuli may be sent to S1 as a prediction of upcoming input, since it is information which may be useful for future (or concurrent) interaction with the specific object. Furthermore, S1 itself may have actively anticipated the upcoming stimulation, yet since the tactile sensation was never received, prediction errors may have been sent to higher-level regions in an

attempt to explain the difference between what was expected and the observed sensory information (Clark, 2013; Rao & Ballard, 1999).

The results from Chapter 3 also provide some support for predictive coding in the brain, since we found high-level influences in the oscillatory response associated with primary sensorimotor areas. This suggests associative links may have been formed from the visual, tactile, and motor aspects of an object such as a wine glass, which, when viewing, would often include the action of reaching out to interact with the object (see also Smith & Goodale, 2015). As such, simply viewing the object could feedback predictions about the likely upcoming interaction to somatosensory or sensorimotor regions, oscillating at a rate between 8-13 Hz. This is supported by previous research that has suggested such low-frequency oscillations are responsible for coordinating predictions along feedback pathways (Bonaiuto et al., 2018; Scheeringa & Fries, 2019), and the mu rhythm has been associated with activity in S1 (Cheyne, 2013; Cheyne et al., 2003). However, due to the weak spatial resolution of EEG we cannot rule out the idea that the effects could have been originating from M1, especially since we found weak evidence for a degree of information about hearing the sound of familiar hand-object interactions in M1 in Chapter 2 (see also Bailey et al., 2019). However, since Smith and Goodale (2015) found decoding for viewing the exact same familiar visual objects only in S1, and not M1, we have reason to believe the effects we observe originate from S1.

Whilst neither of the studies conducted Chapters 2 and 3 measured predictive coding directly, Chapter 4 aimed to explicitly test the predictive coding account by investigating whether a congruent or incongruent visual prime could influence the neural response when participants were asked to subsequently reach out and interact with the object. We found, in contrast to our hypothesis, hints towards higher decoding accuracies in somatosensory and motor-related brain regions when participants interacted with an object which was inconsistent with the visual prime – although it is important to note these decoding accuracies did not survive FDR corrections. Nevertheless, the trend we observe is intriguing, as we believe we may have been detecting signs of prediction errors which were likely being transmitted to high-level brain regions in an attempt to explain the unexpected input (Rao & Ballard, 1999). Furthermore, we observe some very tentative evidence of support for predictive processing whereby minimised prediction errors may be apparent in voxels selective to the task in S1. This is because we observed a reverse pattern of

decoding in $S1_{localiser}$ whereby decoding was lower for Invalid trials compared to Valid trials. This tentatively agrees with previous research which has suggested voxels tuned to the task produce a stronger representation of the stimulus, since an incongruent (and hence, likely unpredicted) event led to weaker decoding in this analysis (Kok et al., 2012; Kok & De Lange, 2015; Yon et al., 2018). However, due to the lack of significant findings after FDR corrections in this study, no strong conclusions can be drawn from these results.

5.3.2. Representation of object concepts to explain cross-sensory processing in the brain.

Understanding how the early sensory cortical areas represent the information from the stimuli used in this thesis can also be explained with theories for how the brain represents knowledge of objects. For example, Martin's (2016) representation of object concepts theory suggests the neural representation of object concepts is distributed across the perceptual, action, and emotion systems in the brain. In terms of object knowledge, the theory suggests that salient information is stored in property-specific, *not* modality-specific, brain regions. In saying this, the idea is that specific object categories comprise a unique circuitry in the brain, in which the entire processing stream that was activated at the time information was acquired or updated can be re-activated in an 'all-or-none' fashion. To take an example from the research conducted in Chapter 2, hearing the sound of typing on a keyboard may activate *all* previously stored information about the object (e.g., the sight, sound, tactile sensation and motor action plans of the keys, in addition to semantic knowledge about what a keyboard is used for). Martin's theory suggests this ability to retain all stored knowledge about an object avoids the need of re-learning the properties of an object at every encounter. This theory also ties in nicely with the work of Barsalou (2016), who suggests object perception or categorization involves a neural re-use of the same systems which were active when a person stored the initial representation of an object in the brain (see also Anderson, 2010).

Together these theories could help to explain how multiple sensory modalities may receive information from a stimulus presented via one independent sense, since the theories suggest object concepts are stored across multiple systems in the brain to enable adaptive and efficient basic-level object category identification

(Barsalou, 2016; Martin, 2016). In terms of the research in this thesis, when presented with a familiar object, activation in early sensory cortical areas independent to that of stimulus presentation may be a reflection of the broad representation of stored knowledge about the object. The idea is that processing the object via one sense activates a neural network of all previously stored associations with that object, rather than the idea that these areas are activated to aid future object interaction in a predictive manner (see Section 5.3.1. above).

Due to this alternative explanation, future research should consider experiments which can explicitly examine whether the observed cross-modal effects are a likely result of predictive coding or stored object concepts becoming re-activated in the brain. To test predictive coding, an element of expectation could be implemented in the experiments used in the present thesis. For example, the study from Chapter 2 could be replicated, adding colour changes in the fixation cross which indicate the likelihood of hearing a certain type of sound category (for example, see Kok et al., 2012). Here, we could investigate the neural responses to the exact same sound when it was either expected, or unexpected, to examine whether the representation of the hand-object sounds are stronger in S1 when they were predicted based upon a cued fixation cross. If this is the case, this would provide support for predictive coding in the brain. Furthermore, since Martin's (2016) account of the representation of object knowledge proposes the primary sensory regions could become re-activated under specific task conditions, future research could consider manipulating task constraints in the studies used in this thesis. Here, we may expect stronger decoding for the hand-object interaction sounds in S1 for a task in which the somatosensory properties of objects and/or actions are more prominent compared to less prominent. If this is the case, the results would provide a heavier weight of support for the account of stored object concepts becoming re-activated in the brain.

5.4. Real world applications

5.4.1. Decoding cross-modal influences in primary sensory areas can aid understanding of neural plasticity in sensory deprivation.

Our results can be used to explain how specific experiences may cause neuroplastic changes in cortical brain structures. Neural plasticity is the ability for the brain to reorganise itself in terms of its functional or structural properties in response to a given event, or a set of events (Huttenlocher, 2002). Furthermore, cross-modal plasticity occurs when neurons or brain regions that would typically process a certain type of sensory information (e.g. visual regions process visual information) can adapt to process a different kind of sensory information if the person has undergone sensory deprivation to that modality (for reviews see Collignon, Champoux, Voss, & Lepore, 2011; Collignon, Voss, Lassonde, & Lepore, 2009; Frasnelli et al, 2011). For example, visual regions can respond to tactile braille reading in blind individuals (Sadato et al., 1996). Interestingly, more recent work has found visual regions also respond to braille reading in trained sighted participants (Siuda-Krzywicka et al., 2016), indicating large-scale neuroplastic changes can occur when learning complex skills.

Previous research has often suggested the brain only undergoes such cross-modal plastic changes when a person experiences sensory deprivation, however, the fact we have observed cross-modal sensory influences in the typically functioning brain in the present thesis suggests these cross-modal connections may exist even if a person has not undergone deprivation to a sensory modality. Indeed, previous research has found evidence that cortico-cortical connections from A1 to V1 exist, yet are weakened, in the typically functioning human brain relative to blind individuals (Klinge et al., 2010). The idea is that these connections remain intact and are brought back to strength following sensory deprivation (Collignon et al., 2009). In the present thesis, we provide some support for this idea by finding that information about a certain stimulus can be found in one sensory modality, such as S1, when triggered via distal independent sensory modalities, such as audition (Bailey et al., 2019; see also Chapter 2) or vision (Meyer et al., 2011; Smith & Goodale, 2015; see also Chapter 3). As such, we suggest that cross-modal connections can transmit content-specific information related to one sensory

modality to an entirely independent sensory modality in a typically functioning human brain, thus supporting the notion that these cross-modal connections exist, yet may become strengthened following deprivation to a primary sensory cortical area (Collignon et al., 2009). However, since we do not know the true nature of the connections used in the cross-modal context effects observed in this thesis, no definitive conclusions can be drawn from this claim. Future research should consider running the studies conducted in this thesis on individuals who have undergone sensory deprivation to investigate whether the cross-modal decoding effects are stronger for blind individuals when compared to the data used from the typically functioning human brain in the present thesis.

5.4.2. Advances for machine learning and the design of intelligent computing chips.

These findings will also be of interest to computational modellers who may be interested in developing intelligent computing chips for building realistic models of human brain function, specifically by taking into consideration the influence of context on early sensory processing. For example, the Generative Query Network (GQN), developed by the artificial intelligence company DeepMind, is a software within which machines learn to represent scenes using only their own sensors (Eslami et al., 2018). The GQN can create an internal representation of a scene by reading information about still images of objects placed in a virtual room, taken from different viewpoints, and can generate predictions about what the scene should look like from an unobserved viewpoint. As mentioned by Eslami et al. (2018), the GQN thus demonstrates representational learning without relying on any human input, such as semantic labelling. The algorithm learns the scene and predicts what may be shown, and continuously takes the difference between its predictions and what is actually observed in order to improve the likelihood of accurately predicting the input in the future, similar to predictive processing theories of human brain function (Clark, 2013). However, whilst this deep learning model can learn to perceive and interpret an internal representation of a scene, including an objects identity and position in 3D space, it is constrained to the visual representation of the 3D structure. As such, the work in the present thesis emphasises the importance of training artificial intelligence models to build representations from multiple sensory

modalities to build a complete and more accurate representation of something such as an object. For example, when building a representation of a scene in terms of where 3D objects are placed in a virtual room, models should be trained on a more similar representation as is present in a human brain – accounting for prior knowledge of interacting with the objects and the associated motor/tactile features of the objects which will be predicted in the primary somatosensory cortex. Indeed, recent work by Jacobs and Zu (2019) trained deep or artificial neural networks either with both visual and haptic signals, or with visual signals alone, and found a network which received multisensory training benefitted in terms of the information it represented when compared to a network which only received visual training.

Our findings are also applicable to state of the art advances in neuroscience in the biotechnology and neural engineering community working on developing neuroprosthetic devices, such as brain-controlled robotic limbs (Burck, Bigelow, & Harshbarger, 2011). For instance, engineers have recently used EEG recordings associated with certain movements or states of alertness, and converted them into commands for robotic arms (Beyrouthy, Al Kork, Korbane, & Abouelela, 2017). These arms are operated via brain activity using neurofeedback from EEG, since the arms are equipped with a network of smart sensors that can provide the patient with intelligent feedback about something such as an object and its surrounding environment. However, a limitation with the field of neuroprosthetics is that the amount of information which can be extracted from the EEG signal is low and is not as flexible as a natural limb (Abbott & Faisal, 2012), thus restricting the potential use of these prosthetics in everyday activities and limiting their overall usage (Thomik, Haber, Faisal, & Ieee, 2013). As such, the results we have observed from Chapter 3 in the present thesis may help to advance the development of neuroprosthetic devices, since we have shown that information specific to the category of different familiar visual objects can be detected within the sensorimotor oscillatory response. Therefore, the future of neuroprosthetics could design a device which can determine the specific tactile and/or motor properties of an object based on a person merely viewing or hearing the object, in turn informing the robotic arms about the appropriate grip aperture and pressure to put on the object when interacting with it based on information present in the primary somatosensory cortex or sensorimotor-related oscillatory responses.

5.4.3. Applications to understanding neurological disorders and conditions of brain function.

Whilst the research conducted in this thesis has examined healthy populations with an aim to test predictive processes in the typically functioning adult brain, this research could give rise to important opportunities which can investigate any deviations in the predictive effects we observe in neurological or psychiatric disorders. For example, research has previously suggested that dysfunctional prediction in sensory processing is a causal mechanism in developing delusions in patients with schizophrenia (Fletcher & Frith, 2009; Frith & Done, 1988; Horga, Schatz, Abi-Dargham, & Peterson, 2014). Therefore, future research could consider applying the experimental paradigms used in this thesis to clinical populations, such as in patients with schizophrenia, to examine whether different cross-modal effects are found between the typical and patient population. If differences in the cross-modal representation of an object are apparent across the two populations, this could provide further support that predictive coding is the underlying theory as to why we have observed such cross-modal effects in the present thesis. In doing this, it would also further confirm the theory that patients with schizophrenia suffer from deficits in elements of predictive coding in the brain.

Our research could also help to further inform the literature as to why people experience neurological conditions such as synaesthesia. Synaesthesia is a condition of the brain whereby one sense is simultaneously perceived by one or more additional senses. For example, people with synaesthesia may report an ability to see sounds or experience colour when reading letters and numbers (Ward, 2013). The fact we have found in the present thesis that a primary sensory cortical area can receive information specific to the content of a stimulus presented via an entirely independent distal modality suggests that feedback connections between the primary sensory areas exist even in the typically functioning human brain. As such, it may be the case that people who experience synaesthesia have over-active cross-modal connections which transmit information between the sensory modalities in a way that the person consciously experiences it. Indeed, previous research has suggested such ‘cross-wiring’ in the brain has been retained in those who experience synaesthesia (Ramachandran & Hubbard, 2001). In future research, it would be interesting to use a cross-modal paradigm such as in the studies conducted in this thesis with people

who experience synaesthesia to determine whether there is a stronger representation in the synesthetic group as compared to a typical population such as those studied in the present thesis.

Another interesting application from the research conducted in this thesis is its potential use on assessing consciousness in clinical populations, such as those diagnosed as being in the vegetative state. A patient is diagnosed as being in a vegetative state if they have suffered from severe damage to the brain which results in them appearing awake yet showing no signs of awareness or responsiveness in any meaningful way. As such, to be diagnosed as being in a vegetative state, it has typically been assumed that the person's sense of self is diminished, with them displaying basic reflexes yet no signs of what it means to actually be conscious. Within the past few decades, however, the development of state of the art neuroimaging techniques has revealed that those diagnosed as being in the vegetative state can, in some cases, communicate and show signs of consciousness when assessing the activity within their *brain*, not from their overt behaviours (Cruse et al., 2012; Owen et al., 2006). For example, ground-breaking research has used fMRI to reveal those diagnosed as vegetative can imagine playing tennis or walking around their house when merely instructed to do so with the word "imagine", which is verified based on analysing the neural activity in their brain (Owen et al., 2006). Furthermore, patients in the vegetative state can display appropriate responses in the brain to the plot of watching a film, which would require a conscious experience beyond the visual information entering the retina (Naci, Cusack, Anello, & Owen, 2014). These are merely a few of a series of studies which have revealed evidence of awareness in patients diagnosed to be in a vegetative state using fMRI (see also Coleman et al., 2007; Monti et al., 2010).

More recently, research has used EEG to detect signs of consciousness in the vegetative state, since it is cheap and transportable, meaning the equipment can be taken to the bedside within a patient's home. For example, Cruse et al. (2011, 2012) have used EEG to find significant modulation of sensorimotor beta oscillations in vegetative patients following a command to try to move their hands or toes. Furthermore, research has suggested alpha oscillations may be the most informative marker of a diagnostic model of consciousness (Sokoliuk & Cruse, 2018), since alpha is considerably reduced in those diagnosed as being in a vegetative state. As such, machine learning methods could help establish whether or not a person is in a

vegetative state by training the machines to differentiate between alpha power in clinical and healthy populations (Engemann et al., 2018). With this in mind, the results from Chapter 3 could be of significant interest to researchers in this field. This is because we have found information specific to the content of different familiar visual objects can be discriminated in the alpha oscillation over sensorimotor areas when healthy participants merely saw the image of the still object. The fact the participants were merely viewing the objects and no explicit haptic interaction was either required or implied suggests predictive processing mechanisms may have been the reason for these effects (Clark, 2013). Furthermore, it is likely that the study from Chapter 2 could be corroborated with EEG, whereby similar distinguishable responses may be found in the central alpha mu rhythm relating to the content of the sound of different hand-object interactions. The reason this could be of interest to researchers detecting awareness in the vegetative state is because we could examine whether the same distinguishable responses are found in the alpha mu rhythm of those diagnosed as being vegetative. If we found comparable responses in this clinical population, this could not only suggest the underlying brain structures known to underlie a patients level of consciousness remain intact (Sokoliuk & Cruse, 2018), but could specifically determine whether the patient's prior knowledge about the tactile or motor features of each individual object is still intact.

5.5. Limitations

There are several limitations from the studies conducted in this thesis which are important to address. Firstly, the largest limitation from the study in Chapter 2 is the limited number of participants needed for a 'gold standard' number for fMRI research (Desmond & Glover, 2002; Poldrack et al., 2017). Whilst our data is strong in terms of the a priori hypotheses we set and survives after FDR corrections thus assumed to be true, the low sample size causes a lack of power for further analyses which may have been informative. For example, the lower sample lead to no significant activations found in the brain in a psychophysical interaction (PPI) connectivity analysis (O'Reilly, Woolrich, Behrens, Smith, & Johansen-Berg, 2012) which we conducted in order to examine whether there was any activity in areas of the brain when S1 was used as the seed region of interest. Therefore, testing more

participants may have increased the power, giving us the ability to run further analyses of interest on the data and determine the potential neural pathway for transmitting cross-modal information.

Furthermore, the experiment would have benefitted from including sounds from an additional familiar object interaction category using a different part of the body, such as the mouth or the foot. Whilst this could determine whether decoding of the sound of different haptic-implying object interactions is localised to the body regions which would be used to interact with the object, the implementation of such a paradigm would be somewhat difficult. For example, whilst we originally planned to include mouth-object interactions in the experiment from Chapter 2, it became increasingly apparent that mouth-object interactions rarely involve the use of the mouth without the hand. For example, brushing teeth is a common mouth action that can be easily identified with its sound, however the action would comprise both the arm and hand action in addition to the mouth sensation. Furthermore, foot-object interactions are relatively hard to find for a sound experiment, since most would involve walking on ground whereby shoes would usually be worn thus perhaps not producing a rich tactile sensation, or kicking an object such as a football which may not be distinct enough for the sound to be classified and represented in the brain with accurate precision.

One limitation from the study conducted in Chapter 3 is the fact there is a heavier weight in the literature stating that the mu rhythm is an index of actual motoric actions, as opposed to somatosensory features of actions (A. Cochin, Barthelemy, Roux, & Martineau, 1999; S. Cochin, Barthelemy, Lejeune, Roux, & Martineau, 1998; Denis, Rowe, Williams, & Milne, 2017; Kumar et al., 2013; Muthukumaraswamy & Johnson, 2004; Pfurtscheller et al., 1997; Pineda, 2005). Therefore, we could have implemented the somatosensory vibro-tactile localiser in the EEG experiment conducted in Chapter 3, in addition to the voluntary motor response task, to determine whether we could find an oscillatory response in the mu rhythm oscillation when participants received tactile stimulation to the hands in the absence of a motor movement. If so, we could have also investigated differences in the mu rhythm response when participants received the vibro-tactile stimulation and when they executed the self-paced motor response experiment. We know from Figure 2.4 in Chapter 2, Section 2.4.3. that the vibro-tactile localiser activates only somatosensory, *not* motor-related cortical regions, therefore using this equipment

with the EEG experiment in Chapter 3 could determine whether the mu rhythm oscillation can uniquely respond to tactile information in addition to a self-paced motor response, as the literature is starting to suggest (Coll et al., 2015, 2017). Furthermore, identifying the average of the significant pixels from the vibro-tactile localiser could have been used to create a mask for extracting each participants ERSP data from the main experiment. This could hence work as a similar tactile/hand-localisation tool as was used for the localiser data in Chapters 2 and 4 (see Chapter 2, Section 2.3.6.2. and Chapter 4, Section 4.3.8. respectively).

Furthermore, the alpha- and beta-band ERSP values extracted from the time-frequency windows assume the exact same significant clusters of desynchronization for all of our participants. This is because one mask was generated for each cluster, based on the average selected time-frequency matrix across *all* participants, and applied to each participant regardless of where the true oscillation in each individual participant may have been. Hence with this method, specific individual differences in the temporal, spatial, and frequency characteristics are ignored, which could be a problem since the boundaries of oscillatory responses are not rigid and tend to vary across participants (M. Cohen, 2014). However, we used this method based on previous research investigating a similar question about the role of the mu rhythm (see Coll et al., 2017). Additionally, we were decoding high-level influences which would not be expected to be detected in the pure oscillatory responses. Rather, we were investigating whether discriminable information about the objects could be found regardless of whether we found an observable mu rhythm response. Whilst we could have considered selecting significant subject-specific clusters from the voluntary motor response task, we may not have successfully identified a mask for each participant since the mu rhythm cannot be detected in every participant (Hobson & Bishop, 2017). Therefore, we believe the best method of analysis was chosen in this case, but acknowledge the accompanying limitation with the method.

Another limitation in the study conducted in Chapter 3 is the lack of an additional control stimulus which is a novel stimulus that is *not* an object. This would have been a beneficial control category to include in order to determine whether any mu suppression is apparent when viewing a novel stimulus which cannot be physically interacted with, such as images of stimulus gratings (e.g. Kok et al., 2012). This type of category would significantly differ from the unfamiliar objects which, despite the lack of familiarity, could be interacted with. If we found

no modulation of a sensorimotor response when participants viewed a novel stimulus which is not an object, we could argue, similar to the study in Chapter 2, that it is not merely any stimulus which causes a mu suppression, but an object which is able to be interacted with.

Limitations from the study conducted in Chapter 4 surround the fact we were interested in the somatosensory (and motor) response of an action, yet the design was largely oriented to vision. An ideal design would have also incorporated a trial in which participants were asked to reach out and touch the object in *both* the prime phase and the target phase of the trial. This could have determined whether any adaptation effects may exist when participants are asked to reach out and touch the same object two times in a row. Lastly, the region of S1 in Chapter 4 is not optimal since hand-drawn masks of the post-central gyrus were not made in each individual participant, but rather a probability map was created based on the mask of S1 created from the participants in Chapter 2. Furthermore, the lower number of participants in the vibro-tactile localiser data from this study has led us to interpret the results with caution. In future work, we plan to create hand-drawn masks of the post-central gyrus in each individual participant in order to accurately define each participant's post-central gyrus along with the relevant sub-divisions of S1. Unfortunately this is a time-consuming task, thus implementing software such as FreeSurfer (Fischl, 2012) to quantify the functional, connectional and structural properties of the human brain could be an option for future analyses with the data collected in Chapter 4.

Finally, it is important to note that the results from the multivariate pattern analyses conducted in all experimental chapters (Chapters 2, 3, and 4) were calculated by entering classification accuracies into a parametric t-test, or non-parametric equivalent Wilcoxon signed-rank test, which were then compared to chance level across all participants. Therefore, the caveats which have been associated with this procedure must be addressed. As mentioned in a relatively recent paper by Allefeld, Görgen, and Haynes (2016), the potential problem with this method is the fact that the true value of classification accuracies here can never be below chance level, therefore this changes the meaning behind the population-level null hypothesis which suggests there is no effect in any participant of the population. As such, rejecting a null hypothesis using this method only allows one to infer that there are some participants within that sample in which there is an information content effect, rather than inferring that there is an information content effect which

generalises to the entire population (see also Brodersen & Chumbley, 2012). However, it is also important to note that despite the caveat that such a procedure may not be able to provide population inference, each experimental chapter in the present thesis compared classification accuracies across different conditions within the same participant populations. For example, the results in Chapter 2 found decoding accuracies in our experimental condition were significantly higher than decoding accuracies in our control conditions, thus providing evidence within our specific participant population for differing levels of information content effects in our hypothesised direction.

5.6. Future directions

5.6.1. Transcranial magnetic stimulation.

There are many interesting avenues that future research could explore with Transcranial Magnetic Stimulation (TMS); a powerful non-invasive method of brain stimulation which can temporarily disrupt a targeted area of the cortex (Barker, Jalinous, & Freeston, 1985; Hallett, 2000). For example, a combined TMS-fMRI study could be used to further explore the results found in Chapter 2, whereby TMS could be applied to a higher-order multisensory relay brain region, such as STS. Since high-level areas such as STS are thought to be a multisensory convergence zone for these cross-modal effects (Beauchamp, 2005; Driver & Noesselt, 2008; Ghazanfar & Schroeder, 2006), this could hence examine whether disruption to this region impairs the ability for the pattern classifier to decode different familiar hand-object sounds in S1 when compared to the results from Chapter 2. If this was found, using TMS would show causal evidence for the role of multisensory areas in these types of effects, as it would suggest multisensory influences are necessary for successful recognition. We have reason to believe this is possible since previous research has found disrupting the occipital face area leads to impairments when recognising faces (Pitcher, Walsh, Yovel, & Duchaine, 2007).

If we can find causal evidence to suggest STS plays a pivotal role in transmitting information specific to the content of hand-object sounds to S1, another interesting avenue that TMS could explore could be to use a novel paradigm known as cortico-cortical paired association stimulation (ccPAS). This is a form of TMS

that induces short-term plastic changes between paired pulses at two regions of interest on the surface of the cortex (Romei, Chiappini, Hibbard, & Avenanti, 2016). With this in mind, TMS could be used to artificially induce the communication between two neuronal populations (e.g. between A1 and STS), to examine whether artificially facilitating the connections improves the categorisation of the hand-object sounds in S1. Similarly, such a paradigm could also be applied to the study conducted in Chapter 3, whereby we could artificially induce the communication between V1 and STS to examine whether categorisation of familiar visual objects is improved in this case when compared to unfamiliar visual objects or compared to a sham condition.

5.6.2. Functional magnetic resonance imaging at 7-Tesla.

Future research could also use layer-specific fMRI to investigate the laminar architecture underlying the cross-sensory contextual effects we have observed in the present thesis. For example, we could replicate the experimental designs used in Chapter 2 and 3 using 7-Tesla fMRI, which would allow us to investigate the layer-specific profile of activity underlying the transmission of visual or auditory information to S1. In order to support predictive coding theories of human brain function, we would expect to find decoding of the sound of familiar hand-object interactions, or familiar visual object categories, in either the deep or superficial layers of S1, regardless of the initial stimulation modality (Muckli et al., 2015; Palomero-Gallagher & Zilles, 2019; Yu et al., 2019). Furthermore, we could use cross-classification techniques to determine whether the same neural code is activated in S1 for the same object category, regardless of stimulation modality. For example, we could present participants with both the sound of typing on a keyboard, and a video of a person typing on a keyboard, to investigate whether the neural signature detected in S1 is the same across these two independent stimulus types which convey similar tactile information. Such results would be of strong interest to the predictive coding literature and would help to richly characterize the functional laminar architecture underlying cross-sensory context effects in primary somatosensory cortex.

5.6.3. Training paradigms to assess familiarity effects of cross-modal processing.

Another interesting area for future research could be to investigate how the neural representation of unfamiliar objects could change if participants are familiarised with 3D printed versions of the unfamiliar objects. For example, we could use 3D printed versions of the cubies and smoothies (see Chapter 3, Section 3.3.2., Figure 3.1C and 3.1D respectively) taken from Op de Beeck et al. (2008). Here, the same design by Smith and Goodale (2015) could be used in an fMRI experiment both before and after participants are asked to pick up, interact with, and familiarise themselves with the tactile properties of the cubies and smoothies. Following the assumption that familiarity is needed for cross-modal connections to carry information related to the tactile features of objects to S1, we would expect to find no significant decoding in S1 when viewing novel objects if participants have not been trained with them, replicating Smith and Goodale (2015). However, if participants have been trained with 3D printed versions of these unfamiliar objects, thus making them familiar to the person, we would expect to be able to significantly decode between the tactile features of the unfamiliar objects in S1 when participants are only viewing them, since they would then be familiarised with the tactile properties of the objects. This would hence permit causal evidence that experience with the tactile features of the objects is necessary for these effects to emerge.

Such a study could also be conducted between other pairs of sensory modalities, for example, a training element could be added to the study in Chapter 2 which investigated the links between sounds conveying hand-object interactions and the classifiers ability to discriminate these sounds in S1. Here, the same fMRI design could be used as in Chapter 2 (see also Bailey et al., 2019) both before and after participants are trained to learn tactile associations with a sample of different arbitrary artificial sounds. Once again, following the assumption that familiarity with the tactile features of the sounds is needed to carry discriminable patterns of activity to S1, we would expect to find significant decoding for different previously novel sounds in S1 when participants have been trained to learn a tactile association with the sounds when compared to the patterns of activity elicited for the same sounds when participants received no training. Furthermore, participants could even learn a tactile association to a sound for each hand independently, thus enabling

investigation into whether the representation in S1 corresponds to the hemisphere relative to the hand they learned the haptic association with. Such a study could further confirm that prior knowledge with the tactile features of an object is essential in order to observe such cross-modal effects and provide further insight into the laterality of such effects in relation to each hand.

Another experiment which could assess familiarity effects could be a replication of the experiment in Chapter 2, however we could ask participants to physically interact with familiar objects with their hands, such as asking them to type on a keyboard, and we could record the sound of each participant's hand-object interaction. The participant could subsequently hear the sounds they personally created in an fMRI scanner, in addition to a series of hand-object sounds they did not personally create. Here, we may expect to observe stronger decoding accuracies for the hand-objects interaction sounds that the participant personally created when compared to hand-object sounds which were not personally created. Such an experiment would strongly validate the idea that familiarity is a key component needed to observe these cross-modal effects by revealing personal familiarity creates the strongest representation of the sound of a hand-object interaction in S1.

5.6.4. An improved direct measure of predictive coding with real action.

It is worth highlighting a potential adapted paradigm from the real action study conducted in Chapter 4, since the results failed to find convincing evidence for a valid measure of predictive coding effects of action in the brain. As mentioned in Chapter 4, Section 4.5.1., the reason why we may not have found evidence for predictive coding may have been due to the fact the brief illumination of the object in the target phase was a sufficient amount of information for the somatosensory (and motor) cortex to predict their determined tactile sensation, thus producing comparable effects regardless of the visual prime. If this was the case, an adapted paradigm could instead include an auditory prime of a distinguishable hand-object sound that is either congruent or incongruent with the object participants are asked to reach out and interact with. For example, participants could view a real object, such as a keyboard, in which they will then be asked to reach out and touch the object. Then, a sound could also be played whilst participants are reaching out to touch the object. This sound could either be congruent (e.g. typing on a keyboard) or

incongruent (e.g. knocking on a door). If predictive coding (Clark, 2013; see also Chapter 1, Section 1.4.2) can explain the functional significance behind these cross-modal effects, we would expect to find stronger decoding of a real object interaction when participants have simultaneously heard a sound that is congruent with the action they are making compared to hearing a sound which is incongruent with the action (Kok et al., 2012). We have further reason to believe this would be possible based on the results in Chapter 2, which found hearing such sounds produced discriminable patterns of information in S1. This would be an improvement to the paradigm in Chapter 4 since the sound could be played whilst the participant is *simultaneously* executing the action, thus making the results comparable to Yon et al. (2018). If such differences were found, we could provide the first evidence for predictive coding in the brain during action with real 3D objects.

5.7. General conclusion

To conclude, the research presented in this thesis has found the content of cross-modal influences can be decoded in the brain by revealing two important results. First, simply hearing the sound of different familiar hand-object interactions can send discriminable patterns of activity to the primary somatosensory cortex (S1), despite the complete absence of external tactile stimulation. This suggests cross-modal context effects can be observed even when the dominant sense of vision is taken out of the equation. Second, viewing different familiar visual objects which imply rich haptic information can be discriminated in the mu rhythm oscillatory response, despite the absence of physical tactile stimulation or a motor response. Therefore, this thesis has also found evidence to support such cross-modal context effects using a different neuroimaging technique (EEG) and has established a potential oscillatory marker for these effects. Whilst no reliable evidence was found for a direct account of predictive coding to explain these cross-modal influences, this thesis has also provided critical insight into the development of experiments which can directly test the assumptions of predictive coding with real action. The research conducted in this thesis has, therefore, provided significant contributions to the literature regarding our understanding of cross-modal influences and cortical feedback in the human brain.

References

Abbott, W. W., & Faisal, A. A. (2012). Ultra-low-cost 3D gaze estimation: An intuitive high information throughput compliment to direct brain-machine interfaces. *Journal of Neural Engineering*, *9*(4). https://doi.org/10.1088/1741-2560/9/4/046016

Akerstedt, T., Anund, A., Axelsson, J., & Kecklund, G. (2014). Subjective sleepiness is a sensitive indicator of insufficient sleep and impaired waking function. *Journal of Sleep Research*, *23*, 240–252.

Åkerstedt, T., & Gillberg, M. (1990). Subjective and objective sleepiness in the active individual. *International Journal of Neuroscience*, *52*, 29–37.

Albers, A. M., Meindertsma, T., Toni, I., & de Lange, F. P. (2018). Decoupling of BOLD amplitude and pattern classification of orientation-selective activity in human visual cortex. *NeuroImage*, *180*, 31–40. https://doi.org/10.1016/j.neuroimage.2017.09.046

Alink, A., Schwiedrzik, C. M., Kohler, A., Singer, W., & Muckli, L. (2010). Stimulus Predictability Reduces Responses in Primary Visual Cortex. *Journal of Neuroscience*, *30*(8), 2960–2966. https://doi.org/10.1523/JNEUROSCI.3730-10.2010

Allefeld, C., Görgen, K., & Haynes, J. D. (2016). Valid population inference for information-based imaging: From the second-level t-test to prevalence inference. *NeuroImage*, *141*, 378–392. https://doi.org/10.1016/j.neuroimage.2016.07.040

Alonso, J.-M., & Chen, Y. (2009). Receptive Field. *Scholarpedia*, *4*(1), 5393.

Altmann, C. F., Doehrmann, O., & Kaiser, J. (2007). Selectivity for animal vocalizations in the human auditory cortex. *Cerebral Cortex*, *17*(11), 2601–2608. https://doi.org/10.1093/cercor/bhl167

Amaral, D. G. (2000). The functional organization of perception and movement. In *Principles of Neural Science* (4th ed., pp. 337–348). McGraw-Hill.

Amedi, A., Von Kriegstein, K., Van Atteveldt, N. M., Beauchamp, M. S., & Naumer, M. J. (2005). Functional imaging of human crossmodal identification and object recognition. *Experimental Brain Research*, *166*(3–4), 559–571. https://doi.org/10.1007/s00221-005-2396-5

Amunts, K., Malikovic, A., Mohlberg, H., Schormann, T., & Zilles, K. (2000). Brodmann's areas 17 and 18 brought into stereotaxic space - Where and how variable? *NeuroImage*, *11*(1), 66–84. https://doi.org/10.1006/nimg.1999.0516

Anderson, M. L. (2010). Neural reuse: A fundamental organizational principle of the brain. *Behavioral and Brain Sciences*, *33*(4), 245–266. https://doi.org/10.1017/S0140525X10000853

Argall, B. D., Saad, Z. S., & Beauchamp, M. S. (2006). Simplified intersubject averaging on the cortical surface using SUMA. *Human Brain Mapping*, *27*(1), 14–27. https://doi.org/10.1002/hbm.20158

Arnott, S. R., Cant, J. S., Dutton, G. N., & Goodale, M. A. (2008). Crinkling and

crumpling: An auditory fMRI study of material properties. *NeuroImage*, *43*(2), 368–378. https://doi.org/10.1016/j.neuroimage.2008.07.033

Arnstein, D., Cui, F., Keysers, C., Maurits, N. M., & Gazzola, V. (2011). Mu-Suppression during Action Observation and Execution Correlates with BOLD in Dorsal Premotor, Inferior Parietal, and SI Cortices. *Journal of Neuroscience*, *31*(40), 14243–14249. https://doi.org/10.1523/JNEUROSCI.0963-11.2011

Aziz-Zadeh, L., Iacoboni, M., Zaidel, E., Wilson, S., & Mazziotta, J. (2004). Left hemisphere motor facilitation in response to manual action sounds. *European Journal of Neuroscience*, *19*(9), 2609–2612. https://doi.org/10.1111/j.0953-816X.2004.03348.x

Bailey, K. M., Giordano, B. L., Kaas, A., & Smith, F. W. (2019). Decoding the sound of hand-object interactions in primary somatosensory cortex. *BioRxiv*, 732669. https://doi.org/10.1101/732669

Bannert, M. M., & Bartels, A. (2013). Decoding the yellow of a gray banana. *Current Biology*, *23*(22), 2268–2272. https://doi.org/10.1016/j.cub.2013.09.016

Barker, A. T., Jalinous, R., & Freeston, I. L. (1985). Non-invasive magnetic stimulation of human motor cortex. *The Lancet*, *325*(8437), 1106–1107. https://doi.org/10.1515/eng-2018-0022

Barone, P., Batardiere, A., Knoblauch, K., & Kennedy, H. (2000). Laminar Distribution of Neurons in Extrastriate Areas Projecting to Visual Areas V1 and V4 Correlates with the Hierarchical Rank and Indicates the Operation of a Distance Rule. *The Journal of Neuroscience*, *20*(9), 3263–3281. https://www.jneurosci.org/content/jneuro/20/9/3263.full.pdf

Barsalou, L. W. (2016). On Staying Grounded and Avoiding Quixotic Dead Ends. *Psychonomic Bulletin and Review*, *23*(4), 1122–1142. https://doi.org/10.3758/s13423-016-1028-3

Bastos, A. M., Usrey, W. M., Adams, R. A., Mangun, G. R., Fries, P., & Friston, K. J. (2012). Canonical Microcircuits for Predictive Coding. *Neuron*, *76*(4), 695–711. https://doi.org/10.1016/j.neuron.2012.10.038

Bastos, A. M., Vezoli, J., Bosman, C. A., Schoffelen, J. M., Oostenveld, R., Dowdall, J. R., DeWeerd, P., Kennedy, H., & Fries, P. (2015). Visual areas exert feedforward and feedback influences through distinct frequency channels. *Neuron*, *85*(2), 390–401. https://doi.org/10.1016/j.neuron.2014.12.018

Bavelier, D., & Neville, H. J. (2002). Cross-modal plasticity: Where and how? *Nature Reviews Neuroscience*, *3*(6), 443–452. https://doi.org/10.1038/nrn848

Bays, P. M., Flanagan, J. R., & Wolpert, D. M. (2006). Attenuation of self-generated tactile sensations is predictive, not postdictive. *PLoS Biology*, *4*(2), 281–284. https://doi.org/10.1371/journal.pbio.0040028

Bays, P. M., & Wolpert, D. M. (2007). Computational principles of sensorimotor control that minimize uncertainty and variability. *Journal of Physiology*, *578*(2), 387–396. https://doi.org/10.1113/jphysiol.2006.120121

Beauchamp, M. S. (2005). See me, hear me, touch me: Multisensory integration in lateral occipital-temporal cortex. *Current Opinion in Neurobiology*, *15*(2), 145–

153. https://doi.org/10.1016/j.conb.2005.03.011

Beauchamp, M. S., Yasar, N. E., Frye, R. E., & Ro, T. (2008). Touch, sound and vision in human superior temporal sulcus. *NeuroImage*, *41*(3), 1011–1020. https://doi.org/10.1016/j.neuroimage.2008.03.015

Belin, P., Zatorre, R. J., Lafaille, P., Ahad, P., & Pike, B. (2000). Voice-selective areas in human auditory cortex. *Nature*, *403*(6767), 309–312.

Bell, A. H., Summerfield, C., Morin, E. L., Malecek, N. J., & Ungerleider, L. G. (2016). Encoding of Stimulus Probability in Macaque Inferior Temporal Cortex. *Current Biology*, *26*(17), 2280–2290. https://doi.org/10.1016/j.cub.2016.07.007

Benjamini, Y., & Hochberg, Y. (1995). Controlling the False Discovery Rate: a Practical and Powerful Approach to Multiple Testing. *Journal of the Royal Statistical Society: Series B (Methodological)*, *57*(1), 289–300. https://doi.org/10.2307/2346101

Benjamini, Y., & Yekutieli, D. (2001). The control of the false discovery rate in multiple testing under dependency. *The Annals of Statistics*, *29*(4), 1165–1188. https://doi.org/10.3390/s130810151

Berger, H. (1929). Ueber das Elektroenkephalogramm das Menschen. *Archiv Fuer Psychiatrie*, *87*, 527–570.

Berman, N. E. (1991). Alterations of visual cortical connections in cats following early removal of retinal input. *Developmental Brain Research*, *63*(1–2), 163–180.

Beyrouthy, T., Al Kork, S., Korbane, J. A., & Abouelela, M. (2017). EEG mind controlled smart prosthetic arm - A comprehensive study. *Advances in Science, Technology and Engineering Systems*, *2*(3), 891–899. https://doi.org/10.25046/aj0203111

Bigdely-Shamlo, N., Mullen, T., Kothe, C., Su, K.-M., & Robbins, K. A. (2015). The PREP pipeline: standardized preprocessing for large-scale EEG analysis. *Frontiers in Neuroinformatics*, *9*(16), 1–20. https://doi.org/10.3389/fninf.2015.00016

Blake, D. T., & Merzenich, M. M. (2002). Changes of AI receptive fields with sound density. *Journal of Neurophysiology*, *88*(6), 3409–3420. https://doi.org/10.1152/jn.00233.2002

Blakemore, S., Wolpert, D. M., & Frith, C. D. (1998). Central cancellation of self-produced tickle sensation. *Nature Neuroscience*, *1*(7), 635–640.

Blankenburg, F., Ruff, C. C., Deichmann, R., Rees, G., & Driver, J. (2006). The cutaneous rabbit illusion affects human primary sensory cortex somatotopically. *PLoS Biology*, *4*(3), 0459–0466. https://doi.org/10.1371/journal.pbio.0040069

Bonaiuto, J. J., Meyer, S. S., Little, S., Rossiter, H., Callaghan, M. F., Dick, F., Barnes, G. R., & Bestmann, S. (2018). Lamina-specific cortical dynamics in human visual and sensorimotor cortices. *ELife*, *7*, 1–32. https://doi.org/10.7554/eLife.33977

Brainard, D. H. (1997). The Psychophysics Toolbox. *Spatial Vision*, *10*(4), 433–436.

Brandi, M.-L., Wohlschlager, A., Sorg, C., & Hermsdorfer, J. (2014). The Neural Correlates of Planning and Executing Actual Tool Use. *Journal of Neuroscience*, *34*(39), 13183–13194. https://doi.org/10.1523/JNEUROSCI.0597-14.2014

Breedlove, S. M., Watson, N. V, & Rosenzweig, M. R. (2010). Sensory Information Processing is Selective and Analytical. In *Biological Psychology* (7th ed., pp. 228–235). Sinauer associates.

Brenner, M. (2015). *The Bayesian Brain Hypothesis*. https://towardsdatascience.com/the-bayesian-brain-hypothesis-35b98847d331

Brewer, A. A., & Barton, B. (2016). Maps of the Auditory Cortex. *Annual Review of Neuroscience*, *39*(1), 385–407. https://doi.org/10.1146/annurev-neuro-070815-014045

Brodersen, K. H., & Chumbley, J. R. (2012). Bayesian Mixed-Effects Inference on Classification Performance in.pdf. *Journal OfMachine Learning Research 13 (2012)*, *13*, 3133–3176.

Brodmann, K. (1994). *Localisation in the Cerebral Cortex*. Smith-Gordon.

Brodmann, K., & Garey, L. J. (2006). *Brodmann's localisation in the cerebral cortex*. Springer. https://doi.org/10.1007/b138298

Brown, R. M., Chen, J. L., Hollinger, A., Penhune, V. B., Palmer, C., & Zatorre, R. J. (2013). Repetition suppression in auditory-motor regions to pitch and temporal structure in music. *Journal of Cognitive Neuroscience*, *25*(2), 313–328. https://doi.org/10.1162/jocn_a_00322

Brown, R. M., Zatorre, R. J., & Penhune, V. B. (2015). Expert music performance: Cognitive, neural, and developmental bases. In *Progress in Brain Research* (1st ed., Vol. 217). Elsevier B.V. https://doi.org/10.1016/bs.pbr.2014.11.021

Bruce, C., Desimone, R., & Gross, C. G. (1981). Visual Properties of Neurons in a Polysensory Area in Superior Temporal Sulcus of the Macaque. *Journal of Neurophysiology*, *46*(2), 369–384.

Buccino, G., Binkofski, F., Fink, G. R., Fadiga, L., Fogassi, L., Gallese, V., Seitz, R. J., Zilles, K., Rizzolatti, G., & Freund, H. J. (2001). Action observation activates premotor and parietal areas in a somatotopic manner: An FMRI study. *European Journal of Neuroscience*, *13*, 400–404. https://doi.org/10.4324/9780203496190

Budinger, E., Heil, P., Hess, A., & Scheich, H. (2006). Multisensory processing via early cortical stages: connections of the primary auditory cortical field with other sensory systems. *Neuroscience*, *143*(4), 1065–1083. https://doi.org/10.3389/conf.neuro.09.2009.01.267

Budinger, E., Laszcz, A., Lison, H., Scheich, H., & Ohl, F. W. (2008). Non-sensory cortical and subcortical connections of the primary auditory cortex in Mongolian gerbils: Bottom-up and top-down processing of neuronal information via field AI. *Brain Research*, *1220*, 2–32. https://doi.org/10.1016/j.brainres.2007.07.084

Buffalo, E. A., Fries, P., Landman, R., Buschman, T. J., & Desimone, R. (2011).

Laminar differences in gamma and alpha coherence in the ventral stream. *Proceedings of the National Academy of Sciences*, *108*(27), 11262–11267. https://doi.org/10.1073/pnas.1011284108

Burck, J. M., Bigelow, J. D., & Harshbarger, S. D. (2011). Revolutionizing Prosthetics: Systems Engineering Challenges and Opportunities. *Johns Hopkins APL Technical Digest*, *30*(3), 186–197.

Calvert, G. (1997). Activation of auditory cortex during silent lip-reading. *Science*, *276*(1997), 593–596. https://doi.org/10.1126/science.276.5312.593

Cannon, E. N., Yoo, K. H., Vanderwert, R. E., Ferrari, P. F., Woodward, A. L., & Fox, N. A. (2014). Action experience, more than observation, influences mu rhythm desynchronization. *PLoS ONE*, *9*(3). https://doi.org/10.1371/journal.pone.0092002

Cappe, C., & Barone, P. (2005). Heteromodal connections supporting multisensory integration at low levels of cortical processing in the monkey. *European Journal of Neuroscience*, *22*(11), 2886–2902. https://doi.org/10.1111/j.1460-9568.2005.04462.x

Carandini, M., Demb, J., Mante, V., Tolhurst, D., Dan, Y., Olshausen, B., Gallant, J., & Rust, N. (2005). Do We Know What the Early Visual System Does? *The Journal of Neuroscience*, *25*(46), 10577–10597. https://doi.org/10.1523/JNEUROSCI.3726-05.2005

Cate, A. D., Herron, T. J., Yund, E. W., Stecker, G. C., Rinne, T., Kang, X., Petkov, C. I., Disbrow, E. A., & Woods, D. L. (2009). Auditory Attention Activates Peripheral Visual Cortex. *PLoS ONE*, *4*(2), e4645. https://doi.org/10.1371/journal.pone.0004645

Cavina-Pratesi, C., Goodale, M. A., & Culham, J. C. (2007). FMRI reveals a dissociation between grasping and perceiving the size of real 3D objects. *PLoS ONE*, *2*(5). https://doi.org/10.1371/journal.pone.0000424

Chang, C.-Y., Hsu, S.-H., Pion-Tonachini, L., & Jung, T.-P. (2018). *Evaluation of Artifact Subspace Reconstruction for Automatic EEG Artifact Removal Mental Health Monitoring with EEG View project Evaluation of Artifact Subspace Reconstruction for Automatic EEG Artifact Removal*. 1242–1245. https://doi.org/10.1109/EMBC.2018.8512547

Chang, C., & Lin, C. (2011). *LIBSVM: a library for support vector machines. ACMTrans Intell Syst Technol. 2:27*.

Changeux, J.-P., Courrpge, P., & Danchin, A. (1973). *A Theory of the Epigenesis of Neuronal Networks by Selective Stabilization of Synapses (control theory/graph theory/learning/synaptic plasticity/neuromuscular junction)*. *70*(10), 2974–2978.

Chapman, B., Zahs, K. R., & Stryker, M. P. (1991). Relation of cortical cell orientation selectivity to alignment of receptive fields of the geniculocortical afferents that arborize within a single orientation column in ferret visual cortex. *Journal of Neuroscience*, *11*(5), 1347–1358. https://doi.org/10.1523/jneurosci.11-05-01347.1991

Chaudhuri, A. (2011). *Fundamentals of Sensory Perception*. Oxford University Press.

Chen, J. L., Penhune, V. B., & Zatorre, R. J. (2009). The role of auditory and premotor cortex in sensorimotor transformations. *Annals of the New York Academy of Sciences, 1169*, 15–34. https://doi.org/10.1111/j.1749-6632.2009.04556.x

Chen, J. L., Rae, C., & Watkins, K. E. (2012). Learning to play a melody: An fMRI study examining the formation of auditory-motor associations. *NeuroImage, 59*(2), 1200–1208. https://doi.org/10.1016/j.neuroimage.2011.08.012

Chen, L. M., Friedman, R. M., & Roe, A. W. (2003). Optical Imaging of a Tactile Illusion in Area 3b of the Primary Somatosensory Cortex. *Science, 302*(5646), 881–885. https://doi.org/10.1126/science.1087846

Cheyne, D. O. (2013). MEG studies of sensorimotor rhythms: A review. *Experimental Neurology, 245*, 27–39. https://doi.org/10.1016/j.expneurol.2012.08.030

Cheyne, D. O., Gaetz, W., Garnero, L., Lachaux, J. P., Ducorps, A., Schwartz, D., & Varela, F. J. (2003). Neuromagnetic imaging of cortical oscillations accompanying tactile stimulation. *Cognitive Brain Research, 17*(3), 599–611. https://doi.org/10.1016/S0926-6410(03)00173-3

Ciuparu, A., & Mureşan, R. C. (2016). Sources of bias in single-trial normalization procedures. *European Journal of Neuroscience, 43*(7), 861–869. https://doi.org/10.1111/ejn.13179

Clark, A. (2013). Whatever next? Predictive brains, situated agents, and the future of cognitive science. *Behavioural and Brain Sciences*, 181–253. https://doi.org/10.1017/S0140525X12000477

Cochin, A., Barthelemy, C., Roux, S., & Martineau, J. (1999). Observation and execution of movement: similarities demonstrated by quanti ed electroencephalography ´. *Neuroscience, 11*, 1839–1842. https://doi.org/10.1046/j.1460-9568.1999.00598.x

Cochin, S., Barthelemy, C., Lejeune, B., Roux, S., & Martineau, J. (1998). Perception of motion and qEEG activity in human adults. *Electroencephalography and Clinical Neurophysiology, 107*(4), 287–295. https://doi.org/10.1016/S0013-4694(98)00071-6

Cohen, J. D. (1988). *Statistical power analysis for the behavioral sciences* (2nd ed.). Erlbaum.

Cohen, M. (2014). *Analyzing neural time series data: theory and practice*. The MIT Press.

Colavita, F. B. (1974). Human sensory dominance. *Perception & Psychophysics, 16*(2), 409–412. https://doi.org/10.3758/BF03203962

Coleman, M. R., Rodd, J. M., Davis, M. H., Johnsrude, I. S., Menon, D. K., Pickard, J. D., & Owen, A. M. (2007). Do vegetative patients retain aspects of language comprehension? Evidence from fMRI. *Brain, 130*(10), 2494–2507. https://doi.org/10.1093/brain/awm170

Coll, M.-P., Bird, G., Catmur, C., & Press, C. (2015). Cross-modal repetition effects in the mu rhythm indicate tactile mirroring during action observation. *Cortex*, *63*, 121–131. https://doi.org/10.1016/j.cortex.2014.08.024

Coll, M.-P., Press, C., Hobson, H., Catmur, C., & Bird, G. (2017). Crossmodal Classification of Mu Rhythm Activity during Action Observation and Execution Suggests Specificity to Somatosensory Features of Actions. *The Journal of Neuroscience*, *37*(24), 5936–5947. https://doi.org/10.1523/JNEUROSCI.3393-16.2017

Collignon, O., Champoux, F., Voss, P., & Lepore, F. (2011). Sensory rehabilitation in the plastic brain. In *Progress in Brain Research* (Vol. 191, pp. 211–231). https://doi.org/10.1016/B978-0-444-53752-2.00003-5

Collignon, O., Voss, P., Lassonde, M., & Lepore, F. (2009). Cross-modal plasticity for the spatial processing of sounds in visually deprived subjects. *Experimental Brain Research*, *192*(3), 343–358. https://doi.org/10.1007/s00221-008-1553-z

Crossman, A. R., & Neary, D. (2015). *Neuroanatomy an illustrated colour text* (5th ed.). Churchill Livingstone, Elsevier.

Cruse, D., Chennu, S., Chatelle, C., Bekinschtein, T. A., Fernández-Espejo, D., Pickard, J. D., Laureys, S., & Owen, A. M. (2011). Bedside detection of awareness in the vegetative state: A cohort study. *The Lancet*, *378*(9809), 2088–2094. https://doi.org/10.1016/S0140-6736(11)61224-5

Cruse, D., Chennu, S., Fernandez-Espejo, D., Payne, W. L., Young, G. B., & Owen, A. M. (2012). Detecting Awareness in the Vegetative State: Electroencephalographic Evidence for Attempted Movements to Command. *PLoS ONE*, *7*(11), 1–9. https://doi.org/10.1371/journal.pone.0049933

Cuellar, M., & Toro, C. del. (2017). Time-Frequency Analysis of Mu Rhythm Activity during Picture and Video Action Naming Tasks. *Brain Sciences*, *7*(9), 114. https://doi.org/10.3390/brainsci7090114

Da Silva, F. L., & Van Leeuwen, W. S. (1977). The cortical source of the alpha rhythm. *Neuroscience Letters*, *6*(2–3), 237–241.

David, S. V, & Gallant, J. L. (2005). Predicting neuronal responses during natural vision. *Network*, *16*(2–3), 239–260. https://doi.org/10.1080/09548980500464030

Davis, T., LaRocque, K. F., Mumford, J. A., Norman, K. A., Wagner, A. D., & Poldrack, R. A. (2014). What do differences between multi-voxel and univariate analysis mean? How subject-, voxel-, and trial-level variance impact fMRI analysis. *NeuroImage*, *97*, 271–283. https://doi.org/10.1016/j.neuroimage.2014.04.037

de Lange, F. P., Heilbron, M., & Kok, P. (2018). How Do Expectations Shape Perception? *Trends in Cognitive Sciences*, *22*(9), 764–779. https://doi.org/10.1016/j.tics.2018.06.002

De Martino, F., Moerel, M., Ugurbil, K., Goebel, R., Yacoub, E., & Formisano, E. (2015). Frequency preference and attention effects across cortical depths in the human primary auditory cortex. *Proceedings of the National Academy of*

Sciences of the United States of America, *112*(52), 16036–16041. https://doi.org/10.1073/pnas.1507552112

Delorme, A., & Makeig, S. (2004). EEGLAB: an open sorce toolbox for analysis of single-trail EEG dynamics including independent component analysis. *Journal of Neuroscience Methods*, *134*, 9–21. https://doi.org/10.1016/j.jneumeth.2003.10.009

Dempsey-Jones, H., Wesselink, D. B., Friedman, J., & Makin, T. R. (2019). Organized Toe Maps in Extreme Foot Users Report Organized Toe Maps in Extreme Foot Users. *Cell ReportsReports*, *28*(11), 2748-2756.e4. https://doi.org/10.1016/j.celrep.2019.08.027

Den Ouden, H. E. M., Friston, K. J., Daw, N. D., McIntosh, A. R., & Stephan, K. E. (2009). A dual role for prediction error in associative learning. *Cerebral Cortex*, *19*(5), 1175–1185. https://doi.org/10.1093/cercor/bhn161

Denis, D., Rowe, R., Williams, A. M., & Milne, E. (2017). The role of cortical sensorimotor oscillations in action anticipation. *NeuroImage*, *146*, 1102–1114. https://doi.org/10.1016/j.neuroimage.2016.10.022

Desimone, R. (1996). Neural mechanisms for visual memory and their role in attention. *Proceedings of the National Academy of Sciences of the United States of America*, *93*(24), 13494–13499. https://doi.org/10.1073/pnas.93.24.13494

Desmond, J. E., & Glover, G. H. (2002). Estimating sample size in functional MRI (fMRI) neuroimaging studies: Statistical power analyses. *Journal of Neuroscience Methods*, *118*(2), 115–128. https://doi.org/10.1016/S0165-0270(02)00121-8

DiCarlo, J. J., & Johnson, K. O. (2002). Receptive field structure in cortical area 3b of the alert monkey. *Behavioural Brain Research*, *135*, 167–178. www.elsevier.com/locate/bbr

DiCarlo, J. J., Johnson, K. O., & Hsiao, S. S. (1998). Structure of receptive fields in area 3b of primary somatosensory cortex in the alert monkey. *Journal of Neuroscience*, *18*(7), 2626–2645. https://doi.org/10.1523/jneurosci.18-07-02626.1998

Driver, J., & Noesselt, T. (2008). Multisensory Interplay Reveals Crossmodal Influences on “Sensory-Specific” Brain Regions, Neural Responses, and Judgments. *Neuron*, *57*(1), 11–23. https://doi.org/10.1016/j.neuron.2007.12.013

Edelman, G., & Mountcastle, V. (1978). *The Mindful Brain: Cortical organisation and the group-selective theory of higher brain function*. The Massachusetts Institute of Technology Press.

Eickhoff, S. B., Stephan, K. E., Mohlberg, H., Grefkes, C., Fink, G. R., Amunts, K., & Zilles, K. (2005). A new SPM toolbox for combining probabilistic cytoarchitectonic maps and functional imaging data. *NeuroImage*, *25*(4), 1325–1335. https://doi.org/10.1016/j.neuroimage.2004.12.034

Elbert, T., Pantev, C., Wienbruch, C., Rockstroh, B., & Taub, E. (1995). Increased cortical representation of the fingers of the left hand in string players. *Science*, *270*(5234), 305–307. https://doi.org/10.1126/science.270.5234.305

Elbert, T., Sterr, A., Rockstroh, B., Pantev, C., Mu, M. M., & Taub, E. (2002). Expansion of the Tonotopic Area in the Auditory Cortex of the Blind. *The Journal of Neuroscience*, *22*(22), 9941–9944. papers2://publication/uuid/6D0C5553-FDC7-43B6-A2B7-40147CD3117A

Engel, L. R., Frum, C., Puce, A., Walker, N. A., & Lewis, J. W. (2009). Different categories of living and non-living sound-sources activate distinct cortical networks. *NeuroImage*, *47*(4), 1778–1791. https://doi.org/10.1016/j.neuroimage.2009.05.041

Engemann, D. A., Raimondo, F., King, J. R., Rohaut, B., Louppe, G., Faugeras, F., Annen, J., Cassol, H., Gosseries, O., Fernandez-Slezak, D., Laureys, S., Naccache, L., Dehaene, S., & Sitt, J. D. (2018). Robust EEG-based cross-site and cross-protocol classification of states of consciousness. *Brain*, *141*(11), 3179–3192. https://doi.org/10.1093/brain/awy251

Ernst, M. O., & Banks, M. S. (2002). Humans integrate visual and haptic information in a statistically optimal fashion. *Nature*, *415*, 429–433.

Eskenasy, A. C. C., & Clarke, S. (2000). Hierarchy within human SI: Supporting data from cytochrome oxidase, acetylcholinesterase and NADPH-diaphorase staining patterns. *Somatosensory and Motor Research*, *17*(2), 123–132.

Eslami, S. M. A., Rezende, D. J., Besse, F., Viola, F., Morcos, A. S., Garnelo, M., Ruderman, A., Rusu, A. A., Danihelka, I., Gregor, K., Reichert, D. P., Buesing, L., Weber, T., Vinyals, O., Rosenbaum, D., Rabinowitz, N., King, H., Hillier, C., Botvinick, M., … Hassabis, D. (2018). Neural scene representation and rendering. *Science*, *360*(6394), 1204–1210. https://doi.org/10.1126/science.aar6170

Etzel, J. A., Gazzola, V., & Keysers, C. (2008). Testing simulation theory with cross-modal multivariate classification of fMRI data. *PLoS ONE*, *3*(11). https://doi.org/10.1371/journal.pone.0003690

Falchier, A., Clavagnier, S., Barone, P., & Kennedy, H. (2002). Anatomical evidence of multimodal integration in primate striate cortex. *The Journal of Neuroscience*, *22*(13), 5749–5759. https://doi.org/20026562

Felleman, D. J., & Van Essen, D. C. (1991). Distributed hierachical processing in the primate cerebral cortex. *Cerebral Cortex*, *1*(1), 1–47.

Finney, E. M., Fine, I., & Dobkins, K. R. (2001). Visual stimuli activate auditory cortex in the deaf. *Nature Neuroscience*, *4*(12), 1171–1173. https://doi.org/10.1038/nn763

Fischl, B. (2012). FreeSurfer. *NeuroImage*, *62*(2), 774–781. https://doi.org/10.1016/j.neuroimage.2012.01.021.FreeSurfer

Fischl, B., Sereno, M. I., Tootell, R. B. H., & Dale, A. M. (1999). High-resolution intersubject averaging and a coordinate system for the cortical surface. *Human Brain Mapping*, *8*(4), 272–284. http://www.nmr.mgh.harvard.edu

Fletcher, P. C., & Frith, C. D. (2009). Perceiving is believing: A Bayesian approach to explaining the positive symptoms of schizophrenia. *Nature Reviews Neuroscience*, *10*(1), 48–58. https://doi.org/10.1038/nrn2536

Formisano, E, De Martino, F., Bonte, M., & Goebel, R. (2008). "Who" is saying "what"? Brain-based decoding of human voice and speech. *Science*, *322*, 970–973.

Formisano, Elia, Kim, D. S., Di Salle, F., Van De Moortele, P. F., Ugurbil, K., & Goebel, R. (2003). Mirror-symmetric tonotopic maps in human primary auditory cortex. *Neuron*. https://doi.org/10.1016/S0896-6273(03)00669-X

Fox, N. a, Bakermans-Kranenburg, M. J., Yoo, K. H., Bowman, L. C., Cannon, E. N., Vanderwert, R. E., Ferrari, P. F., & Van Ijzendoorn, M. H. (2016). Assessing Human Mirror Activity With EEG Mu Rhythm: A Meta-Analysis. *Psychological Bulletin*, *142*(3), 291–313. https://doi.org/10.1037/bul0000031

Frasnelli, J., Collignon, O., Voss, P., & Lepore, F. (2011). Crossmodal plasticity in sensory loss. In *Progress in Brain Research* (1st ed., Vol. 191). Elsevier B.V. https://doi.org/10.1016/B978-0-444-53752-2.00002-3

Friston, K. (2003). Learning and inference in the brain. *Neural Networks*, *16*(9), 1325–1352. https://doi.org/10.1016/j.neunet.2003.06.005

Friston, K. (2005). A theory of cortical responses. *Philosophical Transactions of the Royal Society B: Biological Sciences*, *360*(1456), 815–836. https://doi.org/10.1098/rstb.2005.1622

Friston, K. (2009). The free-energy principle: a rough guide to the brain? *Trends in Cognitive Sciences*, *13*(7), 293–301. https://doi.org/10.1016/j.tics.2009.04.005

Friston, K. (2010). The free-energy principle: a unified brain theory? *Nature Reviews. Neuroscience*, *11*(2), 127–138. https://doi.org/10.1038/nrn2787

Friston, K. (2012). The history of the future of the Bayesian brain. *NeuroImage*, *62*(2), 1230–1233. https://doi.org/10.1016/j.neuroimage.2011.10.004

Friston, K., Kiebel, S., Barlow, H. ., Feynman, R. ., Neal, R. ., Hinton, G. ., & Neisser, U. (2009). Predictive coding under the free-energy principle. *Philosophical Transactions of the Royal Society of London. Series B, Biological Sciences*, *364*(1521), 1211–1221. https://doi.org/10.1098/rstb.2008.0300

Friston, K., & Stephan, K. E. (2007). Free-energy and the brain. *Synthese*, *159*(3), 417–458. https://doi.org/10.1007/s11229-007-9237-y

Frith, C. D., & Done, D. J. (1988). Towards a neuropsychology of schizophrenia. *British Journal of Psychiatry*, *153*(OCT.), 437–443. https://doi.org/10.1192/bjp.153.4.437

Fritz, L., Mulders, J., Breman, H., Peters, J., Bastiani, M., Roebroeck, A., Andersson, J., Ashburner, J., Weiskopf, N., & Goebel, R. (2014). Comparison of EPI distortion correction methods at 3T and 7T. *OHBM Annual Meeting, Hamburg, Germany*.

Fu, K.-M. M., Johnston, T. A., Shah, A. S., Arnold, L., Smiley, J., Hackett, T. A., Garraghty, P. E., & Schroeder, C. E. (2003). Auditory cortical neurons respond to somatosensory stimulation. *Journal of Neuroscience*, *23*(20), 7510–7515. https://doi.org/23/20/7510 [pii]

Gabard-Durnam, L. J., Mendez Leal, A. S., Wilkinson, C. L., & Levin, A. R. (2018). The Harvard Automated Processing Pipeline for Electroencephalography

(HAPPE): Standardized Processing Software for Developmental and High-Artifact Data. *Frontiers in Neuroscience, 12*, 1–24. https://doi.org/10.3389/fnins.2018.00097

Gallese, V., Fadiga, L., Fogassi, L., & Rizzolatti, G. (1996). Action recognition in the premotor cortex. *Brain, 119*, 593–609. https://doi.org/10.1093/brain/awp167

Gallivan, J. P., Cavina-Pratesi, C., & Culham, J. C. (2009). Is that within reach? fMRI reveals that the human superior parieto-occipital cortex encodes objects reachable by the hand. *Journal of Neuroscience*, *29*(14), 4381–4391. https://doi.org/10.1523/JNEUROSCI.0377-09.2009

Gallivan, J. P., McLean, D. A., Valyear, K. F., & Culham, J. C. (2013). Decoding the neural mechanisms of human tool use. *ELife*, *2013*(2), 425. https://doi.org/10.7554/eLife.00425

Gardner, E. P., & Johnson, K. (2012). Touch. In *Principles of Neural Science (Kandel ES, JH; Jessell, TM; Siegelbaum, SA; Hudspeth, AJ)* (5th ed., pp. 498–529). McGraw-Hill.

Gazzola, V., Aziz-Zadeh, L., & Keysers, C. (2006). Empathy and the Somatotopic Auditory Mirror System in Humans. *Current Biology*, *16*(18), 1824–1829. https://doi.org/10.1016/j.cub.2006.07.072

Geldard, F. A., & Sherrick, C. E. (1972). The cutaneous "rabbit": A perceptual illusion. *Science*, *178*(4057), 178–179. https://doi.org/10.1126/science.178.4057.178

Geyer, S. (2003). *The microstructural border between the motor and the cognitive domain in the human cerebral cortex* (1st ed.). Springer.

Geyer, S., Ledberg, A., Schleicher, A., Kinomura, S., Schormann, T., Bürgel, U., Klingberg, T., Larsson, J., Zilles, K., & Roland, P. E. (1996). Two different areas within the primary motor cortex of man. *Nature*, *382*(6594), 805–807. https://doi.org/10.1038/382805a0

Ghazanfar, A. A., & Schroeder, C. E. (2006). Is neocortex essentially multisensory? *Trends in Cognitive Sciences*, *10*(6), 278–285. https://doi.org/10.1016/j.tics.2006.04.008

Giard, M. H., & Peronnet, F. (1999). Auditory-visual integration during multimodal object recognition in humans: a behavioral and electrophysiological study. *Journal of Cognitive Neuroscience*, *11*(5), 473–490. https://www.mitpressjournals.org/doi/pdfplus/10.1162/089892999563544

Giordano, B. L., McAdams, S., Zatorre, R. J., Kriegeskorte, N., & Belin, P. (2013). Abstract encoding of auditory objects in cortical activity patterns. *Cerebral Cortex, 23*, 2025–2037. https://doi.org/10.1093/cercor/bhs162

Giordano, B. L., McDonnell, J., & McAdams, S. (2010). Hearing living symbols and nonliving icons: Category specificities in the cognitive processing of environmental sounds. *Brain and Cognition*, *73*(1), 7–19. https://doi.org/10.1016/j.bandc.2010.01.005

Goebel, R., Esposito, F., & Formisano, E. (2006). Analysis of functional image analysis contest (FIAC) data with Brainvoyager QX: From single-subject to

cortically aligned group general linear model analysis and self-organizing group independent component analysis. *Human Brain Mapping*, *27*, 392–401.

Greening, S. G., Mitchell, D. G. V., & Smith, F. W. (2018). Spatially generalizable representations of facial expressions: Decoding across partial face samples. *Cortex*, *101*, 31–43. https://doi.org/10.1016/j.cortex.2017.11.016

Grefkes, C., Geyer, S., Schormann, T., Roland, P., & Zilles, K. (2001). Human Somatosensory Area 2: Observer-Independent Cytoarchitectonic Mapping, Interindividual Variability, and Population Map. *NeuroImage*, *14*(3), 617–631. https://doi.org/10.1006/nimg.2001.0858

Gregory, R. (1970). *The Intelligent Eye*. Weidenfeld and Nicolson.

Grill-Spector, K., Henson, R., & Martin, A. (2006). Repetition and the brain: Neural models of stimulus-specific effects. *Trends in Cognitive Sciences*, *10*(1), 14–23. https://doi.org/10.1016/j.tics.2005.11.006

Grill-Spector, K., & Malach, R. (2001). fMR-adaptation: A tool for studying the functional properties of human cortical neurons. *Acta Psychologica*, *107*(1–3), 293–321. https://doi.org/10.1016/S0001-6918(01)00019-1

Grootswagers, T., Wardle, S. G., & Carlson, T. A. (2017). Decoding Dynamic Brain Patterns from Evoked Responses: A Tutorial on Multivariate Pattern Analysis Applied to Time Series Neuroimaging Data. *Journal of Cognitive Neuroscience*, *29*(4), 677–697. https://doi.org/10.1162/jocn

Grummett, T. S., Fitzgibbon, S. P., Lewis, T. W., DeLosAngeles, D., Whitham, E. M., Pope, K. J., & Willoughby, J. O. (2014). Constitutive spectral EEG peaks in the gamma range: suppressed by sleep, reduced by mental activity and resistant to sensory stimulation. *Frontiers in Human Neuroscience*, *8*(November), 1–11. https://doi.org/10.3389/fnhum.2014.00927

Haegens, S., Handel, B. F., & Jensen, O. (2011). Top-Down Controlled Alpha Band Activity in Somatosensory Areas Determines Behavioral Performance in a Discrimination Task. *Journal of Neuroscience*, *31*(14), 5197–5204. https://doi.org/10.1523/jneurosci.5199-10.2011

Hallett, M. (2000). Transcranial magnetic stimulation and the human brain. *Nature*, *406*(6792), 147–150. https://doi.org/10.1038/35018000

Halpern, A. R. (2015). Differences in auditory imagery self-report predict neural and behavioral outcomes. *Psychomusicology: Music, Mind, and Brain*, *25*(1), 37–47. https://doi.org/10.1037/pmu0000081

Hari, R., & Salmelin, R. (1997). Human cortical oscillations: A neuromagnetic view through the skull. *Trends in Neurosciences*, *20*(1), 44–49. https://doi.org/10.1016/S0166-2236(96)10065-5

Harrison, J. M. (1946). An examination of the varying effect of certain stimuli upon the alpha rhythm of a single normal individual. *British Journal of Psychology*, *37*(1), 20.

Hawkins, J., & Blakeslee, S. (2004). *On Intelligence*. Holt Paperback.

Hebb, D. O. (1949). *The Organization of Behavior*. Wiley & Sons.

Heeger, D. J. (2017). Theory of cortical function. *Proceedings of the National*

Academy of Sciences of the United States of America, *114*(8), 1773–1782. https://doi.org/10.1073/pnas.1619788114

Henschke, J. U., Noesselt, T., Scheich, H., & Budinger, E. (2015). Possible anatomical pathways for short-latency multisensory integration processes in primary sensory cortices. *Brain Structure and Function*, *220*(2), 955–977. https://doi.org/10.1007/s00429-013-0694-4

Henson, R., Shallice, T., & Dolan, R. (2000). Neuroimaging evidence for dissociable forms of repetition priming. *Science*, *287*(5456), 1269–1272. http://science.sciencemag.org/

Hermsdörfer, J., Terlinden, G., Mühlau, M., Goldenberg, G., & Wohlschläger, A. M. (2007). Neural representations of pantomimed and actual tool use: Evidence from an event-related fMRI study. *NeuroImage*, *36*. https://doi.org/10.1016/j.neuroimage.2007.03.037

Hickok, G., & Poeppel, D. (2004). Dorsal and ventral streams: A framework for understanding aspects of the functional anatomy of language. *Cognition*, *92*(1–2), 67–99. https://doi.org/10.1016/j.cognition.2003.10.011

Hikosaka, K. (1993). The polysensory region in the anterior bank of the caudal superior temporal sulcus of the macaque monkey. *Biomedical Research*, *14*, 41–45.

Hikosaka, K., Iwai, E., Saito, H. A., & Tanaka, K. (1988). Polysensory properties of neurons in the anterior bank of the caudal superior temporal sulcus of the macaque monkey. *Journal of Neurophysiology*, *60*(5), 1615–1637. https://doi.org/10.1152/jn.1988.60.5.1615

Hjortkjær, J., Kassuba, T., Madsen, K. H., Skov, M., & Siebner, H. R. (2018). Task-modulated cortical representations of natural sound source categories. *Cerebral Cortex*, *28*(1), 295–306. https://doi.org/10.1093/cercor/bhx263

Hobson, H. M., & Bishop, D. V. M. (2016). Mu suppression – A good measure of the human mirror neuron system? *Cortex*, *82*, 290–310. https://doi.org/10.1016/j.cortex.2016.03.019

Hobson, H. M., & Bishop, D. V. M. (2017). The interpretation of mu suppression as an index of mirror neuron activity: past, present and future. *Royal Society Open Science*, *4*(3), 160662. https://doi.org/10.1098/rsos.160662

Horga, G., Schatz, K. C., Abi-Dargham, A., & Peterson, B. S. (2014). Deficits in predictive coding underlie hallucinations in schizophrenia. *Journal of Neuroscience*, *34*(24), 8072–8082. https://doi.org/10.1523/JNEUROSCI.0200-14.2014

Howard, I. P., & Templeton, W. B. (1966). *Human spatial orientation*. Wiley.

Hsiao, S. (2008). Central mechanisms of tactile shape perception. *Current Opinion in Neurobiology*, *18*(4), 418–424. https://doi.org/10.1016/j.conb.2008.09.001

Huang, G. T. (2008). Is this a unified theory of the brain? *New Scientist*, 30–33.

Hubel, D. H., & Wiesel, T. N. (1968). Receptive fields and functional architecture of monkey striate cortex. *The Journal of Physiology*, *195*(1), 215–243. https://doi.org/10.1113/jphysiol.1968.sp008455

Hubel, D., & Wiesel, T. (1959). Receptive fields ofsingle neurones in the cat's striate cortex. *Journal of Physiology, 148*, 574–591.

Hubel, David H, & Wiesel, T. (1962). Receptive fields, binocular interaction and functional architecture in the cat's visual cortex. *Journal of Physiology, 160*, 106–154.

Humphries, C., Liebenthal, E., & Binder, J. R. (2010). Tonotopic organization of human auditory cortex. *NeuroImage, 50*(3), 1202–1211.

Huttenlocher, P. R. (2002). *Neural plasticity: the effects of environment on the development of the cerebral cortex*. Harvard University Press.

Imazu, S., Sugio, T., Tanaka, S., & Inui, T. (2007). Differences between actual and imagined usage of chopsticks: an fMRI study. *Cortex, 43*, 301–307.

Innocenti, G. M., & Clarke, S. (1984). Bilateral transitory projection to visual areas from auditory cortex in kittens. *Developmental Brain Research, 14*(1), 143–148.

Ishibashi, R., Pobric, G., Saito, S., & Lambon Ralph, M. A. (2016). The neural network for tool-related cognition: An activation likelihood estimation meta-analysis of 70 neuroimaging contrasts. *Cognitive Neuropsychology, 33*(3–4), 241–256. https://doi.org/10.1080/02643294.2016.1188798

Jacobs, R. A., & Xu, C. (2019). Can multisensory training aid visual learning? A computational investigation. *Journal of Vision, 19*(11), 1. https://doi.org/10.1167/19.11.1

Jensen, O., & Mazaheri, A. (2010). Shaping Functional Architecture by Oscillatory Alpha Activity: Gating by Inhibition. *Frontiers in Human Neuroscience, 4*(November), 1–8. https://doi.org/10.3389/fnhum.2010.00186

Jezzard, P., & Balaban, R. S. (1995). Correction for geometric distortion in echo planar images from B0 field variations. *Magnetic Resonance in Medicine, 34*(1), 65–73.

Jones, E. G., & Powell, T. P. S. (1970). An Anatomical Study of Converging Sensory Pathways. *Brain, 93*, 793–820. https://doi.org/10.1037/a0015325

Kaas, J. H., Nelson, R. J., Sur, M., Lin, C. S., & Merzenich, M. M. (1979). Multiple representations of the body within the primary somatosensory cortex of primates. *Science, 204*(4392), 521–523. https://doi.org/10.1126/science.107591

Kaiser, D., Quek, G. L., Cichy, R. M., & Peelen, M. V. (2019). Object Vision in a Structured World. *Trends in Cognitive Sciences, 23*(8), 672–685. https://doi.org/10.1016/j.tics.2019.04.013

Kaliukhovich, D. A. e., & Vogels, R. (2013). Decoding of Repeated Objects from Local Field Potentials in Macaque Inferior Temporal Cortex. *PLoS ONE, 8*(9), 74665. https://doi.org/10.1371/journal.pone.0074665

Kanizsa, G. (1976). Subjective contours. *Scientific American, 234*(4), 48–52.

Kanizsa, G. (1979). *Organization in vision*. Praeger.

Kaplan, J. T., & Iacoboni, M. (2007). Multimodal action representation in human left ventral premotor cortex. *Cognitive Processing, 8*(2), 103–113. https://doi.org/10.1007/s10339-007-0165-z

Karlen, S. J., Kahn, D. M., & Krubitzer, L. (2006). Early blindness results in abnormal corticocortical and thalamocortical connections. *Neuroscience*, *142*(3), 843–858. https://doi.org/10.1016/j.neuroscience.2006.06.055

Kassuba, T., Menz, M. M., Röder, B., & Siebner, H. R. (2013). Multisensory interactions between auditory and haptic object recognition. *Cerebral Cortex*, *23*(5), 1097–1107. https://doi.org/10.1093/cercor/bhs076

Kayser, C., & Logothetis, N. K. (2007). Do early sensory cortices integrate cross-modal information? *Brain Structure and Function*, *212*(2), 121–132. https://doi.org/10.1007/s00429-007-0154-0

Kayser, C., Petkov, C. I., Augath, M., & Logothetis, N. K. (2005). Integration of touch and sound in auditory cortex. *Neuron*, *48*(2), 373–384. https://doi.org/10.1016/j.neuron.2005.09.018

Kayser, C., & Shams, L. (2015). Multisensory Causal Inference in the Brain. *PLoS Biology*, *13*(2). https://doi.org/10.1371/journal.pbio.1002075

Keysers, C., Kaas, J. H., & Gazzola, V. (2010). Somatosensation in social perception. *Nature Reviews Neuroscience*, *11*(6), 417–428. https://doi.org/10.1038/nrn2833

Kikuchi, T., Sugiura, M., Yamamoto, Y., Sasaki, Y., Hanawa, S., Sakuma, A., Matsumoto, K., Matsuoka, H., & Kawashima, R. (2019). Neural responses to action contingency error in different cortical areas are attributable to forward prediction or sensory processing. *Scientific Reports*, *9*(1), 1–8. https://doi.org/10.1038/s41598-019-46350-1

Klinge, C., Eippert, F., Röder, B., & Büchel, C. (2010). Corticocortical connections mediate primary visual cortex responses to auditory stimulation in the blind. *Journal of Neuroscience*, *30*(38), 12798–12805. https://doi.org/10.1523/JNEUROSCI.2384-10.2010

Koch, C. (2004). *The quest for consciousness: A neurobiological approach*. Roberts & Company.

Koch, S. P., Werner, P., Steinbrink, J., Fries, P., & Obrig, H. (2009). Stimulus-Induced and State-Dependent Sustained Gamma Activity Is Tightly Coupled to the Hemodynamic Response in Humans. *Journal of Neuroscience*, *29*(44), 13962–13970. https://doi.org/10.1523/jneurosci.1402-09.2009

Kohler, E., Keysers, C., Alessandra Umilta, A., Fogassi, L., Gallese, V., & Rizzolatti, G. (2002). Hearing sounds, understanding actions: Action representation in mirror neurons. *Science*, *297*, 846–848. www.sciencemag.org/cgi/content/full/297/5582/846/

Kok, P. (2016). Perceptual Inference: A Matter of Predictions and Errors. *Current Biology*, *26*(17), R809–R811. https://doi.org/10.1016/j.cub.2016.07.061

Kok, P., & De Lange, F. P. (2015). Predictive coding in sensory cortex. In *An Introduction to Model-Based Cognitive Neuroscience* (pp. 221–244). https://doi.org/10.1007/978-1-4939-2236-9_11

Kok, P., Jehee, J. F. M., & de Lange, F. P. (2012). Less Is More: Expectation Sharpens Representations in the Primary Visual Cortex. *Neuron*, *75*(2), 265–

270. https://doi.org/10.1016/j.neuron.2012.04.034

Kok, P., Mostert, P., & De Lange, F. P. (2017). Prior expectations induce prestimulus sensory templates. *Proceedings of the National Academy of Sciences of the United States of America*, *114*(39), 10473–10478. https://doi.org/10.1073/pnas.1705652114

Kording, K. P., Beierholm, U., Ma, W. J., Quartz, S., Tenenbaum, J. B., & Shams, L. (2007). Causal Inference in Multisensory Perception. *PLoS ONE*, *9*. https://doi.org/10.1371/journal.pone.0000943

Kothe, C. A. E., & Jung, T. P. (2016). *ARTIFACT REMOVAL TECHNIQUES WITH SIGNAL RECONSTRUCTION* (Patent No. 14/895,440).

Koutstaal, W., Wagner, A. D., Rotte, M., Maril, A., Buckner, R. L., & Schacter, D. L. (2001). Perceptual specificity in visual object priming: Functional magnetic resonance imaging evidence for a laterality difference in fusiform cortex. *Neuropsychologia*. https://doi.org/10.1016/S0028-3932(00)00087-7

Kovács, G., Kaiser, D., Kaliukhovich, D. A., Zoltán, V., & Vogels, R. (2013). Repetition probability does not affect fMRI repetition suppression for objects. *Journal of Neuroscience*, *33*(23), 9805–9812. https://doi.org/10.1523/JNEUROSCI.3423-12.2013

Kriegeskorte, N., & Bandettini, P. A. (2007). Analyzing for information, not activation, to exploit high-resolution fMRI. *NeuroImage*, *38*(4), 649–662. https://doi.org/10.1016/j.neuroimage.2007.02.022

Kriegeskorte, N., Lindquist, M. A., Nichols, T. E., Poldrack, R. A., & Vul, E. (2010). Everything you never wanted to know about circular analysis, but were afraid to ask. *Journal of Cerebral Blood Flow and Metabolism*, *30*(9), 1551–1557. https://doi.org/10.1038/jcbfm.2010.86

Kriegeskorte, N., Simmons, W. K., Bellgowan, P. S., & Baker, C. I. (2009). Circular analysis in systems neuroscience: The dangers of double dipping. *Nature Neuroscience*, *12*(5), 535–540. https://doi.org/10.1038/nn.2303

Kuhlman, W. N. (1978). Functional topography of the human mu rhythm. *Electroencephalography and Clinical Neurophysiology*, *44*(1), 83–93.

Kujala, T., Palva, M. J., Salonen, O., Alku, P., Huotilainen, M., Järvinen, A., & Näätänen, R. (2005). The role of blind humans' visual cortex in auditory change detection. *Neuroscience Letters*. https://doi.org/10.1016/j.neulet.2004.12.070

Kumar, S., Riddoch, M. J., Humphreys, G., Proverbio, A. M., Bicocca, M., & Vallesi, A. (2013). *Mu rhythm desynchronization reveals motoric influences of hand action on object recognition*. https://doi.org/10.3389/fnhum.2013.00066

Lakens, D. (2013). Calculating and reporting effect sizes to facilitate cumulative science: A practical primer for t-tests and ANOVAs. *Frontiers in Psychology*, *4*(NOV), 1–12. https://doi.org/10.3389/fpsyg.2013.00863

Lamme, V. A. F., Super, H., & Spekreijse, H. (1998). Feedforward, horizontal, and feedback processing in the visual cortex. *Current Opinion in Neurobiology*, *8*(4), 529–535.

Leaver, A. M., & Rauschecker, J. P. (2010). Cortical Representation of Natural

Complex Sounds: Effects of Acoustic Features and Auditory Object Category. *Journal of Neuroscience*, *30*(22), 7604–7612. https://doi.org/10.1523/JNEUROSCI.0296-10.2010

Lee, T. S., & Mumford, D. (2003). Hierarchical Bayesian inference in the visual cortex. *Journal of the Optical Society of America*, *20*(7), 1434–1448. https://doi.org/10.1364/JOSAA.20.001434

Lee, T. S., & Nguyen, M. (2001). Dynamics of subjective contour formation in the early visual cortex. *PNAS*, *98*(4), 1907–1911.

Lega, C., Stephan, M. A., Zatorre, R. J., & Penhune, V. (2016). Testing the role of dorsal premotor cortex in auditory-motor association learning using Transcranical Magnetic Stimulation (TMS). *PLoS ONE*, *11*(9), 1–16. https://doi.org/10.1371/journal.pone.0163380

Lemus, L., Hernández, A., Luna, R., Zainos, A., & Romo, R. (2010). Do sensory cortices process more than one sensory modality during perceptual judgments? *Neuron*, *67*(2), 335–348. https://doi.org/10.1016/j.neuron.2010.06.015

Lewis, J. W., Brefczynski, J. A., Phinney, R. E., Janik, J. J., & DeYoe, E. A. (2005). Distinct Cortical Pathways for Processing Tool versus Animal Sounds. *Journal of Neuroscience*, *25*(21), 5148–5158. https://doi.org/10.1523/JNEUROSCI.0419-05.2005

Lewis, J. W., Phinney, R. E., Brefczynski-Lewis, J. A., & DeYoe, E. a. (2006). Lefties Get It "Right" When Hearing Tool Sounds. *Journal of Cognitive Neuroscience*, *18*(8), 1314–1330. https://doi.org/10.1162/jocn.2006.18.8.1314

Lewis, J. W., Talkington, W. J., Puce, A., Engel, L. R., & Frum, C. (2011). Cortical Networks Representing Object Categories and High-level Attributes of Familiar Real-world Action Sounds. *Journal of Cognitive Neuroscience*, *23*(8), 2079–2101. https://doi.org/10.1162/jocn.2010.21570

Lewis, J. W., Wightman, F. L., Brefczynski, J. A., Phinney, R. E., Binder, J. R., & DeYoe, E. A. (2004). Human brain regions involved in recognizing environmental sounds. *Cerebral Cortex*, *14*(9), 1008–1021. https://doi.org/10.1093/cercor/bhh061

Liang, M., Mouraux, A., Hu, L., & Iannetti, G. D. (2013). Primary sensory cortices contain distinguishable spatial patterns of activity for each sense. *Nature Communications*, *4*. https://doi.org/10.1038/ncomms2979

Limanowski, J., Sarasso, P., & Blankenburg, F. (2018). Different responses of the right superior temporal sulcus to visual movement feedback during self-generated vs. externally generated hand movements. *European Journal of Neuroscience*, *47*(4), 314–320. https://doi.org/10.1111/ejn.13824

Luck, S. J. (2005). *An Introduction to Event-Related Potentials and their Neural Origins*. MIT Press.

Macaluso, E., & Driver, J. (2005). Multisensory spatial interactions: A window onto functional integration in the human brain. *Trends in Neurosciences*, *28*(5), 264–271. https://doi.org/10.1016/j.tins.2005.03.008

Makeig, S. (1993). Effects of Exposure to Pure Tones on Event-Related Dynamics of

the EEG Spectrum. *Electroencephalogr Clin Neurophysiol.*, *86*(4), 283–293. https://doi.org/10.1016/0013-4694(93)90110-H

Man, K., Damasio, A., Meyer, K., & Kaplan, J. T. (2015). Convergent and invariant object representations for sight, sound, and touch. *Human Brain Mapping*, *36*(9), 3629–3640. https://doi.org/10.1002/hbm.22867

Man, K., Kaplan, J. T., Damasio, A., & Meyer, K. (2012). Sight and sound converge to form modality-invariant representations in temporoparietal cortex. *The Journal of Neuroscience : The Official Journal of the Society for Neuroscience*, *32*(47), 16629–16636. https://doi.org/10.1523/JNEUROSCI.2342-12.2012

Marcell, M. M., Borella, D., Greene, M., Kerr, E., & Rogers, S. (2000). Confrontation naming of environmental sounds. *Journal of Clinical and Experimental Neuropsychology*, *22*(6), 830–864. https://doi.org/10.1076/jcen.22.6.830.949

Marini, F., Breeding, K. A., & Snow, J. C. (2019). Distinct visuo-motor brain dynamics for real-world objects versus planar images. *NeuroImage*, *195*, 232–242. https://doi.org/10.1016/j.neuroimage.2019.02.026

Martin, A. (2016). GRAPES—Grounding representations in action, perception, and emotion systems: How object properties and categories are represented in the human brain. *Psychonomic Bulletin and Review*, *23*(4), 979–990. https://doi.org/10.3758/s13423-015-0842-3

Masland, R. H., & Martin, P. R. (2007). The unsolved mystery of vision. *Current Biology*, *17*(15), R577–R582. https://doi.org/10.1016/j.cub.2007.05.040

Massaro, D. W. (1999). Speechreading: illusion or window into pattern recognition. *Trends in Cognitive Sciences*, *3*(8), 310–317.

Maunsell, J. H., & Van Essen, D. C. (1983). Functional properties of neurons in middle temporal visual area of the macaque monkey. I. Selectivity for stimulus direction, speed, and orientation. *Journal of Neurophysiology*, *49*(5), 1127–1147. https://doi.org/10.1016/j.aqpro.2013.07.003

McIntosh, A. R., Cabeza, R. E., & Lobaugh, N. J. (1998). Analysis of Neural Interactions Explains the Activation of Occipital Cortex by an Auditory Stimulus. *Journal of Neurophysiology*, *80*(5), 2790–2796. http://jn.physiology.org/content/jn/80/5/2790.full.pdf

Mesulam, M. M. (1998). From sensation to perception. *Brain*, *121*, 1013–1052. https://doi.org/10.1093/brain/121.6.1013

Meyer, K., & Damasio, A. (2009). Convergence and divergence in a neural architecture for recognition and memory. *Trends in Neurosciences*, *32*(7), 376–382. https://doi.org/10.1016/j.tins.2009.04.002

Meyer, K., Kaplan, J. T., Essex, R., Damasio, H., & Damasio, A. (2011). Seeing touch is correlated with content-specific activity in primary somatosensory cortex. *Cerebral Cortex*, *21*(9), 2113–2121. https://doi.org/10.1093/cercor/bhq289

Meyer, K., Kaplan, J. T., Essex, R., Webber, C., Damasio, H., & Damasio, A. (2010). Predicting visual stimuli on the basis of activity in auditory cortices.

Nature Neuroscience, *13*(6), 667–668. https://doi.org/10.1038/nn.2533

Michalareas, G., Vezoli, J., van Pelt, S., Schoffelen, J. M., Kennedy, H., & Fries, P. (2016). Alpha-Beta and Gamma Rhythms Subserve Feedback and Feedforward Influences among Human Visual Cortical Areas. *Neuron*, *89*(2), 384–397. https://doi.org/10.1016/j.neuron.2015.12.018

Molholm, S., Ritter, W., Murray, M. M., Javitt, D. C., Schroeder, C. E., & Foxe, J. J. (2002). Multisensory auditory-visual interactions during early sensory processing in humans: A high-density electrical mapping study. *Cognitive Brain Research*, *14*(1), 115–128. https://doi.org/10.1016/S0926-6410(02)00066-6

Monti, M. M., Vanhaudenhuyse, A., Coleman, M. R., Boly, M., Pickard, J. D., Tshibanda, L., & Laureys, S. (2010). Willful modulation of brain activity in disorders of consciousness. *New England Journal of Medicine*, *362*(7), 579–589.

Morosan, P., Rademacher, J., Schleicher, A., Amunts, K., Schormann, T., & Zilles, K. (2001). Human primary auditory cortex: Cytoarchitectonic subdivisions and mapping into a spatial reference system. *NeuroImage*, *13*(4), 684–701. https://doi.org/10.1006/nimg.2000.0715

Muckli, L. (2010). What are we missing here? Brain imaging evidence for higher cognitive functions in primary visual cortex V1. *International Journal of Imaging Systems and Technology*, *20*(2), 131–139. https://doi.org/10.1002/ima.20236

Muckli, L., De Martino, F., Vizioli, L., Petro, L. S., Smith, F. W., Ugurbil, K., Goebel, R., & Yacoub, E. (2015). Contextual Feedback to Superficial Layers of V1. *Current Biology*, *25*(20), 2690–2695. https://doi.org/10.1016/j.cub.2015.08.057

Muckli, L., Kohler, A., Kriegeskorte, N., & Singer, W. (2005). Primary visual cortex activity along the apparent-motion trace reflects illusory perception. *PLoS Biology*, *3*(8), e265. https://doi.org/10.1371/journal.pbio.0030265

Muckli, L., & Petro, L. S. (2013). Network interactions: Non-geniculate input to V1. *Current Opinion in Neurobiology*, *23*(2), 195–201. https://doi.org/10.1016/j.conb.2013.01.020

Mulholland, T., & Runnals, S. (1962). Increased occurrence of EEG alpha during increased attention. *The Journal of Psychology*, *54*(2), 317–330.

Mullen, T., Kothe, C., Chi, Y. M., Ojeda, A., Kerth, T., Makeig, S., Cauwenberghs, G., & Jung, T. P. (2013). Real-time modeling and 3D visualization of source dynamics and connectivity using wearable EEG. *Proceedings of the Annual International Conference of the IEEE Engineering in Medicine and Biology Society, EMBS*, 2184–2187. https://doi.org/10.1109/EMBC.2013.6609968

Mumford, D. (1991). On the computational architecture of the neocortex - I. The role of the thalamo-cortical loop. *Biological Cybernetics*, *65*(2), 135–145. https://doi.org/10.1007/BF00202389

Mumford, D. (1992). On the computational architecture of the neocortex - II The

role of cortico-cortical loops. *Biological Cybernetics*, *66*(3), 241–251. https://doi.org/10.1007/BF00198477

Mur, M., Bandettini, P. A., & Kriegeskorte, N. (2009). Revealing representational content with pattern-information fMRI - An introductory guide. *Social Cognitive and Affective Neuroscience*, *4*(1), 101–109. https://doi.org/10.1093/scan/nsn044

Murray, S. O., Boyaci, H., & Kersten, D. (2006). The representation of perceived angular size in human primary visual cortex. *Nature Neuroscience*, *9*(3), 429–434. https://doi.org/10.1038/nn1641

Murray, S. O., Kersten, D., Olshausen, B. A., Schrater, P., & Woods, D. L. (2002). Shape perception reduces activity in human primary visual cortex. *Proceedings of the National Academy of Sciences of the United States of America*, *99*(23), 15164–15169. https://doi.org/10.1073/pnas.192579399

Muthukumaraswamy, S. D., & Johnson, B. W. (2004). Changes in rolandic mu rhythm during observation of a precision grip. *Psychophysiology*, *41*(1), 152–156. https://doi.org/10.1046/j.1469-8986.2003.00129.x

Muthukumaraswamy, S. D., Johnson, B. W., & McNair, N. A. (2004). Mu rhythm modulation during observation of an object-directed grasp. *Cognitive Brain Research*, *19*(2), 195–201. https://doi.org/10.1016/j.cogbrainres.2003.12.001

Naci, L., Cusack, R., Anello, M., & Owen, A. M. (2014). A common neural code for similar conscious experiences in different individuals. *Proceedings of the National Academy of Sciences of the United States of America*, *111*(39), 14277–14282. https://doi.org/10.1073/pnas.1407007111

Nelson, A. J., & Chen, R. (2008). Digit somatotopy within cortical areas of the postcentral gyrus in humans. *Cerebral Cortex*, *18*(10), 2341–2351. https://doi.org/10.1093/cercor/bhm257

Neuper, C., Wörtz, M., & Pfurtscheller, G. (2006). ERD/ERS patterns reflecting sensorimotor activation and deactivation. *Progress in Brain Research*, *159*, 211–222.

Niedermeyer, E., & da Silva, F. (2005). *Electroencephalography: Basic principles, clinical applications, and related fields* (5th ed.). Lippincott Williams & Wilkins.

Nihashi, T., Naganawa, S., Sato, C., Kawai, H., Nakamura, T., Fukatsu, H., Ishigaki, T., & Aoki, I. (2005). Contralateral and ipsilateral responses in primary somatosensory cortex following electrical median nerve stimulation - An fMRI study. *Clinical Neurophysiology*. https://doi.org/10.1016/j.clinph.2004.10.011

Norman, K. A., Polyn, S. M., Detre, G. J., & Haxby, J. V. (2006). Beyond mind-reading: multi-voxel pattern analysis of fMRI data. *Trends in Cognitive Sciences*, *10*(9), 424–430. https://doi.org/10.1016/j.tics.2006.07.005

O'Reilly, J. X., Woolrich, M. W., Behrens, T. E. J., Smith, S. M., & Johansen-Berg, H. (2012). Tools of the trade: Psychophysiological interactions and functional connectivity. *Social Cognitive and Affective Neuroscience*. https://doi.org/10.1093/scan/nss055

Oldfield, R. C. (1971). The assessment and analysis of handedness: The Edinburgh inventory. *Neuropsychologia*, *9*(1), 97–113. https://doi.org/10.1016/0028-3932(71)90067-4

Olshausen, B. A., & Field, D. J. (2005). How close are we to understanding v1? *Neural Computation*, *17*(8), 1665–1699. https://doi.org/10.1162/0899766054026639

Op de Beeck, H. P., Torfs, K., & Wagemans, J. (2008). Perceived Shape Similarity among Unfamiliar Objects and the Organization of the Human Object Vision Pathway. *Journal of Neuroscience*, *28*(40), 10111–10123. https://doi.org/10.1523/JNEUROSCI.2511-08.2008

Owen, A. M., Coleman, M. R., Boly, M., Davis, M. H., Laureys, S., & Pickard, J. D. (2006). Detecting awareness in the vegetative state. *Science*, *313*(5792), 1402. https://doi.org/10.1126/science.1130197

Palmer, S. E. (1975). The effects of contextual scenes on the identification of objects. *Memory & Cognition*, *3*(5), 519–526. https://doi.org/10.3758/BF03197524

Palomero-Gallagher, N., & Zilles, K. (2019). Cortical layers: Cyto-, myelo-, receptor- and synaptic architecture in human cortical areas. *NeuroImage*, *197*, 716–741. https://doi.org/10.1016/j.neuroimage.2017.08.035

Pantev, C., Oostenveld, R., Engelien, A., Ross, B., Roberts, L. E., & Hoke, M. (1998). Increased auditory cortical representation in musicians. *Nature*, *392*(6678), 811–814. https://doi.org/10.1186/s13568-017-0488-9

Paraskevopoulos, E., & Herholz, S. C. (2013). Multisensory integration and neuroplasticity in the human cerebral cortex. *Translational Neuroscience*, *4*(3), 337–348. https://doi.org/10.2478/s13380-013-0134-1

Paraskevopoulos, E., Kuchenbuch, A., Herholz, S. C., & Pantev, C. (2012). Evidence for training-induced plasticity in multisensory brain structures: An meg study. *PLoS ONE*, *7*(5). https://doi.org/10.1371/journal.pone.0036534

Penfield, W., & Boldrey, E. (1937). Somatic motor and sensory representation in the cerebral cortex of man as studied by electrical stimulation. *Brain*, *60*(4), 389–443. https://doi.org/10.1093/brain/60.4.389

Penfield, W., & Rasmussen, T. (1950). *The cerebral cortex of man; a clinical study of localization of function*. MacMillan.

Penfield, W., & Rasmussen, T. (1952). *The Cerebral Cortex of Man.* MacMillan.

Pérez-Bellido, A., Anne Barnes, K., Crommett, L. E., & Yau, J. M. (2018). Auditory Frequency Representations in Human Somatosensory Cortex. *Cerebral Cortex*, *28*(11), 3908–3921. https://doi.org/10.1093/cercor/bhx255

Perry, A., & Bentin, S. (2009). Mirror activity in the human brain while observing hand movements: A comparison between EEG desynchronization in the μ-range and previous fMRI results. *Brain Research*, *1282*, 126–132. https://doi.org/10.1016/j.brainres.2009.05.059

Pfurtscheller, G. (1992). Event-related synchronization (ERS): an electrophysiological correlate of cortical areas at rest. *Electroencephalogr Clin*

Neurophysiol, *83*(1), 62–69.

Pfurtscheller, G. (1997). EEG event-related desynchronization (ERD) and synchronization (ERS). *Electroencephalography and Clinical Neurophysiology*, *1*(103), 26.

Pfurtscheller, G., & Lopes, F. H. (1999). Event-related EEG / MEG synchronization and desynchronization : basic principles. *Clinical Neurophysiology*, *110*, 1842–1857. https://doi.org/10.1016/S1388-2457(99)00141-8

Pfurtscheller, G., Neuper, C., Andrew, C., & Edlinger, G. (1997). Foot and hand area mu rhythms. *International Journal of Psychophysiology*, *26*(1–3), 121–135. https://doi.org/10.1016/S0167-8760(97)00760-5

Pfurtscheller, G., Pregenzer, M., & Neuper, C. (1994). Visualization of sensorimotor areas involved in preparation for hand movement based on classification of μ and central β rhythms in single EEG trials in man. *Neuroscience Letters*, *181*(1–2), 43–46.

Pfurtscheller, G., Stancák, A., & Neuper, C. (1996). Event-related synchronization (ERS) in the alpha band - An electrophysiological correlate of cortical idling: A review. *International Journal of Psychophysiology*, *24*(1–2), 39–46. https://doi.org/10.1016/S0167-8760(96)00066-9

Pineda, J. A. (2005). The functional significance of mu rhythms: Translating "seeing" and "hearing" into "doing." *Brain Research Reviews*, *50*(1), 57–68. https://doi.org/10.1016/j.brainresrev.2005.04.005

Pitcher, D., Walsh, V., Yovel, G., & Duchaine, B. (2007). TMS Evidence for the Involvement of the Right Occipital Face Area in Early Face Processing. *Current Biology*, *17*(18), 1568–1573. https://doi.org/10.1016/j.cub.2007.07.063

Poldrack, R. A., Baker, C. I., Durnez, J., Gorgolewski, K. J., Matthews, P. M., Munafò, M. R., Nichols, T. E., Poline, J. B., Vul, E., & Yarkoni, T. (2017). Scanning the horizon: Towards transparent and reproducible neuroimaging research. *Nature Reviews Neuroscience*, *18*(2), 115–126. https://doi.org/10.1038/nrn.2016.167

Press, C., Kok, P., & Yon, D. (2020). The Perceptual Prediction Paradox. *Trends in Cognitive Sciences*, *24*(1), 13–24. https://doi.org/10.1016/j.tics.2019.11.003

Proverbio, A. M. (2012). Tool perception suppresses 10-12Hz mu rhythm of EEG over the somatosensory area. *Biological Psychology*, *91*(1), 1–7. https://doi.org/10.1016/j.biopsycho.2012.04.003

Puckett, A. M., Bollmann, S., Barth, M., & Cunnington, R. (2017). Measuring the effects of attention to individual fingertips in somatosensory cortex using ultra-high field (7T) fMRI. *NeuroImage*, *161*, 179–187. https://doi.org/10.1016/j.neuroimage.2017.08.014

Puckett, A. M., Bollmann, S., Junday, K., Barth, M., & Cunnington, R. (2020). Bayesian population receptive field modeling in human somatosensory cortex. *NeuroImage*, *208*, 116465. https://doi.org/https://doi.org/10.1016/j.neuroimage.2019.116465

Quandt, L. C., Marshall, P. J., Bouquet, C. A., & Shipley, T. F. (2013).

Somatosensory experiences with action modulate alpha and beta power during subsequent action observation. *Brain Research, 1534*, 55–65. https://doi.org/10.1016/j.brainres.2013.08.043

Quandt, L. C., Marshall, P. J., Shipley, T. F., Beilock, S. L., & Goldin-Meadow, S. (2012). Sensitivity of alpha and beta oscillations to sensorimotor characteristics of action: An EEG study of action production and gesture observation. *Neuropsychologia*, *50*(12), 2745–2751. https://doi.org/10.1016/j.neuropsychologia.2012.08.005

Rademacher, J., Morosan, P., Schormann, T., Schleicher, A., Werner, C., Freund, H. J., & Zilles, K. (2001). Probabilistic mapping and volume measurement of human primary auditory cortex. *NeuroImage*, *13*(4), 669–683. https://doi.org/10.1006/nimg.2000.0714

Ramachandran, V. S. (2002). *Encyclopedia of the Human Brain*. Elsevier Science Publishing Co Inc.

Ramachandran, V. S., & Hubbard, E. M. (2001). Psychophysical investigations into the neural basis of synaesthesia. *Proceedings of the Royal Society B: Biological Sciences*, *268*(1470), 979–983. https://doi.org/10.1098/rspb.2000.1576

Rao, R. P. N., & Ballard, D. H. (1999). Predictive coding in the visual cortex: a functional interpretation of some extra-classical receptive-field effects. *Nature Neuroscience*, *2*(1), 79–87. https://doi.org/10.1038/4580

Rao, R. P. N., & Sejnowski, T. J. (2002). Predictive Coding, Cortical Feedback, and Spike-Timing Dependent Plasticity. In *Probabilistic Models of the Brain: Perception and Neural Function* (pp. 297–315). MIT Press. https://doi.org/10.7551/mitpress/5583.003.0017

Rauschecker, J. P., Tian, B., Pons, T., & Mishkin, M. (1996). Serial and parallel processing in macaque auditory cortex. *The Journal of Comparative Neurology*, *382*, 89–103. https://onlinelibrary.wiley.com/doi/pdf/10.1002/(SICI)1096-9861(19970526)382:1%3C89::AID-CNE6%3E3.0.CO;2-G

Reid, R. C., & Alonso, J. M. (1995). Specificity of monosynaptic connections from thalamus to visual cortex. *Nature*, *378*, 281–284.

Renoult, L., Davidson, P. S. R., Schmitz, E., Park, L., Campbell, K., Moscovitch, M., & Levine, B. (2015). Autobiographically Significant Concepts: More Episodic than Semantic in Nature? An Electrophysiological Investigation of Overlapping Types of Memory. *Journal of Cognitive Neuroscience*, *27*(1), 57–72. https://doi.org/10.1162/jocn_a_00689

Richter, D., Ekman, M., & de Lange, F. P. (2018). Suppressed Sensory Response to Predictable Object Stimuli throughout the Ventral Visual Stream. *The Journal of Neuroscience*, *38*(34), 7452–7461.

Riecke, L., Van Opstal, A. J., Goebel, R., & Formisano, E. (2007). Hearing illusory sounds in noise: Sensory-perceptual transformations in primary auditory cortex. *Journal of Neuroscience*, *27*(46), 12684–12689. https://doi.org/10.1523/JNEUROSCI.2713-07.2007

Ritter, P., Moosmann, M., & Villringer, A. (2009). Rolandic alpha and beta EEG

rhythms' strengths are inversely related to fMRI-BOLD signal in primary somatosensory and motor cortex. *Human Brain Mapping*, *30*(4), 1168–1187. https://doi.org/10.1002/hbm.20585

Rockland, K. S., & Pandya, D. N. (1979). Laminar origins and terminations of cortical connections of the occipital lobe in the rhesus monkey*. *Brain Research*, *179*, 3–20.

Rohe, T., Ehlis, A. C., & Noppeney, U. (2019). The neural dynamics of hierarchical Bayesian causal inference in multisensory perception. *Nature Communications*, *10*(1), 1–17. https://doi.org/10.1038/s41467-019-09664-2

Rohe, T., & Noppeney, U. (2015). Cortical Hierarchies Perform Bayesian Causal Inference in Multisensory Perception. *PLoS Biology*, *13*(2), 1002073. https://doi.org/10.1371/journal.pbio.1002073

Rohe, T., & Noppeney, U. (2016). Distinct computational principles govern multisensory integration in primary sensory and association cortices. *Current Biology*, *26*(4), 509–514. https://doi.org/10.1016/j.cub.2015.12.056

Rolls, E. T. (1991). Neural organization of higher visual functions. *Current Opinion in Neurobiology*, *1*(2), 274–278. https://doi.org/10.1016/0959-4388(91)90090-T

Romei, V., Chiappini, E., Hibbard, P. B., & Avenanti, A. (2016). Empowering Reentrant Projections from V5 to V1 Boosts Sensitivity to Motion. *Current Biology*, *26*(16), 2155–2160. https://doi.org/10.1016/j.cub.2016.06.009

Rorden, C., Karnath, H.-O., & Bonilha, L. (2007). Improving Lesion–Symptom Mapping. *Journal of Cognitive Neuroscience*, *19*(7), 1081–1088. http://www.mitpressjournals.org/doi/pdfplus/10.1162/jocn.2007.19.7.1081

Rosenthal, R. (1991). *Meta-analytic procedures for social research* (2nd ed.). Sage.

Rossit, S., McAdam, T., Mclean, D. A., Goodale, M. A., & Culham, J. C. (2013). FMRI reveals a lower visual field preference for hand actions in human superior parieto-occipital cortex (SPOC) and precuneus. *Cortex*, *49*(9), 2525–2541. https://doi.org/10.1016/j.cortex.2012.12.014

Rust, N. C., Schwartz, O., Movshon, J. A., & Simoncelli, E. P. (2005). Spatiotemporal elements of macaque V1 receptive fields. *Neuron*. https://doi.org/10.1016/j.neuron.2005.05.021

Sadato, N., Pascual-Leone, A Grafman, J., Ibañez, V., Deiber, M. P., Dold, G., & Hallett, M. (1996). Activation of the primary visual cortex by Braille reading in blind subjects. *Nature*, *380*(6574), 526–528.

Samaha, J., Bauer, P., Cimaroli, S., & Postle, B. R. (2015). Top-down control of the phase of alpha-band oscillations as a mechanism for temporal prediction. *Proceedings of the National Academy of Sciences*, *112*(27), 8439–8444. https://doi.org/10.1073/pnas.1503686112

Sayres, R., & Grill-Spector, K. (2006). Object-selective cortex exhibits performance-independent repetition suppression. *Journal of Neurophysiology*, *95*(2), 995–1007. https://doi.org/10.1152/jn.00500.2005

Scheeringa, R., & Fries, P. (2019). Cortical layers, rhythms and BOLD signals. *NeuroImage*, *197*, 689–698. https://doi.org/10.1016/j.neuroimage.2017.11.002

Scheeringa, R., Fries, P., Petersson, K. M., Oostenveld, R., Grothe, I., Norris, D. G., Hagoort, P., & Bastiaansen, M. C. M. (2011). Neuronal Dynamics Underlying High- and Low-Frequency EEG Oscillations Contribute Independently to the Human BOLD Signal. *Neuron*, *69*(3), 572–583. https://doi.org/10.1016/j.neuron.2010.11.044

Schenke, K. C., Wyer, N. A., & Bach, P. (2016). The Things You Do : Internal Models of Others ' Expected Behaviour Guide Action Observation. *PLoS ONE*, 1–22. https://doi.org/10.1371/journal.pone.0158910

Schneider, T. R., Engel, A. K., & Debener, S. (2008). Multisensory identification of natural objects in a two-way crossmodal priming paradigm. *Experimental Psychology*, *55*(2), 121–132. https://doi.org/10.1027/1618-3169.55.2.121

Schroeder, C. E., & Foxe, J. J. (2002). The timing and laminar profile of converging inputs to multisensory areas of the macaque neocortex. *Cognitive Brain Research*, *14*(1), 187–198. https://doi.org/10.1016/S0926-6410(02)00073-3

Schweizer, R., Voit, D., & Frahm, J. (2008). Finger representations in human primary somatosensory cortex as revealed by high-resolution functional MRI of tactile stimulation. *NeuroImage*. https://doi.org/10.1016/j.neuroimage.2008.04.184

Serre, T., Oliva, A., & Poggio, T. (2007). A feedforward architecture accounts for rapid categorization. *Proceedings of the National Academy of Sciences*, *104*(15), 6424–6429.

Seymour, R. A., Rippon, G., Gooding-Williams, G., Schoffelen, J.-M., & Kessler, K. (2018). Dysregulated Oscillatory Connectivity in the Visual System in Autism Spectrum Disorder. *BioRxiv*, 1–43. https://doi.org/10.1101/440586

Sherman, M. T., Kanai, R., Seth, A. K., & Van Rullen, R. (2016). Rhythmic influence of top-down perceptual priors in the phase of prestimulus occipital alpha oscillations. *Journal of Cognitive Neuroscience*, *28*(9), 1318–1330. https://doi.org/10.1162/jocn_a_00973

Sherman, S. M., & Guillery, R. W. (2002). The role of the thalamus in the flow of information to the cortex. *Philosophical Transactions of the Royal Society of London. Series B, Biological Sciences*, *357*(1428), 1695–1708. https://doi.org/10.1098/rstb.2002.1161

Silva, L. R., Amitai, Y., & Connors, B. W. (1991). Intrinsic Oscillations of Neocortex Generated by its importance Layer 5 Pyramidal. *Science*, *251*(4992), 432–435.

Siuda-Krzywicka, K., Bola, Ł., Paplińska, M., Sumera, E., Jednoróg, K., Marchewka, A., Śliwińska, M. W., Amedi, A., & Szwed, M. (2016). Massive cortical reorganization in sighted braille readers. *ELife*, *5*(MARCH2016). https://doi.org/10.7554/eLife.10762

Smith, F. W., & Goodale, M. A. (2015). Decoding visual object categories in early somatosensory cortex. *Cerebral Cortex*, *25*(4), 1020–1031. https://doi.org/10.1093/cercor/bht292

Smith, F. W., & Muckli, L. (2010). Nonstimulated early visual areas carry

information about surrounding context. *Proceedings of the National Academy of Sciences of the United States of America*, *107*(46), 20099–20103. https://doi.org/10.1073/pnas.1000233107

Smith, F. W., & Smith, M. L. (2019). Decoding the dynamic representation of facial expressions of emotion in explicit and incidental tasks. *NeuroImage*, *195*(March), 261–271. https://doi.org/10.1016/j.neuroimage.2019.03.065

Snow, J. C., Pettypiece, C. E., McAdam, T. D., McLean, A. D., Stroman, P. W., Goodale, M. A., & Culham, J. C. (2011). Bringing the real world into the fMRI scanner: Repetition effects for pictures versus real objects. *Scientific Reports*, *1*, 1–10. https://doi.org/10.1038/srep00130

Snow, J. C., Skiba, R. M., Coleman, T. L., & Berryhill, M. E. (2014). Real-world objects are more memorable than photographs of objects. *Frontiers in Human Neuroscience*, *8*(OCT), 1–11. https://doi.org/10.3389/fnhum.2014.00837

Snow, J. C., Strother, L., & Humphreys, G. W. (2014). Haptic Shape Processing in Visual Cortex. *Journal of Cognitive Neuroscience*, *26*(5), 1154–1167. https://doi.org/10.1162/jocn_a_00548

Sokoliuk, R., & Cruse, D. (2018). Listening for the rhythm of a conscious brain. *Brain*, *141*(11), 3095–3097. https://doi.org/10.1093/brain/awy267

Stein, B. E., Meredith, M. A., & Wallace, M. T. (1993). The visually responsive neuron and beyond: multisensory integration in cat and monkey. In *Progress in brain research* (Vol. 95, pp. 79–90). Elsevier.

Stein, B. E., Perrault Jr, T. J., Stanford, T. R., & Rowland, B. A. (2009). Postnatal experiences influence how the brain integrates information from different senses. *Frontiers in Integrative Neuroscience*, *3*(21), 1–12. https://doi.org/10.3389/neuro.07

Steriade, M., & Llinás, R. R. (1988). The functional states of the thalamus and the associated neuronal interplay. *Physiological Reviews*, *68*(3), 649–742. https://doi.org/10.1002/hbm.20728

Sugiyama, S., Takeuchi, N., Inui, K., Nishihara, M., & Shioiri, T. (2018). Effect of acceleration of auditory inputs on the primary somatosensory cortex in humans. *Scientific Reports*, *8*(1), 1–9. https://doi.org/10.1038/s41598-018-31319-3

Summerfield, C., & De Lange, F. P. (2014). Expectation in perceptual decision making: Neural and computational mechanisms. *Nature Reviews Neuroscience*, *15*(11), 745–756. https://doi.org/10.1038/nrn3838

Sun, H. C., Welchman, A. E., Chang, D. H. F., & Di Luca, M. (2016). Look but don't touch: Visual cues to surface structure drive somatosensory cortex. *NeuroImage*, *128*, 353–361. https://doi.org/10.1016/j.neuroimage.2015.12.054

Sun, W., & Dan, Y. (2009). Layer-specific network oscillation and spatiotemporal receptive field in the visual cortex. *Proceedings of the National Academy of Sciences*, *106*(42), 17986–17991. https://doi.org/10.1073/pnas.0903962106

Sur, M., Merzenich, M. M., & Kaas, J. H. (1980). Magnification, receptive-field area, and "hypercolumn" size in areas 3b and 1 of somatosensory cortex in owl monkeys. *Journal of Neurophysiology*, *44*(2), 295–311.

https://doi.org/10.1152/jn.1980.44.2.295

Talavage, T. M., Ledden, P. J., Benson, R. R., Rosen, B. R., & Melcher, J. R. (2000). Frequency-dependent responses exhibited by multiple regions in human auditory cortex. *Hearing Research*, *150*(1–2), 225–244. https://doi.org/10.1016/S0378-5955(00)00203-3

Tanaka, K. (1996). Inferotemporal Cortex and Object Vision. *Annual Review of Neuroscience*, *19*(1), 109–139. https://doi.org/10.1146/annurev.neuro.19.1.109

Tang, H., Buia, C., Madhavan, R., Crone, N. E., Madsen, J. R., Anderson, W. S., & Kreiman, G. (2014). Spatiotemporal Dynamics Underlying Object Completion in Human Ventral Visual Cortex. *Neuron*, *83*(3), 736–748. https://doi.org/10.1016/j.neuron.2014.06.017

Thomik, A. A. C., Haber, D., Faisal, A. A., & Ieee, M. (2013). Real-time movement prediction for improved control of neuroprosthetics. *6th Annual International IEEE EMBS Conference on Neural Engineering*, 2–6. https://doi.org/10.1109/NER.2013.6696012

Thomson, A. M. (2003). Interlaminar Connections in the Neocortex. *Cerebral Cortex*, *13*(1), 5–14. https://doi.org/10.1093/cercor/13.1.5

Toothaker, L. E., & Newman, D. (1994). Nonparametric competitors to the two-way ANOVA. *Journal of Educational Statistics*, *19*(3), 237–273.

Tucciarelli, R., Turella, L., Oosterhof, N. N., Weisz, N., & Lingnau, A. (2015). MEG multivariate analysis reveals early abstract action representations in the lateral occipitotemporal cortex. *Journal of Neuroscience*, *35*(49), 16034–16045. https://doi.org/10.1523/JNEUROSCI.1422-15.2015

Turella, L., Tucciarelli, R., Oosterhof, N. N., Weisz, N., Rumiati, R., & Lingnau, A. (2016). Beta band modulations underlie action representations for movement planning. *NeuroImage*, *136*, 197–207. https://doi.org/10.1016/j.neuroimage.2016.05.027

Udin, S. B., & Fawcett, J. W. (1988). Formation Of Topographic Maps. *Annual Review of Neuroscience*, *11*(1), 289–327. https://doi.org/10.1146/annurev.neuro.11.1.289

Uludag, K., Ugurbil, K., & Berliner, L. (2015). *fMRI: from nuclear spins to brain functions*. Springer.

Valyear, K. F., Gallivan, J. P., McLean, D. A., & Culham, J. C. (2012). fMRI Repetition Suppression for Familiar But Not Arbitrary Actions with Tools. *Journal of Neuroscience*, *32*(12), 4247–4259. https://doi.org/10.1523/JNEUROSCI.5270-11.2012

Van Kerkoerle, T., Self, M. W., Dagnino, B., Gariel-Mathis, M. A., Poort, J., Van Der Togt, C., & Roelfsema, P. R. (2014). Alpha and gamma oscillations characterize feedback and feedforward processing in monkey visual cortex. *Proceedings of the National Academy of Sciences of the United States of America*, *111*(40), 14332–14341. https://doi.org/10.1073/pnas.1402773111

Vetter, P., Smith, F. W., & Muckli, L. (2014). Decoding sound and imagery content in early visual cortex. *Current Biology*, *24*(11), 1256–1262.

https://doi.org/10.1016/j.cub.2014.04.020

Vickery, T. J., Chun, M. M., & Lee, D. (2011). Ubiquity and Specificity of Reinforcement Signals throughout the Human Brain. *Neuron*, *72*(1), 166–177. https://doi.org/10.1016/j.neuron.2011.08.011

Von Der Heydt, R., Peterhans, E., & Baumgartner, G. (1984). Illusory contours and cortical neuron responses. *Science*, *224*(4654), 1260–1262. https://doi.org/10.1126/science.6539501

Wallace, M. T., Carriere, B. N., Perrault, T. J., Vaughan, J. W., & Stein, B. E. (2006). The Development of Cortical Multisensory Integration. *Journal of Neuroscience*, *26*(46), 11844–11849. https://doi.org/10.1523/JNEUROSCI.3295-06.2006

Wallace, M. T., Ramachandran, R., & Stein, B. E. (2004). A revised view of sensory cortical parcellation. *Proceedings of the National Academy of Sciences*, *101*(7), 2167–2172. https://doi.org/10.1073/pnas.0305697101

Wallace, M. T., & Stein, B. E. (1997). Development of multisensory neurons and multisensory integration in cat superior colliculus. *Journal of Neuroscience*, *17*(7), 2429–2444.

Ward, J. (2013). Synesthesia. *Annual Review of Psychology*, *64*, 49–75. https://doi.org/10.1146/annurev-psych-113011-143840

Watson, C., Paxinos, G., & Kirkcaldie, M. (2010). *The Brain : An Introduction to Functional Neuroanatomy* (1st ed.). Academic Press.

Weiner, K. S., Sayres, R., Vinberg, J., & Grill-Spector, K. (2010). fMRI-Adaptation and Category Selectivity in Human Ventral Temporal Cortex: Regional Differences Across Time Scales. *Journal of Neurophysiology*, *103*(6), 3349–3365. https://doi.org/10.1152/jn.01108.2009

Welch, R., & Warren, D. (1986). Intersensory interactions. In *Handbook of perception and human performance: Vol. 1. Sensory processes and human performance*. Wiley.

Wessinger, C. M., Vanmeter, J., Tian, B., Lare, J. Van, Pekar, J., & Rauschecker, J. P. (2000). Hierarchical Organization of the Human Auditory Cortex Revealed by Functional Magnetic Resonance Imaging S7. *Journal of Cognitive Neuroscience*, *13*(1), 1–7. https://www.mitpressjournals.org/doi/pdfplus/10.1162/089892901564108

Wiggs, C. L., & Martin, A. (1998). Properties and mechanisms of perceptual priming. *Current Opinion in Neurobiology*, *8*(2), 227–233. https://doi.org/10.1016/S0959-4388(98)80144-X

Wyart, V., Nobre, A. C., & Summerfield, C. (2012). Dissociable prior influences of signal probability and relevance on visual contrast sensitivity. *Proceedings of the National Academy of Sciences of the United States of America*, *109*(9), 3593–3598. https://doi.org/10.1073/pnas.1120118109

Xu, J., Yu, L., Rowland, B. A., Stanford, T. R., & Stein, B. E. (2014). Noise-rearing disrupts the maturation of multisensory integration. *European Journal of Neuroscience*, *39*(4), 602–613. https://doi.org/10.1111/ejn.12423

Yon, D., Gilbert, S. J., de Lange, F. P., & Press, C. (2018). Action sharpens sensory representations of expected outcomes. *Nature Communications*, *9*(1), 1–8. https://doi.org/10.1038/s41467-018-06752-7

Yon, D., Zainzinger, V., De Lange, F. P., Eimer, M., & Press, C. (2019). Action biases perceptual decisions toward expected outcomes. *PsyArXiv*, 1–25.

Yu, Y., Huber, L., Yang, J., Jangraw, D. C., Handwerker, D. A., Molfese, P. J., Chen, G., Ejima, Y., Wu, J., & Bandettini, P. A. (2019). Layer-specific activation of sensory input and predictive feedback in the human primary somatosensory cortex. *Science Advances*, *5*(5), 1-. https://doi.org/10.1126/sciadv.aav9053

Zaepffel, M., Trachel, R., Kilavik, B. E., & Brochier, T. (2013). Modulations of EEG Beta Power during Planning and Execution of Grasping Movements. *PLoS ONE*, *8*(3), 60060. https://doi.org/10.1371/journal.pone.0060060

Zatorre, R. J., Chen, J. L., & Penhune, V. B. (2007). When the brain plays music: Auditory-motor interactions in music perception and production. *Nature Reviews Neuroscience*, *8*(7), 547–558. https://doi.org/10.1038/nrn2152

Zeki, S. M. (1969). Representation of central visual fields in prestriate cortex of monkey. *Brain Research*, *14*(2), 271–291.

Zhou, Y. Di, & Fuster, J. M. (1997). Neuronal activity of somatosensory cortex in a cross-modal (visuo-haptic) memory task. *Experimental Brain Research*, *116*(3), 551–555. https://doi.org/10.1007/PL00005783

Zhou, Y. Di, & Fuster, J. M. (2000). Visuo-tactile cross-modal associations in cortical somatosensory cells. *Proceedings of the National Academy of Sciences*, *97*(17), 9777–9782. https://doi.org/10.1073/pnas.97.17.9777

Zhou, Y. Di, & Fuster, J. M. (2004). Somatosensory cell response to an auditory cue in a haptic memory task. *Behavioural Brain Research*, *153*(2), 573–578. https://doi.org/10.1016/j.bbr.2003.12.024

Zhu, T., Liu, G., Li, Q., & Yuan, G. (2019). Recognition of Pure Tone Frequency Based on fMRI Voxels Intensity. *IEEE 3rd Information Technology, Networking, Electronic and Automation Control Conference (ITNEC)*, 1325–1329.

Appendices

Appendix A: Pilot Experiment

A behavioural experiment was designed to determine which sounds would be used for the fMRI experiment in Chapter 2. Participants listened to a selection of different sounds, and were asked to identify them, and rate them on a number of different aspects.

Methods.

Participants.

Psychology undergraduate students (N = 29; 5 male) with an age range of 18-37 years (M = 20.36, SD = 3.42) were recruited for this experiment. All participants reported normal or corrected-to-normal vision, and normal hearing. Written consent was obtained following ethical approval from the Research Ethics Committee of the School of Psychology at the University of East Anglia. Participants were awarded virtual course credits for their participation.

Stimuli, Design & Procedure.

Initially, three sound categories were piloted: hand-object interactions (e.g. typing on a keyboard, knocking on a door), mouth-object interactions (e.g. eating an apple, sipping a drink), and animal vocalizations (e.g. dog barking, rooster crowing). Royalty free sounds in WAV format were downloaded from various sound databases such as Soundsnap.com, YouTube.com, and from a sound database used in Giordano, McDonnel, and McAdams (2010). Using Audacity audio software 2.1.2, all sounds were cut to exactly 2000ms in length, ensuring sound filled the entire duration. Sounds were all normalised to the root mean square (Giordano et al., 2013). Overall, 66 different stimuli were piloted; 33 per category, with two exemplars of each stimulus. The experimental session lasted between 45-60 minutes for each participant.

For the experimental task, sounds were loaded into an E-Prime 2.0 experiment. Participants listened to each sound once through professional SONY MDR-7506 headphones, with the volume set at a self-reported comfortable level (as in Leaver & Rauschecker, 2010; Man, Damasio, Meyer, & Kaplan, 2015; Man, Kaplan, Damasio, & Meyer, 2012; Meyer et al., 2010). To begin a trial, participants were asked to press a button, which would initiate a countdown screen from three seconds. Following the countdown, a 2000ms sound was played whilst participants viewed a blank white screen. All sound stimuli were presented in a random order. Once a sound finished playing, participants were automatically redirected to a screen asking them a series of self-paced questions. The questions used in this experiment were derived from a series of previous research using sounds (Giordano et al., 2010, 2013; Marcell et al., 2000; Schneider et al., 2008). The following seven questions were asked:

(1) *Identification.* Participants were asked to identify the sound using at least one verb, and one or two nouns, as seen in Giordano, et al. (2010). Participants were instructed to make their best guess if they did not know.

(2) *Confidence*. Participants were asked to rate how confident they were with their decision. Ratings we on a 1-7 Likert scale from 1 (not at all confident) to 7 (very confident).

(3) *Familiarity*. Participants rated how familiar they were with the sound. In particular, how commonly they heard the sound in day-to-day life, not just in the way it was presented to them. This was important, since the main study was interested in how general familiarity with a sound may evoke traces of activity in other brain areas. Ratings were made from 1 (not at all familiar) to 7 (very familiar).

(4) *Number of sound-generating events.* The next rating was how many sound-generating events participants believed were present. For example, a ticking of a clock would have many events, whereas a simple click of a mouse button would only have one event. It was important to control for this across our sound categories, since the number of sound-generating events has been found to evoke different brain activity patterns important for classifier performance (Meyer et al., 2011). Ratings were made from 1 (no events) to 7 (many events).

(5) *Action and movement related information*. Next, participants were asked to subjectively rate the amount of action and movement related information that was

present for each sound – whilst this was expected to be higher for hand- and mouth-object interactions, participants were given no indication to this. They were simply asked “Did the sound convey action and movement related information?” Ratings were made from 1 (no action and movement related information) to 7 (much action and movement related information).

(6) *Vividness.* Participants also rated how strongly they experienced mental imagery whilst listening to the sound, with the question adapted from the Bucknell Auditory Imagery Scale (Halpern, 2015), and also Meyer, et al. (2010). Participants were asked to rate “the quality of the sound in terms of how strongly it evoked an image in your head”. Ratings were made from 1 (no image evoked at all) to 7 (I could see the image very clearly).

(7) *Perspective.* Finally, participants were asked to specify the perspective they imagined the sound to be taking place. Participants were given five options: 1. You were making the sound yourself. 2. Somebody else was making the sound. 3. A (non-human) animal was making the sound. 4. Nobody was making the sound. 5. Other (please specify).

Results.

Stimuli to be used in the main experiment were primarily selected according to correct identification (average of at least 90% across all participants), with high confidence and familiarity ratings (average of > 5 across all participants). Identification was analysed as strict correct (correct verb and noun, e.g. door knock) or a not so strict correct (either a verb or a noun, e.g. knocking). We also matched the average number of sound-generating events across our final sound categories (see Table A1 and A2 for final stimuli ratings of hand-object interactions and animal vocalizations respectively).

For the final stimulus set, it was decided that mouth-object sounds would be removed due to the ambiguity of these sounds conveying purely a mouth-related action. For example, sounds such as eating an apple or brushing teeth would also involve a hand movement. Thus, ratings from the mouth-object sounds have been excluded. Following this decision, we then decided to include pure tones as an unfamiliar control category, in which the sounds were created by Bruno Giordano.

Once the final stimulus set was decided, sounds were re-normalised to the root mean square (Giordano et al., 2013).

Final selected stimuli.

1) Familiar stimuli: Five hand-object interactions; typing on a keyboard, bouncing a basketball, knocking on a door, crushing paper, and sawing wood.
2) Familiar control stimuli: Five animal vocalizations; dog barking, birds chirping, rooster crowing, fly buzzing, and frog croaking. Animal sounds were chosen as a familiar sound control category, to rule out the idea that any familiar sound can evoke traces of activity to primary somatosensory cortex (Lewis, 2005; Lewis, Phinney, Brefczynski-Lewis, & DeYoe, 2006; Lewis, Talkington, Puce, Engel, & Frum, 2011).
3) Unfamiliar control stimuli: Five pure tones (different frequencies of the same tone; 400Hz, 800Hz, 1600Hz, 3200Hz, and 6400Hz). Tones were included as an unfamiliar control category (Lewis, 2005; Mesulam, 1998) to rule out the idea that merely any sound can lead to discrimination in primary somatosensory cortex.

Table A1.

Mean ratings of selected hand-object interaction stimuli (N = 29)

Stimuli	**Confidence**	**Familiarity**	**Sound gen events**	**Action info**	**Perspective**	**Vividness**	**Strict correct**	**Not strict correct**
Typing keyboard 1	5.93	5.89	5.68	5.07	1.75	5.68	64.29%	96.43%
Typing keyboard 2	5.57	5.86	5.43	5.11	1.54	5.43	60.71%	89.29%
Door knock 1	6.79	6.25	5.46	5.50	1.79	5.93	96.43%	100.00%
Door knock 2	6.36	5.86	5.07	5.43	1.75	5.89	82.14%	85.71%
Sawing wood 1	6.36	4.71	3.93	5.50	1.82	5.79	67.86%	100.00%
Sawing wood 2	5.79	4.36	4.64	5.61	1.89	5.93	67.86%	92.86%
Basketball bounce 1	5.79	4.75	4.82	5.39	1.86	6.07	78.57%	85.71%
Basketball bounce 2	6.32	4.82	4.14	5.50	2.14	5.89	78.57%	85.71%
Paper crush 1	5.54	5.32	3.54	5.11	2.04	5.00	64.29%	100.00%
Paper crush 2	4.93	5.32	3.96	5.11	1.79	5.36	92.86%	96.43%
AVERAGE:	**5.94**	**5.31**	**4.67**	**5.33**	**1.84**	**5.70**	**75.36%**	**93.21%**

Table A2.

Mean ratings of selected animal vocalization stimuli (N = 29)

Stimuli	**Confidence**	**Familiarity**	**Sound gen events**	**Action info**	**Perspective**	**Vividness**	**Strict correct**	**Not strict correct**
Dog bark 1	6.89	6.07	4.68	4.00	2.96	6.43	100.00%	100.00%
Dog bark 2	6.93	6.07	4.75	3.96	3.00	6.25	96.43%	100.00%
Bird chirp 1	6.75	6.46	5.29	4.04	3.00	6.04	85.71%	100.00%
Bird chirp 2	5.39	4.89	4.96	3.61	3.00	5.04	71.43%	96.43%
Rooster crow 1	6.54	4.61	3.82	3.00	3.07	5.86	57.14%	100.00%
Rooster crow 2	6.50	4.79	3.75	3.29	3.00	5.89	60.71%	100.00%
Frog croak 1	6.57	4.43	4.21	3.32	3.00	5.43	60.71%	100.00%
Frog croak 2	6.61	4.61	4.07	3.32	2.93	5.86	60.71%	100.00%
Fly buzz 1	6.11	5.54	4.39	5.18	2.96	5.82	67.86%	96.43%
Fly buzz 2	6.32	5.64	4.96	4.89	3.00	6.00	71.43%	100.00%
AVERAGE:	**6.46**	**5.31**	**4.49**	**3.86**	**2.99**	**5.86**	**73.21%**	**99.29%**

Appendix B: Miniature piezo-tactile stimulator

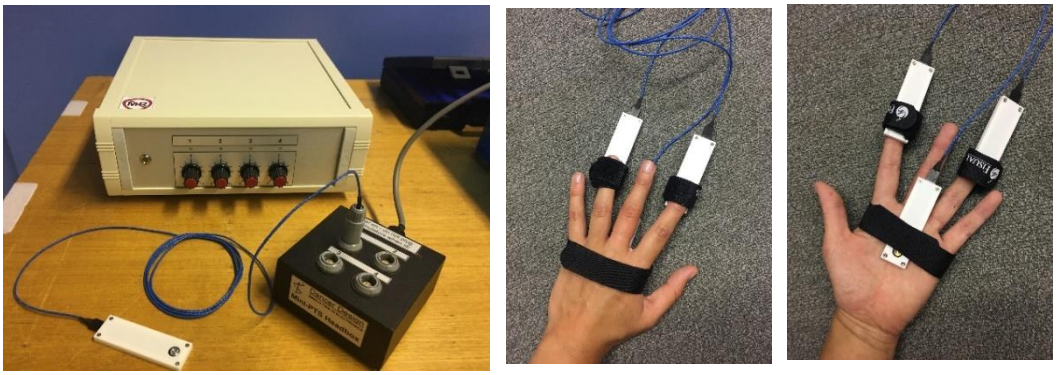

Figure B-1. Image of miniature Piezo-Tactile Stimulator. Demonstration of the three pads placed on the index finger, ring finger, and palm of the left hand.

Appendix C: All hand-drawn masks of the post-central gyri

Table C1.

Number of voxels (and associated cubic volume) in the hand-drawn post-central gyrus for each hemisphere per participant (pooled = left and right combined). Means and standard deviations for each hemisphere are also specified

	Number of Voxels			**Cubic Volume (cm^3)**		
Participant	Right	Left	Pooled	Right	Left	Pooled
1	2373	2257	4630	19.0	18.1	37.0
2	1755	2097	3852	14.0	16.8	30.8
3	1997	1787	3784	16.0	14.3	30.3
4	1638	1950	3588	13.1	15.6	28.7
5	2016	2170	4186	16.1	17.4	33.5
6	1805	1738	3543	14.4	13.9	28.3
7	2180	2303	4483	17.4	18.4	35.9
8	1950	2131	4081	15.6	17.0	32.6
9	2183	2331	4514	17.5	18.6	36.1
10	1790	2296	4086	14.3	18.4	32.7
Mean	**1969**	**2106**	**4075**	**15.7**	**16.9**	**32.6**
St Dev	**229**	**215**	**385**	**1.84**	**1.72**	**3.08**

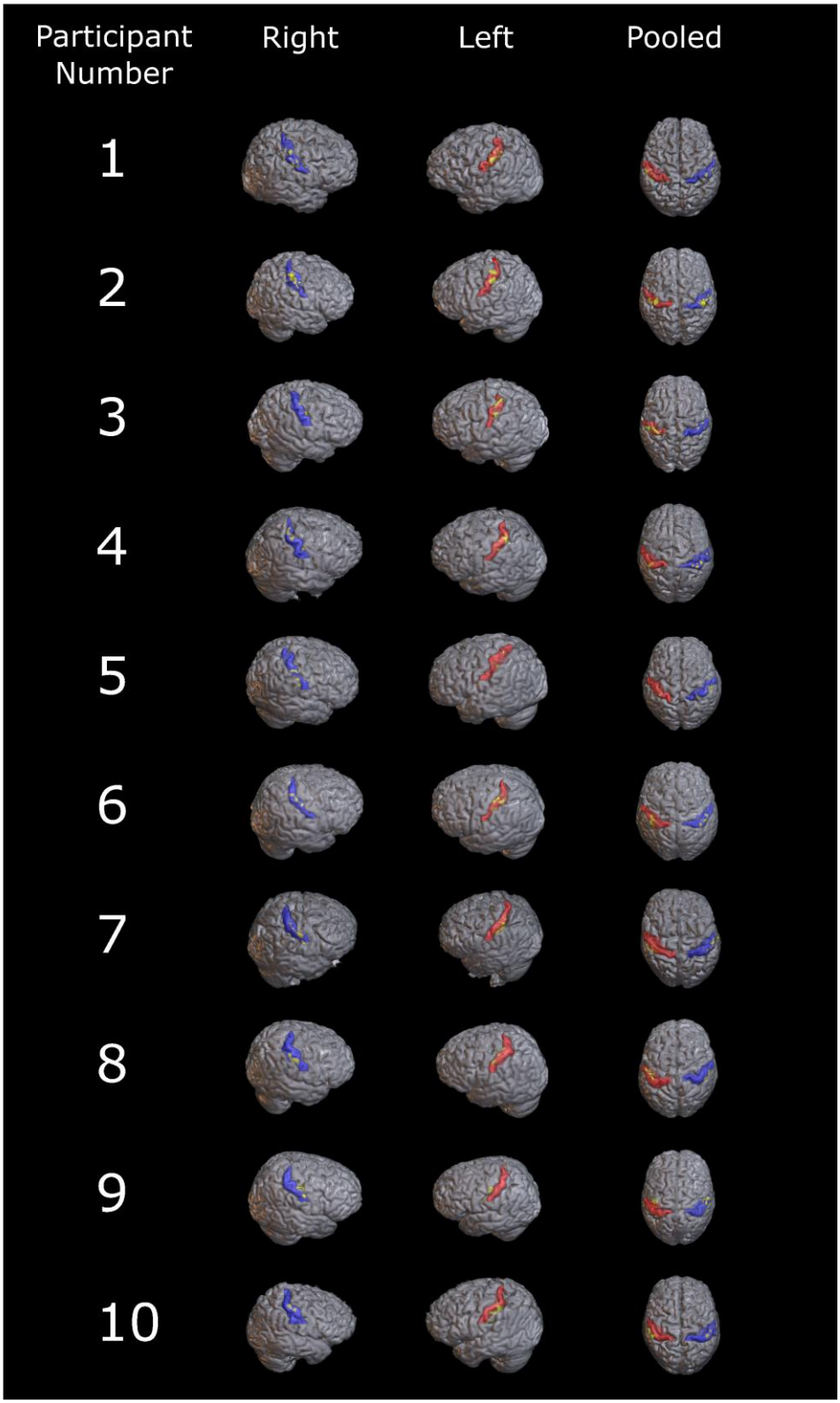

Figure C-1. Anatomical masks of the lateral post-central gyrus (PCG) for all participants. Figures display a 3D rendered version of the right (blue), left (red) and pooled hemispheres. Voxels in yellow indicate the hand-selective voxels (see Chapter 2, Section 2.3.6.2. for more information).

Appendix D: Anatomical masks of the additional ROI's in Chapter 2

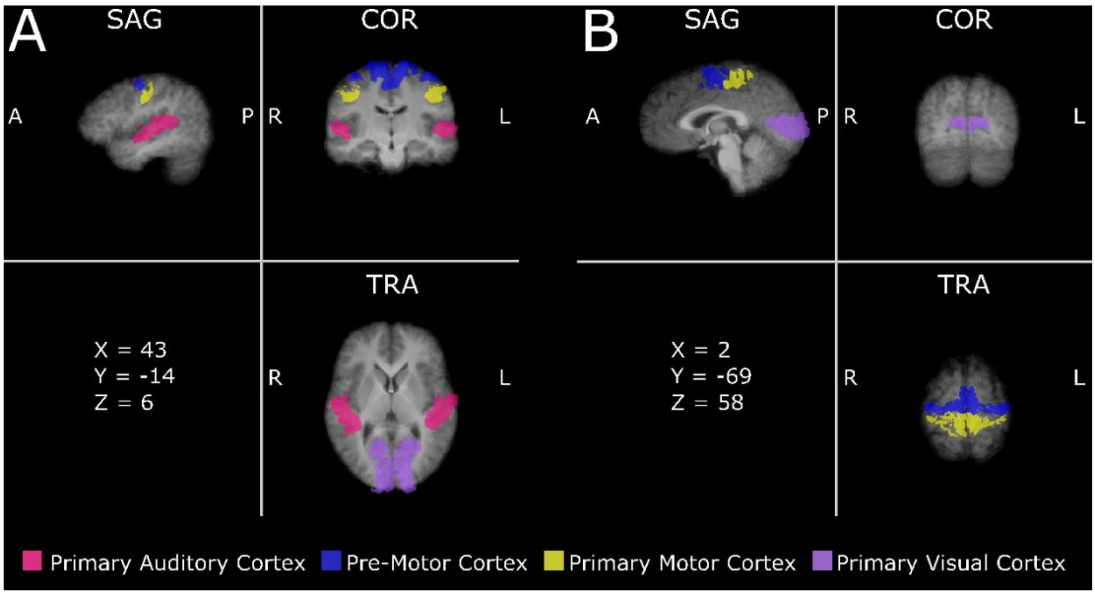

Figure D-1. Image of the four additional anatomical masks taken from the Jüelich Anatomy toolbox. Masks overlaid on the average of 10 participants Talairach brains. Note each mask was transformed to each individual participants ACPC brain.

Appendix E: Table of p values from the univariate deconvolution ANOVA

Table E1

Results from the univariate deconvolution ANOVA, showing main effects and interactions for each ROI. Significant results in bold.

ROI	*Main effect of hemisphere*
$S1_{mask}$	$F_{1.001, 9.013} = .175$, $p = .686$, $\eta_p^2 = .019$
$S1_{localiser}$	$F_{1.200, 10.798} = .342$, $p = .610$, $\eta_p^2 = .037$
A1	$F_{1.001, 9.008} = .056$, $p = .818$, $\eta_p^2 = .006$
PMC	$F_{1, 9.001} = 1.111$, $p = .319$, $\eta_p^2 = .110$
M1	$F_{1.001, 9.005} = .825$, $p = .387$, $\eta_p^2 = .084$
V1	$F_{1, 9.003} = .803$, $p = .393$, $\eta_p^2 = .082$

ROI	*Main effect of sound*
$S1_{mask}$	$F_{1.601, 14.409} = 1.150$, $p = .332$, $\eta_p^2 = .113$
$S1_{localiser}$	$F_{1.369, 12.320} = 1.592$, $p = .238$, $\eta_p^2 = .150$
A1	$\mathbf{F_{1.630, 14.672} = 14.061, p = .001, \eta_p^2 = .610}$
PMC	$F_{1.973, 17..755} = 2.840$, $p = .086$, $\eta_p^2 = .240$
M1	$F_{1.716, 15.444} = 2.906$, $p = .091$, $\eta_p^2 = .244$
V1	$F_{1.370, 12.331} = 1.976$, $p = .185$, $\eta_p^2 = .180$

ROI	*Interaction between hemisphere and sound*
$S1_{mask}$	$F_{1.480, 13.322} = 1.266$, $p = .301$, $\eta_p^2 = .123$
$S1_{localiser}$	$F_{1.981, 17.827} = .224$, $p = .799$, $\eta_p^2 = .024$
A1	$\mathbf{F_{1.579, 14.212} = 9.319, p = .004, \eta_p^2 = .509}$
PMC	$F_{1.463, 13.163} = .388$, $p = .622$, $\eta_p^2 = .041$
M1	$F_{1.599, 14.389} = 1.515$, $p = .250$, $\eta_p^2 = .144$
V1	$F_{1.690, 15.214} = .363$, $p = .667$, $\eta_p^2 = .039$

Appendix F: Actual significant pixels from cluster-based analysis in each visual object category and ROI

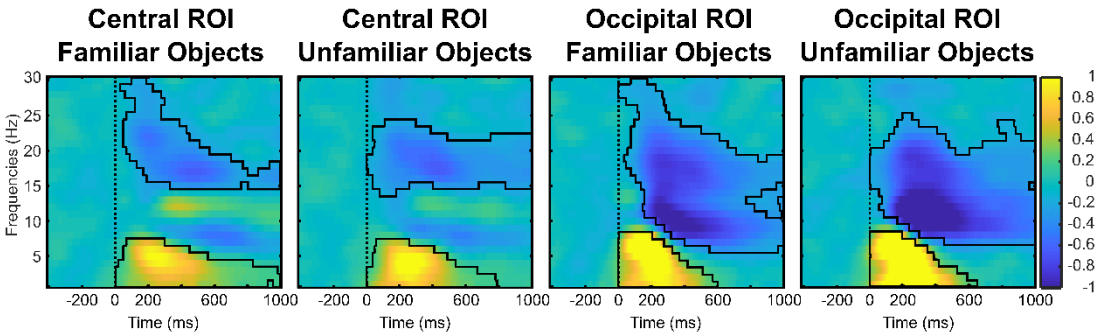

Figure F-1. Masks of actual significant pixels in each condition and ROI. This data was not analysed and is shown for visual purposes.

Appendix G: Anatomical masks of the ROI's in Chapter 4

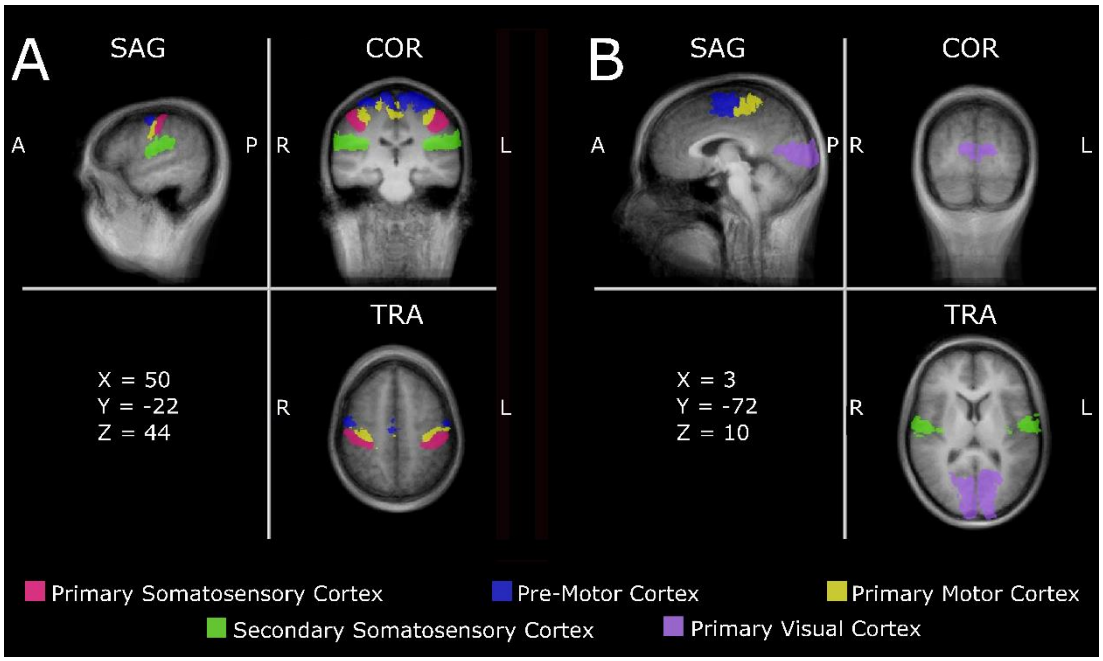

Figure G-1. Image of the anatomical masks taken from the Jüelich Anatomy toolbox and the probability map of S1. Masks overlaid on the average of 18 participants Talairach brains. Note each mask was transformed to each individual participants ACPC brain.

Appendix H: Probability map of the $S1_{localiser}$ cube from 9 participants

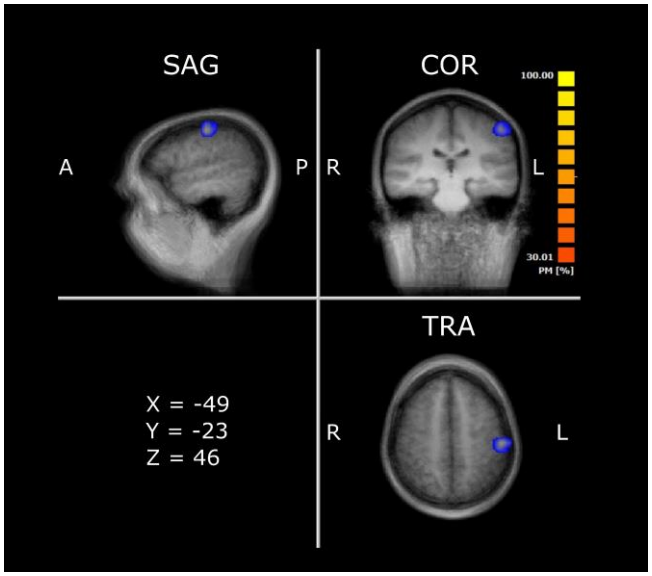

Figure H-1. Image of the probability map created from the $S1_{localiser}$ cubes from 9 participants. Note the probability map is created in Talairach space and overlaid on the average of 18 participants Talairach brains

Appendix I: Plots for all univariate deconvolution analysis

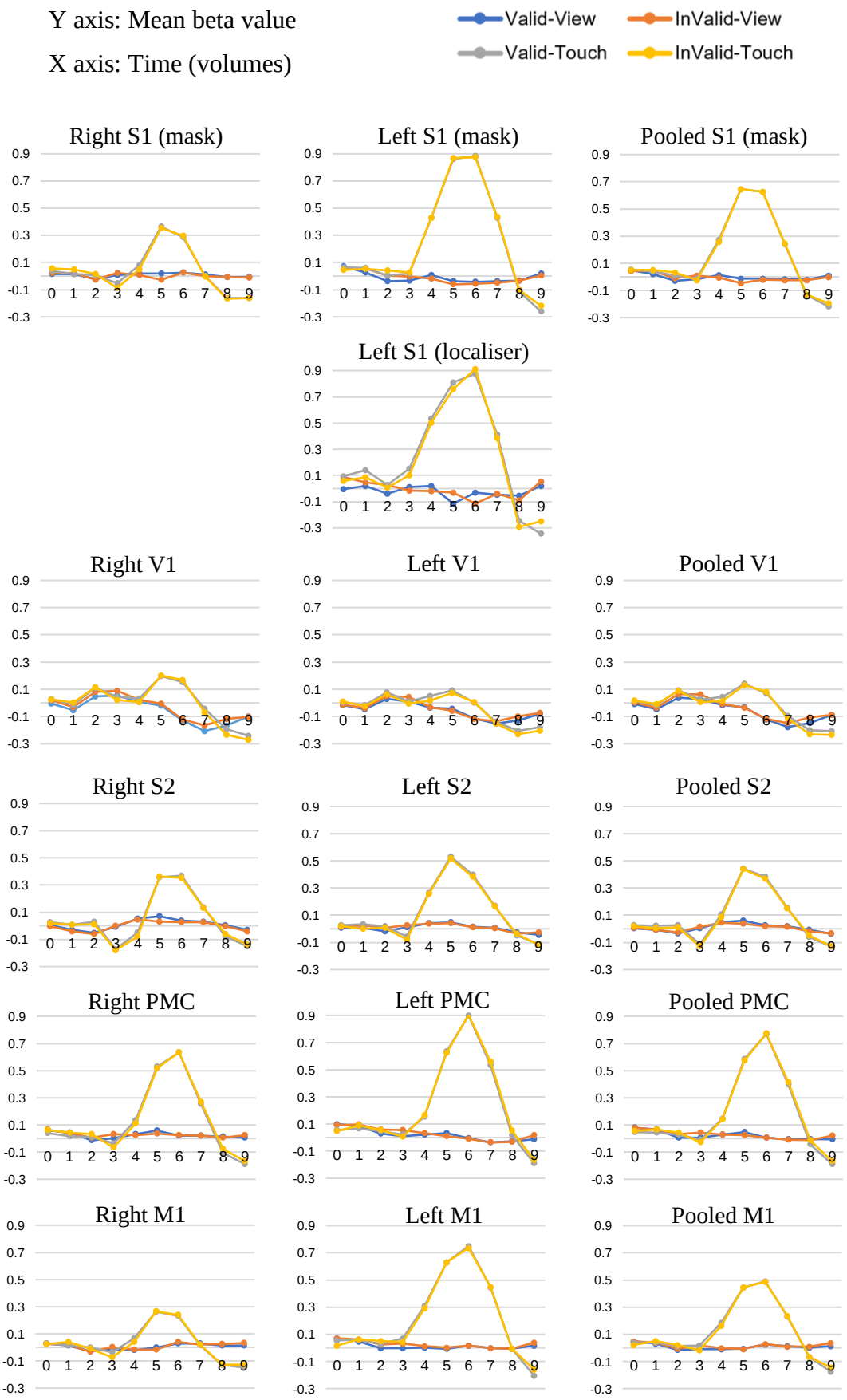

Figure I-1. Deconvolution plots of all volumes in each ROI. Note volumes 5 and 6 were extracted and averaged for the analysis.